NEUROPSYCHOLOGICAL MECHANISMS OF FABRIC TOUCH SENSATIONS

LIAO XIAO

Ph.D

The Hong Kong Polytechnic University

2015

The Hong Kong Polytechnic University

Institute of Textiles and Clothing

Neuropsychological Mechanisms of Fabric Touch Sensations

Liao Xiao

A thesis submitted in partial fulfilment of the requirements

for the degree of Doctor of Philosophy

December 2014

CERTIFICATE OF ORIGINALITY

I hereby declare that this thesis is my own work and that, to the best of my knowledge and belief, it reproduces no material previously published or written, nor material that has been accepted for the award of any other degree or diploma, except where due acknowledgement has been made in the text.

_______________________________ (Signed)

________LIAO, XIAO____(Name of student)

I would like to dedicate my thesis to my beloved wife.

I would not finish this study without her constant love, support and encouragement.

ABSTRACT

The ultimate purpose of this Ph.D. research is to reveal neuropsychological mechanisms of fabric touch sensations by carrying out a systematic study on the process of human tactile sensory perception from physical detection of stimuli, neurophysiological coding and conduction of neural signals, and psychophysiological decoding and formation of sensory perceptions. By uncovering the neuropsychological mechanisms, the underlying grounds of fabric tactile comfort are disclosed. The primary physical stimuli generated form fabric physical properties are identified and transformed with computational algorithms to express how they impact final perceptions, which advance current understanding of human tactile perception of textiles. The research findings can provide guidance for fabric innovation, product development and e-fashion business applications like on-line certificating product tactile comfort performance.

Detection mechanism of physical stimuli was studied by characterizing physical properties of fabrics using “Fabric Touch Tester” (FTT for short), which was designed and engineered for simultaneous measurement on fabric thermal and tactile properties according to the several types of human haptic sensations. The biomimetic neural signals obtained from the measurement of fabric physical and mechanical behaviours using FTT provide multi-channel physical stimuli

information for analysing the thermal, surface texture and softness sensory properties of fabrics.

Neurophysiological coding and transduction of the biomimetic neural signals were investigated by extracting three main types of physical stimuli according to the neurophysiological mechanisms of human skin receptors identified from literature, including thermal stimulus, surface stimulus, as well as force stimulus when deforming the fabrics. The neural coding models of each stimulus reported in neuroscience literatures were modified with consideration of the unique heterogeneous features of textile materials. Several neural responses calculation models were subsequently developed to transform fabric physical properties recorded into skin neural receptor responses. Dynamic thermal responses and mechanical behaviour of fabrics during deformation were analysed according to different stages of neural responses to calculate thermal and force neural indexes. Meanwhile, neural indexes were derived to characterize surface roughness of fabrics according to signal patterns generated from their complex surface properties.

Psychological discrimination of fabric touch sensations from human subjects was examined. Subjective measurements followed standard AATCC Evaluation Procedure 5. Experiment was designed to involve subjects in six climatic conditions and both active and passive haptic evaluation methods. Principle component analysis was performed to extract independent factors from ten sensory descriptors. Three key independent sensory dimensions, named smoothness, softness, and warmth, were derived. They matched well with the three types of physical stimuli. Statistical analyses on subjective results were conducted. Results show significant differences between passive and active touch methods, as well as between different climatic conditions. Psychophysiological study indicates as that active touch method would allow skin to receive more information than passive one due to the anatomical distribution of varied skin receptors and active manipulation of fabrics. It is also found out that acclimation to climatic condition can modify the sensitivity of subjective sensory perception and subsequently induce changes in fabric touch sensations.

Underlying connections between the primary physical stimuli and final psychological perceptions were explored to obtain a complete picture of the process of human tactile sensory perception. Psychophysical relations were explored first by using correlation and regression techniques and further by applying different theories of psychophysical laws. The results show that there is no signal universal psychophysical law applicable for all the tactile sensory perceptions. For different tactile sensory perception, different psychophysical law fits better. It is also observed that interactions between different physical aspects on a single sensory dimension should not be neglected. The integrated sensory perceptions fit with the experimental observations the best by a combination of different equations derived according to different psychophysical law for individual sensations. This finding proved the hypothesis of the need of simultaneous measurement of fabric physical and mechanical behaviors.

Neuropsychological mechanisms were revealed by examining the relations between neural indexes and psychological perceptions. It is concluded that the “Smoothness” was solely affected by the weighted power of PC fiber responses to stimuli with different intensity and frequency; “Softness” is affected by both the SA1 fiber responses to fabric’s resistant force of bending deformation and surface-induced PC fiber responses; “Warmth” is affected by both the maximum and steady thermoreceptor responses and the SA1 fiber response to fabric’s resistant force of compression deformation. Neuropsychological prediction models were developed on the basis of these findings. Models were validated by using the subjective sensory evaluation and physical measurements of a new set of fabrics. The results show that predicted touch sensations from the neuropsychological models are more closely related to subjective obtained scores than those from the psychophysical models.

In summary, this Ph.D. study has generated original research findings that reveal the neuropsychological mechanisms of fabric touch sensations. These findings advance our scientific understanding on fabric tactile sensory comfort and provide a novel neuropsychological approach for sensory engineering of textile materials and products.

OUTPUTS OF THE STUDY

Refereed Journal Paper:

1. **Liao, X.**, Li, Y., Hu, J. Y., Wu, X.X., & Li, Q. H. (2014). A simultaneous measurement method to characterize touch properties of textile materials. *Fibers and Polymers*, 15(7), 1548-1559. doi: 10.1007/s12221-014-1548-2
2. **Liao, X.**, Hu, J. Y., Li, Y., Li, Q. H., & Wu, X.X. (2012). A review on fabric smoothness-roughness sensation studies, *Journal of Fiber Bioengineering and Informatics 4*(2), doi: 105-114. 10.3993/jfbi06201101
3. Zhang, S. J., Li, Y., Hu, J. Y., **Liao, X.**, & Zhang, H. T. (2014). Heat transfer in single-side napped fabrics during compression, *Journal of Fiber Bioengineering and Informatics 7*(1), 103-106. doi: 10.3993/jfbi03201409

Refereed Conference Paper:

4. **Liao, X.**, Hu, J. Y., Li, Y., Wu, X. X., & Li, Q. H. (2014). Psychophysical relations between fabric physical properties and psychological touch perceptions. Paper presented at Textile Bioengineering and Informatics Symposium 2014, Hong Kong, China.
5. **Liao, X.**, Li, Y., Hu, J. Y., Wang, Y. Y., Feng, W. Y., Ding, X. M., Zhang, X., Ying, B. A., Li, Q. H., & Wu, X.X. (2013). An empirical study on the climate effects of fabric touch feels. Paper presented at Textile Bioengineering and Informatics Symposium 2013, Xi'an, China.
6. **Liao, X.**, Hu, J. Y., Li, Y., Wu, X. X., & Li, Q. H. (2012). A Comparison Study of Measuring Fabric Smoothness Using KES-FB and PhabrOmeter.

Paper presented at the Textile Bioengineering and Informatics Symposium 2012, Ueda, Japan.

7. Cai, T., Li, Y., Hu, J. Y., Wang, M. K., **Liao, X.**, Wu, X. X. & Li, Q. H. The influence of water contents on the handle properties of cotton shirt fabrics. Paper presented at Textile Bioengineering and Informatics Symposium 2014, Hong Kong, China.
8. Cai, T., Hu, J. Y., Wang, M. K., **Liao, X.**, Wu, X. X. & Li, Q. H. The influence of fineness on the handle properties of cotton fabric for shirt. Paper presented at Textile Bioengineering and Informatics Symposium 2014, Hong Kong, China.
9. Wu, X. X., Li, Y., Hu, J. Y., **Liao, X.**, & Li, Q. H. (2013). A comparative study of fabric stiffness based on FTT, KES, and subjective testing. Paper presented at Textile Bioengineering and Informatics Symposium 2013, Xi'an, China.
10. Li, Q. H., Li, Y., Hu, J. Y, **Liao, X.**, & Wu, X. X. (2013). A new method to characterize dynamic heat conductivity properties of fabric under various pressure conditions. Paper presented at Textile Bioengineering and Informatics Symposium 2013, Xi'an, China.
11. Zhang, S. J., Li, Y., Hu, J. Y., **Liao, X.**, Liu, X. Q., Li, Q. H., & Wu, X. X. (2013). Analysis on the heat transfer performance of single-side napped fabric, Paper presented at Textile Bioengineering and Informatics Symposium 2013, Xi'an, China.

12. Wang, Y. Y., Feng, W. Y., **Liao, X.**, Li, Y., & Ding, X. M. (2013). Sensory Evaluation and instrumental methods for measuring tactile properties of silk fabrics. Paper presented at Textile Bioengineering and Informatics Symposium 2013, Xi'an, China.

<u>Patent:</u>

1. Li, Y., Hu, J. Y., **Liao, X.**, Li, Q. H., & Wu, X. X. (2012a). A New Method to Characterize Surface Geometry Properties and Surface Friction Properties of Soft Material China Patent File No.: 2012102754856 C. P. Office.
2. Li, Y., Hu, J. Y., **Liao, X.**, Li, Q. H., & Wu, X. X. (2012b). A New Method to Characterize Dynamic Heat Conductivity Prosperities of Soft Materials under Various Pressure China Patent File No.: 2012102756480, C. P. Office.
3. Li, Y., Hu, J. Y., **Liao, X.**, Li, Q. H., & Wu, X. X. (2012c). A New Method to Characterize Dynamic Bending Properties of Soft Material China Patent File No.: 201210278839.2, C. P. Office.

<u>Award:</u>

1. **Liao, X.**, Jiao, J. Liu, X. Q., & Li, G. Chamber of Personal Protection and Health, Shortlisted for final assessment, PolyU Micro Fund 2014 – Entrepreneurship Steam, Hong Kong 2014.
2. Li, Y., Hu, J. Y., & **Liao, X.** Gold Medal with the Congratulations of Jury Prototype: Fabric Touch Tester, Geneva 2013 Invention Exhibition, Geneva, 2013.

3. **Liao, X.** Outstanding Research Presentation Award (Winner), the 8th ITC Research Student Seminar, Hong Kong, 2013.
4. **Liao, X.**, Li, Y., Hu, J. Y., Wang, Y. Y., Feng, W. Y., Ding, X. M., Zhang, X., Ying, B. A., Li, Q. H., & Wu, X.X., Outstanding Student Paper, 6th Textile Bioengineering and Informatics Symposium, China, 2013.

ACKNOWLEDGEMENTS

I am using this opportunity to express my gratitude to everyone who supported me throughout this Ph.D. study. I am thankful for their guidance, criticism, and advice during the work. I am sincerely grateful to them for sharing their thoughts on a number of issues related to the dissertation.

I express my warmness thanks to my chief supervisor, Prof. Yi Li, for being an excellent mentor during my study in both scientific research and personality development. I sincerely appreciate his superior supporting style for allowing me exploring the unknown with all the possibilities while still in the right path. I am also grateful for the healthy research and life atmosphere he leaded in his research team. It reminded me to maintain well balanced between work and life.

I express my gratitude to my supervisor Dr. Jun-Yan Hu, for providing me thorough guidance during all stages of my research work. I could not image how hard it would be to finish this study without his invaluable inspirations and advices. I would also like to extend my thanks to my supervisor Dr. Ji-Yong Hu, for the time and contributions he gave to this dissertation.

I express my thanks to Mr. Xin-Xing Wu and Mr. Quan-Hai Li from the Hong Kong Polytechnic University, as well as Mr. Robert Lattie, Mr. Kenji Kang, Mr. Fred Cheng and Mr. Fu-Ming Li from SDL Atlas Inc., for their supports in manufacturing the instrument prototype in this study. Their views and opinions helped a lot in modifying the measurement principle so that it could be commercial practicable.

I wish to thank Hong Kong Innovation and Technology Commission and Hong Kong Research Institute of Textile and Apparel for proving funding support to this research through projects ITP/024/10TP and ITP/005/14TI. I also wish to thank Hong Kong Polytechnic University and Institute of Textiles and Clothing of it for providing administration and other financial supports.

There are also many people I would like to give my sincere thanks to for their patient assistances in conducting experiments and constructive discussions on my dissertation. They include:

Dr. Lei Yao,

Prof. Xue-Mei Ding,

Prof. Takatera Masayuki,

Prof. Sachiko Sukigara,

Prof. Xin Zhang,

Prof. Fu-Kui Pan,

Dr. Bo-An Ying,

Dr. Yong-Jun Sun,

Ms. Mow-Nin Sun,

Dr. Chun-Hong Zhu,

Ms. Yan-Yan Wang,

Ms. Wen-Yan Feng,

Mr. Sammy Cheng,

Ms. Yan-Xia Han,

Ms. Su-Jian Zhang,

Dr. Tao Cai, and

all the other persons who participated in the subjective measurement as well as all colleagues in Prof. Li's research team.

Finally, and most importantly, I wish to express my deepest gratitude to my wife and my parents, without their support, this dissertation would be impossible.

TABLE OF CONTENT

LIST OF FIGURES

LIST OF TABLES

Chapter 1 Introduction

This research aims to study the neuropsychological mechanism of fabric touch sensations. The study is carried out by investigating three components: physical detection of fabrics as stimuli; neurophysiological coding of neural signals; and psychological discrimination of fabrics through touch sensation. Research outcomes include the simultaneous detection mechanism of fabric physical stimuli; the coding models that identify the physical stimuli from fabric and transduce them into biomimetic neural signal intensities; the discrimination capacities of psychological touch sensations; and the neuropsychological prediction methods on the fabric touch sensations.

A systematic literature review is provided in Chapter 2. Conventional studies on fabric touch sensations began from investigations that recognize their psychological relevance, followed by studies on physical measurements on fabrics and then psychophysical prediction models. There is, however, a lack of studies on revealing the underlying neuropsychological principle of touch sensations, especially in textiles field. With detail summaries of findings from previous publications, six research gaps are identified with regard to the neuropsychological mechanism of fabric touch sensations. To fill these knowledge gaps, six research objectives are derived as listed below:

1. To develop a theoretical framework to outline the potential mechanisms at different stages of neuropsychological perception of fabric touch sensations.

2. To reveal the simultaneous physical detection processes that skin receiving stimuli from fabrics and to explore the principles of simultaneous quantitative measurements on these physical stimuli.
3. To study the neurophysiological coding mechanisms that underlies the transductions from fabric physical stimuli to the nerve signals with development of models on the unique features of fabrics to transfer measured physical properties of the fabric to neurophysiological indexes.
4. To investigate the psychological perception and discrimination of fabric touch sensations with identification of the independent dimensions of psychological sensory perceptions and the differences between passive and active touch, as well as the effects of climatic acclimation.
5. To explore the relations between psychological sensations and physical stimuli as well as their interactions with validation of various psychophysical laws.
6. To reveal the neuropsychological mechanisms of fabric touch sensations and formulate prediction models.

Detailed methodologies are designed and presented to achieve the stated research objectives in Chapter 3. Briefly, in order to quantitatively measure the physical stimuli from the fabrics, a new evaluation instrument has been designed and engineered to measure physical features of selected fabrics. Neurophysiological coding models are established to transduce fabric physical properties to biomimetic neural signals. The psychological discrimination of touch sensations of selected fabrics is studied from subjective measurement. Experiment design has considered the potential effects of passive/active touch methods and different climatic conditions. The neuropsychological mechanisms are revealed by building prediction models, utilizing findings from each stage. Validation of neuropsychological prediction models is carried out by comparing predicted results of a new set of fabrics with the subjective scores.

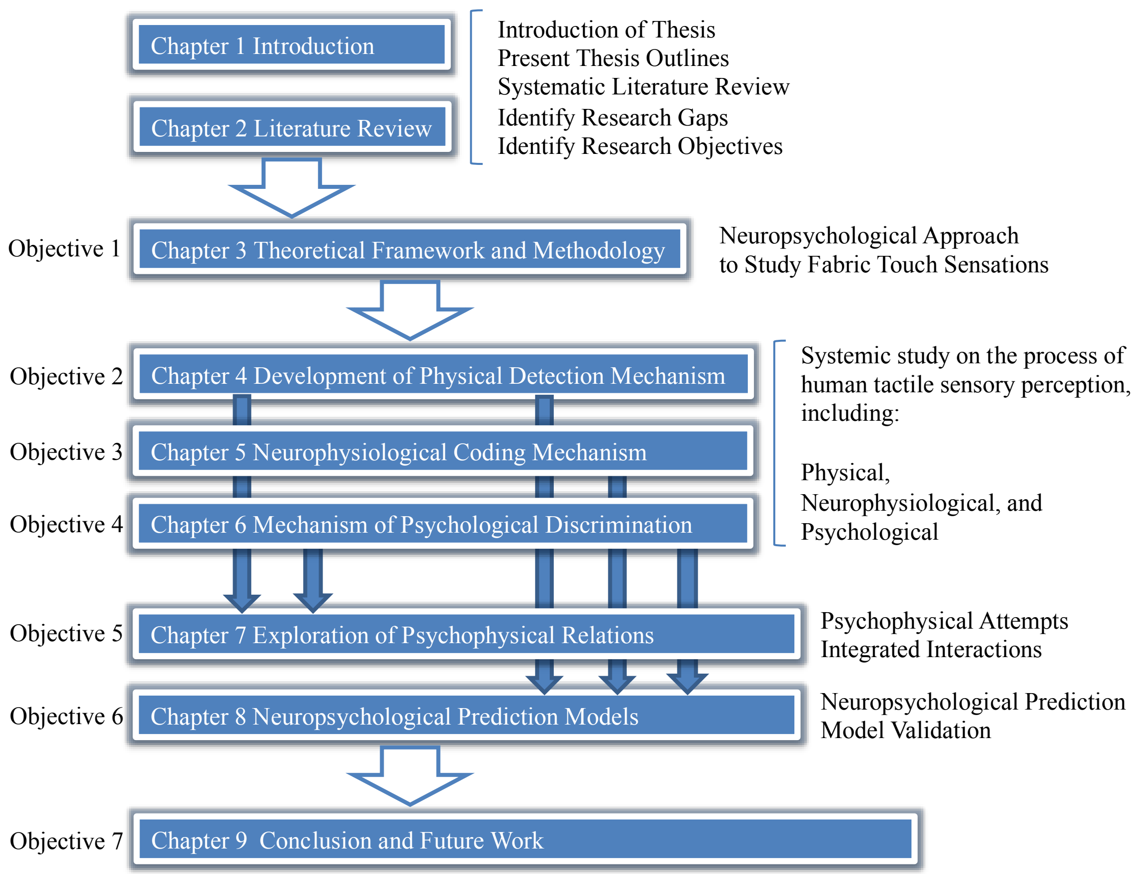

Figure 1-1 Flowchart of Thesis

A flowchart of this thesis is presented in Figure 1-1. There are nine chapters in this Ph.D. dissertation, which clearly express the canvassed neuropsychological mechanism of fabric touch sensations. Chapter 1 presents the research highlights and outline of the whole dissertation. Chapter 2 is the literature review while the theoretical framework for achieving the research objectives is stated in Chapter 3.

Chapters 4 to 6 are discussions on the evaluation of the fabric touch sensations from physical, neurophysiological and psychological three stages respectively. Chapter 4 investigates the physical stimuli produced from fabrics. These physical stimuli can stimulate skin receptors, which can transduce them into neural signals. The physical detection mechanism of these fabric stimuli is revealed. A measurement method that simultaneously records the properties of these physical stimuli is utilized in this chapter.

In Chapter 5, the neurophysiological coding mechanism of signal transduction is explored. Three primary types of stimuli, which can be perceived by human skin when evaluating fabrics, are presented. These stimuli include thermal, texture, and force. Mathematical modeling to transduce these physical stimuli into the biomimetic neural signals is carried out. The coded neural signal responses are subsequently calculated based on the physical measurement results.

Chapter 6 details an investigation on the psychological discrimination capacities of humans. Experiment design of reported behavioral measurements includes over 200 subjects under six different climatic conditions, using both passive and active haptic evaluation of fabrics. Smoothness, softness, and warmth are attributed as factors that contribute to the psychological discrimination of various fabrics. Meanwhile, the effects of active and passive touch and climatic conditions are also reported.

Chapters 7 and 8 present the prediction models that are synthesized from previous findings. Chapter 7 shows the psychophysical prediction models developed to demonstrate the relationship between subjective sensory perception and objective physical properties. The classical psychophysical laws are compared with the test results in this study. The effects of the interactions between different physical aspects on a single sensory dimension are presented.

Chapter 8 is a discussion of the neuropsychological mechanism of fabric touch sensations, which presents the underlying principle of complete perception process of fabric touch sensations. Concluded prediction models based on neuropsychological mechanism provide indexes that directly address the touch sensation of fabrics. The models are validated with a new set of fabrics and good prediction accuracies are observed.

Chapter 9 is a review of the work carried out in this Ph.D. study during the past four years. A conclusion for the present study is provided. Potential commercial applications from this study are given and suggestions on future studies are specified.

Chapter 2 Literature Review

The origin of the use of clothing was to protect the human body from the external environment. Keeping warm during cold days was the principal reason for why ancient humans started to wear clothing, as the belief of anthropologists. Later, aesthetic pleasure was brought on by the wearing of clothing. A number of different styles have been conceived throughout the history of fashion design. Nowadays, the demands of consumers have changed from “works well”, “looks good” to “feels comfortable”. Fabric touch sensations attract the attention of consumers in today’s market. Research carried out ten years ago has already shown that the touch feel of fabric is the most important factor to consumers in Australia, Asia and Europe (Wong & Li, 2002). The importance of the comfort of clothing was accepted and many studies were subsequently conducted to evaluate the touch sensations of textile products.

Fabric touch sensation has been studied since the early 1900s. Researchers began first by studying the definition. In 1930, Peirce first described fabric touch as related to the perception of consumers, including a series of different personal perceptions (Peirce, 1930). Schwartz later conducted technical investigations on the effect of fabric finishing treatments (Schiwarz, 1939). It was concluded that fabric touch consists of three types of contrasting sensations: stiffness-limpness, hardness-softness and roughness-smoothness. Patterson studied the causes of different touch feel in wool fabrics (Patterson, 1947). His research concluded that fabric touch sensations are generated as an individual reaction in the examining of fabrics. These classic instances of research work made the first steps in the field and guided the studies that followed.

With regard to the comprehensive definition of fabric touch sensation, LaMotte and Goldman (LaMotte, 1977) introduced a human-clothing-environment concept in their research. Fabric touch sensations were believed to be greatly influenced by tactile and thermal factors that arise from contact between the skin and the immediate environment. Li further summarized that evaluations of fabric touch feel should include studies into the physical, physiological, and psychological factors (Li, 1998a).

In the following, Section 2.1 provides an explanation on the general processing patterns of sensory perception. Section 2.2 focuses on the physical stimuli that could stimulate skin touch receptors and Section 2.3 is a review on the measurements of these physical stimuli. Section 2.4 concludes on the latest findings on neurophysiological coding mechanisms of touch sensations. Section 2.5 is a discussion on the psychological studies of fabric touch sensations. Section 2.6 is a summary on the prediction methods previously used. In Section 2.7, the research gaps are provided, while the objectives of the study are given in Section 2.9.

2.1 General Mechanism of Sensory Perception

The sensory system is the part of the human nerve system that responds to sensory information, aside from other nerve systems like the motor and the cogitation systems. The majority of the previous studies focused on four types of sensory systems. They were concluded to be responsible for detecting four different types of stimuli, which are mechanical (touch), chemical (taste and smell), sound (auditory) and light (visual) (Avijit Chaudhuri, 2011). Neurons are the very basic cells in these sensory systems. They are the carriers of electrically neural signals within the nerve system. It was concluded that common functions of neurons include three types of processes: receiving stimulus input, transmitting the input into signals, and generating motor outputs when necessary (Levitan & Kaczmarek, 2002).

The sensory system responsible for touch information is called the somatosensory system. Therefore, physical stimuli received when skin comes into contact with objects are processed in the somatosensory system. The physiological mechanisms of this system, as a result, illustrate the perception process of touch sensations. It was concluded that the perception of touch sensations involves several steps. Information transfer would begin from the detection of certain stimuli (for instance through temperature changes, pressure, or skin stretching and indentation). The corresponding neural organics in the human skin, named receptors, would subsequently transduce these stimuli into neural signals (Avijit Chaudhuri, 2011). This step is called the transduction of stimuli. Afterwards, receptors would transmit neural signals to the brain via the central nervous system (Kolb & Whishaw, 2003). The neural signals would finally reach the functioning areas of the human cerebrum and generate sensations (Levitan & Kaczmarek, 2002). In short, literature states the typical pathway of perception would begin from the fingers/skin, pass through the human nerve system, and terminate at the thalamus as illustrated in Figure 2-1.

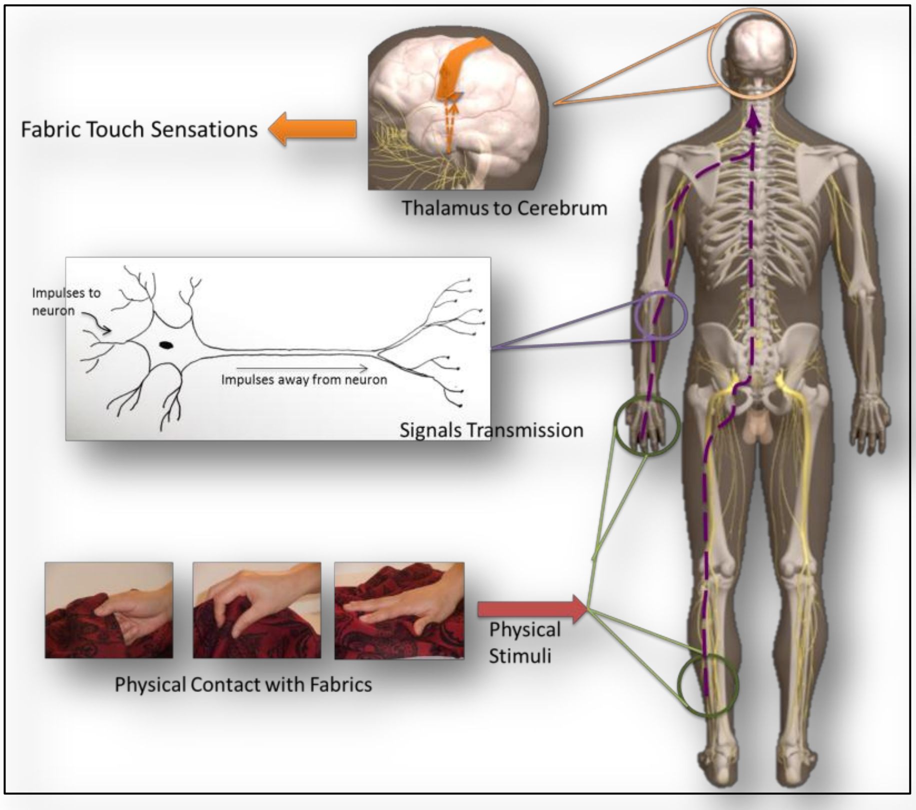

Figure 2-1 General Perception Process of Fabric Touch Sensations

Bottom part of the Figure 2-1 shows that physical contact with fabrics will stimulate certain receptors on human skin. Middle part demonstrates how neurons carry and transmit the neural signals. These signals are transmitted from skin receptors until brain, as presented in purple dashed lines in the right part of the figure. The upper part illustrates that neural signals are received in thalamus and terminates in cerebrum to generate perceived touch sensations.

It was concluded that parallelism takes place in the human nervous system. Parallelism suggests that there are only several pathways that transmit a large number of sensation nerve signals at the same time (Bear, Connors, & Paradiso, 2007). Mountcastle stated that parallelism is especially noticeable in the somatosensory system (Mountcastle, 1998). This phenomenon implies that despite the different receptors responsible for different physical stimuli, the pathways to transmit these nerve signals might be shared and signals are simultaneously transmitted.

Human cerebrum, the destination of these neural signals, is divided into four anatomical parts, including the occipital, temporal, parietal, and frontal lobes. Each lobe responds to a certain type of sensation and/or cognition. Somatosensory perception is carried out in the parietal lobe (Avijit Chaudhuri, 2011). When a sensory signal goes through a neural pathway and reaches the cerebrum, it is the cerebral cortex that first receives the signal and biologically recodes the signal for the perception of sensation. Most modern biological scientists agree on the theory that different parts of the human brain have differences from both anatomical and functional viewpoints (Avijit Chaudhuri, 2011; Kolb & Whishaw, 2003; Kornhuber & Albe-Fessard; Smith, 2000). Brodmann's areas histologically divided the cerebral cortex into 52 functional areas (Brodmann & Garey, 2010). It was stated touch sensation (somatosensory) is carried out by areas 3, 1, and 2. Brodmann's areas 3b and 1 for example, were found to be sensitive to information from the cutaneous receptors (Darian-Smith, Sugitani, Heywood, Karita, & Goodwin, 1982; Iwamura, 1998).

Brodmann's areas 3, 1 and 2 make up an area called the primary somatosensory cortex (SI). The early stage of perceived touch sensation is believed to be generated in the SI, which receives input from the peripheral afferent neurons via thalamocortical projections. Another area located in the parietal operculum was also found related to the processing of somatosensory information. This region, Brodmann's areas 40 and 43, is called the secondary somatosensory cortex (SII) (Burton, 2002). These two parts of the cerebrum are believed to be hierarchically organized in human as well as nonhuman primate brains. Different areas in the SI would receive signals not only from lower organics (like afferent fibers), but also other areas in the SI (Hyvarinen & Poranen, 1978; Iwamura & Tanaka, 1978). It is also believed that information interaction takes place between SI and SII (Iwamura, 2003).

The above concepts with regard to touch sensations perception suggest that humans perceive integrated touch sensations from a group of neural signals transduced from several types of stimuli. These stimuli are simultaneously received when evaluating touch sensations.

2.2 Physical Stimuli of Fabric Touch Sensations

As pointed out in Section 2.1, physical stimuli are the initial inputs in the perception of touch sensation. They are detected and received by the skin receptors. Obviously, fabric is the sources of physical stimuli that will produce touch sensations. Textile material, usually evaluated in the form of fabric, is a kind of soft material that has unique features. Fabric is easily deformed at low stress and rough on the surface. It is the buffering layer that separates the human body and the external environment, which transfers heat and moisture between layers. The following paragraphs first provide information on the biological foundation of skin and receptors, and then a review is provided on the fabric physical properties that can be detected by the skin receptors.

2.2.1 Anatomy of Skin and Receptors

The skin is the part of the human body that touches fabric and receives physical stimuli. There are two types of skin that cover the human body (Coren & Ward, 1989). One is called glabrous skin. It is glabrous, which means there are no hairs. It can be found on the palm of the hand and ventral portion of the finger.

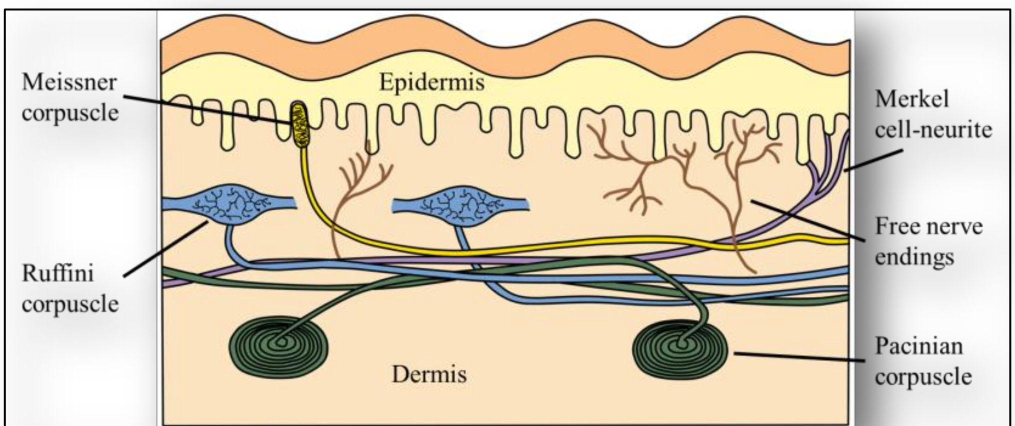

Figure 2-2 Anatomic Location of Neural Receptors in Human Skin

Skin is believed to anatomically comprise two basic layers. The outer layer is called the epidermis while the inner layer is named the dermis. The order of the outer to the inner layers comprises first the layers in the epidermis, which are the stratum corneum (cornified layer), stratum lucidum (clear/translucent layer), stratum granulosum (granular layer), stratum spinosum (spinous layer), and stratum basale/germinativum (basal/germinal layer) (Marks, Miller, & Lookingbill, 2006). Then, the dermis is made of two layers called the stratum papillary and stratum reticular (Arnold, Odom, & James, 1990). Receptors are found in these different layers. The function of these receptors is to receive stimuli from the external environment and transduce them into neural signals.

Previous research showed that there are many ways to distinguish skin receptors. They can be classified as corpuscular and non-corpuscular endings. Coren and Ward concluded that corpuscular nerve endings are responsive to tactile stimuli and are associated with cold or pain fibers (Coren & Ward, 1989). Iggo and Wolfe distinguished sensory receptors by their functions as mechanoreceptors, thermoreceptors, and nociceptors (Iggo, 1988). These receptors are named after the anatomists who first located them. Figure 2-1 illustrates the anatomic location of these skin receptors. The Meissner corpuscle and Merkel cell neurite complexes are found at the junction of the epidermis and dermis while the Pacinian corpuscles and Ruffini endings are located at deeper levels; that is, the dermis and underlying subcutaneous tissue (Molfe et al., 2009). Thermoreceptors are located in both types of skin layers. There are two types of thermoreceptors. They are warm and cold fibers. The cold fibers were found to project into the epidermis in rats (Dhaka, Earley, Watson, & Patapoutian, 2008). Meanwhile, the myelinated afferents were also found to be sensitive to cold. Research showed that Merkel cell neurite complexes and Ruffini endings are also cold-sensitive in the range of 14.5°C to normal skin temperature (Cahusac & Noyce, 2007; Duclaux & Kenshalo, 1972).

2.2.2 Thermal Stimulus from Heat Transfer

In daily life, there are always differences between the temperature of human skin (which remains relatively constant in most environment conditions) and the external atmosphere. Thermal sensation, however, was only considered to be one of the fabric touch sensations after 1975. It was proposed that fabric touch sensation should not comprise only tactile, but also thermal sensations (LaMotte, 1977). The latest review showed that most textile researches agree that the thermal property is an important aspect that influences clothing comfort sensation (Kamalha, Zeng, Mwasiagi, & Kyatuheire, 2013).

It has been long considered that thermal sensation is one of the most distinct sensations of human touch. Somatosensory studies have revealed that humans are able to sense a wide range of temperatures. Thermal sensation is considered to be a very important factor for consequent physiological responses when the temperature of the external environment changes. It is also believed that neurophysiological responses to thermal stimuli would interact with other somatosensory receptors and produce multi-faceted touch sensations (Avi Chaudhuri, 2011).

Humans can detect a wide range of temperatures and perceive both hot and cold sensations (Schepers & Ringkamp, 2009). Extreme temperatures, above 43°C or below 15°C, would produce not only thermal sensations, but also pain sensations (Tominaga & Caterina, 2004). Therefore, innocuous cold and hot sensations are usually discussed separately from cold-pain and hot-pain sensations (Nilius & Voets, 2007). Two different types of receptors are concluded to be responsible for hot or cold sensations. Warm fibers conduct impulses when the skin temperature is above 30°C while cold fibers do so when the skin temperature is in the range of around 16°C to 44°C (Patapoutian, Peier, Story, & Viswanath, 2003). Under daily circumstances, the human body skin temperature is normally around 32°C – 35°C while normal room conditions are around 20°C - 27°C (Freitas, 1999). Therefore, fabrics are more likely to stimulate the cold receptors. In other words, heat will usually transmit from the skin to the fabric.

There are three means by which the skin temperature changes. These include conduction, radiation, and convection (J. Y. Hu, 2006), with conduction as the most significant means (Stanković, Popović, & Poparić, 2008). When we touch fabric, the skin thermoreceptors would be stimulated because of the heat transmission through the fabrics. For fibrous materials like fabric, thermal transmission is jointly determined by the effects of both material (i.e. fibers) and the air.

Humans are found to be able to sense the warmth or coolness of objects even when they are balanced with the same temperature. The reason is believed to be the heat energy transmitted between human skin and the touched objects (Tiest, 2010). Therefore, it has been suggested that thermoreceptors are more sensitive to detecting temperature changes than the absolute temperature of objects (Avi Chaudhuri, 2011). Meanwhile, previous studies on fabric sensation correlated thermal perception with heat transfer properties of fabric as the thermal conductivity and the total energy absorbed (Hes & Dolezal, 1989; Kawabata, 1984; Pac, Bueno, Renner, & El Kasmi, 2001).

2.2.3 Force Stimulus from Fabric Deformation

The manipulation of objects is a very common task that humans perform. In order to successfully manipulate an object, we would actually need to receive many different types of information and perform different reactions. Three types of information are generally agreed on when manipulating an object, including shape of the object, contact position on skin, and direction and magnitude of force (Goodwin & Wheat, 2004). Meanwhile, simpler tasks take place in haptic exploration, which requires smaller number of contact points. As a result, when investigating haptic perception of fabric, researchers usually paid more attention to contact force. Force is often applied onto fabric when we touch them. The reactions would subsequently be exerted onto the hand, and such reaction forces could be received by the receptors as stimuli. In fabric research, a common method to differentiate reactions is to group them as compression and bending forces.

The compressibility of objects was originally investigated as the relationship between the pressure and volume of a specimen (Van Wyk, 1946). Research concluded that there are three layers in the structure of fabric: 1) the incompressible center, 2) surface, and 3) back layers (Dejong, Snaith, & Michie, 1986; Postle, Carnaby, & Dejong, 1988). Hu added two additional layers to the theory, which increased from three to five layers by further dividing both the surface and back layers into the first and secondary outside layers (J. L. Hu, 2004b). These are the hairy fiber and structure layers respectively.

The complete process of fabric compression includes the pressing and recovery stages. Compressibility or compliance is defined as the changes in thickness when applying certain normal pressures onto samples (Ali & Begum, 1994; Elder, Fisher, Armstrong, & Hutchison, 1984). Recovery is also an important physical feature. The forces received during different stages might affect different sensations. Softness has been reported to be associated with pressing forces (Elder et al., 1984). On the other hand, the properties during the recovery stage are usually described with terms such as “fullness” or “bulkiness”. The ratio of energy during pressing and recovery has been used (Kawabata & Niwa, 1989) to address this touch sensation.

The initial findings from neurophysiological studies have indicated that both forces received and displacements of skin (indentation) could be indicative of softness discrimination through compression, whilst later research which was carried out with tools indicated that spatial cues such as indentation are not necessarily required (LaMotte, 2000). A recent study concluded that when softness is evaluated by active tapping or pressing, the ratio of the object deformation and normal force is the most important factor for softness discrimination while maximum compression force and force change rate are the least important factors (Friedman, Hester, Green, & LaMotte, 2008).

Reaction forces could also be received in the conducting of bending. Fabrics are easily bendable. The bending properties of fabrics depend on at least three factors, which are the bending properties of the fibers themselves, the structure of the fabric, and (if any) finishing methods applied. Hu defined two stages during the bending process (J. L. Hu, 2004a). The first stage determines if the fibers are compacted together and the curve of the moment - curvature of bending is non-linear. The second stage illustrates the process after all of the fibers are compacted into tight positions and the curve is close-to-linear.

The bending properties have been concluded as highly correlated to the touch sensation of “softness”. “Stiffness” is the opposite of “softness” and more commonly used when discussing fabric bending features. Bending rigidity, defined as the slope of the bending curves, has been mentioned in a series of early studies (Abbott & Grosberg, 1966; Livesey & Owen, 1964; Owen, 1966). The hysteresis bending moment is also defined to address the bending recoverability (Kawabata, 1982).

Compared to the compression aforementioned, bending also involves tactual information like perceived force, skin indentation, and change of contact position. There are limited neurophysiological studies that have solely focused on bending rigidity.

2.2.4 Texture Stimulus from Fabric Surface

Texture stimulus is another type of cutaneous stimuli. It reflects the external information of form and texture perceptions (K. O. Johnson & Yoshioka, 2002). Fabrics are basically in the form of a flat sheet. In addition, fabrics can be deformed with low stress, which means that there is little three-dimension information produced by them. Therefore, the discussion here mainly focuses on texture information other than form.

In research on fabric touch sensation, it is commonly believed that friction force and surface roughness are related to the sensation of perceived "smoothness", despite the various terms that may otherwise be used. Previous research (Ekman, Hostman, & Lindstrom, 1965) found that the sensation of smoothness has a power function related to the friction coefficient of the surface. Li also found correlation among the sensation of fabric smoothness and surface roughness, compression, fiber diameter, as well as fiber and fabric tensile properties (Li, 1988). Recently, Chen et al. studied the strength and form of sensation and physical properties by using regression modeling (X. J. Chen, Shao, Barnes, Childs, & Henson, 2009). The conclusion of this study was that smoothness is related to the friction coefficient and roughness of the surface. However, the friction force only appears when there is at least some trend of movement. Can we valuate and receive fabrics without relative movement, i.e. without friction force? Comparison experiments carried out by (Morley, Goodwin, & Dariansmith, 1983) showed that lateral movement is not crucial for texture perception. This indicates that texture stimulus could be received without friction force.

Meanwhile, research on texture stimulus was also widely conducted through the use of tactile writing systems, such as Braille Dots. A series of research by (Lederman, 1974; Lederman & Taylor, 1972; Taylor & Lederman, 1975) on recognition of Braille letters concluded that the texture stimulus is received in relation to the groove and ridge widths of these dots. On the other hand, findings from later studies, such as by (Hollins, Fox, & Bishop, 2000), again attracted attention on lateral movement. It was concluded that for very fine texture, lateral movement does help with texture discrimination Subsequently, it was found by (Cascio & Sathian, 2001) that receiving of texture stimulus is also affected by the scanning speed between the skin and surface of the object. Neuroscientists believe that such conflicting findings are mainly due to whether fine or coarse textures were used in the experiments. The reason for the conflicting information received from fine or coarse textures was then proposed. It was concluded by (Hollins, Bensmaia, & Washburn, 2001) that the vibrations caused by lateral movement could stimulate receptors and produce texture stimulus. Such vibrations are critical only for fine textures.

2.2.5 Summary of Physical Stimuli

Previous studies have provided reviews on physical stimuli that could be received by the skin receptors of the human somatosensory system. Research in the textiles field have revealed the mechanism of unique fabric physical properties while recent neuroscience studies have made good progress in uncovering the critical triggers of touch sensations. These findings, however, have their own limitations and are unable to form the full picture with regard to how humans perceive touch sensations from fabric. Table 2-1 is a summary of the findings from textile and neurophysiological researchers.

The interactions between the different aspects in these findings would also influence touch perception. A number of publications have concluded the effects of temperature on the neural responses to tactile stimuli (Ho, Watanabe, Ando, & Kashino, 2011; Li & Wong, 2006; Smit, Hanekom, & Hanekom, 2009; Yang & Kwon, 2008). In other words, thermal stimulus could both stimulate thermal receptors and affect the sensitivity of the other tactile receptors. Since the functional areas of the human cerebrum are hierarchically organized as indicated in (Hyvarinen & Poranen, 1978; Iwamura & Tanaka, 1978), information interaction also takes place between the SI and SII, and humans would perceive touch sensation along with the simultaneous processing of all the different types of touch stimuli.

Table 2-1 Summary of Findings regarding Different Physical Stimuli in Fabric Researches and Neurophysiological Researches

Physical Stimuli	**Findings in Fabric Researches**	**Finding in Neurophysiological Researches**
Thermal Stimulus	Thermal conductivity (Pac et al., 2001)	Skin temperature (Patapoutian et al., 2003)
Force Stimulus	Compliance and bending rigidity (J. L. Hu, 2004a, 2004b)	Degree of deformation and applied forces (Friedman et al., 2008)
Texture Stimulus	Surface roughness (X. J. Chen et al., 2009)	Shape of roughness elements (Lederman, 1974; Lederman & Taylor, 1972; Taylor & Lederman, 1975); Skin vibrations (Hollins et al., 2001);

<u>Derived Research Gap</u>

In summary, this section provides information on the latest research in terms of the physical stimuli of touch sensation. There exist different physical properties of fabric, which will be received as different types of physical stimuli. Although previous research have successfully concluded that there are certain physical properties of fabric which would produce specific fabric touch sensations, there are few studies that have investigated fabric touch sensation based on recent neuroscience findings. The currently found underlying neurophysiological mechanisms of touch sensation have not yet been applied in research with fabric.

2.3 Quantitative Characterization of Physical Stimuli

Along with studying the physical stimuli from fabric that could affect touch sensation, researchers have also derived many different characterization methods to quantitatively measure these physical stimuli. Measurement methods that are well known include Fabric Assurance by Simple Testing (FAST) developed by the Commonwealth Scientific and Industrial Research Organisation (CSIRO) (Pier Giorgio, 1995) and the Kawabata Evaluation System (KES) devised by Kawabata leaded research group (Kawabata, 1980, 1982, 1984).

In the KES measurement method, there are four separate instruments involved. They are responsible for the measurement of tensile and shear (KES-FB1), bending (KES-FB2), compression (KES-FB3), and the surface (KES-FB4). The tested specimen is to be 200 mm x 200 mm in size. For a complete measurement on fabric, 9 specimens are needed (4 to test the tensile and shearing, 2 to test the bending, 1 to test the compression, and 2 to test their surface). The FAST measurement method includes separately testing for compression (FAST-1), bending (FAST-2), extensibility (FAST-3) and dimensional stability (FAST-4). The specimen size for FAST testing is to be 150 mm x 50 mm for the first compression, bending and extensibility, and 300 mm x 300 mm for dimensional stability. In total, 8 specimens are required for a complete measurement: 1 to test the compression, 2 to determine bending; 4 to test the extensibility; and 1 to test the dimensional stability.

In Section 2.2, three types of physical stimuli that are related to fabric touch sensation are reviewed. In the following section, measurements on the different aspects of these physical properties are discussed, respectively. Since the KES and FAST measurement methods use different testers, hence, they are individually discussed in each section.

2.3.1 Measurement of Thermal Stimulus

Previous discussions have mentioned that not only should the absolute temperature be taken into consideration when studying the thermal touch sensation of object, but also the rate of the temperature change should be included. Meanwhile, the thermal conductivity of the material itself is not enough to demonstrate heat transmission during the evaluation of touch sensation. Contact areas, for example, would also affect heat transmission. As a material that is heterogeneous, the thermal conductivity of fabric is usually believed to be influenced by the material (i.e. fiber contents), construction, and sometimes the finishing and coating. Therefore, how fabrics cool the skin is essential for perception of thermal sensation. Such so called “cooling curves” have been previously investigated and their relation to subjective perception evaluated, see (Havenith, Vandelinde, & Heus, 1992; Sarda, Deterre, & Vergneault, 2004; Schneider & Holcombe, 1991). These psychophysical experiments suggest that the thermal response curves could portray the thermal perception of objects.

Further studies have been conducted to mathematically model the thermal responses of different materials. In a study by (Sarda et al., 2004), two-dimensional finite-element modeling was preferred for simulating the temperature changes of skin when touching various materials. The blood flow of the skin and contact resistance between skin and object were also involved in some of the studies, see (Benali-Khoudja, Hafez, Alexandre, Benachour, & Kheddar, 2003; Ho & Jones, 2006). In later research, such as (Tiest & Kappers, 2007, 2008), other physical properties were taken into consideration, such as roughness and thickness. All of these investigations proved that the proposed factors demonstrate that they have important effects on real circumstances of heat extraction and subsequently cold perception. However, currently, there is no available full description of the complete process of heat transmission during skin-object contact. The physical measurement of thermal sensation hence should be based on the actual thermal response of objects.

Therefore, in the studies on thermal sensation from the perspective of the body, a large number of factors are usually considered. The International Organization for Standardization (ISO) published a series of standards that are related to fabric thermal properties (ISO, 1998, 2005, 2007). These include standards derived from work such as simulations with thermal manikins; assessments from wear trials; and measurements on environmental thermal-wet conditions. Discussions from this field cover different aspects that would influence the thermal-balance between the human body and surrounding environment. These factors involve, but are not limited to the metabolic rate, air movement, clothing, etc. (P. Bishop, 2008). Among them, subjective measurement methods are not commonly used as they are inconsistent and costly (Fan & Chen, 2002) while manikins are usually expensive and too complex to perfectly simulate the thermal-wet system in the human body.

However, research work that use common instruments for measuring fabric seldom study the whole heat transmission process. There are generally two types of measurement methods, including "keeping warm" and the conductivity method.

Kawabata introduced an instrument called the Thermolab (KES-FB7) to evaluate the thermal properties of fabric (Kawabata, 1984). To carry out measurement on warmth, or the use of the so called heat retention measurement, the sample is placed on top of a heated plate. The temperature of this BT Box is usually set 10°C higher than the room temperature. The heat flow value is recorded after the temperature stabilizes. Index $\overline{\mathrm{W}}$ is defined as the mean value of heat flow from 60 until 180 seconds. The reading would be significantly affected by the surrounding environment conditions. Therefore, for the KES-FB7, a wind column in a standard chamber to control the micro-environment, including wind velocity, room temperature, and room relative humidity (Yoneda & Kawabata, 1982), was recommended. This equipment for measuring fabric thermal resistance is also used in several other standards (ASTM, 2011; ISO, 1993).

With regard to thermal conductivity measurement, there are two metal plates that come into contact with the samples in the use of the KES-FB7. One of the plates, called the water box, is designed to remain at a temperature that is the same as the room temperature. The other plate is the BT Box, which is pre-heated to a higher temperature. At the beginning of the experiment, the sample, which is 50 mm x 50 mm in size, is placed in the middle of these two plates. An instrument dynamically records the heat flow loss of the BT Box. When it reaches a steady value, the reading is used to calculate the fabric thermal conductivity through the following equation:

$$k = \frac{H * D}{A * \Delta T} \tag{2-1}$$

where H means the heat flux value of the BT Box, D the thickness of sample, A the area of measurement, and ΔT temperature difference between two plates.

Meanwhile, during the measurement, there should be a peak heat flux value, which is measured at 0.2 seconds after contact. This maximum heat flux is called Qmax and related to the feeling of coolness (Kawabata & Yoneda, 1981).

2.3.2 Measurement of Force Stimulus

The KES-FB3 instrument measures the compression properties of fabrics. A metal circle that is the size of 2 cm^2 is used to compress samples. A normal force would be gradually increased at a constant rate of 0.02 gf/sec until it reaches 100 gf (i.e. 50 gf/cm^2). The compression measurement by the KES-FB3 instrument also includes implementation of the recovery process. Normal pressure would be reduced at the same speed during recovery. There are three parameters defined for fabric compression properties. These three parameters are compression linearity (LC), compression energy (WC), and compression resilience (RC), which can be calculated by using following formulas:

$$WC = \int_{D_m}^{D_0} PdD \tag{2-2}$$

$$LC = \frac{\int_{D_m}^{D_0} PdD}{P_m(D_0 - D_m)/2} \tag{2-3}$$

$$RC = \frac{\int_{D_m}^{D_0} PdD}{\int_{D_m}^{D_0} P'dD} \tag{2-4}$$

where D means the thickness of the specimen; D_0 and D_m the thickness of at pressure of 0.5gf/cm^2 and 50gf/cm^2 respectively; P_m the maximum pressure as 50gf/cm^2; P and P' the normal pressure during compression and recovery respectively.

The FAST-1 compression tester uses a similar measurement principle as the KES-FB3 instrument. The pressure device of FAST-1 has a square shape of 10 cm^2. The minimum recorded pressure is 2 gf/cm^2 and maximum is 100 gf/cm^2. Readings of fabric thickness are also taken and recorded under two loads of 2 gf/cm^2 and 100 gf/cm^2 respectively. In addition, samples which are measured by using the FAST-1 tester is expected to measured again after they are steamed on an open Hoffman press for 30 s. The same loads (i.e. 2 gf/cm2 and 100 gf/cm2) of are used for the released thickness values (Boos & Tester, 1994). The differences between the thickness readings under these two pressure loads are also believed to comprise fabric compression properties.

The KES-FB2 instrument measures the bending properties of fabrics. Two vertically installed bending bars hold the samples vertically. One bending bar is fixed while the other is able to move. The length of the sample held between these two bars is maintained as 1 cm. The route of movable bar is fixed so that the bending curvature of the sample would change at a constant rate of 0.5 cm^{-1}/s until maximum curvature takes place, which is set at 2.5 cm^{-1}. After bending of the sample in the clockwise direction, the movable bar would move in an anti-clockwise direction to its original position and then continuously towards the other side, which would bend the fabric again until a curvature of 2.5 cm^{-1}. The test trial is finished when the movable bar travels back to its original position on the second round. A torque sensor is also mounted, which records the bending moment used during the whole process. Figure 2-3 shows the process of how the KES-FB2 instrument measures the force required for fabric bending. Solid lines mean the original position when the sub-process begins while dashed lines mean the future positions during the sub-process. It is clear that the KES-FB2 instrument would actually bend fabrics twice, once on the face and then the back. The bending properties of the fabric are defined as the average of the results from the forward and backward bending.

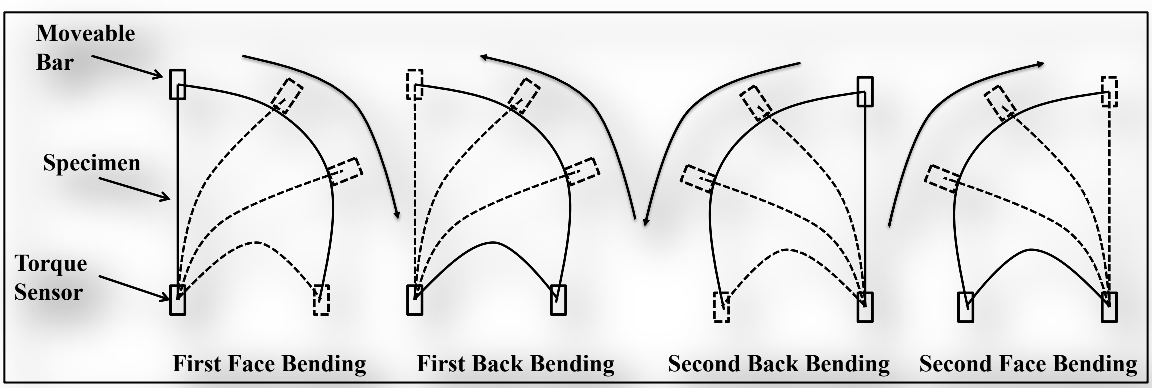

Figure 2-3 A Complete Bending Process of KES-FB2

Indexes defined in KES-FB2 included Bending Rigidity (B) and Moment of Histeresis (2HB) with formula as follows:

$$B = \frac{1}{4}\sum_{i=1}^{4}\frac{|M_{1.5i}-M_{0.5i}|}{1} \qquad (2\text{-}5)$$

$$2HB = \frac{1}{2}\left[\frac{1}{1}\int_{0.5}^{1.5}(M_{f1}-M_{b1})dx + \frac{1}{1}\int_{0.5}^{1.5}(M_{f2}-M_{b2})dx\right] \qquad (2\text{-}6)$$

where $M_{1.5i}$ and $M_{0.5i}$ are the bending moments recorded when the curvature is 1.5cm^{-1} and 0.5cm^{-1} respectively, i number of times of bending process from 0cm^{-1} to 2.5 cm^{-1}, x the bending curvature and M_{f1}, M_{b1}, M_{f2}, and M_{b2} bending moment during the first face bending process, first back bending process, second face bending process and second third bending process respectively.

FAST-2 is used to examine the bending properties of fabrics through the cantilever method. This method is similar to the British Standard Method (BSI, 1990). The bending rigidity is determined from the bending length of a sample obtained by the FAST-2 instrument. A sample is allowed to pass over a platform and subsequently bend itself because of gravity. Unlike other common equipment, FAST-2 uses a photocell to detect the leading edge other than through visual means to improve reliability (Boos & Tester, 1994). The same measurement principle is also applied as early as work carried out by Peirce in 1930 (Peirce, 1930) and later, through commercial instruments such as the Shirley Stiffness Tester and Gurley Stiffness Tester.

There are also other methods that have been used for fabric bending measurements. The hanging loop method, as defined by Wang et al. (X. Wang, Liu, & Hurren, 2008), folds one end of the sample back to its other end. In (Stuart & Baird, 1966), the height of the folded loop was found proportional to the bending length as measured by the cantilever method. However, the physical validity of this measurement method was questioned in (Ghosh & Zhou, 2003; Zhou & Ghosh, 1997).

2.3.3 Measurement of Texture Stimulus

The KES-FB4 instrument measures the surface properties of samples. The KES surface tester includes measurements on both surface friction and surface roughness. Fabric specimens are placed onto a flat platform and held by a clip at the end as shown in the Figure 2-4. Fabric sample is moved towards right side of the figure. The clip, which is mounted onto a roller, can produce a traction force of 20 gf/cm onto the specimen. It would drag the specimen and move at a stable speed of 1 mm/sec. The total movement of the specimen is set as 2 cm forward and 2 cm backward. A friction detector is placed on the top of the sample to record the friction force during testing. The normal force placed onto the sample is 50 gf. The friction detector is made of 10 parallel wires, with a diameter of 0.5 mm.

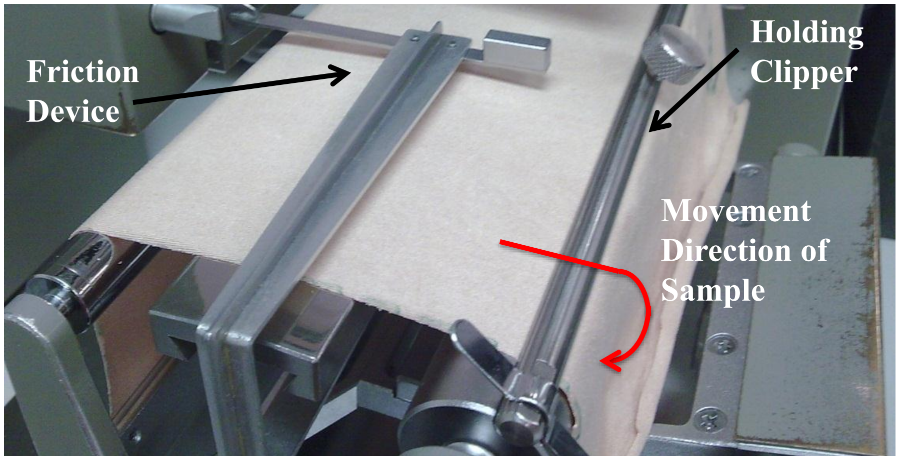

Figure 2-4 KES-FB4 Friction Testing Part

Output included the coefficient of friction (MIU) and the standard deviation of the friction coefficient (MMD) (Kawabata, 1982). Formulas of these indexes are shown as follows:

$$\text{MIU} = \frac{1}{X}\int_0^x \mu dx \qquad (2\text{-}7)$$

$$\text{MMD} = \frac{1}{X}\int_0^x |\mu - \bar{\mu}| dx \qquad (2\text{-}8)$$

Where X is the total displacement of sample (i.e.: 2cm); x displacement of the top device on the sample surface; μ friction force recorded;

The measurement of roughness is conducted together with friction measurement. A different detector is placed parallel to the previously mentioned friction force detector onto the sample surface. The normal force here is set as 10 gf. The detector is made of only one wire with a diameter of 0.5 mm. The displacement of the detector is recorded as the roughness of the sample fabric. During the duration of the testing, there is 2 cm in the movement of the sample. The output parameters include SMD, which is the mean deviation of the surface roughness. Calculation equation of SMD is:

$$\text{SMD} = \frac{1}{X}\int_0^x |D - \bar{D}|dx \qquad (2\text{-}9)$$

Where X is the total displacement of sample (i.e.: 2cm); x displacement of the top device on the sample surface; D the geometric thickness of sample.

There are also many other tactile methods to measure the friction properties of One of these methods is the use of a modified tensile tester to evaluate the friction properties. This method also includes a specially designed detector. The friction defined as the force that prevents the relative movement of fabric and the detector. tensile tester then pulls the detector along the fabric surface while the forces movement are recorded. A sample prototype is illustrated in

Figure 2-5. A metal cube is used as friction-surface device, which is placed on top of the sample. A tensile tester can pull the cube through a fixed pulley and record the forces during experiment. The Instron® machine was widely used in this method (Ajayi, 1992a, 1992b; Zurek, Jankowiak, & Frydrych, 1985).

Another method to measure friction force is called the inclined plane method. This method uses gravity, instead of a tensile instrument, to measure the friction force. A fabric sample is placed onto a sled for testing. The sled is placed on a level platform, which can be lifted up on one end to change the horizontal angle of the platform with a micro switch. The resultant angle is recorded when the sled slips off the platform.

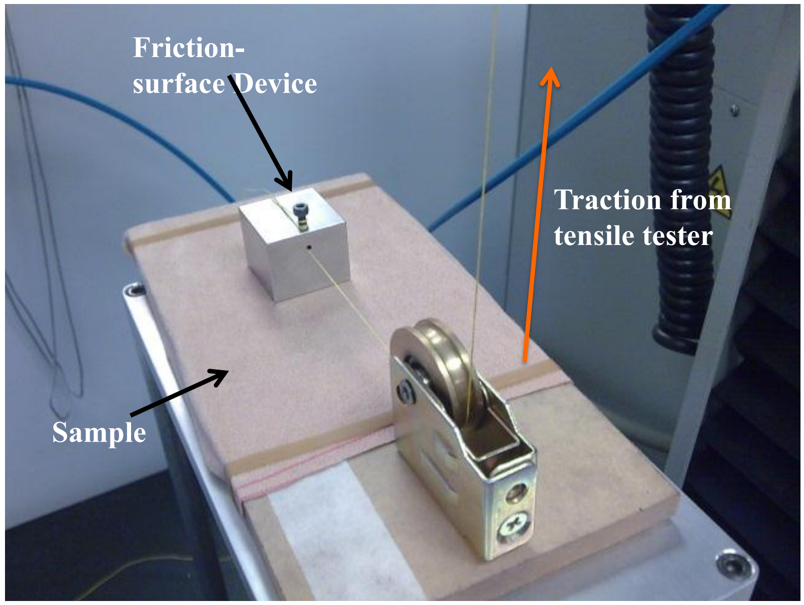

Figure 2-5 A Laboratory Prototype of Modified Tensile Tester for Friction Testing

Another means is the optical method, which is widely used in the measurement of the properties of the fabric surface geometry, i.e. roughness. Kang and colleagues (Kang, Cho, & Kim, 2001; Kang, Kim, Sul, Youn, & Chung, 2005; Kang & Lee, 2000) did a series of research from 2000 to 2005 by using the optical method to evaluate fabric surface smoothness. By following AATCC Test Method 124, which is used to evaluate the fabric smoothness by visual assessment through the use of standard replica (AATCC, 2000), Kang and colleagues (Kang et al., 2001; Kang et al., 2005; Kang & Lee, 2000) developed a new grading method based on 3D vision and fractal dimension techniques. A commercial instrument, called the FabricEye, uses a high-speed charge coupled device (CCD) camera and scanner to objectively measure the surface roughness of samples and apply digital evaluation methods to measure the fabric roughness properties (J. L. Hu, 2004b). Xin et al. (B. X. Xin, Hu, & Baciu, 2010) also recently used silhouette image analysis to determine the surface roughness of textile.

2.3.4 "Ring" Measurement Method

There are also measurement methods that bypass direct measurements on physical stimuli. The "ring" method is one of latest available means to do so. The basic idea of the "ring" methods is to have the sample fabric go through a flexible light circle. Researchers pull or push specimens through a designed circle. The circle is considered to be a better medium for the simulation of different aspects of fabric hand, including drop ability, stretch, internal compression, lateral pressure and surface friction. The force when pulling or pushing the sample fabric is measured as a function of time and the curve generated is recorded.

Although the ring methods all apply the same concept by pulling or pushing a fabric sample through a metallic ring, there are shared variances on the sample and ring sizes or output value. The concept of the ring method was discussed as early as 1988 (Pan, Yen, Zhao, & Yang, 1988). PhabrOmeter, a commercial instrument, was invented based on this concept. A test specimen, with a size of 100 cm^2 in a circular shape, is pulled through a circular metal hole. Force is recorded as a function of time. A complete test would only take 22 seconds.

With 110 recorded data points, Pan (Pan, 2007) used a statistical pattern recognition tool and then the Karhunen-Loeve (K-L) orthonormal expansion to analyze the force-time curves. The data points were then statistically refined to eight parameters (Pan, 2007). These eight parameters were believed to represent different aspects of fabric touch sensations, although some of them remained no suitable names. Pan defined the first three parameters as stiffness, smoothness, and softness (Y_1-Y_3 respectively), because they were found correlated to Primary Hand Value (PHVs) results stiffness, smoothness, and softness from the KES system. The other parameters are still called Y_4-Y_8 respectively. Pan also conducted calibration for the physical meanings of the named three parameters. He performed finishing treatments, which was believed to change one aspect of fabric hand on fabric (e.g. plasma treatment), on the sample fabric. The treated fabrics were re-tested by using the PhabrOmeter to calibrate the physical meaning of one parameter (e.g. smoothness value in the case of plasma treatment). In addition, with a reference fabric, the Euclidean distance of the 8 parameters (with different weights) was calculated as the overall fabric hand value, named the PH value.

There is a new method that uses a funnel to replace the "ring" (El Mogahzy, Kilinc, & Hassan, 2005). A funnel is considered to better simulate the interaction between fabric and hand during touching. A force-time curve similar to one that is given by the PhabrOmeter can be generated by using this method. The under area of this curve is divided into four parts; each indicates one aspect of the fabric physical properties. The fabric hand index is defined as the total area under the force-time curve. In a study by (Kilinc, 2004), a significant correlation was found between this index and subjective hand assessment results. Similar "ring" methods can also be found in many other research, see (J. O. Kim & Slater, 1996, 1999; Sultan & Sheta, 1994) while it was found in (El Mogahzy et al., 2005) that there are disagreements about how the "ring" methods are physically interpreted.

The “ring” method, commercially represented by PhabrOmeter, remarkably reduces the testing time of the measurement of physical stimuli for fabric touch sensation. Nevertheless, there are still difficulties in clearly describing the physical properties of samples (Liao, Hu, Li, Wu, & Li, 2012). The method fails to provide physical interpretations of the test results.

2.3.5 Summary of measurement of related physical stimuli

In the following table, reviews on the above measurement methods are summarized. The major concerns of the FAST and KES systems are the relatively high cost and that they are time consuming, which have reduced their applications in the industry (Behery, 1986; El Mogahzy et al., 2005; J. O. Kim & Slater, 1999). The PhabrOmeter provides a quick means, but is unable to provide clear results of the fabric physical properties. Moreover, none of the methods include thermal properties as a factor in evaluating fabric touch sensation. Some of the latest developed techniques could be used to replace conventional mechanical measurement methods. However, these methods, like image analysis, have not yet been applied in the testing of all the aspects of fabric touch sensations.

Table 2-2 Summary of Measurements on Physical Stimuli

Measurement Concepts	Example Products	Dimensions	Test Time, and Test Cost	Physical Results
Mechanical Direct	KES, FAST	Compression, Bending, Surface, and Tensile (Kawabata, 1982) (Boos & Tester, 1994)	Long, High	Yes

Mechanical Indirect	PhabrOmeter	Smoothness, Softness, Stiffness (Pan, Zeronian, & Ryu, 1993)	Fast, Low	No
Optical	FabricEye	Surface (J. L. Hu, Xin, & Yan, 2002; B. J. Xin, Hu, & Yan, 2002)	Fast, Medium	Yes
Simulation	Human Manikin	Thermal (Fan & Chen, 2002; Romeli, Barigozzi, Esposito, Rosace, & Salesi, 2013)	Medium, High	No

<u>Derived Research Gap</u>

Currently available measurement methods do not give enough attention on the neurophysiological foundation of touch sensation. Most of the instruments reviewed are designed and validated by using psychophysical methods. The underlying neurophysiological mechanism is neither explored nor applied in these instruments. With the latest progress in neurophysiological studies on touch sensation, a new measurement method of physical stimuli is needed. A measurement method that clearly and directly focuses on physical stimuli could be useful for future neuropsychological research on fabric touch sensations.

2.4 Neurophysiological Coding from Physical Stimuli to Neural Signals

An environmental event detected will stimulate the responsible human sensory system. Receptors are transducers of physical external environments and electrical neural signals. The neural coding process is defined as the responses of neural receptors when they receive physical stimuli (Avijit Chaudhuri, 2011). Afferent fibers are the key organics for determining the response to a stimulus as well as the transmission speed of coded neural signals. The transmission speed, as a characteristic of afferent fibers, was found to be affected by the diameter of the fibers and their degree of myelination (Morley, 1998; Smith, 2000). It was revealed that neural receptors continuously fire pulses under normal conditions. When stimulus is recognized by the receptor organics, they fire impulses instead.

Another feature of neural receptors is their adaptation. It has been often observed that continuously applied stimulus could make humans less aware of its presence. This phenomenon is called diminished awareness and lasts until one is no longer aware of the stimulus (Avijit Chaudhuri, 2011). Afferent fibers could subsequently be divided into two categories: those that are slowly adapting and rapidly adapting (Johansson & Vallbo, 1983).

There are four different types of afferent fibers that are classified as cutaneous mechanoreceptors. The slow adapting afferents only respond to sustained deformation or motion detected on skin. They are also more sensitive to skin movement than to static deformation. These afferent fibers include slowly adapting type I (SA1) and slowly adapting type II (SA2). The other types of rapidly adapting afferents only respond to stimulus that would cause sudden, steady indentation. These afferent fibers include rapidly adapting (RA) and Pacinian afferent (PC) fibers.

Neurophysiological studies aim to reveal the underlying mechanisms of how different afferent fibers would act when receiving different stimuli. Investigations in the neural coding field focus on the characterizing of the relationship between the stimulus and response of afferent fibers, see (E. N. Brown, Kass, & Mitra, 2004). The initial idea of finding a consistent relation between the physical stimulus and human response actually began as early as the Psychophysical Laws, which is covered in detail in Section 2.6. Modern experiments usually directly record the responses of neural afferent fibers from monkeys and even humans, as in (K. O. Johnson, Hsiao, & Yoshioka, 2002). The objectives of such experiments are to develop statistical estimates of neural responses based on the feature (or intensity) of the stimulus.

Several different putative neural codes have been previously mentioned. Researchers recorded the firing rates of a given population of mechanoreceptor afferent fibers and calculated their average value. It was anticipated that there would be differences in the firing rate between afferents; those that are under stimulation and those that are not. Variances found in these two groups can be differentiated as temporal and spatial. Temporal variability means the mean firing rates change over time while spatial variability refers to the differences across location.

2.4.1 Neurophysiological Coding of Thermal Stimulus

Thermal sensations are usually classified as innocuous cold/hot or painful cold/hot (sometimes called a burning feeling). With regard to cold sensations, a general conclusion is that when the temperature is lower than 20 degrees Celsius, a painful feeling would be perceived (Hatem, Attal, Willer, & Bouhassira, 2006; Namer, Seifert, Handwerker, & Maihofner, 2005). In terms of the identification of the responsible afferent fibers of innocuous cold, a series of human studies have concluded that cooling sensations are transmitted by cold-sensitive A-fibers (or myelinated A delta fibers, Aδ) (Fruhstorfer, 1984; Mackenzie, Burke, Skuse, & Lethlean, 1975; Yarnitsky & Ochoa, 1990). Nevertheless, current research on the sub-classes of C fibers has proposed that afferent C fibers could also be responsible for innocuous cold perception (Campero & Bostock, 2010; Campero, Serra, Bostock, & Ochoa, 2001).

The general responses of thermoreceptors have been investigated in previous studies, such as (Hensel, 1981). Such thermoreceptors were first identified as those responsible for only non-pain causing temperatures. It was hypothesized that thermoreceptors would demonstrate static impulse rates when the temperature is constant. The dynamic changes of temperature would transiently influence the responses of thermoreceptors. Meanwhile, thermoreceptors would not be stimulated by mechanical stimuli. On the basis of these assumptions, a mathematical model was proposed by (Ring & de Dear, 1991) to calculate thermoreceptor responses to a stimulus. The equation contained both impacts from static temperature and kinetic temperature change rates.

On the other hand, the transduction mechanism of innocuous cold is now widely accepted. Transient receptor potential melastatin 8 (TRPM8) is a nonselective Ca^{2+}-permeable cation channel that is considered to be the nuclear responsible organic for cold perception (Latorre, Brauchi, Madrid, & Orio, 2011; McKemy, Neuhausser, &

Julius, 2002; Peier et al., 2002). In a series of studies with TRPM-deficient mice, the role of the channel in innocuous cold perception has been generally ascertained, see (Bautista et al., 2007; Colburn et al., 2007; Dhaka et al., 2007).

There are several hypotheses on how TRPM8 channels would respond to thermal stimuli. Unlike other somatosensory receptors, cold receptors would fire at a "baseline" speed with normal skin temperature. Upon a temperature decrease, the firing rate would be increased upon receiving temperature decrease. In addition, adaptation of temperature changes could be as short as one minute (Braun, Bade, & Hensel, 1980). For the purpose of investigating this TRPM8 protein, scientists have cloned the protein and recorded their responses under various stimuli. Original hypotheses included that temperature shifting could stimulate the production and binding of channel-activating ligands; the channel opening structure could be temperature-dependent; or the temperature could affect the lipid bilayer rearrangement and then causes the membrane tension changes as sensed by the TRPM8 (Clapham, 2003). While there are no experiments reported to prove these hypotheses, a study by (Voets et al., 2004) showed that TRPM8 is activated by depolarization.

A number of studies have been conducted on steady-state whole-cell currents for TRPM8 channels under different voltages and temperature conditions (Brauchi, Orio, & Latorre, 2004; Mahieu et al., 2010; Matta & Ahern, 2007; McKemy et al., 2002; Peier et al., 2002; Voets et al., 2004; Voets, Owsianik, Janssens, Talavera, & Nilius, 2007). They revealed that the temperature sensitivity of TRPM8 channels should not be presented by cellular signaling pathways, but the intrinsic property of the channel. The experimental results showed that variance in temperature could shift the voltage-current relations of TRPM8 channels (Voets, 2012). Therefore, the voltage-current relations of TRPM8 channels, which would stand for their intrinsic properties under different temperatures, could be considered as the neural responses to thermal stimuli.

2.4.2 Neurophysiological Coding of Force Stimulus

Reaction force has been concluded as another primary type of information received when humans explore objects. There are two types of hand tasks which are concluded as manipulation and tactile exploration. Tactile exploration is a simpler task (Goodwin & Wheat, 2004). A number of experiments have proved that cutaneous mechanoreceptors are important for tactile exploration tasks, see (Klatzky & Lederman, 2003). The resistance of an object to deformation is one aspect of tactile exploration. The reaction force received would cause the skin to stretch and indent, which would subsequently simulate the receptors (Friedman et al., 2008). This type of physical stimulation is usually referred to as the psychological perception of "softness".

Examination on softness perception began with the compliance of objects, which was usually defined as the ratio of the amount of deformation to an applied force. Humans could discriminate between the compliance of objects through basically two kinds of received information. One is cutaneous information (or tactile cues) from skin and the other one is the kinesthetic cues from the muscles and joints. Objects are classified as deformable or rigid. For rigid objects, e.g. a piano key, it was found in (Condon et al.,

2014) that both tactile and kinesthetic inputs are needed, whilst for deformable objects, which include fabrics, neuroscientists concluded that the absence of either one would not significantly reduce the capacity of compliance discrimination, see (LaMotte, 2000).

There are a series of research conducted to address the cues in coding softness. It has been concluded that the perception of softness would require information on the deformation of objects and associated contact force (Friedman et al., 2008). Experiments by (Srinivasan & Lamotte, 1995) found that compliance discrimination can be conducted even when the peak force and velocity are randomly varied. A likely cue of this perception is the change in the pressure distribution or finger displacement over time. In an earlier report by (Peine & Howe, 1998), it was stated that finger displacement rather than object displacement might be the cue for hardness sensation. It was also observed that the perception of softness is independent of the rate of skin indentation (Pare, Carnahan, & Smith, 2002). Meanwhile, the maximum normal pressure as well as the rate of change of normal pressure show no relation to softness perception (Friedman et al., 2008). Different modes of touch, which include active or passive touch, with or without tools, are considered to impact the judgment of softness as well (Lederman & Klatzky, 2004).

SAI fibers were first revealed as the receptor of this type of physical stimulation by (Srinivasan & Lamotte, 1995). A more recent research investigated the possibility of other receptors, including RA and SAII. The results showed that SAI strongly and consistently alters in relation to the compliance of the object. The firing of RA was observed to alter as a result of changing compliance only during the loading phase while SAII demonstrated significant compliance only at the largest load (Condon et al., 2014).

2.4.3 Neurophysiological Coding of Texture Stimulus

Work carried out in both psychophysical and neurophysiological studies have tested many putative neural codes on how texture stimulus is transduced. They use the same textured surfaces in their experiments and hypotheses were rejected only when no consistent relationship with human subjective judgment was found. In the following reviewed studies, gratings that usually contain a set of dot patterns were used. These elements were placed with a certain amount of space and also designed with a specific shape; that was, a constant height and radius. As a result, the subjects repeatedly received stimuli during the experiments. A summary of the findings from these studies is provided in Table 2-3.

Connor et al. (Connor, Hsiao, Phillips, & Johnson, 1990) began a series of experiments in 1990. The conclusion of their study was that the underlying coding mechanism of texture stimulus might be spatial or temporal variations of SA1 or RA fibers. Subsequently, a study in 1992 by (Connor & Johnson, 1992) further evaluated the coding mechanism of spatial and temporal variation separately. From the results, the researchers of the two studies agree on spatial coding. In 1997, Blake et al. investigated whether SA1 or RA afferent fibers were responsible for texture stimulus and concluded on the SA1 fibers (D. T. Blake, Hsiao, & Johnson, 1997). Another study by (David T Blake, Johnson, & Hsiao, 1997) further showed that SA1 fibers are sensitive to height and radius while RA fibers are only sensitive to the center-to-center spacing. In a later publication, Yoshioka et al. (Yoshioka, Gibb, Dorsch, Hsiao, & Johnson, 2001) agreed that spatial variation in the firing rates of SA1 fibers is preferable for the coding of texture stimulus.

The transmission process of these neural signals was examined in another set of neurophysiological experiments in (DiCarlo & Johnson, 1999, 2000; DiCarlo, Johnson, & Hsiao, 1998). They found that texture stimuli from gratings could be recorded in SI neurons; to be more specific, functional area 3b. Aside from this area, it was also discovered that area 1 is also responsive to texture stimulus (Randolph & Semmes, 1974). Similar findings were also reached in area 5 (Roland, O'Sullivan, & Kawashima, 1998) and the SII (Pruett, Sinclair, & Burton, 2001). There has yet to be common agreement on the coding mechanism inside the cortical areas.

Since the coding mechanism for spatial variation has only been recognized for texture stimulus with interelement spacing larger than 2 mm, hypotheses have been put forth on the coding mechanisms of fine texture. In the research work by (S. Bensmaia & Hollins, 2005; Mackevicius, Best, Saal, & Bensmaia, 2012), it was considered that spatial coding is used for the perception of coarse textures while vibrotactile coding for the perception of fine textures.

Table 2-3 Summary of Psychophysical Studies on Texture Stimulus Coding Mechanisms

Nature of Coding	Afferent Fibers	Conclusion	Remarks
Mean Firing Rate	SA1, SA2, RA, PC	Rejected (Connor et al., 1990)	
Temporal or Spatial Variability	SA1, RA	Agreed (Connor et al., 1990)	
Spatial Variability	SA1, RA	Agreed (Connor & Johnson, 1992)	
Spatial Variability	RA	Rejected (D. T. Blake et al., 1997)	Only sensitive to center-to-center distance (David T Blake et al., 1997)
Spatial Variability	SA1	Agreed (D. T. Blake et al., 1997; David T Blake et al., 1997; Connor et al., 1990; Connor & Johnson, 1992; Yoshioka et al., 2001)	Sensitive to element height and radius (David T Blake et al., 1997) For distance of elements larger than 2mm (Yoshioka et al., 2001)

Vibrotactile coding method describes another perception process. Tiny geometric variations of fine textures are sensed through eliciting skin vibrations. These vibrations are received and transduced as neural signals, see (S. J. Bensmaia & Hollins, 2003; Hollins, Bensmaia, & Roy, 2002). The conclusion in the work by (Mackevicius et al., 2012) further pointed out that vibrations could significantly influence discrimination performance with fine texture.

Similarly, a set of psychophysical experiments was conducted by Hollins et al. (Hollins et al., 2001) to reveal the underlying coding method of temporal coding. Hollins et al. (Hollins et al., 2001) investigated responses from RA and PC fibers and concluded a preference for PC fibers. Early research by (Barlow, 1987; Hollins, Delemos, & Goble, 1991; Verrillo & Ecker, 1977) concluded that PC fibers cannot be found in the lower skin level. Therefore, Hollins and Bensmaia (Hollins & Bensmaia, 2007) examined whether the absence of PC fibers would lead to disadvantages in the discrimination of fine texture. Based on the study results, they agreed with the expectation that PC fibers seem to be critical for the discrimination of fine.

Bensmaia and Hollins (S. J. Bensmaia & Hollins, 2003) studied the potential codes for PC fibers. Between temporal vibrations (their peak frequency) and intensive vibrations (power of the vibrations-weighted), they proposed that the perceived roughness for fine texture is a function of latter codes. An index of PC vibration weighted power, provided by Makous et al. (Makous, Friedman, & Vierck, 1995), was adopted in a separate study (S. Bensmaia & Hollins, 2005). It was found that perceived roughness is a logarithmic function of this index

A previous conclusion made by (Hollins, Fox, et al., 2000) on the neurophysiological coding mechanism of texture stimulus is that either spatial or temporal coding would be effective for texture within a certain range. Two different types of mechanoreceptors (SA1 and PC) enable texture discrimination by using these two codes. Scientists then hypothesized whether these two types of afferent fibers could be combined together to perceive texture stimuli. This assumption was then proven under strict controlled conditions (perception of texture with a spatial period of 298 μm) (Hollins, Fox, et al., 2000). A more recent research work by (Weber et al., 2013) used stimuli with coarse to fine textures with the intent to test the precision of the two codes. It revealed that the correlation between afferent fibers and perceived roughness showed that RA fibers demonstrate even stronger results than PC fibers for coarse textures.

Most previous studies on the neurophysiological coding of texture stimulus used pre-designed gratings as stimuli. Only a handful of researchers have examined the texture perception of the surfaces of different objects while research on fabrics is scarce. Fabrics, however, differ much in terms of surface texture and people can perceive even minimal differences. The findings from neuroscience should be applied towards fabric smoothness perception.

2.4.4 Summary of Neural Coding Mechanisms

It is found in the literature review of recent research on studies of the underlying neurophysiological mechanisms of somatosensory stimuli, including those that involve heat, force, and texture, that there is a focus on revealing the fundamental electrophysiological patterns of signal transduction and transmission.

Derived Research Gap

Still, there are few studies on the application of the related hypotheses to the discrimination of touch sensation in practice. In addition, fabric is considered as a heterogeneous material with unique features. There is the need to encourage investigation on fabric touch sensation on the exploring of neurophysiological coding of fabric touch sensation.

2.5 Psychological Discrimination of Fabric Touch Sensations

The brain is where sensations are generated and neurophysiological signals are received. Psychological processing is the final stage of sensation perception. The outcome of this process is that humans can discriminate between different types of fabrics from touch sensations. Investigations on the psychological perception of fabric touch sensations usually involve direct measurements from subject response, including those of mammals, primates, and humans. Besides discussions on psychological results, psychophysiological studies that have revealed the physiological bases of psychological processing have also been carried out in previous publications.

2.5.1 Psychological Measurement Methods

Fabric touch sensations cannot be studied in a purely objective manner (i.e. the subject's response cannot be considered as right or wrong). The literature shows that most researchers conducted subjective measurements to determine the sensory response from fabrics. Subjective sensory measurement as a method was first published by Binns in 1926 (Binns, 1926). This method has been recently coined "behavioral measures of touch" by (C. Brown, Filion, & Weiss, 2011). These behavioral measurements usually require subjects to examine fabrics by following certain procedures. Questionnaires would be used and then responses recorded, in which the respondents are to express their subjective feelings about the fabrics evaluated. In the following paragraphs, a review on the variations in different behavioral measures is presented in terms of judge/subject type, rating scale, and semantics.

It is obviously important for researchers to determine their subjects before measurement since behavioral measurements are based on their evaluation. In 1972, Matsuo chose trained judges for a study (Matsuo, 1972). Kawabata selected expert panel members as part of a committee to evaluate fabric hand (Kawabata, 1980). Winakor et al. recruited both ordinary and expert judges in their evaluation. (Winakor, Kim, & Wolins, 1980). There were also studies that collected subjective assessments from unskilled users (reviewed in (Ciesielska-Wrobel & Van Langenhove, 2012). University students have also been commonly recruited as unskilled subjects (S.-W. Park, Y.-G. Hwang, B.-C. Kang, & S.-W. Yeo, 2000). There are no findings on preference for subject type but comparisons between these unskilled and skilled judges came to the conclusion that they tend to use different descriptors (Hallos, Burnip, & Weir, 1990). The same terminology could mean different things to the respective party. As a result, in order to ascertain the uniformity of subjective assessments, descriptors used in evaluations should be precisely defined and explained to the subjects.

The second difference among behavioral measurements is the use of rating scales. Two types of rating scales have been previously used in research work, including direct measurements and paired comparisons, see (M. S. Byrne, Gardner, & Fritz, 1993; P. L. Chen, Barker, Smith, & Scruggs, 1992; Fritz, 1992; Osgood, Suci, & Tannenbaum, 1957; Winakor et al., 1980). In studies that used direct measurements, the subjects were asked to evaluate samples and directly give feedback on the fabric touch. In studies that used paired comparisons, the subjects were introduced to a reference fabric and then requested to make a comparison with other samples based on the reference. It is evident that direct measurements could be largely affected by the experience of the subjects.

The last common variance is the semantics. There are basically two kinds of semantics: the single and bipolar approaches. The former will use a single descriptor term and a scale where the subjects would rate how well the terms describe a fabric, such as in a study carried out by Kawabata (Kawabata, 1980). The latter will use two descriptor terms that are antonyms, and the subjects will rate between these two terms based on a semantic differential scale (Winakor et al., 1980).

Table 2-4 is a summary on the variations among behavioral measurement methods as discussed. The AATCC published a standard for the subjective evaluation of fabric in 2011 (AATCC, 2011), the AATCC Evaluation Procedure 5 (EP5), and proposed recommendations for future studies. No preference was stated on the type of subject, but the paired comparison approach was suggested as the rating scale. In addition, this standard also suggested that hand evaluation methods and descriptors to be used for the evaluation of fabric touch sensation. Therefore, by following the standard, the subjective results would be more appropriate for cross-comparisons and future follow-up studies.

Table 2-4 Variance of Behavioral Measurement Methods

Judge/Subject Type	Rating Scales	Semantics
Trained Judges/ Experts (Matsuo, 1972) (Kawabata, 1980)	Unforced Scales (Winakor et al., 1980)	Single Method (Kawabata, 1980)
Unskilled Subjects (Ciesielska-Wrobel & Van Langenhove, 2012; S.-W. Park et al., 2000)	Paired Comparison (M. S. Byrne et al., 1993; P. L. Chen et al., 1992; Fritz, 1992)	Bipolar Method (Winakor et al., 1980)

2.5.2 Dimensions of Psychological Sensations

In order to better understand fabric touch sensations, researchers have conducted many studies with different descriptors and tried to identify the different dimensions of psychological touch sensations.

Howorth and Oliver (Howorth, 1964; Howorth & Oliver, 1958) used nine descriptors in their research from 1958 to 1964, which included smoothness, softness, firmness, coarseness, thickness, weight, warmth, harshness and stiffness. Hollies, Hollies et al., and Hollies and Goldman (Hollies, 1965, 1975; Hollies, Custer, Morin, & Howard, 1979; Hollies & Goldman, 1977) further enriched the sensory descriptor list with: snug, loose, heavy, lightweight, stiff, sticky, non-absorbent, cold, clammy, damp, clingy, picky, rough and scratchy in their research between 1965 and 1979. Owen (Owen, 1971) suggested eight important factors: stiffness, smoothness, weight, thickness, compressibility, liveliness, ease of skewing or shearing, and cold feeling. Mahar et al. (T. J. Mahar, Wheelwright, Dhingra, & Postle, 1990) proposed that the attributes of fabric touch sensation should include stiffness, softness, smoothness, warmth, coolness, crispness, and smooth drape. The number of descriptors in this list continued to increase and in 1998, Li summarized 26 sensory descriptors (Li, 1998b).

It is evident that these descriptors are all correlated to each other to some extent. Their similarities and differences, meanwhile, should also be clarified. The principal component analysis (PCA) is the most widely used method to group these descriptors (Okamoto, Nagano, & Yamada, 2013). Howorth, and Howorth and Oliver (Howorth, 1964; Howorth & Oliver, 1958) used four factors as descriptors: smoothness, stiffness, bulk, and thermal character. Li (Li, 1988, 1998c) summed up his descriptors and condensed them as three factors : thermal-wet, pressure and tactile comfort. In a recent study, four textures were categorized by (Ju & Ryu, 2006), which are roughness, softness, bulkiness, and stretch-ability. The aforementioned AATCC EP5 suggested four categories for evaluation, which are compression, bending, shearing, and surface (AATCC, 2011).

In Table 2-5, a summary is provided on the previous conclusions on the dimensions of touch discrimination. In spite of the variances on the number of dimensions and slight differences of terminologies, most studies concluded that the two most important dimensions are smooth/rough and soft/hard. All of the studies that involved thermal perception defined cold/warm as the third factor. The last study by Asaga et al. (Asaga, Takemura, Maeno, Ban, & Toriumi, 2013) provided the factors in relation to neurophysiological mechanisms and divided tactile touch perception into two properties:

roughness and softness. Therefore, it is reasonable to expect that fabric touch sensation would constitute the following factors: coolness, roughness, and softness.

Table 2-5 Summary of Concluded Discrimination Dimensions

Study	Dimension 1	Dimension 2	Dimension 3	Dimension 4
Howorth, 1964 (Howorth, 1964)	Smoothness	Stiffness	Thermal	Bulkiness
Hollins, 1993 (Hollins, Faldowski, Rao, & Young, 1993)	Rough/Smooth	Hard/Soft		
Li, 1998 (Li, 1998b)		Tactile	Thermal-Wet	Pressure
Hollins, 2000 (Hollins, Bensmaia, Karlof, & Young, 2000)*	Rough/Smooth	Hard/Soft		Sticky
Picard, 2003 (Picard, Dacremont, Valentin, & Giboreau, 2003)	Rough	Hard/Soft		Relief
Ballesteros, 2005 (Ballesteros, Reales, de Leon, & Garcia, 2005)	Rough/Smooth	Hard/Soft		Sticky
Shirado, 2005 (Shirado & Maeno, 2005)	Rough/Smooth	Hard/Soft	Cold/Warm	Moist/Dry
Tiest, 2006 (Tiest & Kappers, 2006)	Smooth/Rough	Hard/Soft	Not Named	Not Named
Ju, 2006 (Ju & Ryu, 2006)*	Roughness	Softness		Bulkiness
Tanaka, 2006 (Tanaka, Tanaka, & Chonan, 2006)	Rough/Smooth	Hard/Soft	Cold/Warm	Moist/Dry
Yoshioka, 2007 (Yoshioka, Bensmaia, Craig, & Hsiao, 2007)	Rough/Smooth	Hard/Soft		Sticky
Guest, 2012 (Guest et al., 2012)	Rough/Smooth	Hard/Soft		Moist/Dry
Asaga, 2013 (Asaga et al., 2013)	Roughness	Softness		

* There are more dimensions that are not shown in the table

2.5.3 Environmental Factors of Psychological Discriminations

Meanwhile, there are other environmental factors that are taken into consideration for psychological discrimination tasks. Contact method is an element that should be prioritized, but usually omitted. Four means of hand evaluation are defined in the AATCC EP5 (AATCC, 2011). The assessment of fabrics should follow this sequence:

the finger tips should have the first contact with the fabric; the fabric should be stroked or touched by the hands; the fabric is lightly grabbed by the fingers and palm; the fabric is picked up and rubbed with the fingers; and finally, the fabric is pinched. These steps are considered to comprise the "active touching of stimuli" in neuroscience studies.

"Active touch" is defined as an evaluation method where subjects actively manipulate samples, whilst "passive touch" is described as an evaluation method where samples are placed onto the skin of the subjects (they are touched with the samples) (Fernandes & Albuquerque, 2012). Research work on active and passive touch was reviewed in detail by Symmons et al. (Symmons, Richardson, & Wuillemin, 2004). They summarized the conclusions of previous studies. A comparison study of these two categories of touch, however, showed different preferences. Although 30 out of the 76 studies concluded that active touch is preferable, 15 suggested that passive touch is better for discrimination and 19 claimed that there is no difference between the two methods. On the other hand, in an fMRI study, the authors of (Ackerley et al., 2012; Simoes-Franklin, Whitaker, & Newell, 2011) pointed that active touch significantly produces more signals than passive touch. Stimulations on neural receptors implied that active touch involves information from proprioception, kinesthesia, and cutaneous receptors, while passive touch only involves information from the cutaneous receptors (Fernandes & Albuquerque, 2012). As regards fabric touch, wearing the fabric on the body is to some extent considered passive touch while evaluation by hand is obviously active touch. Nevertheless, relevant research on investigating the variances on the effect of these two methods on fabric touch sensation is limited.

Furthermore, local climatic conditions could also affect fabric touch sensation. It is commonly agreed that there are significant variances in fabric touch sensation depending on the region. Researchers have conducted experiments in different countries to evaluate the underlying correlations. A series of studies on fabric touch perception was conducted worldwide in the 1980s by (T.J. Mahar, Dhingra, & Postle, 1982; T.J. Mahar & Postle, 1989). Kim and Winakor (H. Kim & G., 1996) later conducted comparison research and concluded that cultural differences exist for fabric hand among the Koreans and Americans. These experiments suggest that fashion preference and cultural differences could affect the perceived feeling in fabric touch.

In another point of view based on psychophysiological studies, climatic conditions are also a factor that may affect the functions of the human body. The human body has the capacity to acclimatize to new environments. Acclimation is a terminology that describes the process of human self-adaption to new climatic conditions. A new climatic condition usually includes changes in temperature, humidity, photoperiod, and/or pH value. Researchers have concluded that human organics might change their physiological characteristics in response to acclimation. For instance, finger cold-induced vasodilation (CIVD) is considered as a self-protection response of human beings to reduce the risk of injury when exposed to extreme cold environments (Daanen, 2003). Mathew et al. (Mathew, Purkayastha, Jayashankar, & Nayar, 1981) repeatedly exposed subjects to a cold environment and recorded improvement in the CIVD among them due to acclimation. A study by Makinen et al. (Mäkinen et al., 2004) confirmed that acclimation due to climate changes would lead to a reduction of cold detection threshold in the hand.

The results from other subsequent acclimation studies also showed effects on other tactile sensations. Many recent research work, for instance, (Ho et al., 2011; Li & Wong, 2006; Smit et al., 2009; Yang & Kwon, 2008), concluded that temperature has effects on the neural response to tactile stimuli. In other words, thermal sensation could affect the sensitivity of other aspects of touch sensation. Moreover, it was also proven by (Hyvarinen & Poranen, 1978; Iwamura & Tanaka, 1978) that in the hierarchical organization of the functional areas of the human cerebrum, information interaction also takes place between the cortex levels, as indicated above.

2.5.4 Summary of Psychological Discrimination

In this section, the most recent studies on the psychological discrimination of touch sensations have been reviewed. Behavioral measurement is the most commonly used method for the psychological measurement of touch sensation. Although previous researchers have used methods that varied in subject, rating scale, and semantics, the AATCC EP5 has provided a standard guideline for future psychological studies. The literature has also pointed out that interpretations of descriptors should be expressed in detail to subjects prior to assessments. With regard to the factors of fabric touch sensation, researchers generally agree that there should be at least the following: smoothness, softness (and/or fullness) and thermal characteristics.

Derived Research Gap

In terms of environmental factors, one important issue would be the variances between the evaluation methods of passive and active touch. There is evidence that suggest differences exist in touch sensation between evaluations that involve wear and those of hand. Previous research has also reached the conclusion that individuals in different regions demonstrate different reactions to touch preference of fabrics, whilst physiological mechanisms imply that climatic conditions could also be a factor. Acclimation affects the perception of thermal feel, which is highly likely to subsequently affect other tactile perceptions.

In summary, the psychological measurement methods that will be used in this Ph.D. study have been illuminated in this section. Two limitations in previous psychological studies have also been identified: the effects of touch and climatic conditions on fabric touch sensation.

2.6 Predictions of Fabric Touch Sensations

After obtaining physical stimuli properties and psychological sensory responses, researchers usually explore the establishment of prediction models that link these two items. A number of methods have been developed to simulate the perception process of fabric touch sensation. In the following reviewed literature, a wide range of prediction methods is discussed that are derived from previous studies.

2.6.1 Regression Relations

Statistical regression prediction methods of fabric touch sensation are the most commonly used, and linear regression analysis is one such method which includes a group of modeling and prediction techniques that are useful for establishing a relationship between a dependent variable and many independent variables. This method has been widely used for forecasting. The anticipated value of the dependent variable would be estimated through a built model equation, after the independent variables are inputted.

Kawabata (Kawabata, 1982) used a stepwise-linear-regression in his KES-F system. Stepwise regression is an option in statistical software (e.g. SPSS) in which significantly affected predictors will be automatically selected (Harrell, 2001). Multiple regression analyses would be conducted afterwards, as in the case of many studies, see (Cardello, Winterhalter, & Schutz, 2003; P. L. Chen et al., 1992; Morino, Matsudaira, & Furutani, 2005).

However, there are limitations in using linear regression. An important limitation is in generalization. Regression analysis methods build prediction equations on the basis of the samples tested. Generalization means the possibility of extending the prediction model to all populations. The population in studying fabric hand sensation should theoretically be as large as possible to include all kinds of fabrics and all human beings. Some researchers have managed to conduct experiments in more than one country to increase the reliability of the prediction model. Nevertheless, the selecting of samples that can represent large populations has been a significant challenge in the use of regression statistical analysis.

In addition, regression methods disregard the underlying mechanism of these relations. It is common knowledge that there are certain principles that underlie the transfer of information within the human nerve system, but the use of the regression method means that such principles are treated as black box without considering the need for detailed evaluations of the processing mechanisms involved. Consequently, it is highly possible that the resultant models would have misleading implications.

2.6.2 Psychophysical Laws

Psychophysical laws are based on explorations that aimed to find the possible correlations between physical stimuli and perceived sensation. One assumption of psychophysical laws is that such correlations should apply to any type of sensation. Fechner et al. (Fechner, Boring, & Howes, 1966) defined sensation perception as "outer psychophysics" and "inner psychophysics"; the former is the direct relationship between physical stimuli and subjective perception, and the latter introduces the subjective concept of an "inner stimulus" as opposed to physical stimulus. They raised the ultimate question as to whether there are universal laws that could be used to explain how we subjectively sense the world. Although Fechner et al. were aware there would be always limitations on the generality of built linkages between physical stimuli and subjective perceptions, they believed that general laws exist for "inner psychophysics" (K. O. Johnson et al., 2002).

The well-known Weber-Fechner law incorporates two findings from the work of Ernst H. Weber and Gustav T. Fechner respectively. Weber's finding indicated that the minimum difference between stimuli that can be detected, Just-Noticeable Difference (JND), would be proportional to the magnitude of the stimuli. Fechner later stated that there is a relationship between stimulus intensity and sensation perceived by the subject, with JND as the connecting factor. The Weber-Fechner Law, consequently, describes this relationship as a logarithmic function. Nearly a hundred years later, the Stevens' Power Law was introduced (Stevens, 1957). Stevens revised the relationship between JND and subjective perception as a power function (Stevens, 1961).

These psychophysical laws were used afterwards in studies of fabric touch perception. Hu et al. (J. L. Hu, Chen, & Newton, 1993) compared the accuracy of prediction models based on linear functional, mixed linear and log-linear analyses, and the Weber-Fechner law and Stevens' power law. The most optimal result was derived by the Stevens' power law. However, other reports tended to agree with the Weber-Fechner law (Li, 2005; Mazzuchetti, Demichelis, Songia, & Rombaldoni, 2008; Rombaldoni, Demichelis, & Mazzuchetti, 2010).

Based on the psychophysical laws, there have been previous attempts to build solid relations between psychological perception and physical stimuli. Nevertheless, comparison studies could not adequately explain the mechanism of the generation of touch sensation, see (Anttila, 1988; J. Y. Hu, Ding, & Wang, 2006). MacKay published his findings soon after introduction of the Stevens' power law. He suggested that focus should be on revealing the underlying mechanism of sensory perceptions rather than adding to the psychophysical laws (MacKay, 1963). The assumption in the psychological laws that there are equal JNDs of all the senses has also been questioned by recent studies, such as (Heidelberger, 2004; Masin, Zudini, & Antonelli, 2009). Some studies even proved that there is no consistent relationship, see (J. H. Johnson, Turner, Zwislocki, & Margolis, 1993; Schroder, Viemeister, & Nelson, 1994).

The advantage of the use of psychophysical laws in studies that utilize regression methods is that they try to hypothesize about the mechanisms of sensory perception. However, the accuracy of the hypothesized perception principles can be easily questionable. The assumption that all types of sensations should share the same "law" has also been disputed, see (K. O. Johnson et al., 2002).

2.6.3 Machine Learning Prediction Methods

Given the uncertainty of the mechanisms of sensory perception, machine learning prediction methods could provide further means to link physical stimuli and psychological perception. Artificial Neural Network (ANNs) were inspired by the structure of biological neural networks (C. M. Bishop, 1995). Artificial neural networking is usually used to simulate non-linear relationships between inputs and outputs. One major characteristic of artificial neural networking is the ability to self-learn. The entire model could be trained by using real life cases so that prediction would gradually become more accurate. In other words, the ANN technique allows the model to “find out” the perception mechanisms itself through a training process. Such mechanisms concluded would be subsequently inputted for future predictions.

With comparison to the prediction capacity of regression models, Park et al. (S. W. Park, Y. G. Hwang, B. C. Kang, & S. W. Yeo, 2000) concluded on the advantage of ANN over regression predictions. This finding was also supported by a number of other experiments, see (Gao, 2003; Meng, 2010; L. M. Zhang, 1993). Lai et al. (Lai, Shyr, & Lin, 2002) also investigated the prediction capacities of artificial neural networking by using KES measurement data and FAST data, and obtained better results from the former. Meanwhile, the accuracy of ANN prediction models is largely affected by the number of layers and training cases. Wong et al. (Shyr, Lai, & Lin, 2004; Wong, Li, & Yeung, 2004) included four layers in their model while Shyr et al. (Shyr et al., 2004; Wong et al., 2004) investigated up to 114 types of fabrics. It appears that a large database would be needed for a model with high accuracy.

The fuzzy logic analysis is also conducted for the prediction of fabric touch sensation in previous studies. The fuzzy logic analysis transforms the quantitative prediction of perception magnitude to the rank of the touch perception of the fabric. For example, Raheel and Liu (Raheel & Liu, 1991) defined 0 as “very poor” and 1 as “excellent” in terms of the true values of the fuzzy logic variables. Among the studies that use fuzzy logic, variances could be found in terms of membership functions and weighting factors of different physical properties (Y. Chen, Collier, Hu, & Quebedeaux, 2000; Pan et al., 1993).

Machine learning methods for predicting fabric touch perception have the advantage of accuracy. More cases inputted means higher accuracy of the model. Still, the use of machine learning fails to investigate the underlying mechanisms of how we can perceive touch sensation. Researchers have generally concluded on different models for the prediction of fabric touch sensation. This makes cross-comparisons of the models impossible. Consequently, prediction models cannot be examined and revised after they have been reported.

2.6.4 Summary of Prediction Methods

In summary, many approaches have been proposed and used to predict the psychological sensation of fabric touch on the basis of physical properties. These methods have been individually proven to successfully address the psychophysical relations whilst limitations still exist.

Derived Research Gap

One of most important disadvantages as mentioned above is the investigation of the underlying mechanisms of perception. The focus of the reviewed prediction methods is on building solid psychophysical relations and revealing universal relations. Still, with the advancements of current neurophysiological findings, the investigation of fabric touch sensation could be extended to the neural level. The direct implementation of neurophysiological coding mechanisms in prediction model building should also be encouraged.

Another possible reason for limitations of current prediction methods for fabric touch sensation could be due to the lack of attention on the effects of the interaction. Academic work that supports the interaction between different types of physical stimuli has been reviewed in previous sections. When building prediction methods, efforts put forth to investigate the effects of the interaction, however, appear to be weak.

2.7 Summary of Literature Review

In this literature review chapter, different stages of the process of fabric touch sensation perception have been summarized. Despite the individual focuses of different research work, it is generally agreed that there are three levels of sensation perception: physical, neurophysiological, and psychological. Therefore, neuropsychological studies, as the title indicates, should encompass all three levels of sensation perception. In these three levels, much research work and efforts have been made to determine the perception of fabric touch sensation. However, the knowledge gaps that remain are as follows.

1. Overall speaking, there is lack of approaches attempting to comprehensively investigate the neuropsychological perception process of fabric touch sensation.

Within each processing stage, the research gaps are:

2. The physical detection mechanisms of fabric properties have not been completely uncovered and presented in the physical measurement instruments.
3. Neurophysiological studies of different physical stimuli that generate nerve signals have not yet specified the underlying coding mechanisms of fabrics with regard to their thermal, reaction force, and texture information.

4. Psychological discrimination in the touch sensation of fabric has not yet been evaluated considering the effects of passive and active touch, as well as climatic conditions.

With regard to the synthesizing of the three levels of sensation perception, the research gaps are:

5. The effects of the interaction of different types of physical stimuli have not yet been completely investigated in research work on psychophysical relations.
6. The prediction methods of fabric touch sensation have not included the underlying neurophysiological coding mechanisms. Neuropsychological prediction methods should be applied to all three levels of sensation perception.

To fill these knowledge gaps, six objectives are derived and research methodologies are developed, as presented in Chapter 1.

Chapter 3 Theoretical Framework and Methodology

This chapter focuses on the objective 1 to develop a theoretical research framework of neuropsychological study of fabric touch sensations. On the basis of the literature review in Chapter 2, it can be concluded that the perception of fabric touch sensation should involve three levels: physical, neurophysiological and psychological. Research gaps as well as the objectives have been identified from the literature on these three levels of sensation perception. In this chapter, a theoretical framework that addresses the research gaps and attains the objectives is proposed.

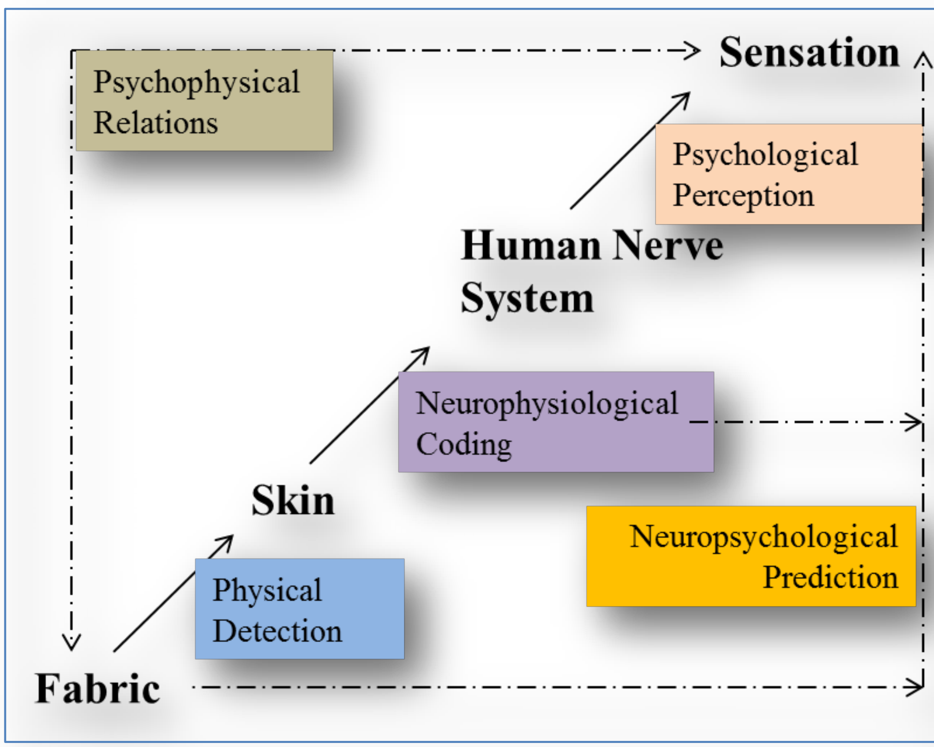

Figure 3-1 Systematic Map of Areas involved for Investigating Fabric Touch Sensations

A detailed study on fabric touch sensation should involve the underlying mechanisms of touch perception. A systematical map of five aspects related to such is shown in Figure 3-1. These five areas, as provided in Chapter 2, should be involved when investigating fabric touch sensation. Therefore, this Ph.D. study covers research in each of these five areas, which are physical detection, neurophysiological coding, psychological perception, psychophysical relations and neuropsychological prediction. The thesis logic basically follows the transmission processing of touch sensation information in the human nerve system.

The left-bottom corner of the figure shows the physical inputting into the human nerve system. External physical stimuli, provided by fabrics in this study, would be detected by the corresponding skin receptors. These receptors characterize certain physical properties of the fabrics and input the information into the human nerve system. Their neurophysiological transduction process subsequently occurs as shown in the middle part of Figure 3-1. Organics in the nerve system respond to the received information by following certain coding mechanisms. The coded electrophysiological information is carried through the human nerve system until it reaches the cerebrum, where they will stimulate different functioning areas and generate psychological touch sensations, as illustrated in the top right corner of Figure 3-1.

Besides direct investigation on these three levels of sensory perception, effort will also be put forth to link them. The conventional process is to link the physical and psychological aspects. Psychophysical relations could then be explored through mathematical models. Neuropsychological prediction methods will also be used in this study, which would involve all three levels of information transfer and address the underlying mechanisms.

3.1 Detection of Physical Stimuli

As previously reviewed in Chapter 2, studies on the physical properties of fabric generally agree that there are three main types of stimuli that could be received by human skin receptors. These include thermal, force, and texture stimuli. It has been found that tactile properties have solely been the main concern of studies on fabric touch sensation previously.

The thermal-tactile method is a new concept based on findings from neurophysiological studies, which reveals the importance of interactions between thermal and tactile sensations (reviewed in detail in Chapter 2). That the measurement of the physical stimuli of touch sensation should include both thermal and tactile aspects is now generally accepted (Kamalha et al., 2013).

Measurement methods have been developed to characterize the physical properties of fabric, although the current instruments were not invented on the basis of neuroscience understandings. The shortages of such instruments have been reviewed. Most of them have a high cost and require a lengthy amount of time for testing. None of reviewed instruments consider thermal properties as part of fabric touch sensation. Meanwhile, it is difficult to investigate the interactions of different stimuli human skin simultaneously that are perceived through current measurement methods on fabric touch.

In order to solve these limitations, the first objective of this Ph.D. study is to reveal the complete physical detection mechanism of stimuli from fabrics. These stimuli could simultaneously stimulate the touch receptors on skin. Therefore, quantitative measurement method should simulate the simultaneous characterization of touch in the hand evaluation process and clearly express the physical meanings of the measured parameters.

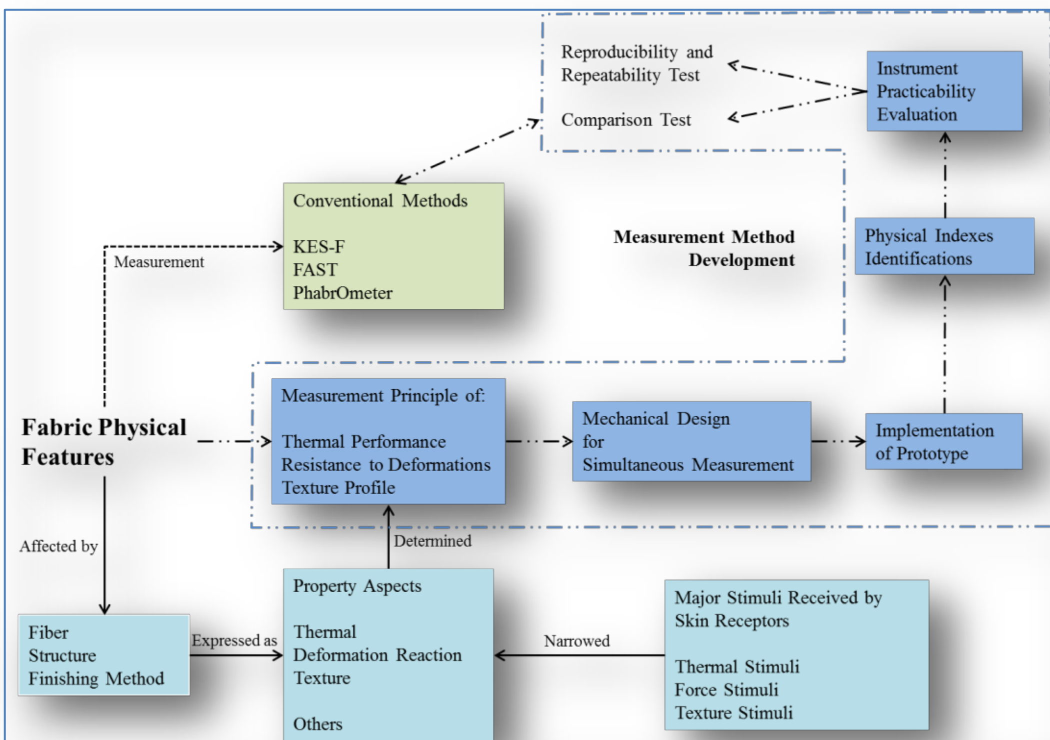

Figure 3-2 Framework of Physical Stage Investigation: Detection of Physical Stimuli

The bottom of Figure 3-2 shows the generally accepted background knowledge with regard to the physical properties of fabric. These could be affected by many factors, including the fiber, structure, and finishing method. Their expression methods also involve many formats. Among these properties, three were concluded as the major stimuli that are received by the skin receptors and generate touch sensations. They are thermal, deformation reaction and texture properties. Tensile property is also an important factor that may affect the fabric touch sensations. Tensile properties of fabrics are generally detected during large movement of human body. The reported PhD study aims to evaluate the fabric touch sensations under a steady circumstance. Therefore, tensile properties are not expected. This part of the figure is mainly a summarization of previous research.

The middle part of Figure 3-2 (circled with a dashed line) shows the development process of the measurement method. Three measurement variables of fabric, which are thermal performance, resistance to deformation, and texture profile, were proposed. A unique mechanical design was subsequently given to enable a measurement protocol that can simultaneously characterize the physical properties of fabric on all aspects. The implementation of the prototype based on the variables was conducted afterwards. On the basis of typical output curves from the prototype, physical indexes were identified to present the physical properties of the tested fabrics.

On the top of Figure 3-2, the practicability of this newly developed instrument was examined. The evaluations mainly consisted of two parts, reproducibility and

repeatability testing, and comparison testing. The former was expected to ascertain relatively low variances in the results due to the operators and repeated testing. The latter was conducted to ensure that similar results of the fabric properties could be obtained from the fabrics, since conventional methods have been well accepted.
The results based on this new instrument were one of the fundamentals in this Ph.D. study. The physical properties, which are attributed to fabric touch sensation, were quantitatively characterized by using this measurement method.

Development and manufacturing of the instrument was complete along with the research project ITP/024/10TP and ITP/005/14TI, which was supported by Hong Kong Research Institutes of Textile and Apparel and Innovation Technology Commission of Hong Kong SAR Government.

3.2 Coding of Neurophysiological Signals

The neurophysiological stage encompasses neurophysiological coding in the human nerve system. After the studies on physical detection, the fabric physical properties of fabrics, which would stimulate neural receptors, would have been obtained. Subsequent discussions can be on how neural receptors would respond to these physical stimuli.

Neurophysiological coding is the underlying mechanism of transmitting external physical stimuli into neural signals. The responsible organics under the human skin are called receptors. They would respond accordingly to the detected physical stimuli and transmit the neural signals into the human nerve system.

The literature review in Chapter 2 provides a summary of the latest findings as regards thermal, force and texture stimuli. Neuroscientists have generally concluded on the responsible receptors for each of the three stimuli while the coding mechanisms have also been proposed and verified through various experiments. These findings, nevertheless, have not yet been applied in the textile research field.

In order to fill the research gap, the objective in neurophysiological study is to specify the neurophysiological coding mechanisms that underlie the transduction process from physical stimuli of fabric into nerve signals. The models should be based on the unique features of fabrics and able to transfer the measured physical property values of the fabric into neurophysiological indexes.

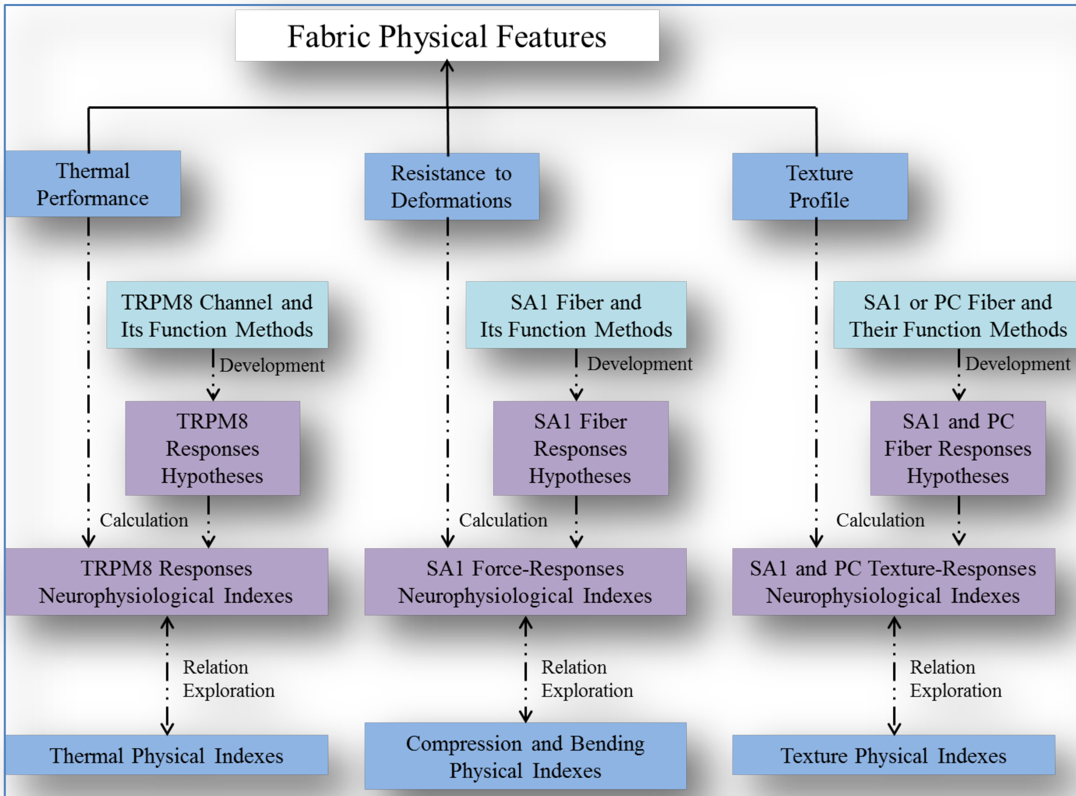

Figure 3-3 Framework of Neurophysiological Stage Investigation: Coding from Physical Stimuli to Neural Signals

Consequently, the research framework of this study is designed as shown in Figure 3-3. The physical properties of the fabrics were inputted into the neurophysiological process. Based on the findings from previous studies, the fabric physical properties were characterized with regard to three aspects. These three aspects are thermal performance, resistance to deformation, and texture profile. They are shown at the top of Figure 3-3.

The literature on the corresponding organics and their function mechanisms were reviewed and summarized in detail. Since research on the neurophysiological mechanisms of various neural receptors in the human nerve system is still forthcoming, common agreement was available. In addition, previous neurophysiological conclusions required modifications before application to the fabrics. Therefore, neural fiber response hypotheses on fabrics were first developed, as illustrated in the middle part of Figure 3-3.

On the basis of the hypotheses on neural fiber response, the physical properties measured on the fabrics were inputted into the models and generated feedback from the neurons when receiving the fabric stimuli. Neurophysiological indexes were subsequently identified to present the responses.

Finally, the relations between the identified neurophysiological indexes and the physical properties of the fabric were explored. It is usually anticipated that the measured physical indexes of fabric would be related to their properties and, most of the time, based on experience. However, there have been limited reported discussions on the relation between fabric properties and the neural responses that they elicit. The bottom part of Figure 3-3 shows this part of the study on exploring such relations.

Statistical analyses comprised the majority of this part of the study. Hypothesis development included physical and electrophysiological model building. However, this Ph.D. study did not directly measure the neurophysiological responses from neurons. One, such measurements usually require relatively high levels of financial support and human resources. Second, this study aims to explore a new approach, the use of neuropsychological methods, to investigate fabric touch sensation. This simpler approach could encourage more future studies in this field.

3.3 Discrimination of Psychological Sensations

The psychological stage directly addresses the final outputs, i.e. touch sensation. As discussed in detail in Chapter 2, when an environmental event is detected, the corresponding organics would transduce the stimulus into neural signals and transmit the signals through pathways in the nerve system until they reach the cerebral cortex. Afterwards, the human brain discriminates touch sensations in different ways while obtaining the overall perception of touch comfort. The dimensions of fabric touch sensation have been discussed although few studies have covered the psychophysiological mechanisms of the achieved groups. There has been a lack of research on the abilities of passive and active touch, and climatic conditions.

Therefore, in response, the objective is to investigate the psychological discrimination ability of fabric touch sensation. The dimensions of psychological discriminations should be clarified based on psychophysiological mechanisms. The effects from touch and acclimation should also be examined.

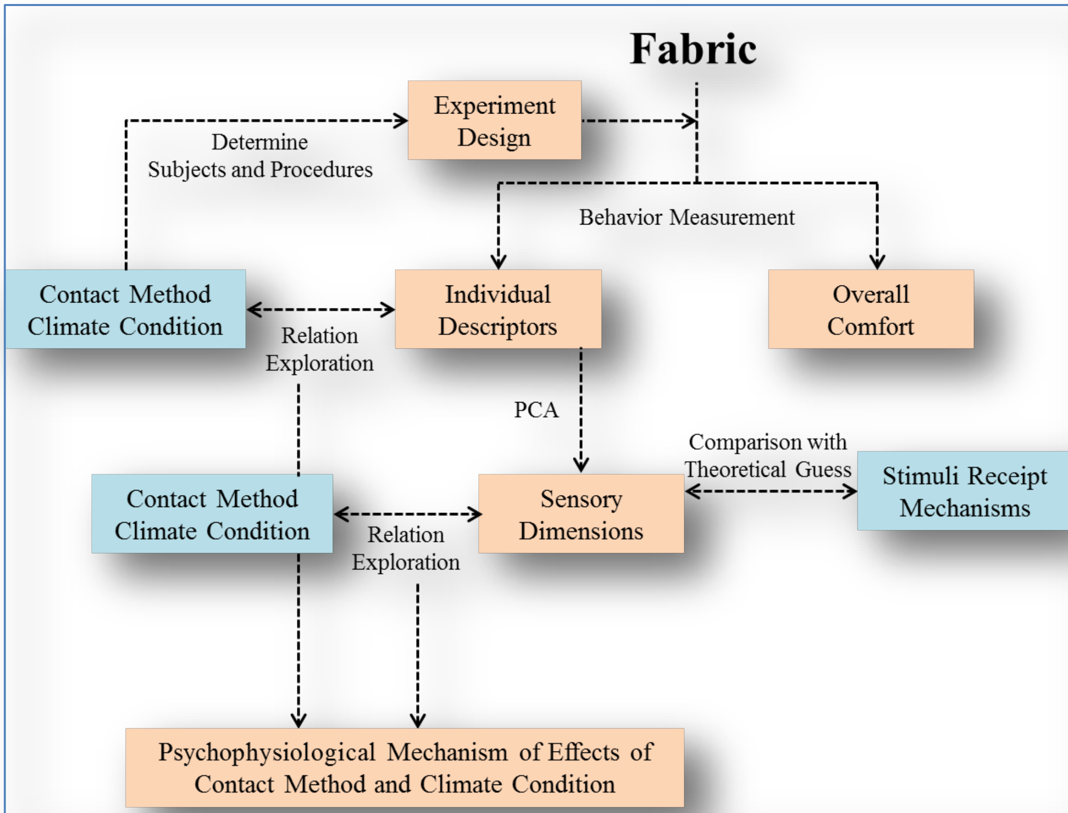

Figure 3-4 Framework of Psychological Stage Investigation: Obtaining Psychological Discrimination Results

In order to attain this objective, the framework as shown in Figure 3-4 was followed. Fabrics were directly measured by using behavior measurement methods. The subjective evaluation on touch sensation constituted of the use of two data sets. The first set of data contained ten individual descriptors, each of which present one aspect of fabric touch sensations. The other set of data included only data based on one type of measurement, i.e. overall comfort rating. They are separated because that the perception of "comfort" maybe more subjective than the specified "feelings". These two set of subjective measurement data were directly obtained from the subjects. They provide the final part of the needed information on the touch sensation of the selected fabrics.

For the purpose of subsequent investigations on the effect of active and passive touch and climatic conditions, the experimental design on subjective measurements included two additional independent variables. The selected subjects were under different climatic conditions. Researchers have concluded that the physiological characteristics of human organics might change in response to acclimation (Daanen, 2003; Mäkinen et al., 2004; Mathew et al., 1981), especially in terms of thermal perception. Acclimation would be observed after half a month exposure in a different climate condition. In the meantime, the temperature environment could affect tactile perception. In view of these two reasons, there are likely potential impacts from climatic conditions. As a result, subjective measurements were performed under different climatic conditions including various temperatures and relative humidity.

In order to explore the effect of active and passive touch, subjective measurements were carried out involving the two types of touch: on the forearm (passive) and the hand (active). There is evidence that indicates somatosensory information received by active and passive touch is different, see (Fernandes & Albuquerque, 2012). The relationship between the distribution of the variance of the receptors and disagreement of the advantages of the two types of touch was examined.

After obtaining the subjective evaluation results from the behavior measurements, the sensory dimensions of fabric touch sensation were extracted. These sensory dimensions are expected to present the different aspects of fabric touch sensations. The literature review has already shown a number of more or less similar conclusions on the specific dimensions. However, none of these studies that identified the dimensions are based on neurophysiological understandings. The relations of the sensory dimensions and stimuli types were not explored. A recent study by (Asaga et al., 2013) investigated the tactile sensory dimensions on the basis of different neural signal types. This technique will be utilized to analyze other sensory responses such as thermal-tactile sensations.

3.4 Exploration of Interactive Psychophysical Relations

Based on full investigations at the physical, neurophysiological, and psychological levels, possible relations between them are discussed. The most common approach is to explore the psychophysical relations, which link physical stimuli and psychological perception. In Chapter 2, previous studies were reviewed which explored the psychophysical relations via different approaches. The effects of the interactions of different types of physical stimuli have not yet been completely investigated.

Therefore, the objective to address this research gap is to explore the relation between psychological sensations and physical stimuli as well as the effects of the interaction of different types of physical stimuli on each sensory dimension.

Figure 3-5 displays the framework of the psychophysical study. On the top-left of this figure, psychophysical studies that directly link fabric and sensations regardless of the neurophysiological stage are shown, as illustrated by the dashed square. The bottom-left of Figure 3-5 represents the investigations in Chapter 4, which includes the detection of physical stimuli. They were be categorized into those on thermal performance, resistance to deformation, and texture profile. The top-right of the figure shows the psychological measurements, which is discussed in Chapter 6. Two types of subjective results were obtained, which are overall comfort and individual descriptors. The sensory dimensions were also defined from individual descriptors in Chapter 6.

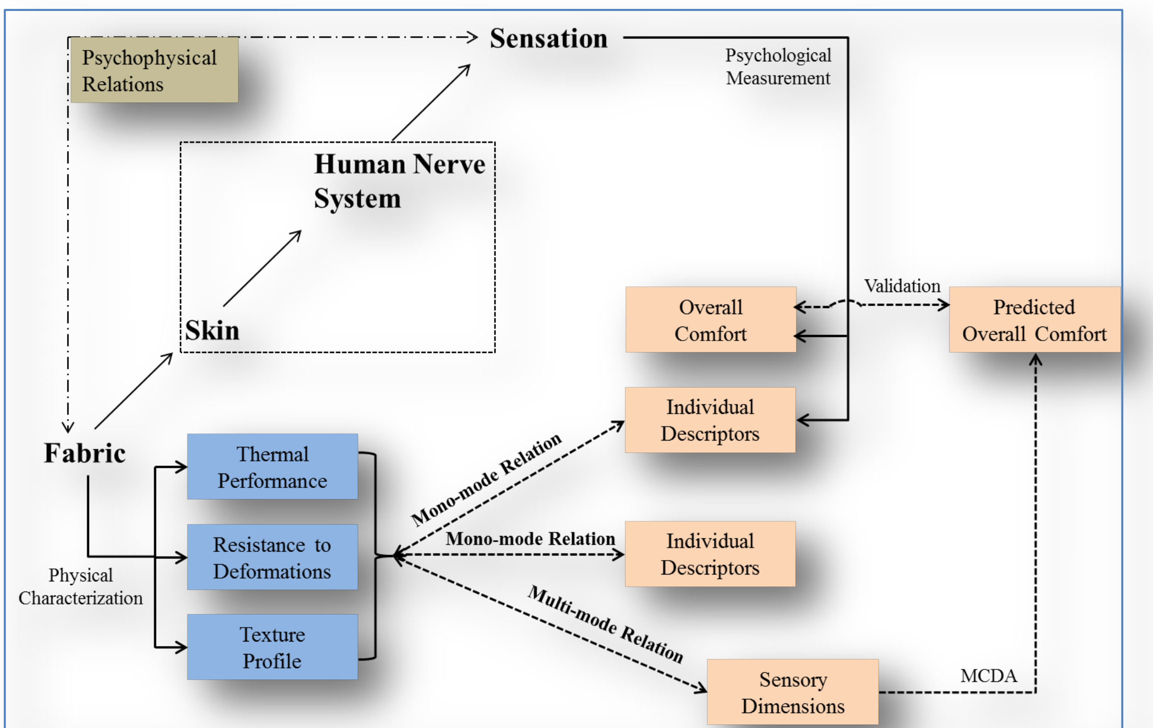

Figure 3-5 Framework of Psychophysical Stage Investigation: Exploration Psychophysical Relations

Studies on the exploration of psychophysical relations began from the building of relations between fabric physical properties and individual psychological descriptors. Among them, the mono-mode relationship hypothesis was tested. The mono-mode relationship stands for the hypothesized linkages between a single physical stimulus and an individual psychological descriptor. An example is the linkage between feelings of cool-warm and thermal properties of a fabric. There are many indexes and methods that concern fabric thermal properties. As a result, either the most relevant of these defined thermal indexes or the integration of all the defined thermal indexes was linked to the cool-warm subjective rating. In Figure 3-5, the latter is called the "mono-mode relation (integrated)".

Next, an investigation was conducted on the psychophysical relations between physical properties and sensory dimensions. Since the sensory dimensions were extracted from individual descriptors through a PCA, it is reasonable to assume the existence of multi-mode relations. The physical properties from the physical, neurophysiological and psychological information could show significant effects on the results of the sensory dimensions. In addition, interactions between different physical properties were included in the exploration of the multi-mode relations.

Finally, the predicted sensory dimension results based on exploration of multi-mode relations were used to calculate the predicted overall comfort via a multiple-criteria decision analysis (MCDA). A check for validity by using the predicted overall comfort values and subjectively obtained values was subsequently conducted.

3.5 Development of Neuropsychological Prediction Methods

The above psychophysical approach evaluates the relationship between psychological perception and physical stimuli. Nevertheless, as pointed out, the neurophysiological stage has been neglected in this approach. In the literature review in Chapter 2, it was mentioned that psychophysical prediction models have limitations in explaining the underlying mechanisms behind mathematical relations.

Therefore, in response, the objective is to formulate prediction models that take into consideration the neuropsychological mechanisms of fabric touch sensation. These models will contain findings from previous objectives to provide a complete explanation for the perception of fabric touch sensation.

The neuropsychological method is proposed to have the ability to predict touch sensations that involve the underlying neurophysiological mechanisms of touch perception. Psychophysical and neurophysiological studies are both referenced for this method. Physical stimuli were first characterized. Neurophysiological coding relations were subsequently investigated, through which statistical functions between the neural population responses and physical stimuli were established. The neuropsychological method consequently linked the coded neural responses with psychological sensations. This method identified the mechanisms between neurons and perception. Such mechanisms were purely based on experimental findings from neurophysiological evaluations in (K. O. Johnson et al., 2002).

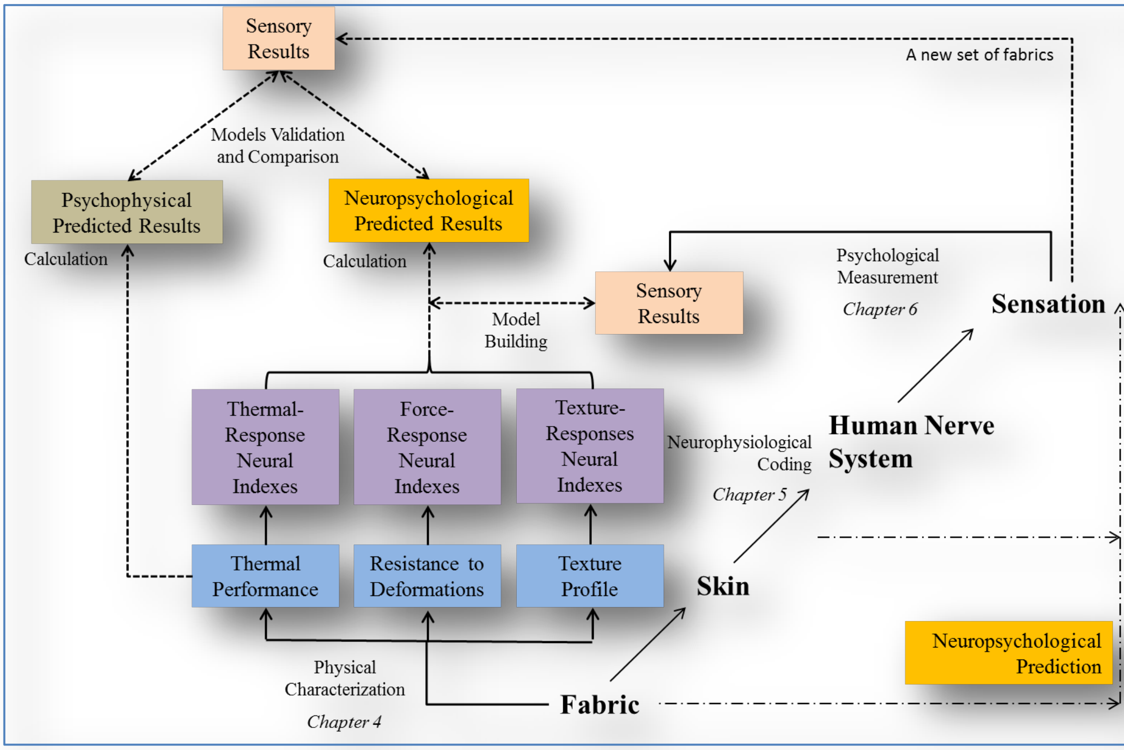

Figure 3-6 Framework of Neuropsychological Stage Investigation: Building Neuropsychological Models

Figure 3-6 illustrates the framework of the neuropsychological component of this study. Similar to Figure 3-5, progress at the physical, neurophysiological, and psychological levels is shown (bottom-right corner). Neurophysiological coding studies are also included as mentioned.

On the left part of Figure 3-6, physical stimuli and neurophysiological indexes accordingly are demonstrated at the bottom since they were obtained in the studies at the physical and neurophysiological levels. The first task at the neuropsychological level was to investigate the relations between neurophysiological indexes and psychological sensory results. Through these explorations of the relations, neuropsychological prediction models were developed. These prediction models were lean towards sensory dimensions rather than individual descriptors.

Another set of fabrics were used to obtain the psychological sensory results afterwards. These fabrics are different from those used in the model development. Their physical properties were characterized by the FTT instrument mentioned in Chapter 4. Subsequently, the anticipated psychological responses were calculated based on the developed neuropsychological prediction models. Model validation was then conducted by comparing the estimated and subjectively obtained responses. The predicted psychological responses were also determined by using the psychophysical methods found in Chapter 7. A comparison between the proposed neuropsychological prediction and conventional models was conducted.

This part of the study is a complete integration of all the other parts of the study. Investigations on physical stimuli detection, neurophysiological signal coding, psychological perception discrimination, and the effects of psychophysical interactions were synthesized to reveal the neuropsychological mechanisms of fabric touch sensation. The final prediction models addressed all of the findings. The neuropsychological approach would provide an alternate research method that could be used to evaluate the underlying reasons for the touch sensations of different fabrics.

3.6 Conclusion

In this chapter, the first objective has been completed by developing a theoretical framework for studying the human tactile sensory perceptions of fabrics from the neuropsychological point of view. The framework links the information from fabric physical stimuli, human neural system to human psychological touch sensations. Therefore, following this framework, a series of systematic investigations and analyses will be carried out and the quantitative models will be developed in the following chapters.

Chapter 4 Fabric Sensory Properties and Physical Stimuli

In this chapter, the objective 2 will be addressed by characterizing the fabric physical properties related to touch sensations with development of a measurement method The literature review in Chapter 2 concluded that current characterization methods of fabric touch sensation have several limitations. The researchers have not implemented work based on neuroscience, which reveals the mechanisms of sensation perception. None have included the measurement of thermal properties. In addition, the evaluation process of touch is normally quick and simultaneous, which would involve the effects of the interactions of different physical stimuli (J. Hu, Ding, Wang, & Cai, 2009). The major concerns about the studies also include that they are relatively high in cost and time consuming, which have reduced their applications in the industry, see (Behery, 1986; El Mogahzy et al., 2005; J. O. Kim & Slater, 1999).

In accordance with the perception mechanisms of fabric touch sensation. This characterization method should be able to simultaneously address different physical factors. Meanwhile, it is expected to clearly express the fabric physical properties.

This chapter is organized as follows. The methodology of the investigation is first introduced. Identification of the physical modeling of stimuli perception is subsequently covered in the sequence as follows: thermal, compression, bending, and surface. The proposed measurement design is also presented. The prototype (FTT) description and index definition are shown afterwards. The results obtained from the FTT prototype are consequently presented. Finally, discussions include repeatability and reproducibility testing on the prototype, as well as a comparison between the FTT prototype and KES instruments.

4.1 Methodology

4.1.1 Identification of Physical Parameters

From the literature review, it can be concluded that the perception of fabric touch sensation could be generally categorized into three indicators: thermal, deformation resistance, and texture (reviewed in detail in Chapter 2). Therefore, the identification of the physical parameters was conducted by following these three indicators. For each indicator, previous agreements were first evaluated, followed by neurophysiological interpretations of how related stimuli would be perceived. Afterwards, the measurement principle of each indicator was proposed. A design to simultaneously measure all of the indicators at the same time was explored.

4.1.2 Prototype Implementation and Indexes Identifications

A prototype, named the FTT, was developed on the basis of the proposed measurement principle that simultaneously characterizes different aspects of the physical properties of fabric. The Hong Kong Innovation and Technology Commission and Hong Kong Research Institute of Textile and Apparel supported the development of the FTT through research project ITP/024/10TP. An external private company, SDL ATLAS, INC, supported the manufacturing of the prototype. The project team members conducted the mechanical and electronic engineering, and software programing of the prototype. The contribution of the thesis author included physical detection mechanism exploration, measurement principle development, and mechanical design of the instrument. The thesis author also conducted the mathematical transformation of the obtained data as well as the identification of the physical indexes and the development of their calculation formulas. The prototype was used to measure several types of fabrics to obtain typical output curves, based on which indexes that present the characteristics of the fabrics were identified.

4.1.3 Sample Selection

For the purpose of testing the capability of the FTT, 54 types of fabrics were tested. In the fabric selection, the aim was to have a wide variation of commonly used textiles. These included woven, knitted, and non-woven fabrics with different fiber contents and structures. There were in total 54 types of fabrics as shown in Table 4-1 to Table 4-3. The weight and thickness of the selected fabrics were tested by following ASTM standards D3776 (ASTM, 2009) and D1777 (ASTM, 1996) respectively. In order to verify the practicability and sensitivity of the design of this new instrument, these fabrics constituted those with relatively larger differences and those with very similar physical properties. The fabric samples could be generally divided into three groups. Group 1 (Fabrics 1-11) consisted of fabrics bought on the market. They comprised most of the daily used fabric types. A private company, ACE Style Intimate Apparel Ltd, provided the fabrics in Group 2 (Fabrics 12-35). The company indicated that all of the samples in this group are used in intimate clothing. Another private company, Babei Group Co. Ltd, sponsored the fabrics in Group 3 (Fabrics 36-54). These fabrics are used for ties. The fabrics in Groups 2 and 3 were randomly selected from the available stock in both companies.

Table 4-1 List of Selected Fabrics (Group 1)

Code	Fabric Description	Weight (g/m^2)		Thickness (mm)	
		Mean	S.D.	Mean	S.D
1	100% Cotton Plain Woven	127.70	0.82	0.39	0.01
2	100% Linen Plain Woven	203.12	2.07	0.59	0.02
3	100% Cotton Non-Woven	33.80	1.90	0.37	0.03
4	100% Cotton Single Yarn Drill Khaki	265.52	1.26	0.70	0.05
5	100% Linen Plain Woven	175.74	2.56	0.54	0.04
6	100% Cotton Single Jersey Knitted	115.54	1.87	0.38	0.00
7	100% Cotton Double Jersey Knitted	203.22	1.32	0.77	0.02
8	100% Polyester Chiffon Knitted	78.26	0.86	0.22	0.00
9	100% Rayon Satin Woven	196.96	2.53	1.09	0.02
10	100% Wool Satin Woven	252.50	2.10	0.34	0.00
11	60% Polytester/ 40% Wool Single Side Flannel Woven	340.84	2.35	1.29	0.01

S.D. stands for Standard Deviation.

4.1.4 Experiment

The fabric samples were conditioned in standard testing conditions (20±1°C and relative humidity (RH) 65±5%) for at least 24 hours. Obvious wrinkles were also removed before the testing. The sample preparation followed ASTM standard D1776 (ASTM, 2008). All of the samples were tested under conditions that were tension free with no forces exerted onto any part.

A design of experiment (DOE) was performed when preparing the testing in order to evaluate the repeatability and reproducibility of the FTT. These two aspects are often challenging yet very important to any instrument (Nuffel et al., 2013). Therefore, two experienced technicians were chosen to conduct the FTT testing. Each technician conducted FTT testing on three samples of each fabric type. The testing sequences of the fabrics were randomly pre-designed.

Table 4-2 List of Selected Fabrics (Group 2)

Code	Fabric Description	Weight (g/m^2)		Thickness (mm)	
		Mean	S.D.	Mean	S.D.
12	94% Cotton 6% Elasthan 3X3 RIB	123.45	3.45	1.30	0.02
13	90% Nylon 10% Elasthan Single Jersey	141.20	2.33	0.62	0.03
14	90% Polyester/10% Elasthan(Spandex) Single Jersey	178.10	2.87	0.26	0.00
15	75% Rayon 15% Nylon 10% Elasthan Single Jersey	157.66	2.20	0.52	0.01
16	91% Polyester/9% Elasthan(Spandex) Single Jersey	123.43	3.46	0.68	0.03
17	100% Modal Interlock	206.93	1.09	1.26	0.05
18	56% Cupro 24% Nylon 20% Elasthan Single Jersey	137.65	1.03	0.34	0.04
19	83% Nylon 17% Elasthan Single Jersey	154.23	3.22	0.73	0.02
20	96% Tencel 4% Elasthan Jacquard	144.67	2.12	1.15	0.04
21	75% Nylon/25% Elasthan(Spandex) Single Jersey	90.45	1.09	0.49	0.00
22	87% Nylon 13% Elasthan Jacquard	113.31	1.31	0.77	0.00
23	91% Nylon/9% Elasthan(Lycra) Single Jersey	157.60	1.98	0.77	0.00
24	45% Polyester 41% Nylon 14% Elasthan Jacquard	112.48	1.07	0.88	0.02
25	39% Modal 55% Nylon 6% Elasthan Jacquard	146.32	1.17	0.94	0.01
26	85% Nylon 18% Elasthan Single Jersey	129.03	1.42	0.79	0.02
27	83% Nylon/17% Elasthan(Lycra) Single Jersey	205.55	2.93	0.76	0.03
28	91% Nylon/9% Elasthan(Lycra) Single Jersey	171.41	1.76	0.74	0.02
29	95% Nylon 5% Elasthan Single Jersey	154.92	1.18	0.58	0.00
30	87% Nylon 13% Elasthan (Spandex) Single Jersey	104.50	0.98	0.55	0.01
31	79% Nylon 22% Elasthan (Spandex) Single Jersey	93.45	1.10	0.52	0.01
32	75% Nylon 25% Elasthan (Spandex) Single Jersey	86.65	1.54	0.50	0.01
33	94% Modal 6% Elasthan Single Jersey	141.22	2.41	0.66	0.02
34	88% Nylon 12% Spandex Single Jersey	119.09	0.77	0.70	0.00
35	83% Nylon 17% Elasthan (Spandex) Single Jersey	105.09	0.81	0.77	0.02

S.D. stands for Standard Deviation.

In order the test the reliability of the measurement results of the FTT, 20 types of fabrics were selected from the list and tested on the KES system. Each fabric type was tested six times. Seven types of fabrics were randomly selected from Group 1; seven from Group 2; and six from Group 3. They are listed in the following table in which the S/N values are the same as their code in the above lists of the 54 types of fabrics. These 20 fabrics could include both samples with large variances and samples with similar properties. The models and statistical analyses then would not be affected by the sample variances. The remaining fabrics, 32 types, were afterwards used in model validation process, with detailed experiment designs covered in Chapter 8.

Table 4-3 List of Selected Fabrics (Group 3)

Code	Fabric Description	Weight (g/m^2)		Thickness (mm)	
		Mean	S.D.	Mean	S.D.
36	100% Silk Jacquard Knitted	142.25	0.50	0.59	0.02
37	100% Silk Jacquard Knitted	139.75	0.96	0.56	0.01
38	100% Silk Jacquard Knitted	117.75	0.50	0.48	0.01
39	100% Silk Jacquard Knitted	122.25	0.50	0.36	0.00
40	100% Silk Jacquard Knitted	126.80	1.10	0.56	0.00
41	100% Silk Jacquard Knitted	162.25	1.50	0.92	0.04
42	100% Silk Jacquard Knitted	166.80	0.84	0.59	0.02
43	100% Silk Jacquard Knitted	115.00	0.00	0.44	0.05
44	100% Silk Jacquard Knitted	124.40	1.14	0.49	0.01
45	100% Silk Jacquard Knitted	123.80	0.84	0.37	0.01
46	100% Silk Jacquard Knitted	117.40	0.89	0.48	0.00
47	100% Silk Jacquard Knitted	169.50	0.58	0.63	0.01
48	100% Silk Jacquard Knitted	124.25	0.96	0.54	0.02
49	100% Silk Jacquard Knitted	138.00	11.00	0.45	0.03
50	100% Silk Jacquard Knitted	165.50	1.73	0.70	0.02
51	100% Silk Jacquard Knitted	121.75	0.96	0.44	0.03
52	100% Silk Jacquard Knitted	133.60	1.14	0.42	0.01
53	100% Silk Jacquard Knitted	119.80	0.84	0.39	0.01
54	100% Silk Jacquard Knitted	131.40	1.14	0.62	0.00

S.D. stands for Standard Deviation.

Table 4-4 Selected 20 Fabrics

S/N	Fabric Description
1	100% Cotton Plain Woven
2	100% Linen Plain Woven
3	100% Cotton Non-Woven
4	100% Cotton Twill Woven
8	100% Polyester Chiffon Knitted
10	100% Wool Satin Woven
11	60% Polytester/ 40% Wool Single Side Flannel Woven
12	94% Cotton 6% Elasthan 3X3 RIB
14	90% Polyester/10% Elasthan(Spandex) Single Jersey
15	75% Viscose 15% Nylon 10% Elasthan Single Jersey
18	56% Cupro 24% Nylon 20% Elasthan Single Jersey
20	96% Tencel 4% Elasthan Jacquard
24	45% Polyester 41% Nylon 14% Elasthan Jacquard
29	95% Nylon 5% Elasthan Single Jersey
36	100% Silk Jacquard Knitted
37	100% Silk Jacquard Knitted
39	100% Silk Jacquard Knitted
46	100% Silk Jacquard Knitted
47	100% Silk Jacquard Knitted
52	100% Silk Jacquard Knitted

4.1.5 Data Analysis

The parameters that define the repeatability and reproducibility of the FTT included two indexes of the result variances in comparisons made with different components. According to the analysis of variance (ANOVA), the total variances on the test results constitute four types: a) variances from the effects of fabrics (degree of freedom: 53); b) variances from the effects of operators (degree of freedom: 1); c) variances from the effects of the interactions between fabrics and operators (degree of freedom: 53); and d) variances from repeated tests or sample errors (degree of freedom: 216). Repeatability (R_a) is defined as the variances caused by the instrument or repeated testing on samples of the same fabric. Reproducibility (R_o) is defined as the variances induced by different operators (Allen, 2010).

$$R_a = \frac{VC_E}{VC_E+VC_F+VC_O+VC_{FO}} * 100\% \quad (4\text{-}1)$$

$$R_O = \frac{VC_O + VC_{SO}}{VC_E + VC_F + VC_O + VC_{FO}} * 100\% \quad (4\text{-}2)$$

where VC_E, VC_F, VC_O, and VC_{FO} represent variance component of error, fabric, operator, and interaction of fabric and operator respectively. They are calculated from variance mean square according to:

$$VC_E = MS_E \quad (4\text{-}3)$$

$$VC_F = (MS_F - MS_E)/(Df_O * Df_E) \quad (4\text{-}4)$$

$$VC_O = (MS_O - MS_E)/(Df_F * Df_E) \quad (4\text{-}5)$$

$$VC_{FO} = (MS_{SO} - MS_E)/Df_E \quad (4\text{-}6)$$

where MS_E, MS_F, MS_O, and MS_{SO} mean variance mean square of error, fabric, operator, and interaction of fabric and operator respectively, Df_E, Df_F, and Df_O represent degree of freedom of error, fabric, and operator with value at 3, 54 and 2 respectively.

4.2 Development of Measurement Principle

4.2.1 Thermal Property

The thermal property is an important factor that influences fabric touch sensation. However, previous research has only focused on its effects on tactile sensation. The thermal stimulus is triggered by the temperature difference between the human skin and external environment as shown in Figure 4-1(a). Thermal perception takes place when one comes into contact with fabric as illustrated in Figure 4-1(b). The skin temperature of the human body is normally around 305.15 K – 308.15 K (32°C – 35°C) while normal room temperature is around 293.15 K (20°C) (Freitas, 1999), which is a difference of slightly over ten degrees Celsius. Therefore, energy transmission exists between hand and fabric. Variances on the properties of such energy transmission would then cause different thermal sensations.

For the purpose of simulating this process, a measurement principle, as shown in Figure 4-2, is proposed. Two plates (hot and cold plates) with different temperatures are clamped to the fabric. The plate with the higher temperature represents human skin while the plate with the lower temperature is the external environment. The fabric acts as a buffer between them. As mentioned, there is usually a temperature difference of about 10°C between the skin and external environment. The temperature difference subsequently should be set as 10°C as well. The heat flux is the main measured parameter here.

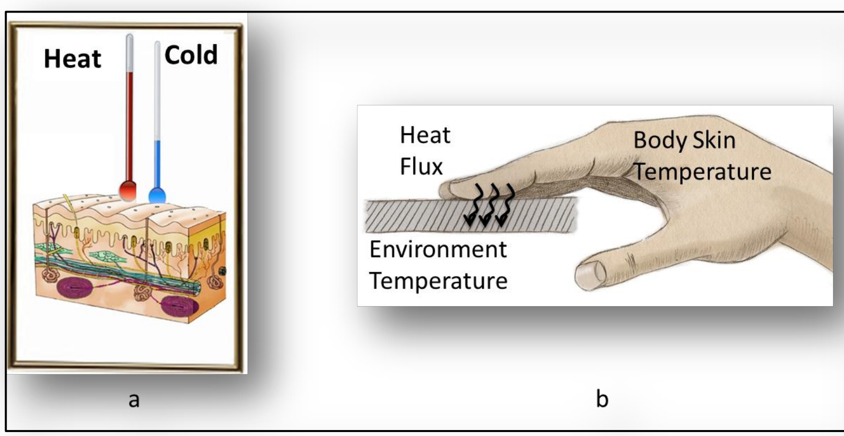

Figure 4-1 Illustration Diagram of Receiving Thermal Stimuli: (a) temperature variance between fabric and skin stimulate skin thermal receptors; (b) human perceive the thermal sensation on fabric as long as skin contact it

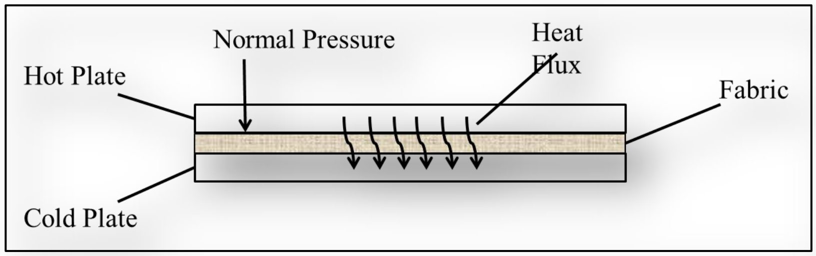

Figure 4-2 Measurement Principle of Fabric Thermal Property

During the measurement of the fabric thermal property, one important factor is the normal pressure applied. In daily life, this pressure usually comes from the gravity force of the cloth itself. Meanwhile, a recent phenomenon has attracted the attention of researchers. It has been noticed that clothing under different pressures would significantly affect thermal perception, since normal pressure would directly affect the thermal conductivity of fabric (Karunamoorthy & Das, 2014; S. J. Zhang, Li, Hu, Liao, & Zhang, 2014). For instance, a real life scenario would be sitting in the snow. Highly compressed clothing on the sitting area would significantly lose its thermal protective capability and induce a cold sensation to its wearer. Consequently, it is proposed in this thesis work that the measurement of fabric thermal property should also include characterization during varied normal pressure conditions. Therefore, applied normal pressure and fabric thickness were both recorded.

4.2.2 Deformation Properties: Compression

Pressure is generally concluded as another perceived fabric touch sensation. The basis of detecting pressure information is clearly on the force received. This kind of force would be received when one is trying to deform the fabric. Compression is one of the common deformations of fabrics when evaluating their touch sensation. The received force can lead to skin indentation and then stimulate the somatosensory receptors as illustrated in Figure 4-3(a). Figure 4-3(b) shows how humans compress fabrics. The process could be physically described as the fingers that provide normal forces to change the thickness of the sample held. Subsequently, the fingers receive a reaction based on Newton's third law of motion.

For simulation, the two-plate method was also proposed. One plate acts as the supporting platform while the other applies a normal force on the top of the sample. A hypothesized mechanical design is shown in Figure 4-4. The main parameters recorded should include fabric thickness and applied normal pressures.

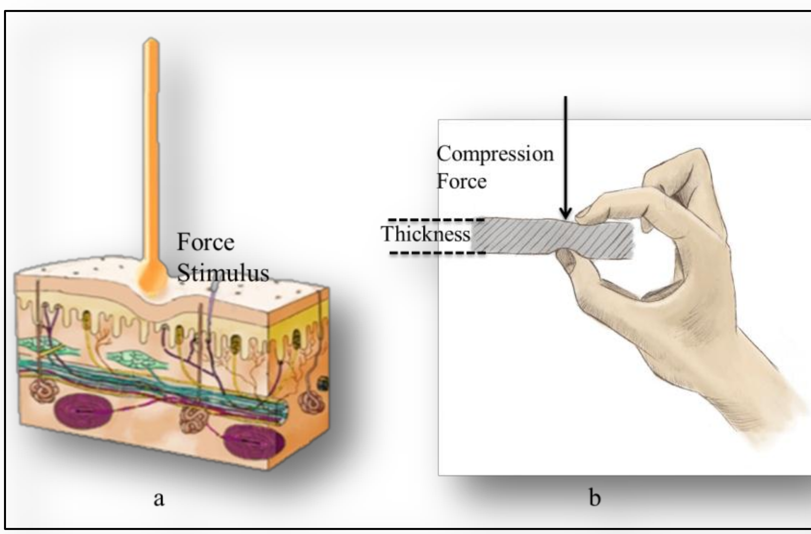

Figure 4-3 **Illustration Diagram of Receiving Compression Force Stimuli:** (a) external force could cause skin indentation and stimulate receptors; (b) human evaluate fabric's compression property by clamping it with certain compression force

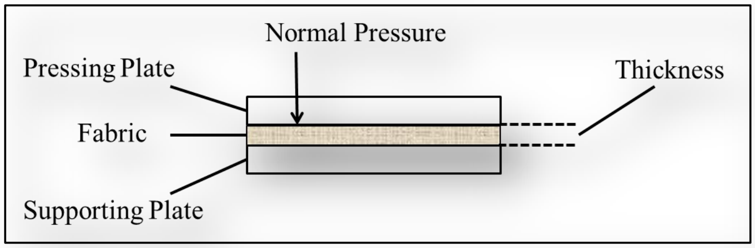

Figure 4-4 Measurement Principle of Fabric Compression Property

4.2.3 Deformation Property: Bending

Bending is another kind of deformation in which force is received by the skin receptors. A bending task would also induce skin indentation similar to the compression process. Figure 4-5 shows the bending process.

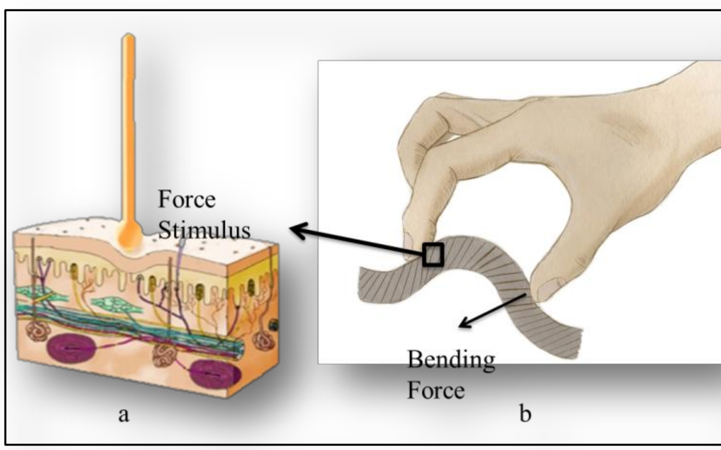

Figure 4-5 Illustration Diagram of Receiving Bending Force Stimuli: (a) external force could cause skin indentation and stimulate receptors; (b) human evaluate fabric bending property by curving it with certain force

In order to characterize this property, the instrument should bend fabric as well as record the force needed. Figure 4-6 shows the principle of this type of measurement. The design as shown in Figure 4-6(a)-(b) is conventionally used for instruments on the market. The fixed and bending clamps hold fabric in the middle while the bending clamp could freely move in a circular motion. The actual bending point of the fabric is indicated in the figure. The bending displacement of this design is the moved curvature. This design has limitations in that the bending clamp has to move in a circular shape. For the purpose of ensuring simultaneous measurement (discussed later), it is proposed here that an alternate measurement principle be used, as shown in Figure 4-6(c)-(d). The bending clamp could straight downwards with a specified normal force on the top. As shown in Figure 4-6(d), this method does not change the actual bending point whilst simplifying the mechanical design.

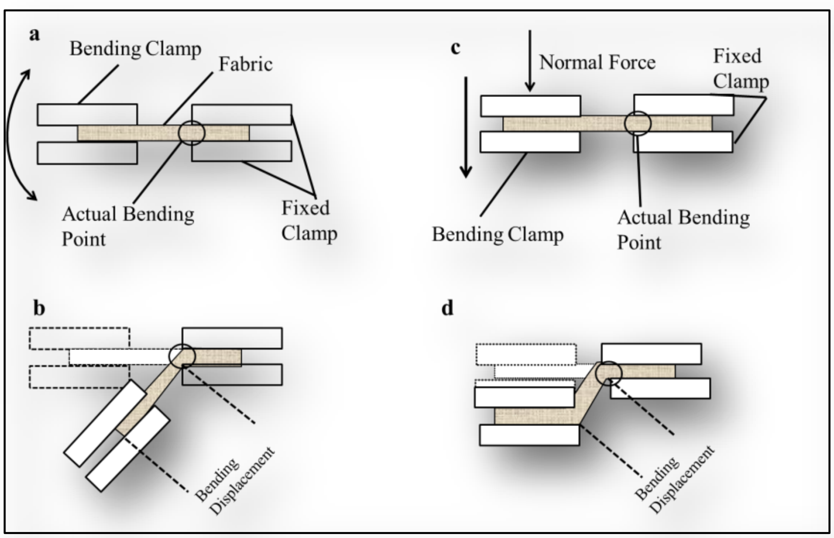

Figure 4-6 Measurement Principle of Fabric Bending Property: (a) conventional movement design; (b) and (c) proposed new movement design

4.2.4 Surface Property

Texture information is the last of the three perceived touch sensations that will be discussed in this work. A relatively rough fabric surface means more sensitivity towards the texture information as shown in Figure 4-7(a). Evaluation on this property is conducted when the finger statically contacts or kinetically moves across the fabric surface as illustrated in Figure 4-7(b).

For measurement of the surface property, usually the surface texture (also described as roughness) is measured together with the surface friction properties. Figure 4-8 is the design of the surface property measurement principle. Figure 4-8(a) is a bird's-eye view of the design while Figure 4-8(b) shows the design from a side view. Both probes are placed parallel to the fabric surface. Movement could be either from the fabric or by the probes. It has also been noticed that sometimes fabric has patterns on its surface. When evaluating friction, our hands or skin surface move across the fabric. This process would involve evaluation within a certain scanned area. Meanwhile, when evaluating roughness, a small but intense area would induce a discriminated sensation. As a result, friction measurement could include the averaging of an area while roughness measurement should scan details. The most ideal size of a texture-detecting probe would be the same as the JNDs. This value will be discussed later in the neural studies in the following chapters. Figure 4-8(c) is the proposed design of these two probes. The friction probe is a cube with one face that comes into contact with the fabric surface. The texture probe has a ball on the top. This design should prevent hooking from yarns.

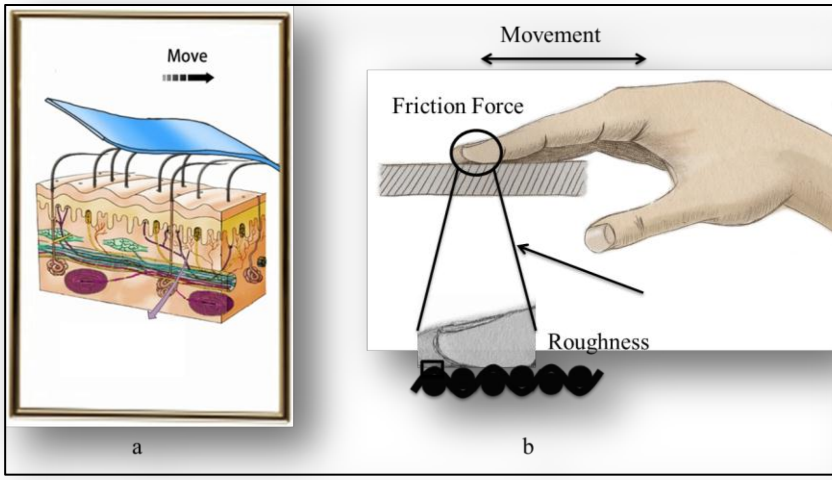

Figure 4-7 Illustration Diagram of Receiving Texture Stimuli: (a) unevenness surface of fabrics would stimulate skin receptor; (b) human evaluate fabric surface texture property by statically touch it or kinetically move along its surface

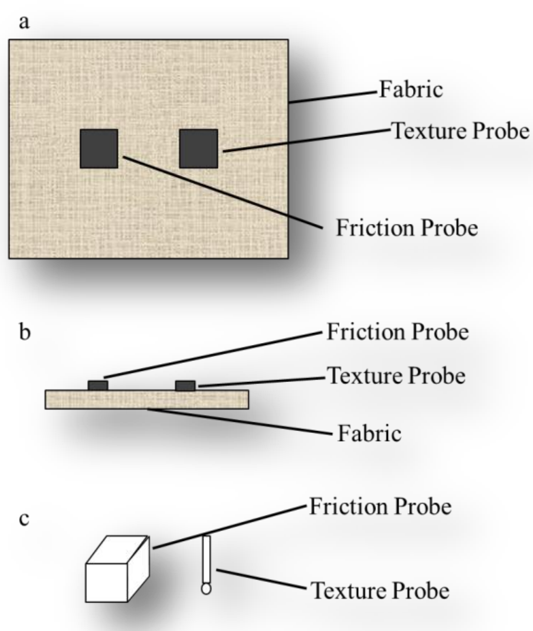

Figure 4-8 Measurement Principle of Fabric Surface Property: (a) bird's-eye view of surface measurement principle; (b) side view of the surface measurement principle; (c) schematic diagram of friction and texture measurement probes

4.2.5 Simultaneous Measurement Design

The above is an introduction of the measurement principle of an instrument that will characterize fabric physical properties with four indicators: thermal, compression, bending and surface property. Meanwhile, it is also necessary that all of these properties are simultaneously measured as they activate the skin receptors at the same time when producing touch sensations.

A design that combines the measurements from all four indictors was subsequently proposed, as shown in Figure 4-9. The sample swatch should be made to be long enough so that it could be divided into two parts. The left side of the sample as shown in Figure 4-9 would be brought downwards while the right side would remain at the initial horizontal level. After the movement, the right side of the fabric would be bent and pulled to allow bending and surface measurements. Meanwhile, two plates at the left side of the sample are used to measure both the thermal and compression properties. This design makes it possible to measure multiple aspects of physical properties simultaneously, which is the same as evaluating fabric touch sensation with the hands.

The design could be further modified to allow one-time measurement in two directions of the fabric. It is well known that fabrics usually have distinct properties in the warp/wale and weft/course directions depending on their fabrication method (for simplification purposes, this is depicted as the warp/weft directions in the following text). Except for non-woven fabrics, the yarns used as well as deformations applied in the warp and weft directions could be different. Therefore, it is appropriate to measure fabric properties in both directions. A simple modification based on the proposed method could carry out this task, as illustrated in Figure 4-10. The same components on the right side could be duplicate implanted on the topside, with each of them measuring one direction. In addition, it is proposed in this research work that both sides of the fabric should be measured since we come into contact with different sides of the fabric during hand evaluation (face side) and during wear (back side).

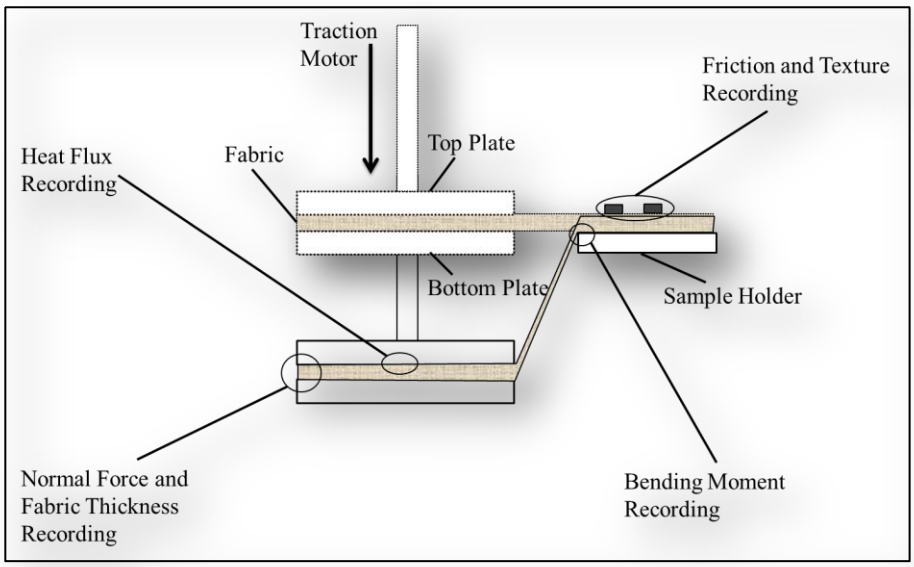

Figure 4-9 Design of Simultaneous Measurement of Fabric Physical Features

4.3 Implementation of Prototype and Indexes Identification

The prototype instrument, the FTT, was manufactured with support from an external private company. The FTT has four modules that could be activated at the same time. Sensors were installed to record the dynamic values. The modules include compression, thermal, bending and surface as shown in Figure 4-11. The samples are to be cut into an

L shape as described previously. They would be placed on the lower plate with the extension arms lying on the adjacent platforms. The center of the sample square would be pushed downwards, which leads to horizontal movement of the two arms. The compression and thermal modules measure the center of the sample while the bending and surface modules evaluate the area with the arms. There are two mirror-duplicated designs for the bending and surface property modules, so that both the warp and weft directions of the sample could be measured in one single testing.

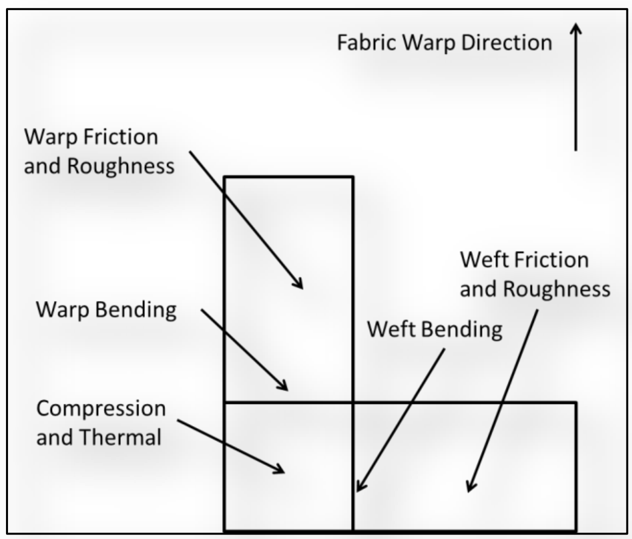

Figure 4-10 Illustration of Method Allowing Concurrent Measurements on Both Warp Direction and Weft Direction

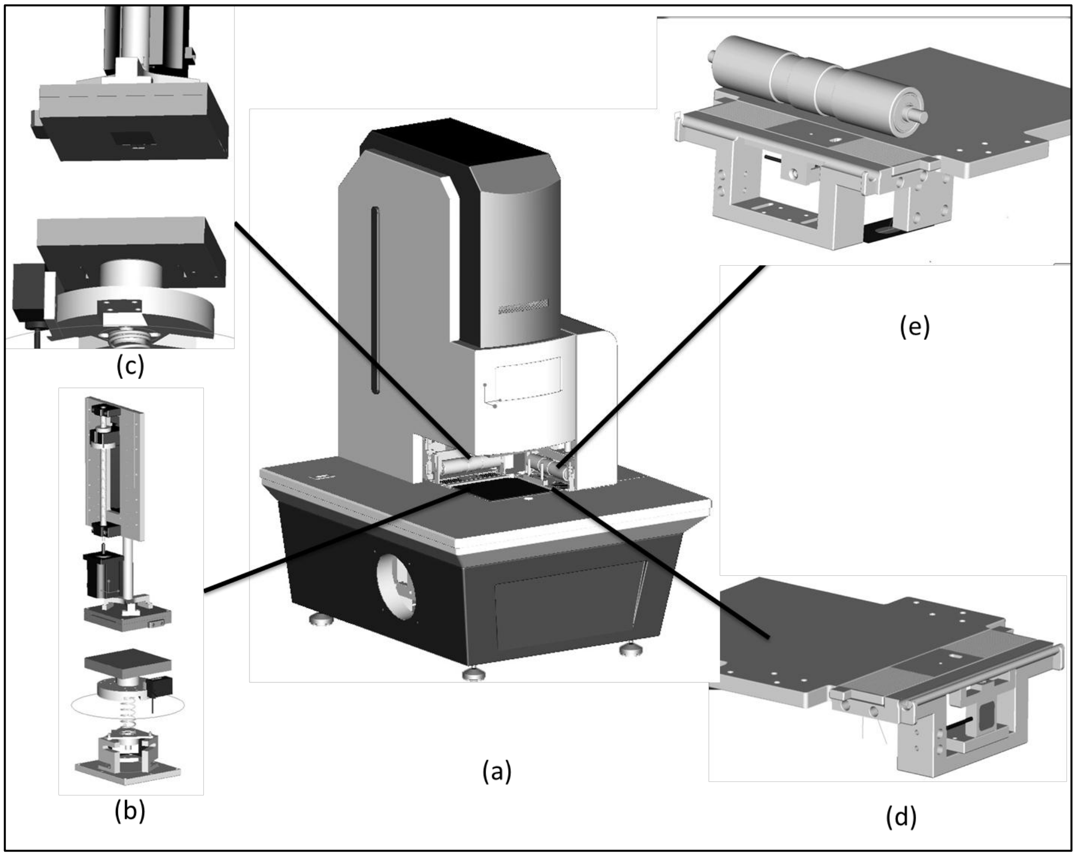

Figure 4-11 Mechanical Design of FTT Includes Overall Structure: Components of FTT includes (a), compression module (b), thermal module (c), bending module (d), and surface module (e).

4.3.1 Identification of Thermal Index

The temperature of the upper plate of the FTT is heated to 10 K higher than that of the lower plate while the latter remains at the same temperature as the surrounding environment. A commercial heat flux sensor was installed at the very center of the upper plate. It dynamically records the heat flux through the fabric during the compression process (Li, Hu, Liao, Li, & Wu, 2012b). The thermal module of the FTT is synchronously performed with the compression module.

A typical measurement curve is shown in Figure 4-12(a). The digital signals recorded from the thermal receptor are calculated according to the heat flux per square meter that uses W/m^2 as the unit while the distance is converted into the sample thickness which uses mm as the unit. The distance (i.e. thickness) data are the same data collected in the compression module.

Three indexes are defined to illustrate the fabric thermal properties. Their calculations are provided in Figure 4-12(b). The standard pressure is defined as 41 gf/cm^2 by following ASTM standard D1777 (ASTM, 1996). The thermal conductivity when compressing and recovering (TCC and TCR respectively) are calculated accordingly. Another index named the thermal maximum flux (TMF) is also defined as the maximum thermal flux during the measurement process.

$$\mathrm{TCC} = (\mathrm{H_i} * \mathrm{D_i})/\mathrm{C} \qquad (4\text{-}7)$$

$$\mathrm{TCR} = (\mathrm{H_j} * \mathrm{D_j})/\mathrm{C} \qquad (4\text{-}8)$$

$$\mathrm{TMF} = \max(\mathrm{H}) \qquad (4\text{-}9)$$

where D_i and D_j are the thickness of the sample under a pressure of 41 gf/cm^2 during compression and recovery, respectively; H_p and H_q the heat flux when the sample thickness is D_i, and D_j respectively; C the temperature difference between the top and bottom of the sample.

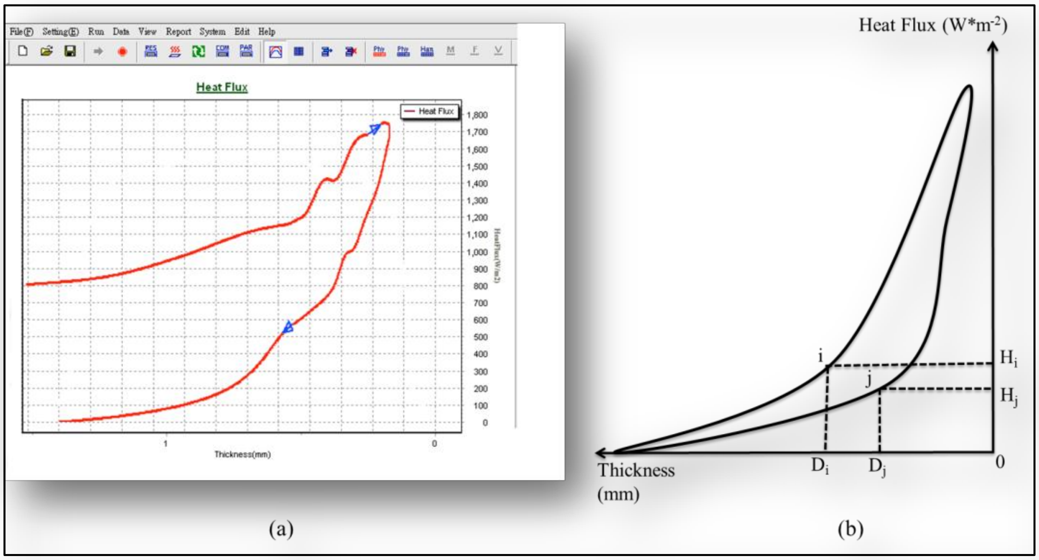

Figure 4-12 Typical Curve and Accordingly Defined Indexes on FTT Thermal Module: (a) a typical measurement curve from FTT is draw with x-axis stands for thickness and y-axis presents heat flux; (b) Calculation diagrams of indices TCC, TCR and TMF

4.3.2 Compression Indexes Identification

The upper plate of the FTT would apply a continuously increasing normal force from 0 gf to 8470 gf (i.e. 0 gf/cm^2 – 70 gf/cm^2) during compression, while also reduce the normal force at the same speed during recovery. The sample should be placed in the middle of the upper and lower plates. As a result, the same amount of normal force would be received by the lower plate. The lower plate is connected to three force sensors to record the normal force. The same three sensors are used to ascertain the horizontal leveling of the two plates, (i.e. sample) during the whole measurement process. A laser distance sensor is used to record the distance between the two plates at the same time (Li et al., 2012b).

A typical measurement curve is shown in Figure 4-13(a). The load cell digital signals recorded are calculated as the pressure which uses gf/mm^2 as the unit while the distance is converted into sample thickness which uses mm as the unit. Both the compression and recovery curves are presented together to show that they form an irregular shape.

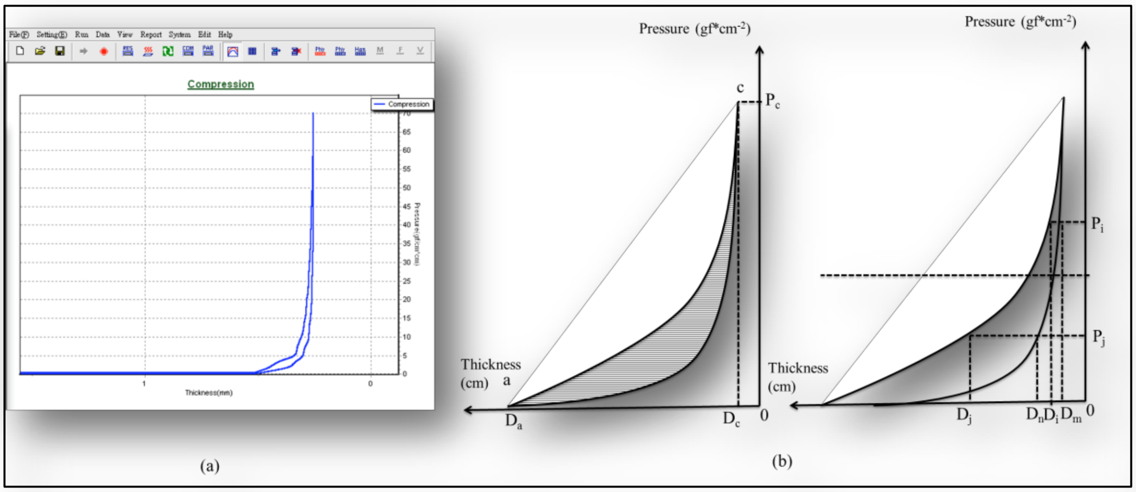

Figure 4-13 Typical Curve and Accordingly Defined Indexes on FTT Compression Module: (a) a typical measurement curve of FTT is draw with x-axis stands for thickness and y-axis presents normal pressure; (b) Calculation diagrams of indices, the left one illustrates the calculations of CW and CRR while right one illustrates calculations of CAR and RAR

There are four indexes defined accordingly. The integral of both the compression and recovery curves (shape formed by curve, y and x bars) are calculated. As shown in Figure 4-13(b), compression work (CW) is defined as the integral of the compression curve while the compression recovery rate (CRR) is the area of the shaded shape (variances between the integrals of the compression and recovery curves) divided by the

CW. These two indexes present the total energy consumed during the measurement process. They are calculated by using the following equations:

$$\mathrm{CW} = \mathrm{A}\int_{\mathrm{D_a}}^{\mathrm{D_c}} \mathrm{PdD} \tag{4-10}$$

$$\mathrm{CRR} = \frac{A\int_{\mathrm{D_a}}^{\mathrm{D_c}} \mathrm{PdD} - \mathrm{A}\int_{\mathrm{D_c}}^{\mathrm{D_a}} \mathrm{P'dD'}}{A\int_{\mathrm{D_c}}^{\mathrm{D_a}} \mathrm{PdD}} \tag{4-11}$$

where A is the measurement area, D_a the initial thickness at zero pressure, D_c the thickness at the maximum pressure, P the measured pressure and D the measured thickness when compressed. P' and D' are measured pressure and thickness for recovery respectively.

Figure 4-13(c) shows the calculation on the slopes of each curve. On the basis of the previously mentioned physical mechanisms of fabric compression in Chapter 2, the center 60%, according to the pressure, of the curves are counted. They are named the compression average rigidity (CAR) and recovery average rigidity (RAR) respectively. These two indexes show the changing rate of pressure during compression and recovery. They are dynamical indexes interpreted as the average pressure needed to change 1 mm of sample thickness.

$$\mathrm{CAR} = (\mathrm{P_i} - \mathrm{P_j})/(\mathrm{D_j} - \mathrm{D_i}) \tag{4-12}$$

$$\mathrm{RAR} = (\mathrm{P_i} - \mathrm{P_j})/(\mathrm{D_m} - \mathrm{D_n}) \tag{4-13}$$

where i to j denotes the limits of the center 60% of the compression curve. P_i and P_j the pressure forces recorded while D_i and D_j the thicknesses recorded. m to n the limits of the center 60% of the recovery curve. P_m and P_n are the pressure forces recorded while D_m and D_n are the thicknesses recorded.

4.3.3 Identification of Bending Index

The bending bars of the FTT are installed at the same level as the lower plate. They could be pushed downwards to exert bending forces during testing. Force sensors are placed under the bending bars to record the dynamic bending forces (Li, Hu, Liao, Li, & Wu, 2012a).

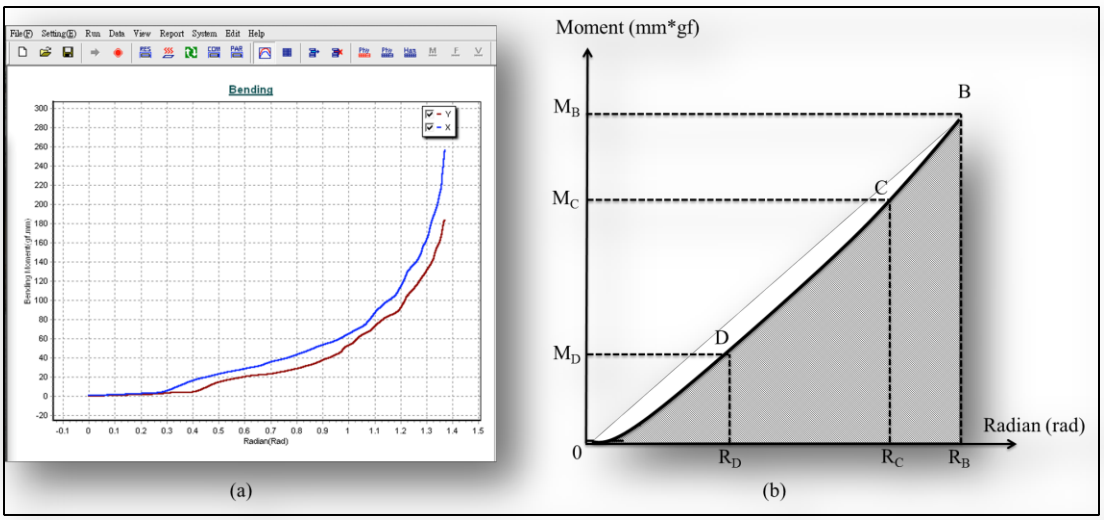

Figure 4-14 Typical Curve and Accordingly Defined Indexes on FTT Bending Module: (a) a typical measurement curve from FTT is draw with x-axis stands for bending radius and y-axis presents bending moment. Blue and red lines represent measurements on warp and weft directions respectively. (b) Calculation diagrams of indices BAR and BW

A typical measure curve is shown in Figure 4-14(a). Digital signals from load cell receptor recorded would be calculated to bending moment in the unit of gf*mm while the distances were converted to the bending radius in the unit of rad.

Indexes similar to the compression module are defined in the bending module. The two indexes are shown in Figure 4-14(b), including the bending average rigidity (BAR) and bending work (BW). The integral of the curve is calculated as the BW while the slope of the curve, center 60% according to the bending moment, is defined as the BAR. The calculation formulas of these two indexes are:

$$\mathrm{BAR} = (\mathrm{M_D} - \mathrm{M_C})/(\mathrm{R_D} - \mathrm{R_C}) \tag{4-14}$$

$$\mathrm{BW} = \int_1^B \mathrm{MdR} \tag{4-15}$$

where D to C denotes the limits of the center 60% of the bending curve. M_D and M_C the bending moments recorded while R_D and R_C are the radian recorded.

4.3.4 Identification of Surface Related Index

The surface property module of the FTT contains measurements on both the fabric friction and roughness properties. The module is located just beside the bending module. The samples should be mounted horizontally on the platforms. With regard to the measurement of surface friction, a standard metal cube that could move freely is used as the detector. Dynamic friction force would take place between the friction and sample surfaces. A roller is placed on the top of the sample to provide a normal force of 140±5 gf. Another needle-shape detector is used to measure the fabric surface unevenness (roughness). Through a lever system, laser sensors, which are the same as the ones used in the compression module, can measure the movement of the detectors. The movement of these detectors during testing corresponded to the geometrical variances on the sample surface (Li, Hu, Liao, Li, & Wu, 2012c).

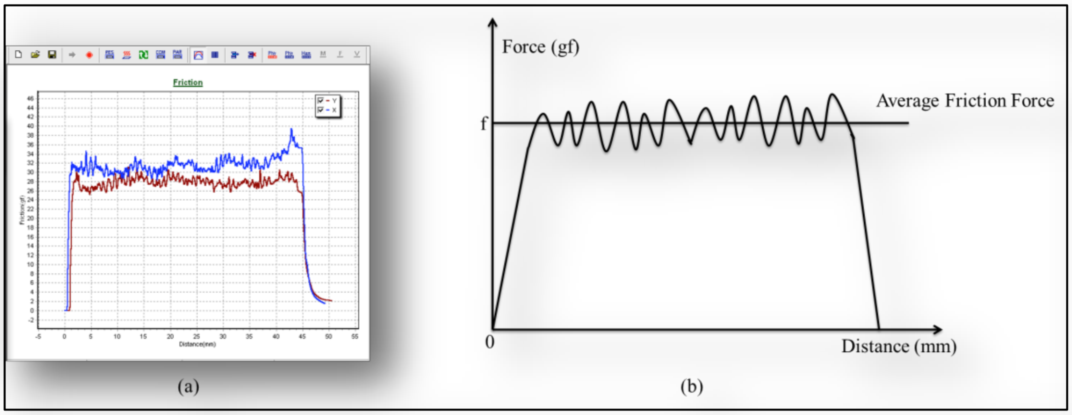

Figure 4-15 Typical Curve and Accordingly Defined Index on FTT Surface Friction Module: (a) a typical measurement curve from FTT is draw with x-axis stands for scanned distance and y-axis presents friction force. Blue and red lines represent measurements on warp and weft directions respectively. (b) Calculation diagrams of index SFC

The friction coefficient is defined in the friction measurement. A typical friction curve generated is shown in Figure 4-15(a). The surface friction coefficient (SFC) is defined as the average value of the measured kinetic friction forces divided by constant normal force, as shown in Figure 4-15(b).

$$\mathrm{SFC} = \mathrm{f/N} = \frac{1}{\mathrm{N(b-c)}} \int_{c}^{b} \mathrm{Fdx} \qquad (4\text{-}16)$$

where *N* is the normal force applied, *c* the start of the kinetic friction movement, *b* the end of the kinetic friction movement, *F* the measured friction force when the sample has moved a distance of *x*.

With regard to the surface roughness, the measurement curves are considered to be waves. A typical curve from the FTT is shown in Figure 4-16(a). A line that represents the measured height of the average roughness curve is first calculated. The peak and trough values for the curve are defined. Within every three intersections of the measured curve and the average roughness line, the maximum value is defined as the peak and the minimum value is defined as the trough.

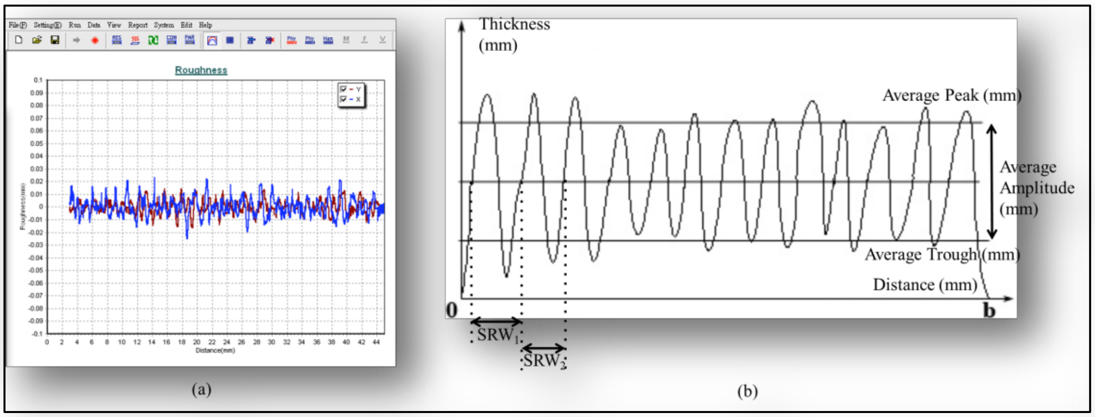

Figure 4-16 Typical Curve and Accordingly Defined Index on FTT Surface Roughness Module: (a) a typical measurement curve from FTT is draw with x-axis stands for scanned distance and y-axis presents roughness geometric height. Blue and red lines represent measurements on warp and weft directions respectively. (b) Calculation diagrams of indices SRA and SRW

Two indexes, the surface roughness amplitude (SRA) and surface roughness wavelength (SRW), are defined accordingly as shown in Figure 4-16 (b). These two indexes describe the basic shape of one repeat unit measured from this module, since the shape of these units of roughness is believed to produce stimulations on the receptors.

$$\mathrm{SRA} = \overline{\mathrm{R_p}} - \overline{\mathrm{R_t}} = \frac{1}{\mathrm{b}}\sum_{\mathrm{x}=1}^{\mathrm{b}} \mathrm{R_{px}} - \frac{1}{\mathrm{b}}\sum_{\mathrm{x}=1}^{\mathrm{b}} \mathrm{R_{tx}} \qquad (4\text{-}17)$$

$$\mathrm{SRW} = \frac{1}{\mathrm{M}}\sum_{\mathrm{x}=1}^{\mathrm{M}} \left|\mathrm{X_{pn}} - \mathrm{X_{tn}}\right| \qquad (4\text{-}18)$$

where R_{px} and R_{tx} are the measured peak and trough values of the roughness curve when the sample has moved a distance of x, b the maximum distance moved during the measurement, X_{pn} and X_{tn} distance moved when the peak and trough values are found, M the total number of groups of three successive intersections of the measured curve.

Table 4-5 List of indices defined in FTT.

Indices	Description	Unit
CW	Compression Work	gf*mm
CRR	Compression Recovery Rate	nul (gf*mm*gf^{-1}*mm^{-1})
CAR	Compression Average Rigidity	gf*mm^{-3}
RAR	Recovery Average Rigidity	gf*mm^{-3}
TCC	Thermal Conductivity when Compression	W*m^{-1}*K^{-1}
TCR	Thermal Conductivity when Recovery	W*m^{-1}*K^{-1}
TMF	Thermal Maximum Flux	W*m^{-2}
BAR	Bending Average Rigidity	gf*mm*rad^{-1}
BW	Bending Work	gf*mm*rad
SFC	Surface Friction Coefficient	nul (gf*gf^{-1})
SRA	Surface Roughness Amplitude	µm
SRW	Surface Roughness Wavelength	mm

In summary, 12 indices are defined to characterize sample physical properties as summarized in Table 4-5. They provide an overall description of textiles with clear physical meanings.

4.4 Repeatability and Reproducibility Test

By following the instructions presented previously, the repeatability and reproducibility test of the FTT was conducted Table 4-6 and Table 4-7 show the results of the repeatability and reproducibility testing on the face and back sides of the selected 54 types of fabrics respectively. The results indicate that for 18 of the defined indexes (including those for the warp and the weft directions), variances caused by repeatability are lower than 10% and those caused by reproducibility are even lower (less than 5%).

Table 4-6 Repeatability and Reproducibility of FTT Results (Face Side)

Indexes	Sample	Repeatability	Reproducibility
BARa	92.57%	3.43%	4.00%
BARe	88.40%	4.42%	7.18%
BWa	95.33%	0.77%	3.91%
BWe	92.35%	1.08%	6.57%
T	98.91%	0.36%	0.73%
CW	95.52%	0.95%	3.53%
CRR	86.59%	4.77%	8.64%
CAR	96.43%	1.06%	2.51%
RAR	93.69%	3.86%	2.45%
TCC	95.89%	0.90%	3.21%
TCR	93.73%	0.89%	5.37%
TMF	98.33%	1.62%	0.05%
SFCa	91.01%	3.75%	5.24%
SFCe	87.49%	8.52%	4.00%
SRAa	88.22%	5.87%	5.91%
SRAe	89.06%	2.89%	8.05%
SRWa	89.68%	7.13%	3.19%
SRWe	85.46%	7.66%	6.87%

Table 4-7 Repeatability and Reproducibility of FTT Results (Back Side)

Indexes	Sample	Repeatability	Reproducibility
BARa	89.35%	6.90%	3.75%
BARe	83.91%	9.56%	6.53%
BWa	95.56%	1.48%	2.97%
BWe	90.62%	5.39%	3.99%
T	96.47%	0.70%	2.83%
CW	93.81%	1.95%	4.24%
CRR	84.69%	8.79%	6.52%
CAR	92.61%	1.95%	5.45%
RAR	90.10%	5.02%	4.88%
TCC	94.81%	2.10%	3.09%
TCR	95.12%	2.16%	2.72%
TMF	97.43%	1.87%	0.70%
SFCa	87.82%	5.31%	6.87%
SFCe	89.69%	4.82%	5.49%
SRAa	84.81%	9.39%	5.80%
SRAe	83.05%	8.81%	8.14%
SRWa	82.60%	8.56%	8.84%
SRWe	83.30%	7.60%	9.10%

The repeatability and reproducibility of the work calculated by the BWa, BWe, and CW indexes are better than those calculated by the BARa, BARe and CAR, and RAR slopes. This is because the integration algorithm removes variances on each recorded data point while the slopes largely rely on the variances of the used points (start and end data points). Indexes related to surface roughness measurement demonstrate the highest repeatability and reproducibility. This finding is not surprising since the design concept of the FTT stipulates that measurements of surface roughness are only to be conducted on very narrow strips on the samples. Different structures and pattern designs could easily induce more variances into these indexes, especially when calculating the repeat pattern of surface unevenness, i.e. SRW.

Generally speaking, the practicability of FTT is satisfied. This new mechanical design aims to implement the above mentioned simultaneous measurement of all physical stimuli related to touch sensation. The repeatability and reproducibility of the FTT have proven that this prototype has commercial potential with the ability to provide stable physical results on various kinds of fabrics.

4.5 Comparison on Objective Measurement Methods

For the purpose of ascertaining the validity and preciseness of this testing method, fabrics were also tested on the KES-F systems, including KES-FB2, KES-FB3, KES-FB4 and KES-Thermolab II. Six repeated tests on each fabric were conducted. The preparation of the samples was the same as that for the testing by the FTT. Table 4-8 is a summary of the Spearman's correlation results between two measurement methods. Significant correlations could be found in the modules, including thermal, compression, and bending.

Figure 4-17 illustrates a comparison between thermal indexes obtained from the FTT and KES respectively. Strong correlations that follow linear functions can be observed from both indexes. The measurement principles of the FTT and KES are similar. They both basically use the "hot plate method" as reviewed in Chapter 2.

Table 4-8 Correlation Results of KES and FTT

Module	KES Indexes	Statistic	FTT Indexes			
Thermal			TMF	TCC		
	Qmax	Coefficient	0.880			
		p Value	0.000			
	k	Coefficient		0.971		
		p Value		0.000		
Compression			CAR	CW	CRR	
	LC	Coefficient	--			
		p Value	--			
	WC	Coefficient		0.868		
		p Value		0.000		
	RC	Coefficient			0.717	
		p Value			0.000	
Bending			Warp BW	Warp BAR	Weft BW	Weft BAR
	Warp B-Mean	Coefficient	0.629	--		
		p Value	0.003	--		
	Weft B-Mean	Coefficient			0.750	--
		p Value			0.000	--
Surface			Warp SFC	Warp SRA	Weft SFC	Weft SRA
	Warp MIU	Coefficient	--			
		p Value	--			
	Warp SMD	Coefficient		--		
		p Value		--		
	Weft MIU	Coefficient			--	
		p Value			--	
	Weft SMD	Coefficient				--
		p Value				--

The KES defines "Qmax" as the measured heat flux value at 0.2 second from contact while FTT defines "TMF" as the maximum heat flux. Nevertheless, the comparison indicates that their results are highly correlated to each other. With regard to the TCC and k, they both describe the thermal conductivity of fabrics. The correlation coefficient is even higher. Since calculation of thermal conductivity shows the effect of temperature differences, contact area and thickness of fabrics, the only variance of the measurement methods is normal pressure. The results imply that for these fabrics, limited differences can be observed between those under normal pressure at 10 gf/cm^2 and 42 gf/cm^2.

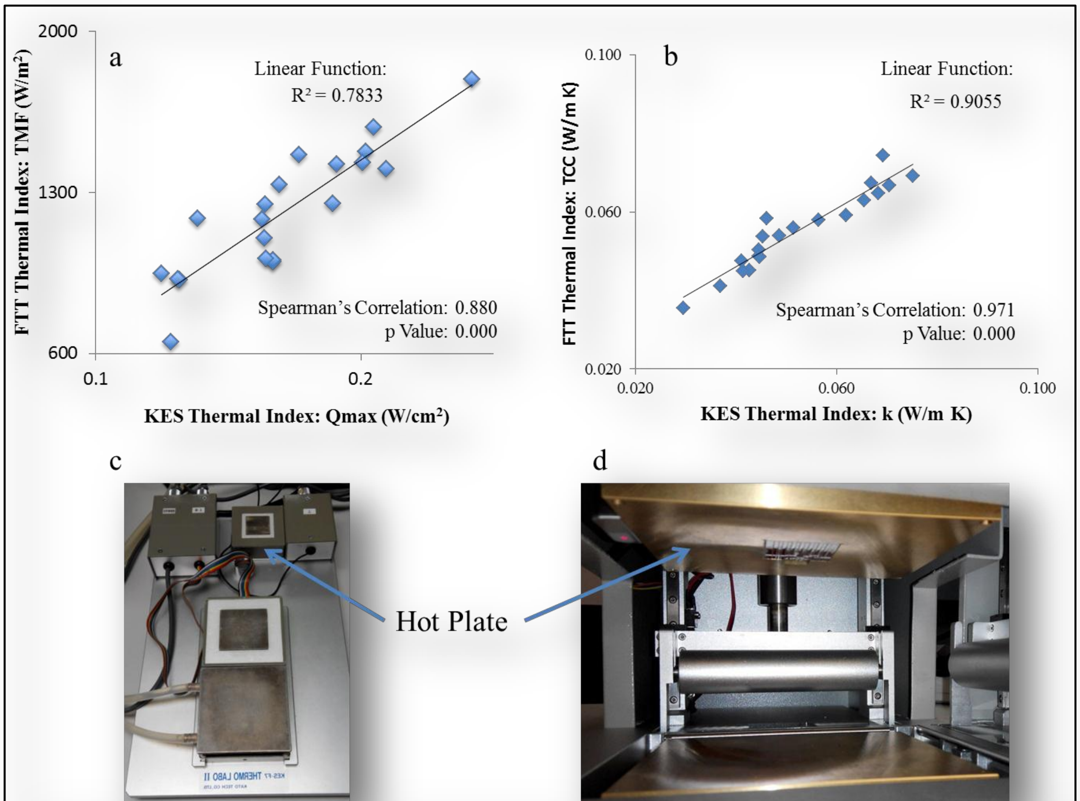

Figure 4-17 Comparison of Thermal Measurement of KES and FTT: (a) comparison scatter-plot between FTT index TMF and KES index Qmax; (b) comparison scatter-plot between FTT index TCC and KES index k; (c) photo of KES Thermolab II instrument. d. photo of FTT instrument (thermal module)

Figure 4-18 shows a comparison of a compression measurement made by the FTT and the KES. Figure 4-18(a) and Figure 4-18(b) show that the both of their indexes follow a linear function. Indexes related to compression work show better correlation coefficients than those related to compression recovery. The physical mechanisms of both instruments comprise two metal plates to compress fabrics. The force and change in distance are recorded to calculate the indexes. The measurement area of the KES-FB3 is 2 cm^2 and that of the FTT is 144 cm^2. The KES-FB3 measures fabrics with compression forces that ranges from 0 to 50 gf/cm^2, compared to 0-71 gf/cm^2 of the FTT. It is therefore not surprising that these two variances lead to different results based on the two types of equipment although they seem to be similar.

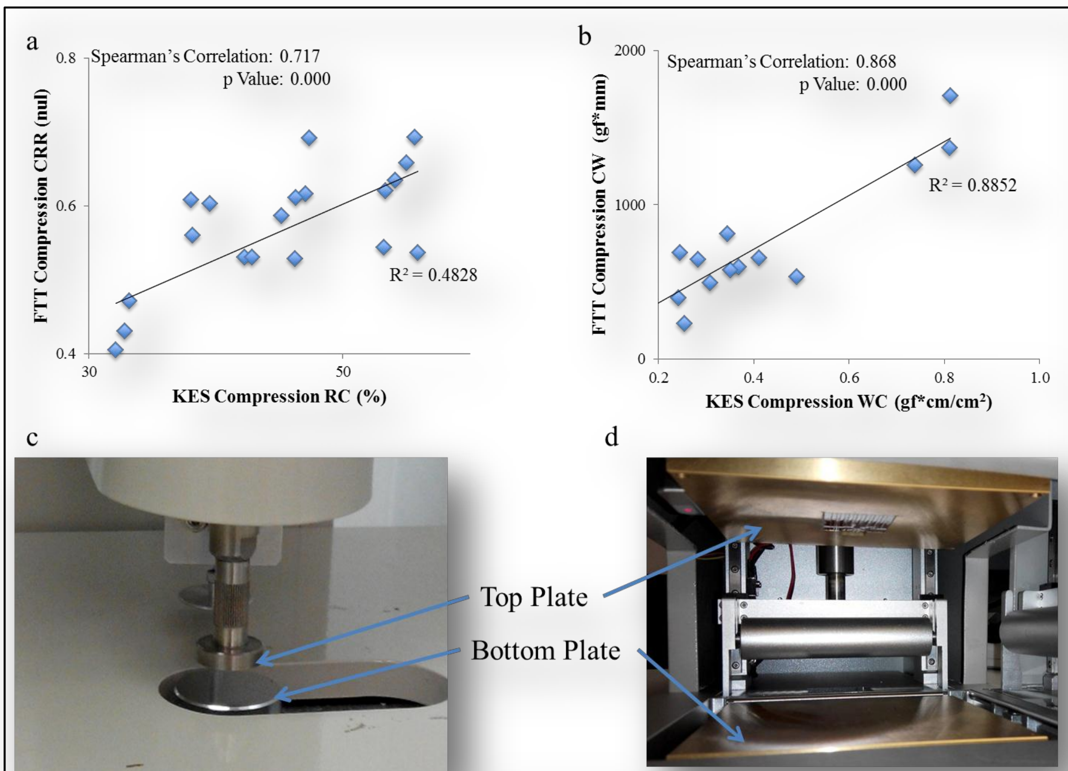

Figure 4-18 Comparison of Compression Measurement of KES and FTT: (a) comparison scatter-plot between FTT index CRR and KES index RC; (b) comparison scatter-plot between FTT index CW and KES index WC; (c) photo of KES-FB3 instrument. d. photo of FTT instrument (compression module)

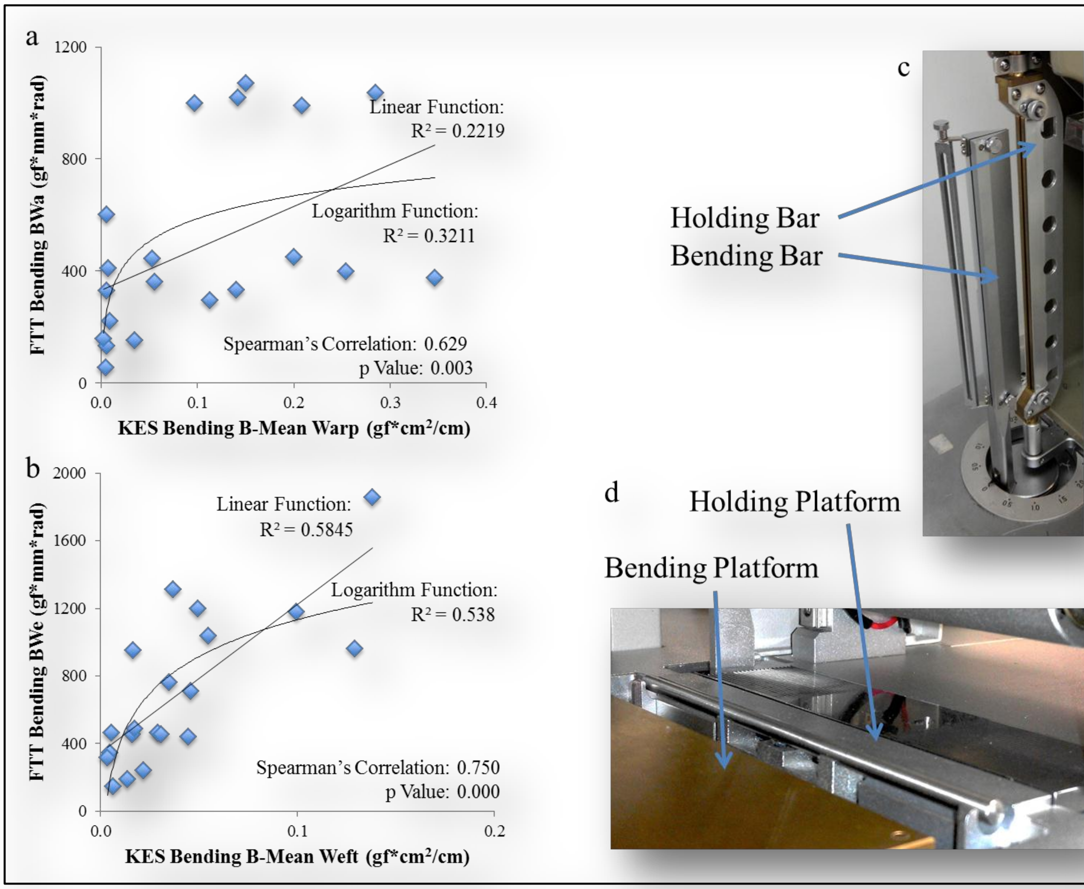

Figure 4-19 Comparison of Bending Measurement of KES and FTT: (a) comparison scatter-plot between FTT index BWa and KES index Warp B-Mean; (b) comparison scatter-plot between FTT index BWe and KES index Weft B-Mean; (c) photo of KES-FB2 instrument. d. photo of FTT instrument (bending module)

Figure 4-19 shows the bending measurements made by the FTT and KES. The measurement mechanisms for bending are different this time. Figure 4-19(a) and Figure 4-19(b) show that the correlations between the indexes obtained from the KES and the FTT are not strong enough, even though a Spearman's correlation test concludes that the p value is lower than 0.01. The KES holds the samples vertically as shown in Figure 4-19(c) while the FTT holds the samples horizontally as illustrated in Figure 4-19(d). In addition, the bending curves measured by the KES ranges from -2.5 to 2.5 cm^{-1} forward and backward (a detailed description is provided in Chapter 2). On the other hand, the bending measurement made by the KES for the bending task ranges from 0 to 2.5 rad, since the bent sample length remains at 1 cm. When calculating index B, the KES system reports the slope of the bending moment curve recorded from 0.5 to 1.5 rad. Meanwhile, for the bending measurement made by the FTT, the maximum bending radian is set at 1 rad. The calculation of BAR index use the slope of the bending moment curve recorded from 0.2 to 0.8 rad. Clearly, the measured ranges by the two instruments are distinctly different. As mentioned before, the KES bends the fabric vertically while the FTT does so horizontally. Together, they could lead to significant but not very strong correlations between the results obtained by the KES and FTT.

In addition, there is no significant correlation found between the surface indexes obtained by the KES-FB4 and FTT. Figure 4-20 is a comparison of the two instruments. It can be easily observed that the measurement probes of the two instruments are different. Due to the relatively high degree of unevenness of the fabric surface texture, different scanned values of the fabric texture properties are likely to be the reason for the non-correlated results. Also, the roughness index identified by using the KES-FB4 (SMD) is different from that obtained by the FTT (SRA and SRW). The former index provides an overall picture of the fabric surface unevenness while the latter two respectively show the average height and width of the repeatedly appearing surface unevenness.

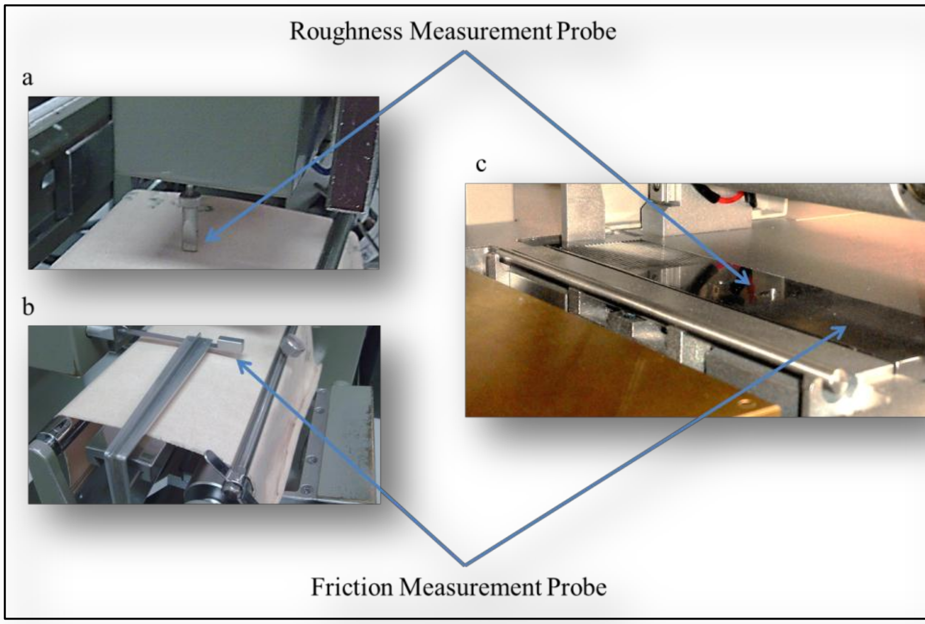

Figure 4-20 Comparison of Surface Measurement of KES and FTT: (a) photo of KES-FB4 roughness probe; (b) photo of KES-FB4 friction probe; (c) photo of FTT instrument (surface module)

In short, some of the indexes show highly correlated results obtained by the KES and FTT, but this is not the case for the other indexes. It can be concluded from the comparison analyses that different measurement principles and index calculation methods lead to non-correlated results. Overall speaking, the FTT is demonstrated to be an alternate testing instrument that gives reasonable results compared to other well-accepted instruments within the KES system.

4.6 Conclusion

The objective 2 has been achieved by developing a simultaneous measurement method to characterizing fabric sensory touch properties in this chapter. The prototype that is based on this principle, the FTT, can simultaneously measure four modules, including compression, thermal, bending and the surface. These four modules address four types of stimuli that could be received by the human somatosensory system. With its unique design, the FTT is able to characterize multiple thermal-tactile properties related to fabric touch sensation in one single trial.

The reported new design of the FTT prototype is capable of completing one test trial in a very short time period and output the test results for both the warp and weft directions. The test results for the 54 types of fabric samples show that the FTT can differentiate significant differences among them in terms of all the defined indexes. Repeatability and reproducibility analysis from two operators on the one instrument confirms that compared to the differences in the fabrics, variations caused by the FTT or operators are much fewer. The comparison between the newly designed FTT and well-known KES shows that the test results of the FTT are generally correlated to those of the KES as long as the measurement concepts are similar. Therefore, the preciseness of the test results from using the FTT should be satisfied.

The FTT provides an objective measurement means of simultaneous characterization of fabric touch sensory properties. The responses obtained from fabrics by using this instrument are used for later discussions in this thesis since they represent their physical properties (i.e. the intensity of touch stimuli).

Chapter 5 Neurophysiological Coding Mechanisms

In this chapter, the objective 3 will be completed by identifying relevant neurophysiological coding mechanisms and developing models for fabric touch sensations. Hypotheses are made based on the physical properties of fabric and neural responses when fabrics are touched. Neurophysiological indexes that represent the neural response after receiving quantified physical stimuli from fabrics are identified. After detecting physical stimuli from the external environment, the skin receptors would subsequently transfer the information into neural signals. In neurophysiological studies, there are discussions on the transduction and transmission of such neural signals. The coding mechanisms of a variety of physical stimuli are one of major areas investigated.

The neurophysiological processing of sensation perception begins from the transduction of physical stimuli into neural signals. As previously reviewed in Chapter 2, there are different kinds of receptors found under the human skin. Each is considered to be responsible for several types of stimuli. In the Figure 5-1, a general classification of the types of physical stimuli that relate to the somatosensory system is given. Human skin can surely receive other types of information, including chemical and physical pain, moisture, etc. However, the shown stimuli are commonly perceived ones when humans evaluate fabric touch sensation. These receptors include Pacinian corpuscles, Meissner's corpuscles, Merkel's discs, Ruffini endings and free nerve endings. It has been generally concluded that these transduce different types of physical stimuli as concluded in Chapter 2.

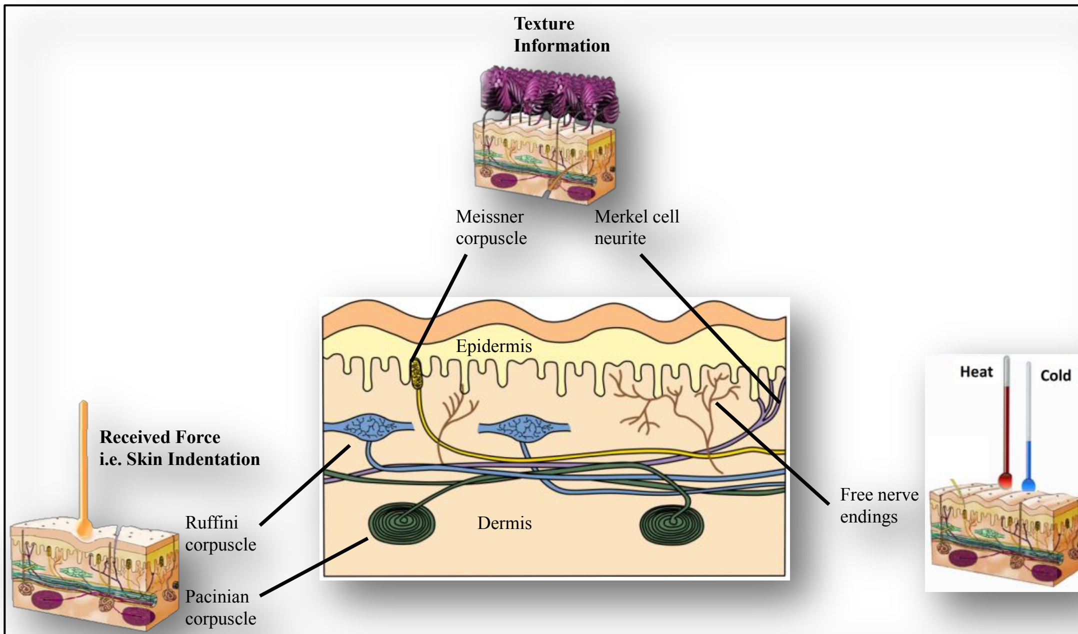

Figure 5-1 Illustration of Skin Receptors and Their Functions

Meanwhile, in neurophysiological studies, skin receptors are also usually categorized according to their rate of adaptation. Slow adapting type 1 (SA1) and slow adapting type 2 (SA2) fibers are usually referred to as Merkel corpuscle and Ruffini corpuscle respectively. Rapidly adapting type 1 (RA) and rapidly adapting type 2 (PC) fibers are concluded as Meissner corpuscle and Pacinian corpuscle respectively. Since the coding mechanisms of these receptors are closely related to their impulse patterns, in the following, the categorization terms are based on their adaptation.

As mentioned in the literature review, most of the neurophysiological studies discussed evaluated homogeneous materials, like silicon or metal. These have quite different physical properties compared to most objects that we use in daily life and come into contact, such as fabric. Therefore, the focus here is on investigating the neurophysiological coding mechanisms of fabric touch sensation. With exceptional findings based on homogeneous materials, applications of these theories on fabric can further the knowledge of how humans sense the external world.

5.1 Methodology

Figure 5-2 is a schematic diagram of the neurophysiological coding mechanism. The left of the figure shows the hand evaluation of fabric. An enlarged illustration of the fabric-skin contact shows that various receptors detect the physical stimuli produced during the evaluation of the fabric. Neural signals are then be transduced by the receptors and transmitted by afferent fibers until they reach the spinal cord. The information is subsequently passed from the spinal cord to the brain. Finally, the "hand feel" is perceived. Neurophysiological coding mechanisms aim to draw the relation between physical stimuli and neural signals. As shown in the bottom-right of the figure, during the rest stage, pulses are produced by fibers while impulses are observed during the presence of stimulus.

In neurophysiological studies, the hypotheses made generally have two focuses. The first is how the stimulus intensity is detected. From previous studies, the aspects of physical properties that are related to touch perception have been summarized. On the basis of such, the proposed physical measurement principle is introduced in Chapter 4. However, the exact algorithms to analyze the measured data have not been found yet. The hypotheses therefore are raised according to the unique features of fabrics.

Secondly, correct quantitative calculation methods should be determined for neural responses. There are many ways to express neural responses, for example, impulse rate in signal fibers and the fiber population or even the membrane currents of fibers. The following hypotheses are made to properly link stimulus intensity and neural response. This chapter is organized according to three types of stimulus information, including thermal, force, and texture information.

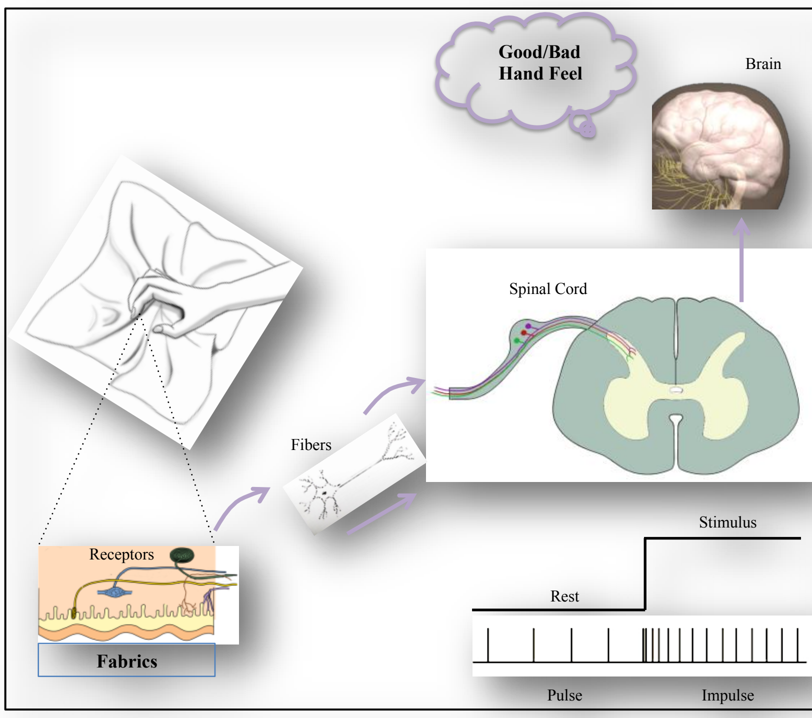

Figure 5-2 Schematic Diagram of Neurophysiological Coding Mechanism

20 types of fabrics were selected, as shown in Table 5-1. The numbers in the column labeled "S/N" are the same as their code in the lists of the 54 types of fabrics as provided in Chapter 4. Since the measurements made by the FTT record dynamic

mechanical responses from the fabrics, the results from the FTT were used to calculate the estimated neurophysiological responses. Algorithm development and statistical analyses in this chapter were conducted by using Matlab version R2013a and IBM SPSS version 20.0.

Table 5-1 List of Fabrics for Neurophysiological Evaluation

S/N	Fabric Description	Weight (g/m^2)		Thickness (mm)	
		Mean	S.D.	Mean	S.D.
1	100% Cotton Plain Woven	127.70	0.82	0.39	0.01
2	100% Linen Plain Woven	203.12	2.07	0.59	0.02
3	100% Cotton Non-Woven	33.80	1.90	0.37	0.03
4	100% Cotton Twill Woven	265.52	1.26	0.70	0.05
8	100% Polyester Chiffon Knitted	78.26	0.86	0.22	0.00
10	100% Wool Satin Woven	252.50	2.10	0.34	0.00
11	60% Polyester/ 40% Wool Single Side Flannel Woven	340.84	2.35	1.29	0.01
12	94% Cotton/6% Elasthan 3X3 RIB	123.45	3.45	1.30	0.02
14	90% Polyester/10% Spandex Single Jersey	178.10	2.87	0.26	0.00
15	75% Viscose 15% Nylon 10% Spandex Single Jersey	157.66	2.20	0.52	0.01
18	56% Cupro 24% Nylon 20% Spandex Single Jersey	137.65	1.03	0.34	0.04
20	96% Tencel 4% Spandex Jacquard	144.67	2.12	1.15	0.04
24	45% Polyester 41% Nylon 14% Spandex Jacquard	112.48	1.07	0.88	0.02
29	95% Nylon 5% Spandex Single Jersey	154.92	1.18	0.58	0.00
36	100% Silk Jacquard Knitted	142.25	0.50	0.59	0.02
37	100% Silk Jacquard Knitted	139.75	0.96	0.56	0.01
39	100% Silk Jacquard Knitted	122.25	0.50	0.36	0.00
46	100% Silk Jacquard Knitted	117.40	0.89	0.48	0.00
47	100% Silk Jacquard Knitted	169.50	0.58	0.63	0.01
52	100% Silk Jacquard Knitted	133.60	1.14	0.42	0.01

S.D. means standard deviation

5.2 Coding Mechanism of Thermal Information

Neurophysiological studies have revealed that humans can detect a wide range of ambient temperatures, see (Hatem et al., 2006; Namer et al., 2005). We can also determine different thermal sensations for two objects even they have been rest at the same (Avi Chaudhuri, 2011). Many textile-related studies have mentioned that there is a peak of the heat flux before there is stabilization in the skin-fabric system (Kawabata & Yoneda, 1981). The measurement of fabric thermal properties also require that they should be recorded under a steady-state (ASTM, 2011; ISO, 1993). Therefore, it is generally agreed that dynamic fabric thermal status during the period where there is contact is quite important for thermal sensation discrimination (Havenith et al., 1992; Sarda et al., 2004; Schneider & Holcombe, 1991).

The FTT dynamically records the heat flux (heat transfer per unit time in per unit area) of fabrics under a continuously compression process. Subsequently, hypotheses are made to link the heat flux measured to the neural signals that fabrics could evoke.

5.2.1 Hypothesis and Data Analysis

Since the FTT kinetically records the heat flux of fabric along with compression measurement, the fabric thickness continuously changes during the measurement. Different values of fabric conductivity are obtained at each time point. Therefore, three specified fabric thickness values were chosen for the following analyses. They include fabric thickness with normal pressure at 5, 42, and 70 gf/cm^2 respectively during the compression process.

According the law of heat conduction (Fourier's law), the thermodynamic equation of fabric when it is measured could be expressed as:

$$q = k\frac{\Delta T}{x} \tag{5-1}$$

where q is heat flux measured, k fabric conductivity, ΔT temperature difference, and x fabric thickness. For the purpose of eliminating the impact of changes in the thickness, a formula was used to transfer the measured heat flux q into an equivalent heat flux h.

$$h = q\frac{x}{D} \tag{5-2}$$

where D is the fabric thickness under specified normal pressure conditions (i.e. 5, 42, and 70 gf/cm^2). Figure 5-3 shows a typical curve after this transformation. Sample shown is Fabric 1. Blue line demonstrates the original data obtained from FTT while red line presents calculated data by equation (5-2). This curve shares a similar pattern with those of previous studies (J. Y. Hu, Hes, Li, Yeung, & Yao, 2006).

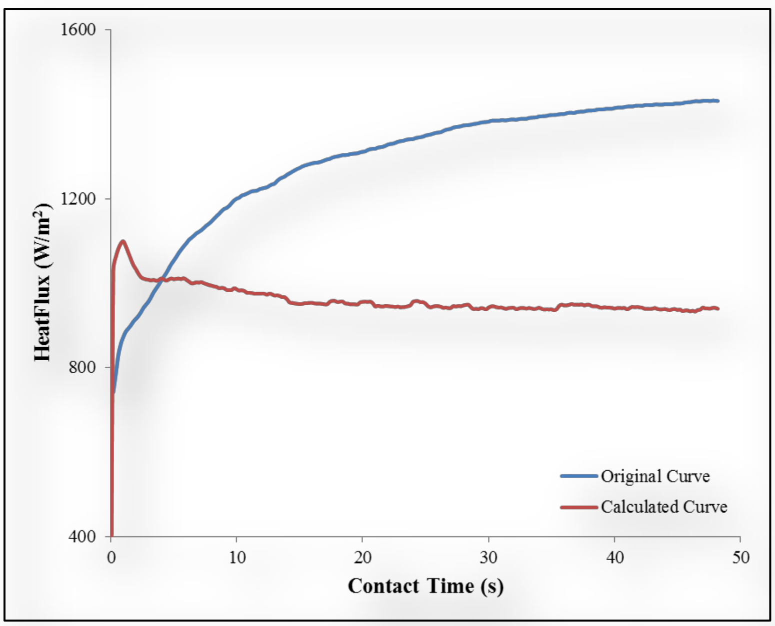

Figure 5-3 Typical Heat Flux Curves Original Measured and After Calculation

Meanwhile, most thermal sensation studies reviewed are based on sensing the ambient temperature as mentioned in Chapter 2. In order to use the concluded mathematical models, a thermodynamic model is proposed here to transform transient fabric thermal behavior into an equivalent skin-air circumstance. This skin-air circumstance could be expressed as shown in Figure 5-4(a). The air temperature is T_2 while the skin temperature is T_0. The heat flux h_2 could be expected in this thermodynamic system. For air at a temperature around 20°C (i.e. 293.15 K), its conductivity is 0.02 $Wm^{-1}K^{-1}$. The L value is set as 0.2 mm. Figure 5-4(b) is a thermodynamic illustration of the skin-fabric system. While the human skin and fabric temperatures balanced at T_0 and T_1, the heat flux h_1 would transfer from the human skin to the fabric as well. A and x represent the size of the contact area and fabric thickness, respectively.

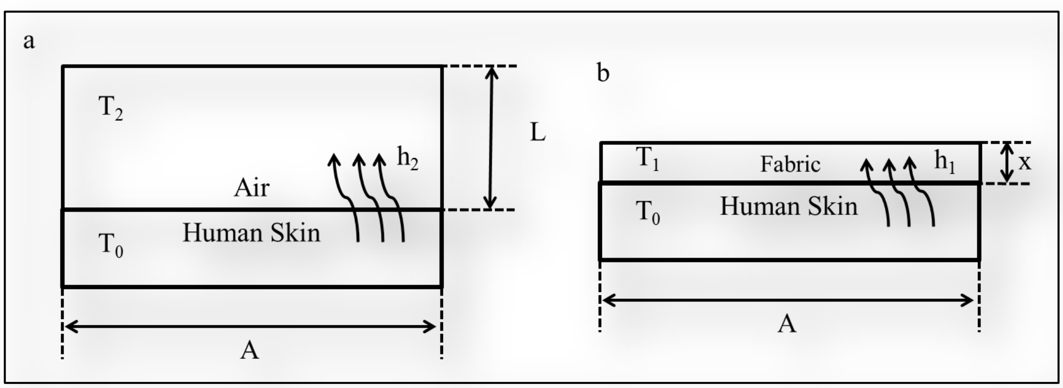

Figure 5-4 Illustration Figure of Thermodynamic System during Temperature Detection: (a) thermodynamic figure of skin-air system; (b) thermodynamic figure skin-fabric system

The thermodynamic formula of the skin-air and skin-fabric systems could be expressed by the following equations respectively.

$$h_2 = k_{air} \frac{\Delta T_2}{L} \quad (5\text{-}3)$$

$$h_1 = k_{fabric} \frac{\Delta T_1}{x} \quad (5\text{-}4)$$

where h_1, h_2 are the heat flux, k_{air} thermal conductivity of air, ΔT_2 temperature difference of the skin-air system (T_0-T_2), L sensitive distance, k_{fabric} thermal conductivity of the fabric, ΔT_1 the temperature difference of the skin-fabric (T_0-T_1), and x the thickness of the fabric.

The heat flux should be the same for these two thermodynamic equal systems (i.e. h_1=h_2), since the heat flux from the skin to the external environment is physiologically due to the body heat loss, which in other words, is the body response to the external environment. The basic idea of linking the two systems is to have them produce the same thermal stimulus, which obviously should cause the same body response. Therefore, the equation is expressed as:

$$k_{air} \frac{\Delta T_2}{L} = k_{fabric} \frac{\Delta T_1}{x} \quad (5\text{-}5)$$

This ΔT_2 could be then addressed by using:

$$\Delta T_2 = \frac{k_{fabric} * \Delta T_1 * L}{k_{air} * x} \quad (5\text{-}6)$$

Thermoreceptor response index

An index that defines psychosensory intensity (PSI) was proposed in prior studies (Ring & de Dear, 1991). The definition of this index was based on a theory from Hensel (Hensel, 1981) as reviewed in Chapter 2. Hensel's model showed that the impulse firing rate of the cold receptors would be integrally impacted by both the static environment temperature and dynamic temperature change rate. The relationship could be expressed as (Ring & de Dear, 1991):

$$Q(y,t) = K_s T_{sk}(y,t) + K_d \frac{\partial T_{sk}(y,t)}{\partial t} \tag{5-7}$$

where $Q(y,t)$ is the impulse firing of the cold receptors with specified time t and vertical depth of receptor y. $T_{sk}(y,t)$ the skin temperature with specified time t and vertical depth from the skin surface y. K_s and K_d the coefficients of these two parts.

In an application of this model, the dynamic property of heat flux during fabric thermal property measurement was proposed to represent the impulse responses of the cold receptors (J. Y. Hu, Hes, et al., 2006). The changes in the rate of heat flux were plotted and the PSI was calculated as the integral of the change rate curve with the following equation:

$$PSI = \int_{t_{d1}}^{t_{d2}} \frac{\partial HF(t)}{\partial t} dt \tag{5-8}$$

where HF(t) is the heat flux at time t, t_{d1} and t_{d2} are defined as the time when contact starts and when the intensity of heat flow is steady respectively. This method, however, neglects the temperature variances of fabric during contact.

Empirical modifications to Equation (5-7) was further made recently in (Z. Wang, Li, Kowk, & Yeung, 2002). The values of the coefficients K_s, K_d, and S were calculated as -0.72, -50, and 28.1 respectively based on animal research with the hand of monkeys and nose of cats (Hensel, 1981).

$$Q(y,t) = K_s T_{sk}(y,t) + K_d \frac{\partial T_{sk}(y,t)}{\partial t} + S \qquad (5\text{-}9)$$

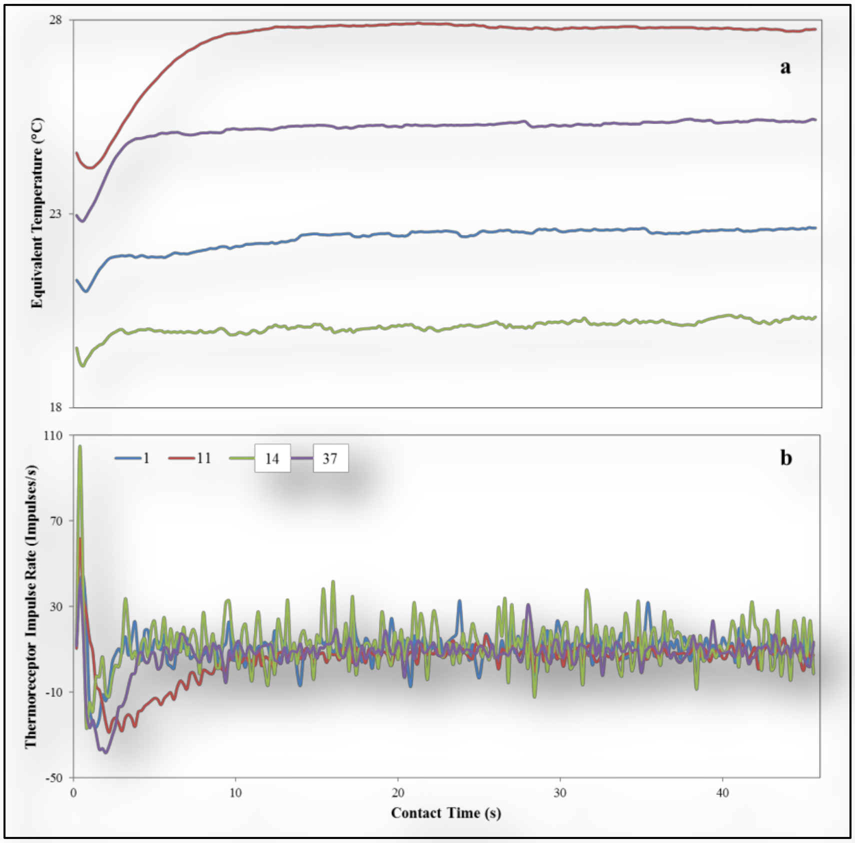

Figure 5-5 Typical Figures of Equivalent Temperature of Fabric and Responses of Thermoreceptor: (a) calculated equivalent temperature of contacted fabrics based on equation (5-6); (b) responses of thermoreceptors when contacting based on equation (5-9).

Figure 5-5(a) shows that there is always a reduction in the equivalent temperature in a short period of time, that is, within 5 seconds, after contact takes place. X-axis of Figure 5-5 stands for the contact time in second. Shown fabrics include Code 1, 11, 15 and 38. The equivalent temperature gradually increases afterwards until a static value is reached. This phenomenon is in agreement with the previous result from the heat flux curve. A sudden “cold” feeling would be anticipated followed by the approaching of the steady state. Figure 5-5(b) shows the calculated thermoreceptor responses (Q) based on equivalent temperature via Equation (5-9). It is obvious that the peak value is obtained soon after contact. The thermoreceptor response subsequently declines and then gradually returns to a relatively stable value. It is noticed that the thermoreceptor response has negative values. There are two components described in Equation (5-9) for determining thermoreceptor responses. The coefficient of the dynamic part, K_d, is negative. Therefore, when the temperature is increasing, the contributed value of the dynamic part $k_d \frac{\partial \mathrm{T_{sk}(y,t)}}{\partial \mathrm{t}}$ is negative. As a result, it is reasonable that the calculated thermoreceptor response is less than zero. These negative values are believed to indicate that a “warm feeling” could actually be perceived during those periods of time.

On the base of these typical curves, three indexes were identified named Q_{upsum}. $Q_{downsum}$, and Q_{steady}. Q_{upsum} was calculated as integral of Q from contact begins till when the minimum response value appears. $Q_{downsum}$ was calculated as integral of Q from the minimum response value appears till when it became steady. Q_{steady} was calculated as the mean value during steady state.

$$Q_{upsum} = \int_{t_{d1}}^{t_{d2}} \frac{\partial Q(t)}{\partial t} dt \qquad (5\text{-}10)$$

$$Q_{downsum} = \int_{t_{d2}}^{t_{d3}} \frac{\partial Q(t)}{\partial t} dt \qquad (5\text{-}11)$$

$$Q_{steady} = \frac{1}{t_{dm} - t_{d3}} \int_{t_{d3}}^{t_{dm}} \frac{\partial Q(t)}{\partial t} dt \qquad (5\text{-}12)$$

where Q(t) is the impulse rate of the thermoreceptor at time t. t_{d1}, t_{d2} and t_{d3} are defined as the time when contact starts, when Q reaches the minimum value, and when the intensity of Q is steady respectively.

<u>Relative membrane current of TRPM8 channel</u>

Meanwhile, in research on thermal perception that concerns the sensing of air temperature, neuroscientists have managed to identify the responsible transducer and its function mechanism. They have recently agreed that TRPM8, a type of protein which is a member of the transient receptor potential (TRP) family, has a significant, if not the only role in sensing temperature. With regard to innocuous cold sensation, TRPM8 was concluded as the main affecting protein (Bautista et al., 2007; Colburn et al., 2007; Dhaka et al., 2007). A significant amount of attention has been paid to the thermal sensitivity function of these TRPs recently (see review in (Voets, 2012)). This channel is considered to be a voltage-gating channel and experiments have indicated that temperature sensing via the TRPM8 channel is accomplished by its intrinsic changes other than cellular signaling (Tominaga et al., 1998; Voets et al., 2004; Zakharian, Cao, & Rohacs, 2010).

A two-state model is proposed to illustrate the simple gating mechanism of the TRPM8 channel as follows:

$$Close \underset{\beta(V,T)}{\overset{\alpha(V,T)}{\rightleftarrows}} Open \qquad (5\text{-}13)$$

where α and β represent the opening and closing rates respectively. They are related to the membrane voltage, V, and absolute temperature, T, based on the model in Hodgkin and Huxley (Hille, 2001). With K defined as the equilibrium between the open and closed states, the open probability of the TRPM8 channel can be calculated by (Voets, 2012):

$$P_{open} = \frac{\alpha}{\alpha+\beta} = \frac{1}{1+\frac{1}{K}} = \frac{1}{1+\exp\left(\frac{\Delta H - T\Delta S - zFV}{RT}\right)} \qquad (5\text{-}14)$$

where ΔH and ΔS are, respectively, the difference in the enthalpy and entropy (the unit is $Jmol^{-1}K^{-1}$) between the open and closed states, z is the gating charge, F the Faraday constant, and R the universal gas constant. In order to convert the unit of all the variables into the SI unit, the above equation could be revised as (Voets et al., 2007):

$$P_{open} = \frac{1}{1+\exp\left(-\frac{z}{k_B T}(V - V_{1/2}\right)} \qquad (5\text{-}15)$$

where k_B is the Boltzmann constant, and $V_{1/2}$ is the voltage for half-maximal activation. $V_{1/2}$ is defined by:

$$V_{1/2} = \frac{\Delta H - T\Delta S}{zF} \qquad (5\text{-}16)$$

By following these equations, free parameters, ΔH, ΔS, and z, were obtained through many electrophysiological cell experiments. The results revealed that these values of these three parameters for the TRPM8 channel are generally constant (Voets, 2012; Voets et al., 2007).

In a simulation of the TRPM8 current, P_{open} is usually first obtained by a function of T, V and t. The membrane currents are then calculated based on single-channel current times, $P_{open,}$ as (Siegelbaum & Koester, 2013):

$$Current = i * n * P_{open} \tag{5-17}$$

where n is the number of channels and i is the single channel current, which could be identified by:

$$i = (V - V_e)g \tag{5-18}$$

where V_e is the equilibrium membrane potential and g single channel conductance. The Q_{10} value for the single-channel conductance, which is used to define the temperature-dependence of a channel, was set as 1.35 (Voets, 2012).

For different thermo-TRPs, the above approach has been reported to accurately simulate the temperature-dependent behavior of these channels under both kinetics and steady-state conditions (Karashima et al., 2009; Talavera et al., 2005; Voets et al., 2004; Vriens et al., 2011).

In the membrane current simulation carried out in this Ph.D. research, the values of the above free parameters and constant were set to be the same as those in the published data (Voets et al., 2007), which are: $z=0.89e_o$ ($1.42*10^{-19}$ C equivalent); $\Delta S=-560\ Jmol^{-1}K^{-1}$; $k_B=1.38*10^{-23}\ JK^{-1}$; $F=9.65*10^{-4}\ Cmol^{-1}$, and V=-80 mv.

Based on Equation (5-18), the single channel current *i* is a linear temperature-dependent under a certain membrane voltage. Single channel conductance g is a linear temperature-dependent with a slope of 0.135. Therefore, when calculating the total membrane currents of TRPM8, a relative current value would be estimated other than the absolute value.

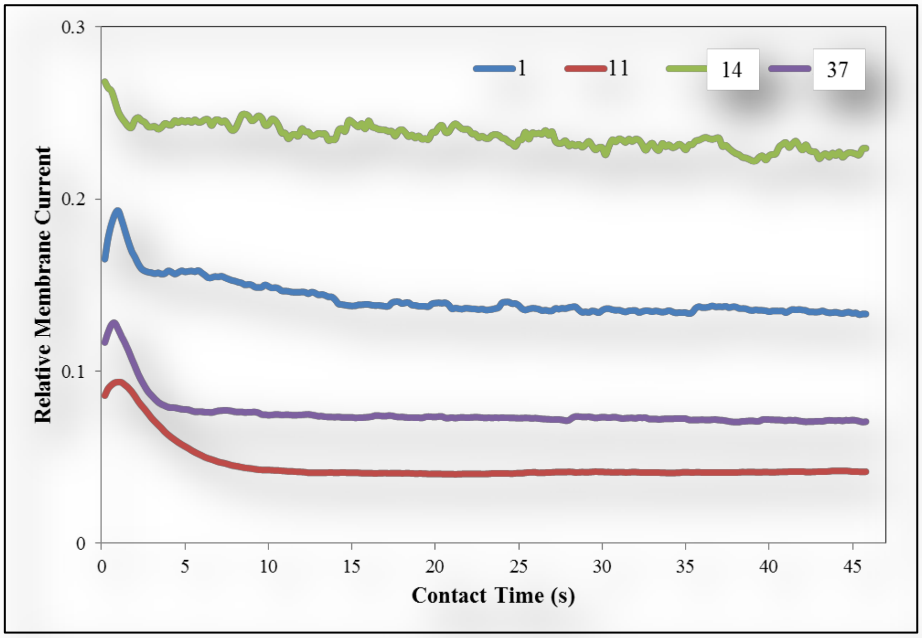

Figure 5-6 Typical Curves of Calculated TRPM8 Channel Membrane Currents

Figure 5-6 displays four typical curves calculated for the TRPM8 channel membrane currents. Membrane voltage values were set at -80mv. Fabric thickness values were calculated at normal pressure of 5gf/cm2. They are one specimen tested on Fabrics 1, 11, 15, and 38, and calculated under a normal pressure of 5 gf/cm^2. It is obvious that all of the fabrics show a peak pattern at the very beginning of the contact. In following the peak, relative steady patterns can be found. The differences between the maximum and steady values also vary from fabric to fabric.

Identification of the neurophysiological indexes based on the calculated relative membrane currents is shown in Figure 5-7. The related calculation formulas are as follows.

$$C_{max} = \max \ (C) \qquad (5\text{-}19)$$

$$C_{steady} = \frac{1}{t_{max} - t_{steady}} \int_{t_{steady}}^{t_{max}} C dt \qquad (5\text{-}20)$$

$$C_{diff} = C_{max} - C_{steady} \qquad (5\text{-}21)$$

where t is the contact time, t_{steady} is the time when the current value remains steady and t_{max} is the maximum measured time.

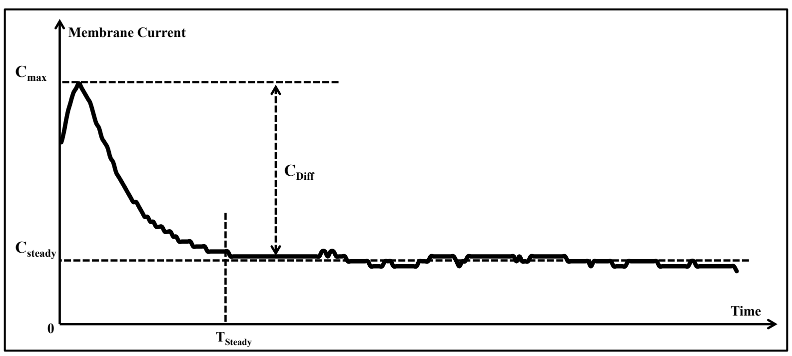

Figure 5-7 Identification of Neurophysiological Indexes

<u>Modified thermoreceptor response</u>

Previous findings have also stated that nerve response to cold stimulus depends on both the changing temperature and rate of temperature change, see (Heinz, Schafer, & Braun, 1990; Schafer, Braun, & Kurten, 1988). Studies on the molecular mechanism of these findings are still currently undergoing. Few hypotheses have been made to quantitatively describe the effect of the rate of temperature change on nerve response (Carr et al., 2003).

Equations for calculating TRPM8 currents as described above include absolute temperature as a parameter while the rate of the temperature change has not been mentioned. For the purpose of containing potential impacts from both steady and dynamic temperature changes, further evaluation of the electrophysiological findings of the TRPM8 transduction mechanism was proposed. The classic model, Equation (5-7), has been used to reveal the impulse rate based on both static and dynamic temperature influences.

The relative membrane current is calculated from the second hypothesis whilst the impulse rate is calculated by using Hensel's model. The impulse rate, or otherwise known as the frequency of action potentials, is proportional to how differently the neurons in the membrane current behave (J. H. Byrne, 2010). In order to apply Equation (5-7), a normalized value should be used for the steady and dynamic components with the same component coefficients.

$$Q2(t) = K_s{}'\mathrm{C}(\mathrm{t}) + K_d{}'O(t) \qquad (5\text{-}22)$$

where C is the relative membrane current at time t and O, the normalized rate of the temperature change at time t. K_s' and K_d' are the standardized coefficients of these components, which were calculated as 0.035 and -0.986 respectively. Theoretically speaking, lower temperatures would lead to higher membrane currents of TRPM8, which would also elicit a stronger thermoreceptor response. Therefore, K_s' should present a positive coefficient to Q2. K_s is negative because it influences Q2 on the basis of the absolute temperature. A higher absolute temperature is theoretically believed to reduce the thermoreceptor response. The normalization of the obtained O values follow the feature scaling approach. Indexes similar to Q have been identified for Q2, including $Q2_{upsum}$, $Q2_{downsum}$ and $Q2_{steady}$.

5.2.2 Discussion on Coded Thermal Information

Multi-ANOVA tests were first conducted on the defined neurophysiological indexes for thermal sensation. Table 5-3 shows a summary of the results while detailed results are provided in the appendix. All of the defined indexes show significant differences between 20 types of fabrics ($p<0.001$). As regards the effects of interaction from the fabric and normal pressure, based on Hypothesis 1, $Q_{downsum}$ and Q_{steady} demonstrate significant differences ($p<0.01$); and C_{max}, C_{steady}, and C_{diff} on the basis of Hypothesis 2 all show significant differences ($p<0.001$). It is also observed that the F values of the indexes related to Q2 are relatively low among these indexes. This implies that the differences of fabrics with regard to the Q2-base indexes are not as large as those of the other two groups.

Spearman's correlation tests were then performed to evaluate the relations between indexes based on the three different hypotheses. Table 5-2 shows the correlation results of the indexes obtained with a normal pressure of 5 gf/cm^2. There is no significant correlation observed between the Q2 indexes based on Hypothesis 3. The only significant correlation shown for the Q-base indexes is between $Q_{downsum}$ and Q_{steady} and their correlation is positive. With regard to the relative membrane current, C, C_{max} is observed to be significantly correlated to both C_{steady} and C_{diff}. It can also be noticed that C_{max} and C_{steady} show significant correlations, although with different coefficients, to

$Q_{downsum}$ and Q_{steady}. The results of the comparison with normal pressures of 42 and 70 gf/cm^2 show similarities, while $Q2_{downsum}$ and $Q2_{steady}$ present significant correlations ($p<0.01$). The results are presented in the appendix in detail.

Table 5-2 Correlation of Thermal Neurophysiological Indexes Obtained with Normal Pressure of 5gf/cm^2

Index	Statistic	$Q2_{upsum}$	$Q2_{downsum}$	$Q2_{Steady}$	Q_{upsum}	$Q_{downsum}$	Q_{steady}	C_{max}	C_{steady}	C_{diff}
$Q2_{upsum}$	Coefficient	1								
	p Value									
$Q2_{downsum}$	Coefficient	--	1							
	p Value	--								
$Q2_{Steady}$	Coefficient	--	--	1						
	p Value	--	--							
Q_{upsum}	Coefficient	--	--	--	1					
	p Value	--	--	--						
$Q_{downsum}$	Coefficient	--	--	--	--	1				
	p Value	--	--	--	--					
Q_{steady}	Coefficient	--	--	--	--	0.486	1			
	p Value	--	--	--	--	0.030				
C_{max}	Coefficient	--	--	--	--	--	0.899	1		
	p Value	--	--	--	--	--	0.000			
C_{steady}	Coefficient	--	--	--	--	0.641	0.935	0.920	1	
	p Value	--	--	--	--	0.002	0.000	0.000		
C_{diff}	Coefficient	--	--	--	--	--	--	0.526	--	1
	p Value	--	--	--	--	--	--	0.017	--	

Table 5-3 Summary of Multi-ANOVA Analysis Results

Source	Fabric Code		Normal Pressure		Fabric Code* Normal Pressure	
	F Value	p Value	F Value	p Value	F Value	p Value
Q_{upsum}	63.4	0.000	--	--	--	--
$Q_{downsum}$	158.0	0.000	83.8	0.000	2.8	0.000
Q_{steady}	259.7	0.000	449.4	0.000	1.9	0.002
C_{max}	87.2	0.000	457.9	0.000	5.9	0.000
C_{steady}	195.1	0.000	381.5	0.000	10.1	0.000
C_{diff}	31.3	0.000	191.9	0.000	3.4	0.000
$Q2_{upsum}$	24.5	0.000	5.8	0.003	--	--
$Q2_{downsum}$	29.6	0.000	--	--	--	--
$Q2_{steady}$	8.6	0.000	5.1	0.000	--	--

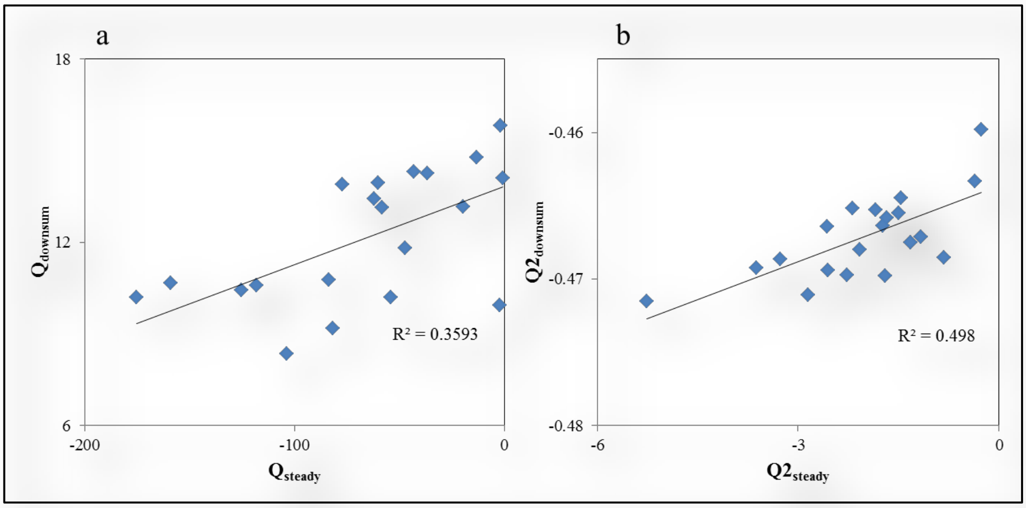

Figure 5-8 Scatterplots between Q_{steady} and $Q_{downsum}$ as well as $Q2_{steady}$ and $Q2_{downsum}$ (obtained with normal pressure at 42gf/cm^2)

Figure 5-8 shows the scatterplots of Q_{steady} and $Q_{downsum}$ as well as $Q2_{steady}$ and $Q2_{downsum}$. There are general linear correlations observed in both pairs. According to the definition of the indexes based on thermoreceptor response, Q_{upsum} and $Q2_{upsum}$ are the neural responses during periods of sudden temperature reduction while

$Q_{downsum}$ and $Q2_{downsum}$, during the stage of temperature increase before reaching the steady state. Q_{steady} and $Q2_{steady}$ demonstrate steady-state response rates. The finding suggests that larger steady-state values of the thermoreceptor response are roughly linked to larger impulses during temperature increasing stage.

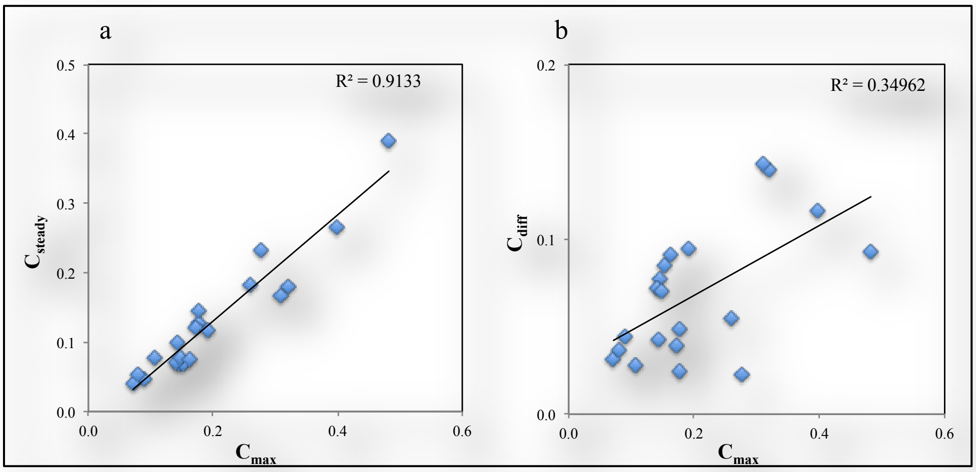

Figure 5-9 Scatterplots between C_{max} and C_{steady} as well as C_{max} and C_{diff} (obtained with normal pressure at 5gf/cm^2)

Similar situations are observed for the C-base indexes as well. Figure 5-9 shows the scatterplots of the indexes defined on the basis of Hypothesis 3. Fabrics with higher C_{max} values are very likely to also show higher C_{steady} values. The correlation coefficient implies that the C_{max} value is also positively related to C_{diff}. However, the scatterplot in Figure 5-9(b) suggests that such a relation is actually quite weak.

Hypotheses 1 and 3 both calculate the thermoreceptor responses based on Hensel's model, through different characterization methods of the component related to the absolute temperature. Q is calculated based on the equivalent absolute temperature and rate of temperature change while Q2 is calculated on the basis of the calculated relative membrane current and rate of temperature change. Spearman's correlation test as mentioned, however, indicates that there is no significant correlation between the indexes that are calculated based on Hypotheses 1 and 3.

Table 5-4 Correlation Results between Neurophysiological Indexes and Corresponding Physical Indexes

Index	Statistic	TCC	T	TMF
$Q2_{upsum}$	Coefficient	--	--	--
	p Value	--	--	--
$Q2_{downsum}$	Coefficient	--	--	--
	p Value	--	--	--
$Q2_{steady}$	Coefficient	--	--	--
	p Value	--	--	--
Q_{upsum}	Coefficient	--	--	--
	p Value	--	--	--
$Q_{downsum}$	Coefficient	--	-0.564	0.621
	p Value	--	0.010	0.003
Q_{steady}	Coefficient	--	-0.492	0.839
	p Value	--	0.028	0.000
C_{max}	Coefficient	--	-0.672	0.885
	p Value	--	0.001	0.000
C_{steady}	Coefficient	--	-0.717	0.952
	p Value	--	0.000	0.000
C_{diff}	Coefficient	-0.453	-0.466	--
	p Value	0.045	0.038	--

A comparison between these neurophysiological indexes and previously defined physical indexes was conducted as well. Table 5-4 shows the correlation coefficients and p values by using the Spearman's correlation test. The thermal indexes TCC and TMF as well as the thickness index T are examined. The neurophysiological indexes calculated under a normal pressure of 5 gf/cm^2 are presented. The coefficient relations observed are similar for the three normal pressure conditions. Comparisons under the other two normal pressure conditions are provided in the appendix. It can be observed that both C_{max} and C_{steady} show high correlation to the physical index

TMF while the coefficients of C_{steady} and TMF are even larger than 0.9. They are also found to be negatively correlated to physical index T. $Q_{downsum}$ and Q_{steady} also show positive correlation to TMF and negative correlation to T.

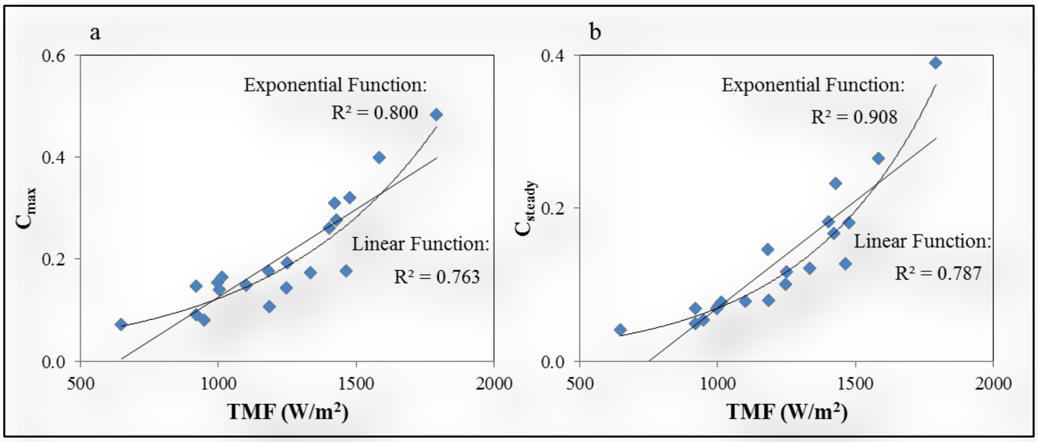

Figure 5-10 Scatterplots between Neurophysiological Indexes C_{max} and C_{steady} and Physical Index TMF

Figure 5-10 shows the scatterplots for the TMF physical index and C-base neurophysiological indexes. Calculations of Cmax and Csteady were conducted under normal pressure at 5gf/cm2. The Spearman's correlation coefficients were concluded as 0.885 and 0.952 respectively. The correlations of both types of indexes are found with a better model fit (R^2 value) with exponential functions. Such a relation implies that molecular thermal neural responses are likely to be correlated to the maximum heat flux measured. In addition, the correlations between C_{max} and C_{steady} with the TCC physical index are not significant. Therefore, a special value like the TMF may better represent the molecular responses of thermal transducers other than standard calculated values of the TCC.

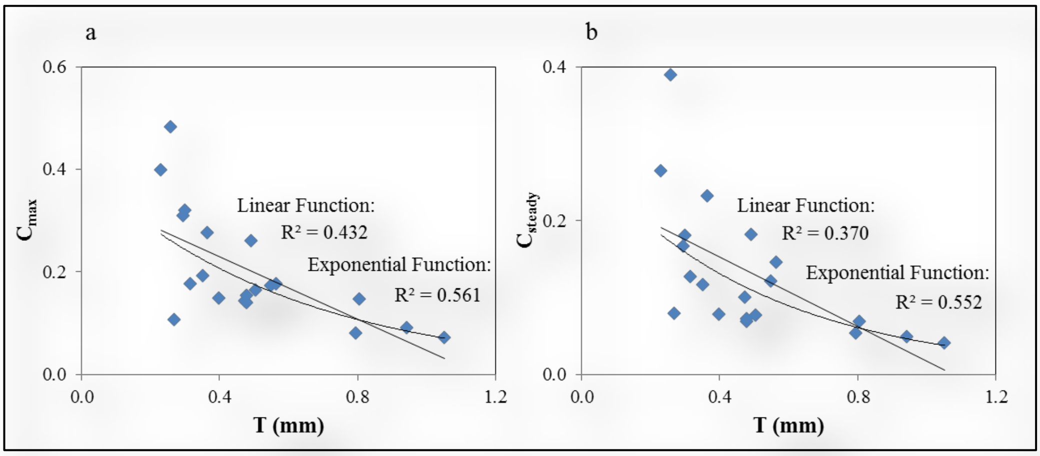

Figure 5-11 Scatter Plots between Neurophysiological Indexes C_{max} and C_{steady} and Physical Index T respectively

Meanwhile, significant negative correlations are found between C_{max}, C_{steady} and the T physical index. Figure 5-11 shows the scatterplots. Calculations of Cmax and Csteady were conducted under normal pressure at 5gf/cm2. The Spearman's correlation coefficients were concluded as -0.672 and -0.717 respectively. Generally speaking, fabrics with lower values in T show higher TRPM8 membrane currents, regardless of the maximum or the steady value. TCC is defined as an index to express the conductivity of fabric regardless of its thickness. It describes more about the fibers other than the construction of the fabric, whilst for textile materials, the final state of the fabric could largely affect its properties. It is hardly possible to change thickness of fabrics without affecting their conductivity. As a result, correlation testing suggests that fabric conductivity only shows a limited relationship to the thermal responses that it may cause. It would be inadequate to address the thermal sensation of fabrics if their thickness is not taken into consideration.

The primary discussion on defined neural responses of received thermal information based on the three hypotheses is that all of the defined neurophysiological indexes show significant differences in terms of the 20 types of examined fabrics. Among them, four indexes, including $Q_{downsum}$, Q_{steady}, C_{max}, and $C_{diff,}$ show high correlation to the defined physical indexes, TMF and T. The TCC physical index is not significantly related to these neural responses. This suggests that physical indexes only describe the material properties of fabrics but not address the actual sensation that fabric may provide while the transient characteristic of fabric defined by the TMF might impact the thermal sensation of fabric. Limited correlation is found between Q2-base neurophysiological and physical indexes. There is neither significant correlation between Q2-base indexes and indexes calculated from the other two hypotheses. It seems that Hypothesis 3 has led to unique simulated neural responses to thermal information. Their relations and actual psychological perception will be analyzed in a later related discussion on neuropsychology in Chapter 8.

5.3 Coding Mechanism of Texture Information

Humans are able to discriminate the texture differences of objects that have even very similar features. Such texture discrimination is linked to the neural fiber response of SA1 or PC fibers in neurophysiological studies. A commonly derived conclusion is that the unevenness of the surface is triggered by SA1 or PC fibers. The literature review in Chapter 2 provided that element shape significantly affects the responses of afferent fibers and consequential stimulated sensation perception. The element features investigated mainly included height and center-to-center spacing. Meanwhile, despite modern research progress on the neurophysiological coding mechanism of smoothness perception, applications of these studies on daily used materials have been seldom evaluated (Weber et al., 2013).

Since uneven features of surface geometry are agreed to be the major reason that affects neural receptors, the test results from the FTT surface roughness module, are used in the following. Two physical indexes are defined, which include the surface roughness amplitude (SRA) and surface roughness wavelength (SRW). The FTT measured results in both the warp and weft directions. However, it is difficult to define the direction of touch evaluation when using human touch. As a result, the mean value from the warp and weft directions was used.

5.3.1 Hypothesis and Data Analysis

Simple linear coding of SA1 spatial variances

The relationship between the unevenness and the afferent fibers of mechanoreceptors was evaluated from a series of neurophysiological studies. As concluded from the majority of the literature, the spatial coding of SA1 fibers is responsible for texture information (D. T. Blake et al., 1997; Connor et al., 1990; Connor & Johnson, 1992; DiCarlo & Johnson, 2000; Phillips, Johansson, & Johnson, 1990).

In a study by Blake et al. (David T Blake et al., 1997), the effect of the unevenness of the height of an element was investigated. They found that the height of an element has a major effect on SA1 impulse rates if the element diameter is less than 2.0 mm. An experiment by Yoshioka et al. (Yoshioka et al., 2001) confirmed that grooved and ridge widths have an effect on surface roughness perception. Grooved and ridge widths could also be summed up as element width (or center-to-center distance). An interpolated equation from these two studies is linearly expressed as:

$$I = \mathrm{b} + K_h S_h + K_w S_w \qquad (5\text{-}23)$$

where I denotes the estimated impulse rate of a single SA1 fiber, S_h and S_w are the height and width of the stimulus, K_h (166.437) and K_w (-5.957) are the coefficients of the height and width of the stimulus, and b is a constant (116.508).

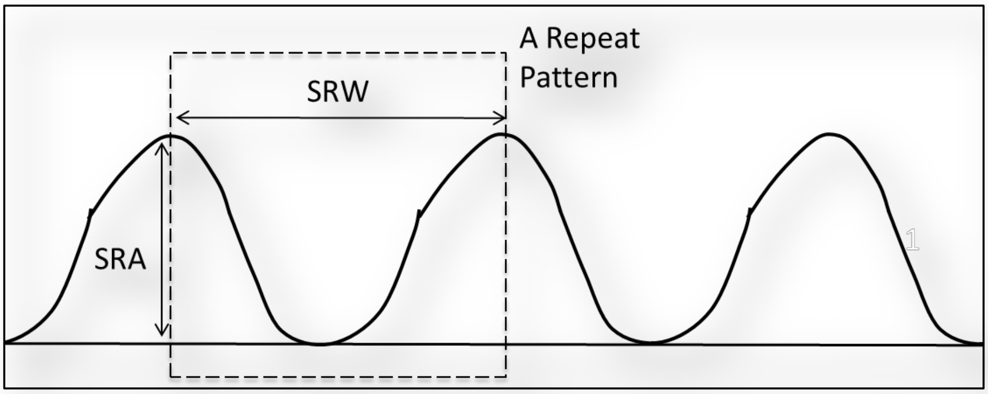

Figure 5-12 Sinusoid Characterization of Fabric Unevenness Elements on Its Surface

In Hypothesis 1, the unevenness element of fabrics is simplified as repeated patterns that are similar to sinusoids. Consequently, the height of unevenness could be addressed by using the FTT index, SRA, while the width of unevenness can be represented by using the FTT index, SRW, as illustrated in Figure 5-12. Solid curve stands for unevenness elements on the fabric surface. Dashed part represents one characterized repeat pattern. The mathematical relations between the SA1 impulse rate and unevenness height and width could therefore be used to predict the SA1 impulse rate from the FTT indexes, SRA and SRW, by using Equation (5-23). It is implied in this hypothesis that regular sinusoid components on the fabric surface would produce a constant response from SA1 fibers during surface texture evaluation.

Weighted power coding of PC temporal variances

Besides coding mechanisms based on spatial variances of SA1 fibers, questions have been raised on the effects of other afferent fibers. Hollins and Risner, and Hollins and Sigurdsson (Hollins & Risner, 2000; Hollins & Sigurdsson, 1998) proposed a duplex theory of roughness perception. They agreed that the coding mechanism for coarse texture is spatial encoding and proposed that vibrotactile encoding would be more appropriate for fine texture. In later studies by (S. J. Bensmaia & Hollins, 2003; Hollins et al., 2002), it was indicated that minor unevenness at a micrometer scale would lead to skin vibrations received by the nerve receptors; that is, the PC fibers.

Between the temporal (peak frequency) and intensive information (power of the vibrations-weighted) of skin vibration, Bensmaia and Hollins (S. J. Bensmaia & Hollins, 2003) proposed that the perceived roughness of fine textures is a function of the latter code. As a result, an index of the PC vibration weighted power, proposed by Makous et al. (Makous et al., 1995) was adopted in later studies. This study found that perceived roughness is a logarithmic function of the weighted power of PC fiber responses (S. Bensmaia & Hollins, 2005). The index of the weighted power (W) of PC fiber vibration was calculated according to:

$$W = \sum_{i=1}^{200} {A_i}^2 {f_i}^2 H_i \qquad (5\text{-}24)$$

where A_i refers to the stimuli amplitude at frequency f_i, f_i is set with a constant interval, 2 in the study by Bensmaia and Hollins (S. J. Bensmaia & Hollins, 2003), and H_i denotes the weight of the sensitivity of the PC fibers . H_i is given by

$$H_i = \frac{\min \ \{T_i{}^2 f_i{}^2 -- T_i{}^2 f_i{}^2\}}{[T_i]^2 f_i{}^2} \qquad (5\text{-}25)$$

where T_i denotes the PC fiber threshold at frequency f_i.

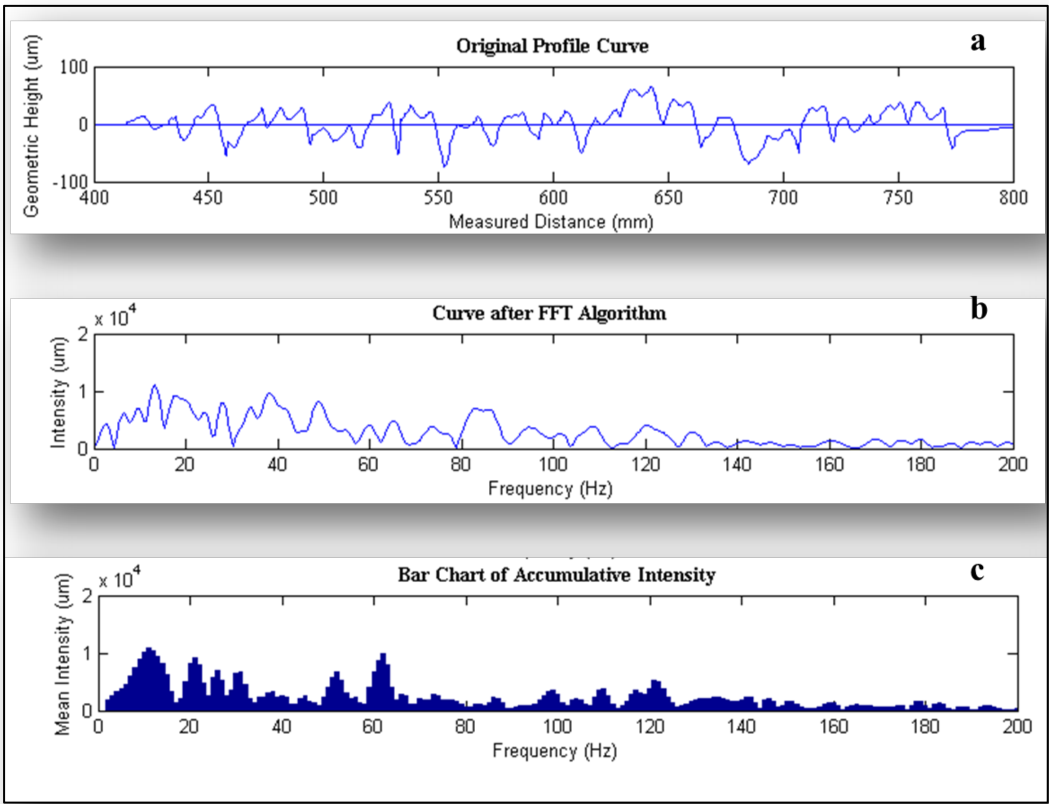

Figure 5-13 Fast Fourier Transform Algorithm on Fabric Surface Profile: (a) original FTT measured surface profile curve is made of discrete points along measured distance (x axis); (b) Spectrum curve after FFT with x axis as frequency and y axis as intensity; (c) Intensities in frequency bin of 1 Hz are averaged and plotted as bar chart.

The thresholds of the PC fibers used by Bensmaia and Hollins (S. J. Bensmaia & Hollins, 2003) were interpolated from the findings of Bolanowski et al. in 1988

(Bolanowski, Gescheider, Verrillo, & Checkosky, 1988) and linearly extrapolated until 1500 Hz. It was also reported that human skin vibrations basically mirror the geometric properties on the stimuli surface (S. J. Bensmaia & Hollins, 2003). As a result, Hypothesis 2 requires a detailed characterization of the surface geometric properties of the stimuli. The fast Fourier transform (FFT) is usually used to obtain such information.

The FFT algorithm is used to analyze the wave-form results and classify the number of sinusoid components that form the wave. The outputs of the FTT measurement are in pairs of distance and height. These two indexes actually present the intensities and frequencies (distance based) of the unevenness, as shown in Figure 5-13(a). After the FFT algorithm is used, as shown in Figure 5-13(b), sinusoid components with different intensities are arranged according to their frequencies. Meanwhile, the frequencies of these elements after using FFT are based on the measured distance. On the other hand, frequency information that the skin receives would be clearly based on time. Therefore, a transformation was conducted, as follows:

$$f = vF \tag{5-26}$$

where f is frequency based on time, F is frequency based on distance, and v is the scanning speed. The scanning speed when the subjects were evaluating stimuli is concluded to be 70±5 mm/s based on a psychophysical subjective measurement, which is reported in Chapter 6.

The maximum investigated frequency was set at 200 Hz, i.e. the minimum repeated distance evaluated was 0.35 mm. The frequency bin applied in this study is 1 Hz.

The intensities recorded within the frequency bin were averaged. The thresholds of the PC fibers were extrapolated as a linear function of the vibration frequencies from 10 to 1000 Hz (Muniak, Ray, Hsiao, Dammann, & Bensmaia, 2007).

This hypothesis addresses in more detail the fabric surface texture. It is proposed that every uneven element on the surface of a fabric would stimulate neural signals as long as their intensity exceeds the perception threshold. Therefore Hypothesis 2 includes studies not only on the roughness caused by the fabrication structure, but also the roughness of the yarns themselves, in contrast to those of Hypothesis 1.

<u>Average coding of temporal variances of SA1 and PC</u>

In a recent study, three different quantitative methods were used to determine the neural impulses, and they were summarized and compared in (Muniak et al., 2007). These three methods include the firing rate of individual afferents, mean firing rate of the entire population of active afferents, and number of active afferents. It was concluded that the logarithmic of the population firing rate has the best fit for psychological sensation. The mean firing evoked in a particular population was calculated in accordance with the stimulus amplitude and threshold. The thresholds were found to be linearly correlated to the stimulus frequency in a certain range (10 to 200 Hz for PC and SA1 fibers). The concluded formula of the mean population rate of SA1 and PC fibers is:

$$P = \frac{1}{N}\sum_{i=1}^{N}[k_i(\log_{10} A_i - \log_{10} T_i)] \qquad (5\text{-}27)$$

where k_i, A_i and T_i are the coefficient, stimulus intensity and fiber threshold respectively. N stands for the total number of stimuli calculated.

Similar to the analysis made for Hypothesis 2, first, the obtained roughness profile data were transformed by using FFT. The frequency bin was also set at 1 Hz. The FFT results that are within one frequency bin were averaged. The values of k_i and T_i were extrapolated as a linear function of the frequencies from 10 to 1000 Hz (Muniak et al., 2007).

This hypothesis provides a more direct calculation means of the impulse rates of both the SA1 and PC fibers, compared to that of Hypothesis 2. Their distinguishing criterion is considered to be the width of the unevenness (Weber et al., 2013). However, as for the heterogeneous texture surface of fabrics, there seems to be no clear conclusion on which types of neural fibers are responsible for the smoothness sensation. Therefore, an investigation on both types of fibers should be conducted.

5.3.2 Discussion on Coded Texture Information

An ANOVA test was first conducted on the calculated neurophysiological indexes. As shown in Table 5-5, it can be confirmed that there are significant differences between the fabrics examined in terms of all the calculated neurophysiological indexes.

Table 5-5 Summary of ANOVA Test on Neurophysiological Indexes

Neurophysiological Indexes	F Value	p Value
I, Coded SA1 Fiber Impulses Rate (H1)	45.596	0.000
W, Coded PC Fiber Weighted Power (H2)	41.795	0.000
P_1, Coded SA1 Fiber Population Impulses Rate (H3)	118.153	0.000
P_2, Coded PC Fiber Population Impulses Rate (H3)	155.967	0.000

Hypotheses 1 and 3 provide two different methods to calculate SA1 fiber responses when receiving texture information from the surface of fabrics. In the following figure, Figure 5-14, the results are shown. Error-bars for each data point represent the standard deviations in this figure and followings in this Chapter. The lowest value of I is found for Fabric 37, which is a 100% silk jacquard fabric, and the highest value of I is observed for Fabric 24, which is a polyester blended jacquard fabric. On the other hand, the lowest value of P_1 is recorded for Fabric 29, a nylon blend single jersey fabric while the highest value is found in Fabric 11, a polyester-wool blend woven flannel fabric. There are some similarities between the coded responses of these two SA1 fibers. For example, relatively low values are found for Fabrics 3 and 15. However, there seems to be no clear agreement on the results from these two hypotheses.

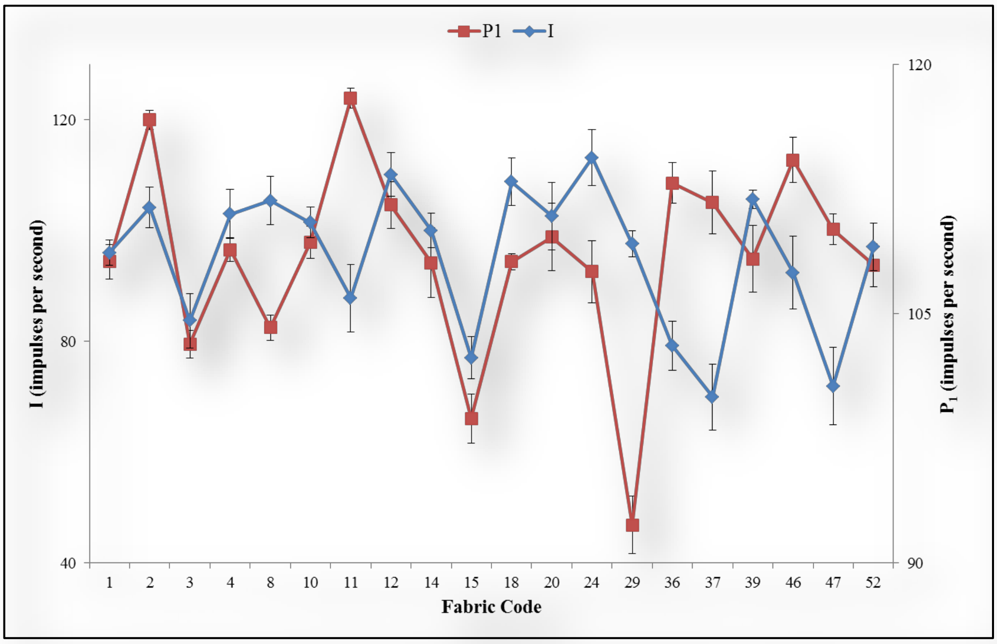

Figure 5-14 Results of Coded SA1 Fiber Responses I and P_1 respectively

Another correlation analysis carried out, as shown in Figure 5-15, indicated that there is no significant relation. The Spearman's correlation analysis showed that no monotonic relations could be found between them. Although both methods are similar in principle in that the unevenness of the height and width would affect the response of SA1 fibers, different calculation means have led to different outcomes.

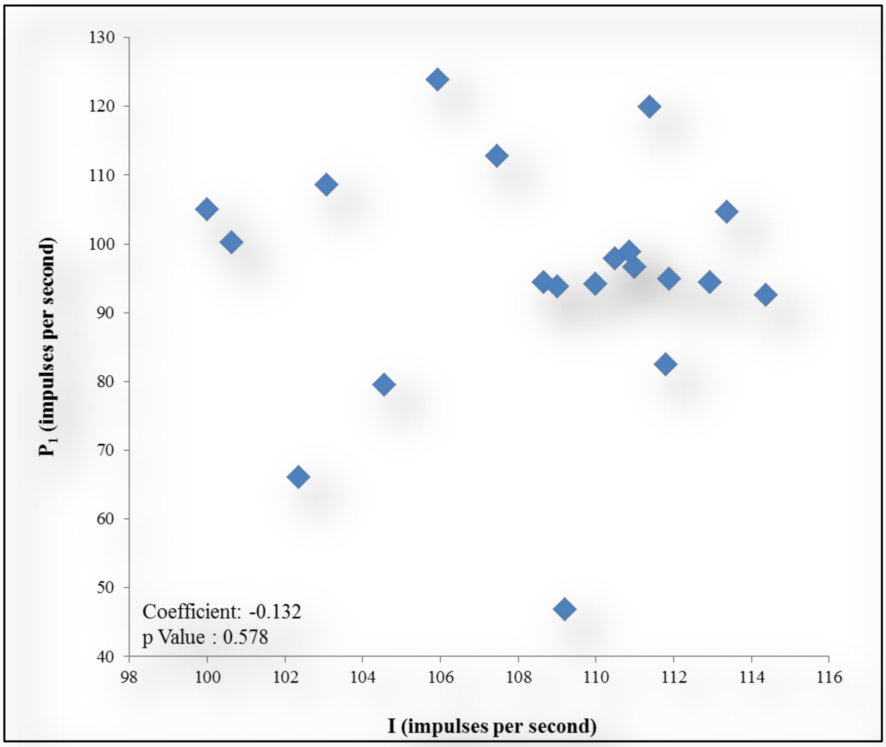

Figure 5-15 Relation Scatterplot of Coded SA1 Fiber Responses I and P_1

Meanwhile, Hypotheses 2 and 3 also demonstrate two distinct approaches to characterizing the responses from the PC fibers. Figure 5-16 shows the results calculated. Generally speaking, the variances for PC weighted power (W) are larger than those for impulse rate based on the PC population (P_2). The lowest values from both methods are found for Fabric 31, the nylon blend single jersey fabric. The highest values for both methods are observed for Fabric 11, the polyester-wool blend woven flannel fabric. These findings are in agreement with the results of P_1. It is also clear that the relation between the two hypotheses on PC fiber response is strong.

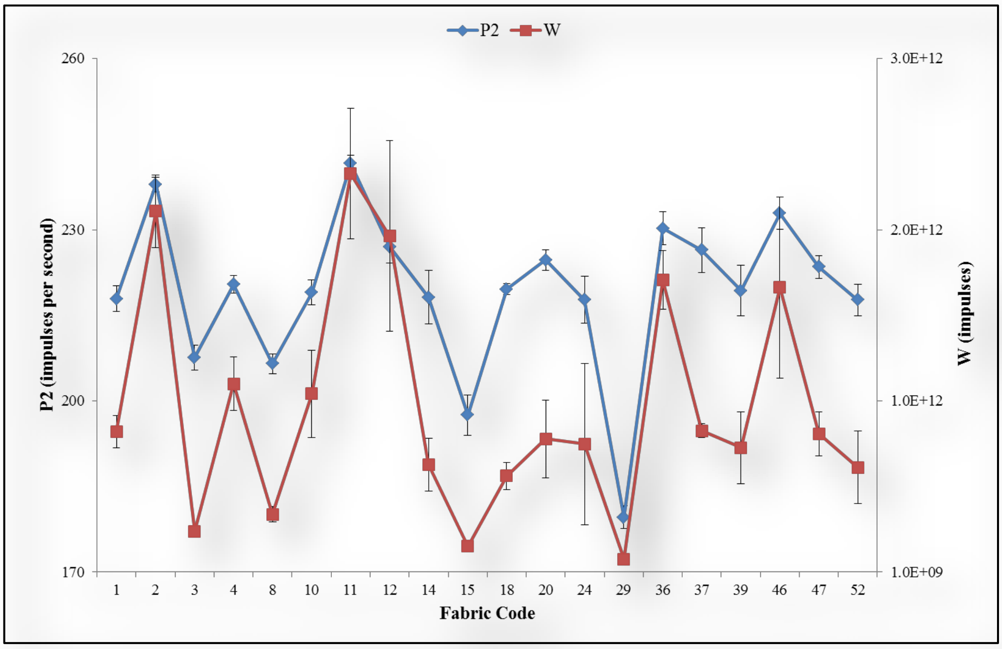

Figure 5-16 Results of Coded PC Fiber Responses W and P_2

As shown in Figure 5-17, the relation between these two neurophysiological indexes seems to fit in the logarithmic function. Their Spearman's coefficient is as high as 0.838. These two methods both examine the unevenness of elements on the fabric surface through sinusoid components after using FFT. This suggests that different degrees of the details examined may be the reason for the uncorrelated relation between indexes I and P_1.

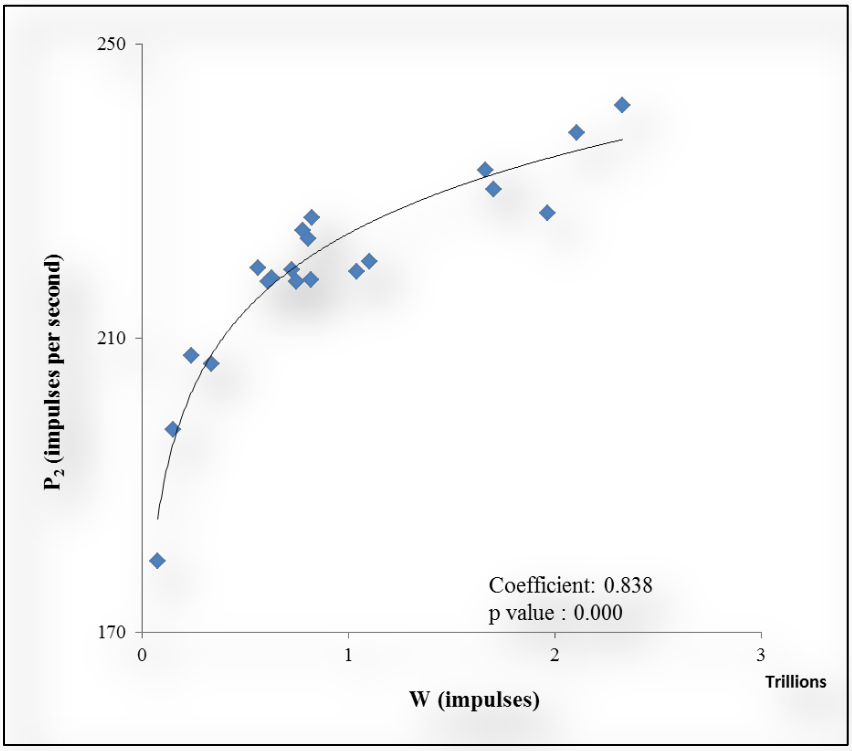

Figure 5-17 Scatterplot of Coded PC Fiber Responses W and P_2

Since Hypothesis 3 addresses both SA1 and PC fibers, their results are verified through a scatter plot as shown in Figure 5-18. A strong Spearman's correlation (0.983) is observed. In spite of the dissimilar coefficient k_i and threshold T_i as shown in Equation (5-27), these fibers demonstrate linear relations with each other. It can be concluded that under this calculation hypothesis of the impulse rate of a population of SA1 and PC fibers, the responses of these two types of receptors to stimulation such as those from fabric would be highly correlated.

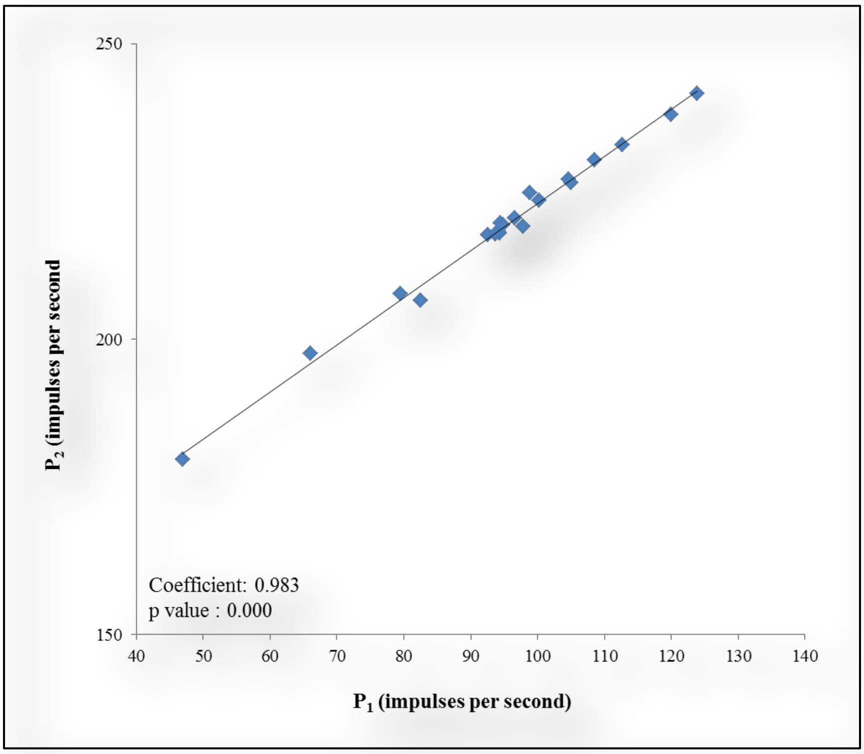

Figure 5-18 Relation Scatterplot of Coded SA1 (P_1) and PC (P_2) Fiber Population Impulses Rate

Table 5-6 shows the correlation results between the surface-related physical and neurophysiological indexes. Based on Hypothesis 3, the impulse rates of the population, regardless whether they are SA1 or PC fibers, show a significant correlation to both the SRA and SRW physical indexes. The weighted power of the PC fibers based on Hypothesis 2 does not show any correlation to the physical indexes while the impulse rate of SA1 fibers based on Hypothesis 1 only shows correlation to SRW.

Table 5-6 Correlation between Surface Physical Indexes and Neurophysiological Indexes

Index	Statistic	*I* (SA1)	*W* (PC)	P_1(SA1)	P_2 (PC)
SRA	Coefficient	--	--	.481	.573
	p Value	--	--	.032	.008
SRW	Coefficient	-.522	--	.448	.489
	p Value	.018	--	.048	.029

To further examine the relationship between the physical and the neurophysiological indexes, the sinusoid components after using FFT were compared with the SRA and SRW indexes. The highest intensity of the extracted sinusoid components were plotted against the SRA physical index obtained by the FTT. The frequencies of these components were also verified with the SRW physical index obtained by the FTT. The results are shown in Table 5-7. It can be observed that the highest intensity of the extracted sinusoid components shows a high correlation to the SRA physical index obtained by the FTT. However, the frequency of the components shows no correlation to SRW.

Table 5-7 Correlation between FTT Physical Indexes and Frequency and Intensity of Sinusoid Elements with Highest Intensity

Physical Index	Statistic	Frequency	Intensity
SRA	Coefficient	--	.940
	p Value	--	.000
SRW	Coefficient	--	.758
	p Value	--	.000

Since the basic concept of textile fabrication is to repeat the interlacing of two groups of yarns, there are two components that may constitute the surface geometric roughness. They include the unevenness of the yarn surface and fabrication structure. According to the definition of the SRA and SRW, these two indexes reflect roughness due to structure since their types of unevenness are usually much greater. Meanwhile, the FFT algorithm classifies various sinusoid components. The components with the highest intensity are therefore considered to be unevenness caused by the fabric structure. A strong correlation found confirms this logic. Nevertheless, the frequency of the component with the highest intensity shows no monotonic relation to the SRW index. This finding implies that despite the strong correlation of the SRA, this pattern recognition method is limited when it comes to characterizing the frequency of unevenness.

In this study, the unevenness of fabrics was measured up to a frequency of 200 Hz. In order to ascertain whether this pre-designed criterion is valid, an analysis was conducted to evaluate the intensity of the components with a frequency greater than 200 Hz. On average, based on the 20 types of fabrics examined, the intensity of the components at 200 Hz is only 6±6% of the highest intensity. This means that only vibrations with small amplitude could be recorded after 200 Hz. Unevenness at 200 Hz means that the smallest width is 0.35 mm.

5.4 Coding Mechanism of Received Force Information

The physical processing of compression and bending is actually similar. Although these two deformation processes are commonly classified as providing different physical properties of fabric, their stimulation principle is the same. In attempts to deform fabric, regardless of the compression or bending format, forces are applied onto the sample and resistance forces from the sample are perceived by the human skin. Such forces could lead to skin indentation and stimulate the response of skin receptors. Therefore, the coding mechanism of these two fabric processing means should be the same. The coding is called the coding of received force information in this study.

As reviewed in Chapter 2, it is generally agreed upon that SA1 fibers are responsible for external information in terms of received force and skin indentation. However, neurophysiologists have not reached an agreement on whether proprioceptive information is essential aside from cutaneous information. This means that aside from the forces received by the human skin, the distance that human fingers move may also provide information for softness discrimination. In following defined neurophysiological hypotheses, these two circumstances are therefore addressed.

5.4.1 Hypothesis and Data Analysis

Total impulses of SA1 fiber

The compression process has two stages, which are pressing and recovering. During pressing, force (F_P) is applied onto the fabric and subsequently the resistance force (F_R) would be received by the human skin. During fabric recovering, the F_P is gradually being reduced. The recovery force of the fabric (F_R) is made towards the skin.

The firing properties of SA1 fibers were concluded in (Wheat, Salo, & Goodwin, 2010) as a linear function to the normal force applied onto fingers. Normal forces were applied onto the fingertips of monkeys, which ranged from 0.2 N to 2.5 N. The contact area was approximately 452.16 mm^2 (with a contact probe that had a diameter of 24 mm). For the purpose of easier future comparisons, the normal forces recorded were transmitted into the amount of normal forces in an area of 1 mm^2 (i.e. pressure) accordingly. The linear formula was interpolated (with linear regression coefficient R^2 at 0.962 and p value at 0.000) as:

$$M = mF + n \qquad (5\text{-}28)$$

where M is the predicted impulse rate of the SA1 fibers when receiving force at F. m and n are empirically defined coefficients at 10,632 and 2 respectively.

The physical data obtained from the FTT measurement show normal pressures and corresponding fabric thickness. The measured normal pressure, which is the y axis in Figure 5-19, is the normal pressure that is expected to be received by the skin when the fabric is compressed; in other words, normal force in an area of 1 mm^2. Thickness is a commonly used dimension in describing fabric compressibility. While compression is conducted at a steady speed, thickness change is proportional to the time that taken to carry out the compression. Therefore, the total impulses during compression are calculated by using the following equation:

$$T_{cj} = \int dt f(P_i) \qquad (5\text{-}29)$$

where T_{cj} is the total impulses of the SA1 fibers during the j^{th} period, t is the time used for the j^{th} period, P_i is the pressure measured and $f(P_i)$ is the impulse rate of the SA1 fiber as calculated by Equation (5-28).

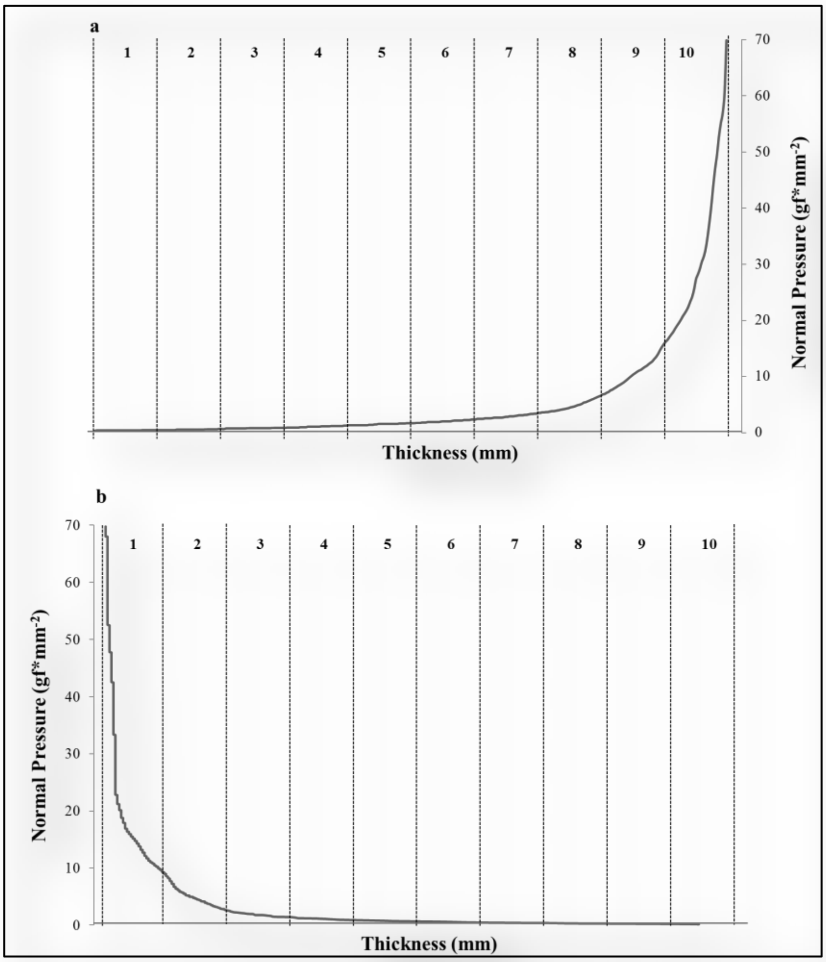

Figure 5-19 Classification of Compression Stages on the basis of Thickness Changed: (a) presents pressing process while (b) shows recovering process. Numbers on the top represent pressing stages and recovering stages respectively.

The deformation process of textile material is usually not consistent, and the physical properties of fabrics vary in terms of different degrees of compression. Consequently, both pressing and recovering processes are categorized into ten stages according to the changes in thickness, as illustrated in Figure 5-19.

Similarly, the bending properties of textile material also vary at different bending radians. The physical properties measured are shown with ten bending stages by using the bending radius as shown in Figure 5-20.

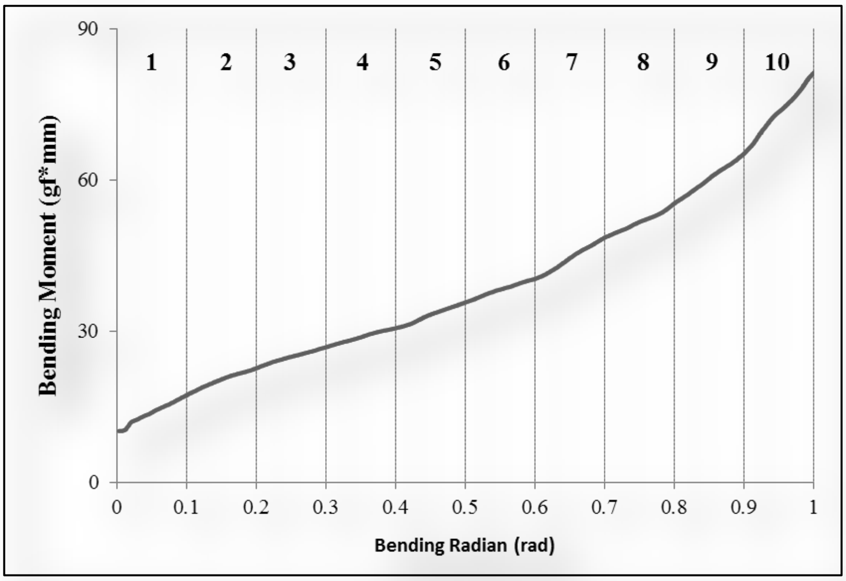

Figure 5-20 Classification of Bending Stages on the basis of Bent Radian

The physical data obtained from the FTT are in pairs of bending moment and bending radian. These two measured parameters represent the received force and distance moved, respectively. Since the bending process was constantly carried out by using the FTT until 1 radian, there would be same bending radian for each application. The bending moment in the use of the FTT is defined with gf*mm as the unit. Since the bending force required does not make sense without defining the bending torque, the bending moment is redefined as bending force with a torque of 1 mm. With an assumed constant bending speed of 1 radian per second, the total impulses of the SA1 fibers can be consequently calculated by using the following equation:

$$T_{bj} = \int dt f(M_i) \qquad (5\text{-}30)$$

where T_{bj} is the total impulses of the SA1 fibers during the j^{th} period, t is the time taken for the j^{th} period, M_i is the bending moment measured and $f(M_i)$ is the impulse rate of the SA1 fibers calculated by using Equation (5-28).

This hypothesis aims to examine the SA1 fiber responses in terms of total impulses when receiving external forces. These forces could be received in the deformation of fabric, such as by compression or bending. Neurophysiological information coded on the basis of force is expected to address psychological touch sensation related to softness perception.

Integration of total SA1 fiber impulses and distance information

There are two types of distance information that could be received by the skin neural system. One is the distance that a finger has moved, which could be received as proprioceptive stimulus. The other is skin indentation, which is another type of cutaneous information perceived by the skin receptors.

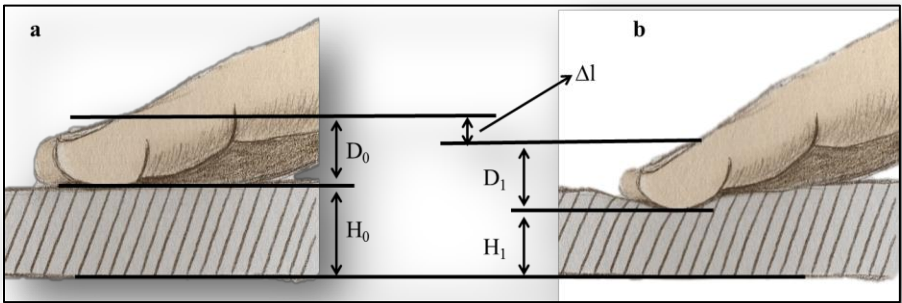

Figure 5-21 Moved Distance of Finger during Compression Task: (a) illustration before compression task; (b). illustration during compression task

As illustrated in Figure 5-21, the distance perceived (Δl) actually has two aspects, which are skin indentation (ΔD) and changes in fabric thickness (ΔH). Research by (Friedman et al., 2008) conducted with 22 subjects showed that skin indentation generally follows a logarithmic function to normal pressure. Their relation is interpolated as the following equation (R^2: 0.976 and p value: 0.000).

$$\Delta D = m \ln F + n \tag{5-31}$$

where F is the normal pressure received, and m and n are constants calculated as 0.617 and 4.738 respectively.

The distance that the finger has moved is calculated by summing ΔD and ΔH. The impulse ratio per unit of moved distance for SA1 fibers is subsequently calculated by dividing the total impulses of the SA1 fibers by the distance moved during each stage.

$$R_{cj} = \frac{\int dt f(P_i)}{\sum(H_{i+1} - H_i) + \sum\left(f\prime(D_{i+1}) - f\prime(D_i)\right)} \tag{5-32}$$

where R_{cj} is the ratio of the total impulses of the SA1 fibers per unit distance moved during the j^{th} period, H_i is the measured fabric thickness, and $f'(P_i)$ is the result from using Equation (5-31).

Similarly, the calculation of the ratio of the total impulses of SA1 fibers per unit distance moved for each bending stage is calculated by using the following equation:

$$R_{bj} = \frac{\int dt f(M_i)}{\sum(Radian_{i+1} - Radian_i) + \sum\left(f\prime(D_{i+1}) - f\prime(D_i)\right)} \tag{5-33}$$

This hypothesis adds another source of information that is the distance moved by the fingers during deformation. The ratio of the total impulses of the SA1 fibers and distance moved is therefore defined to include the impact from both cutaneous and kinesthetic neural information.

5.4.2 Discussion on Coded Received Forces Information

The results of the coded SA1 fiber responses on the selected 20 types of fabrics are examined. Table 5-8 shows the multi-ANOVA analysis results. The impact of fabric is as anticipated, while that of the deformation stage is proven from this statistical analysis. It can be noticed that the stage is an even more important factor than the fabric, which are expressed by using F values. The impact of the interaction of the fabric and application of deformation also shows a significant effect.

Table 5-8 Multi-ANOVA Analysis on the Impact of Fabric and Deformation Stage on Compression Neural Indexes

Factor	Index	F Value	p Value
Main Factor: Fabric	T_c	472.046	0.000
	R_c	470.564	0.000
Main Factor: Stage	T_c	2863.396	0.000
	R_c	4539.115	0.000
Interaction: Fabric * Stage	T_c	50.240	0.000
	R_c	82.459	0.000

ANOVA testing on these neural indexes was conducted and the results are shown in Table 5-9. It can be observed that the total impulses of the SA1 fibers show a greater difference between the different types of fabrics than the ratio of the total impulses of the SA1 fibers and distance moved do. The latter, during some of the deformation stages, even show no significant differences among the examined fabrics. As indicated by the F value, the most relevant results appear during the tenth stage of compression and fourth recovery stage for the neural index T_c, whilst with regard to R_c, the largest F values are found during the tenth stage of compression and first recovery stage. These two stages both represent fabrics under greatest compression.

Table 5-9 ANOVA Table of Compression Neural Indexes on Different Fabrics

Stages	SA1 Total Impulses T_c (H1)		Ratio of SA1 Total Impulses and Moved Distance R_c (H2)	
	F Value	p Value	F Value	p Value
Compressing 1st	43.879	0.000	1.882	0.023
Compressing 2nd	37.568	0.000	--	--
Compressing 3rd	91.112	0.000	8.610	0.000
Compressing 4th	99.724	0.000	25.185	0.000
Compressing 5th	93.398	0.000	33.239	0.000
Compressing 6th	97.232	0.000	28.066	0.000
Compressing 7th	87.756	0.000	7.088	0.000
Compressing 8th	87.653	0.000	9.730	0.000
Compressing 9th	78.365	0.000	7.412	0.000
Compressing 10th	103.112	0.000	55.985	0.000
Recovering 1st	133.078	0.000	110.860	0.000
Recovering 2nd	106.127	0.000	12.765	0.000
Recovering 3rd	129.177	0.000	3.082	0.000
Recovering 4th	158.877	0.000	21.946	0.000
Recovering 5th	153.671	0.000	25.981	0.000
Recovering 6th	89.952	0.000	11.019	0.000
Recovering 7th	53.561	0.000	1.884	0.023
Recovering 8th	23.344	0.000	--	--
Recovering 9th	12.874	0.000	--	--
Recovering 10th	4.436	0.000	--	--

The results imply that most fabrics display similar compressibility with small amounts of compression, i.e. early stages of compression and later stages of recovery. As discussed earlier in Chapter 4, these stages demonstrate that the fabric properties are influenced by their structures and surface free fibers. This finding suggests that humans would receive similar neural responses while the stimuli are affected by the fabric structures and surface free fibers, which also implies that the discrimination of softness perception by touching fabrics is mainly affected by the properties of the yarns that are utilized.

The following figures are the detailed evaluation results of T_c and R_c on different fabrics during different stages. Figure 5-22 shows the T_c results. It is clear that all ten curves, which represent different deformation applications, generally follow a similar pattern among the 20 types of fabrics. Relatively low values appear for Fabrics 29 and 8. They are a nylon-blend single jersey fabric and a 100% polyester chiffon fabric respectively. Relatively high values are evident for Fabrics 11, 12, and 18, which are flannel woven, rib knitted, and single jersey fabrics respectively. A similar conclusion could be made for the neural index R_c, as illustrated in Figure 5-23.

A further comparison between the results based on these two hypotheses was made. As shown in Table 5-10, the correlation coefficients and p values shown are statistics from the Spearman's correlation tests between the results of Hypotheses 1 and 2 in pairs. Strong correlations are found at the fourth, fifth, sixth, and tenth compression stages as well as the first, fifth, and sixth recovery stages. The results imply that differences in the SA1 fiber response during compression deformation mainly appear when a relatively small normal pressure is applied. Since the results based on Hypothesis 1 are concluded to be proportional to those based on Hypothesis 2 during most applications, it appears that the distance moved would not alter the softness discrimination of an object.

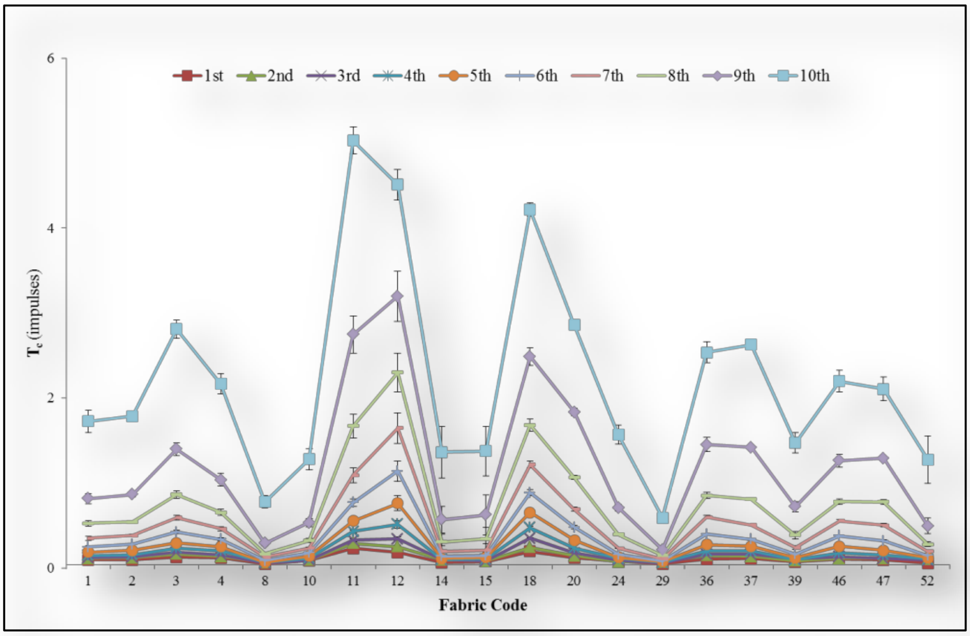

Figure 5-22 Results of T_c on Different Fabrics during Different Compressing Stages

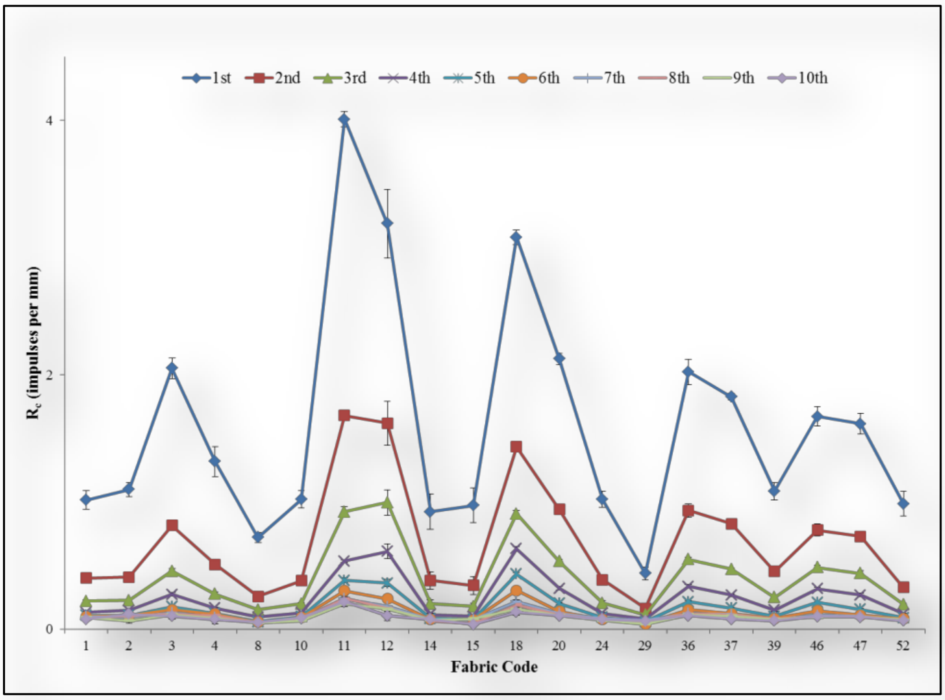

Figure 5-23 Results of R_c on Different Fabrics during Different Recovering Stages

Table 5-10 Correlation Summary of Compression Neural Indexes between H1 and H2 during Different Stages

Task	Statistic	Correlation during Different Stages				
Compressing	Stage	**1st**	**2nd**	**3rd**	**4th**	**5th**
	Coefficient	--	--	--	.957	.961
	p Value	--	--	--	.000	.000
	Stage	**6th**	**7th**	**8th**	**9th**	**10th**
	Coefficient	.887	.544	--	.585	.989
	p Value	.000	.013	--	.007	.000
Recovering	Stage	**1st**	**2nd**	**3rd**	**4th**	**5th**
	Coefficient	.994	--	-.447	.778	.801
	p Value	.000	--	.048	.000	.000
	Stage	**6th**	**7th**	**8th**	**9th**	**10th**
	Coefficient	.814	--	.467	--	--
	p Value	.000	--	.038	--	--

The following focuses on the neural indexes for fabric bending deformations. Similarly, a multi-ANOVA analysis was first conducted. The results in Table 5-11 show that the total impulses of the SA1 fibers and distance moved by the finger as well as the effects of their interaction have a significant impact on T_b and R_b. Again, as indicated by the F value, the bending stage is a more important factor than the fabric itself. Table 5-12 shows in more detail, the differences among the selected 20 types of fabrics with regard to the bending indexes of neural mechanisms, T_b and R_b. Both indexes have the highest F values during the first bending stage and the lowest values during the third stage. In addition, it can be observed that T_b shows larger variances among these fabrics than R_b.

Table 5-11 Summary of Multi-ANOVA Analysis on the Impact of Fabric and Deformation Stage on Bending Neural Indexes

Factor	Index	F Value	p Value
Main Factor: Fabric	T_b	185.365	0.000
	R_b	225.852	0.000
Main Factor: Stage	T_b	541.648	0.000
	R_b	647.307	0.000
Interaction: Fabric * Stage	T_b	7.081	0.000
	R_b	8.685	0.000

Table 5-12 ANOVA Table of Bending Neural Indexes on Different Fabrics

Stages	SA1 Total Impulses (H_1)		Ratio of SA1 Total Impulses and Moved Distance (H_2)	
	F Value	p Value	F Value	p Value
Bending 1st	60.037	0.000	53.734	0.000
Bending 2nd	13.587	0.000	13.083	0.000
Bending 3rd	9.415	0.000	9.100	0.000

Bending 4th	13.652	0.000	12.479	0.000
Bending 5th	12.868	0.000	11.638	0.000
Bending 6th	54.242	0.000	38.043	0.000
Bending 7th	53.854	0.000	37.248	0.000
Bending 8th	47.561	0.000	33.763	0.000
Bending 9th	39.473	0.000	29.595	0.000
Bending 10th	32.358	0.000	27.084	0.000

This finding indicates that fabric elicits more variations in total impulses of the SA1 fibers during the initial fabric bending stage. The F values remain relatively low during the second to the fifth stage. The second highest value is found for the sixth stage and subsequently, is reduced again until the end of the bending process. A similar pattern is found for the ratio of the total impulses of the SA1 fibers and distance moved.

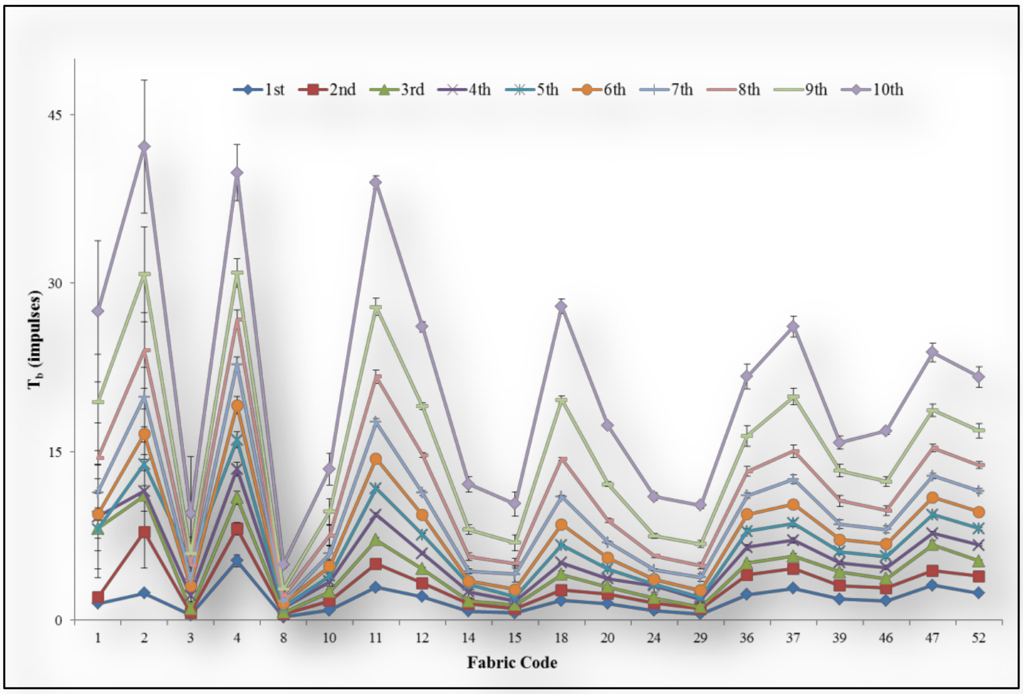

Figure 5-24 Results of T_b on Different Fabrics during Different Bending Stages

Figure 5-24 and Figure 5-25 show the results of the neural indexes based on Hypotheses 1 and 2 during different bending stages. They show that the general patterns are the same for all ten bending stages. The minimum values of T_b are observed for Fabric 8 and then Fabric 3. They are 100% polyester chiffon and 100% cotton non-woven fabrics respectively. Relatively large values of T_b are found for Fabrics 2, 4, and 11. These are 100% linen plain woven, 100% cotton twill woven, and polyester/wool blend single side flannel woven respectively. Meanwhile, with regard to the results of the R_b, low values are evident for Fabrics 4 and 10 (100% satin woven). The highest value of R_b is found for Fabric 3. It seems that, unlike the findings in compression deformation, there is a negative relation between T_b and R_b.

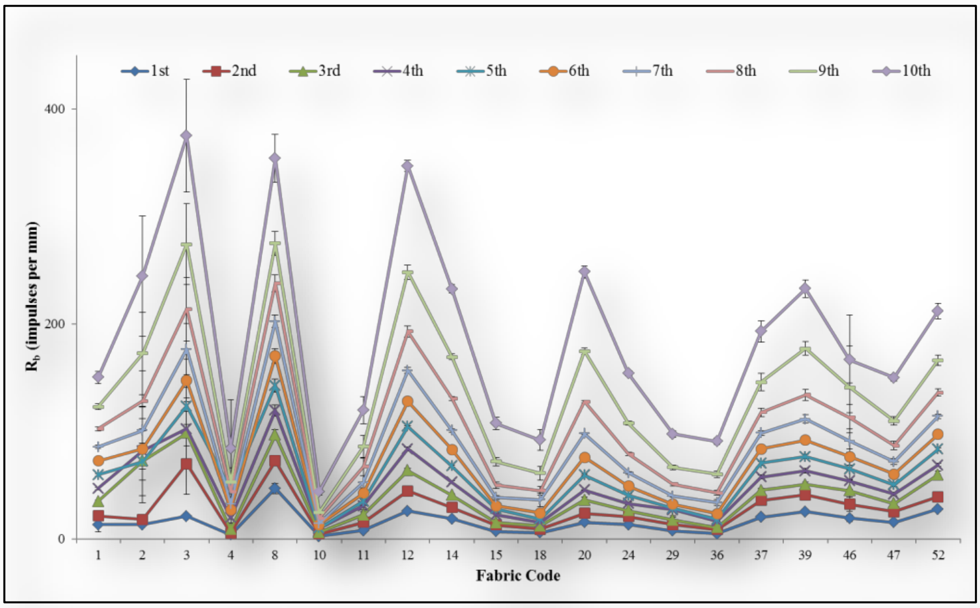

Figure 5-25 Results of R_b on Different Fabrics during Different Bending Stages

The Spearman's correlation test was therefore conducted for T_b and R_b. However, in contrast, there were no significant correlations found between any pairs of T_b and R_b. This finding, nevertheless, suggests that for the bending process, information as provided by Hypotheses 1 and 2 is not proportional. It is obviously worthy to investigate which would be more closely correlated to psychological perception.

Table 5-13 shows the Spearman's correlation results between T_b and the physical indexes of bending during different bending applications. It is clear that all of the T_b values share positive monotonic relations with all four defined physical indexes of bending. The relations to BW are stronger than those to BAR. Nevertheless, the other calculated neural index for bending, R_b, shows no significant relation to any of the physical indexes.

Table 5-13 Correlation between Bending Neural Indexes and Physical Indexes

Stage	Statistic	Correlation to Physical Indexes			
		BARa	BARe	BWa	BWe
1st	Coefficient	0.589	0.662	0.838	0.895
	p Value	0.006	0.001	0.000	0.000
2nd	Coefficient	0.595	0.653	0.836	0.902
	p Value	0.006	0.002	0.000	0.000
3rd	Coefficient	0.647	0.570	0.848	0.815
	p Value	0.002	0.009	0.000	0.000
4th	Coefficient	0.644	0.598	0.877	0.827
	p Value	0.002	0.005	0.000	0.000
5th	Coefficient	0.614	0.579	0.847	0.824
	p Value	0.004	0.007	0.000	0.000
6th	Coefficient	0.639	0.624	0.875	0.865
	p Value	0.002	0.003	0.000	0.000
7th	Coefficient	0.692	0.647	0.887	0.853
	p Value	0.001	0.002	0.000	0.000
8th	Coefficient	0.716	0.692	0.884	0.866
	p Value	0.000	0.001	0.000	0.000
9th	Coefficient	0.767	0.723	0.905	0.851
	p Value	0.000	0.000	0.000	0.000
10th	Coefficient	0.795	0.735	0.902	0.832
	p Value	0.000	0.000	0.000	0.000

5.5 Conclusion

In this chapter, the objective 3 has been accomplished by presenting the neurophysiological coding process from physical stimuli to neural signals for each of the three types of neural simulations. Hypotheses have been made with regard to thermal, texture, and received force information, respectively.

Neural responses to thermal stimuli are expressed by the thermoreceptors. At the molecular level, the membrane current of TRPM8 channels is concluded as the transducer of thermal stimulus. On the basis of modified neurophysiological coding models and heat flux results recorded by the FTT instrument, neurophysiological indexes are defined according to three hypotheses. Comparison analyses found that C-base index C_{max} and C_{steady}, as well as Q-base index $Q_{downsum}$ and Q_{steady} are significantly correlated to the TMF and T physical indexes. The findings imply that to better express the thermal response that fabric could stimulate, fabric thickness should be considered together with the thermal conductivity of the fabric. Generally speaking, fabrics with higher TMF and lower T values are likely to produce higher thermal receptor response.

The spatial and temporal variances of SA1 and PC fibers are due to texture stimuli. Relations are found between the impulse rate of the SA1 and PC fibers and texture component profile. In this study, the measured fabric surface roughness profiles are characterized by using a single sinusoid pattern or the FFT. Based on different hypothesized methods, neurophysiological indexes including the I, W, P_1, and P_2, have been identified to express neural responses to texture stimuli. Correlation analyses between these indexes and the SRA and SRW physical indexes suggest that the impulse rate of the population of P_1 and P_2 is significantly correlated to both the SRA and SRW indexes while I and W show no or limited relationships. The results indicate that fabric surface with higher values in the SRA and SRW would likely to produce higher impulse rate of the population of both the SA1 (P_1) and PC (P_2) fibers.

With regard to the received force information, the total impulses of the SA1 fibers are found to be linearly correlated to the received forces by the finger. Meanwhile, the distance moved could also be an affecting factor of softness discrimination. Two hypotheses, including neural response to force and distance that the finger has moved, are proposed afterwards. It has also been proposed that bending and compression deformation, despite the distinct type of task carried out by hand, should stimulate the same neural receptors. Since fabric would show different resistance properties to external deformation forces during different stages, neurophysiological indexes here are identified according to the deformation stages. Ten stages are used for both bending and compression deformation. The results T_c, R_c, T_b, and R_b are examined by comparing them with the corresponding physical indexes. Their correlation coefficients vary although a general proportional relation between the physical indexes is observed.

After the evaluation in this chapter, the neurophysiological responses from the respective receptors to each type of stimulus have been clarified and quantitatively expressed. These neurophysiological indexes provide novel means to further studies on touch sensation from the transition of the physical into the neurophysiological. Their relations to the psychological subjective sensory results will be examined in Chapter 8. They will also be the predictors in the development of neuropsychological prediction models for fabric touch sensation.

Chapter 6 Mechanisms of Psychological Sensory Discrimination

For the purpose of completing the objective 4, a systematic study will be carried out in this chapter to reveal the patterns of the psychological touch sensory perception and discrimination of different fabrics. The dimensions of psychological discriminations should be clarified based on psychophysiological mechanisms. The effects from touch and acclimation should also be examined.

As reviewed in Chapter 2, although there have been many previous studies, few have covered the psychophysiological principles of sensation perception. Since different terminologies are used to describe fabric touch sensation in daily life, many classification methods had been reported. Nevertheless, they have not managed to connect sensory dimensions to the psychophysiological mechanisms of sensation perception. In addition, it is well accepted that touch (passive or active) and climatic conditions can influence the physiological features of touch sensation perception. Yet there is a lack of discussion on their influences towards fabric touch sensations.

In Chapter 6, the focus is on studies on the final process of the perception of fabric touch sensation, i.e. psychological discrimination. As illustrated in Figure 6-1, a task as simple as sitting can produce psychological touch sensations from clothing in many aspects. We can evaluate the touch sensation of fabric in three ways: next-to-skin for feelings of smoothness, forces needed to cause deformation for feelings of softness, and temperature changes for feelings of warmth. Smoothness sensation is possible to sense when clothing directly contact to skin. Softness sensation is likely to be received when clothing is deformed. Warmness sensation is always perceived because of temperature differences between human body and external environment. Whilst contact method including passive or active touch and climatic conditions like temperature and relative humidity are also believed to impact the perception of touch sensations.

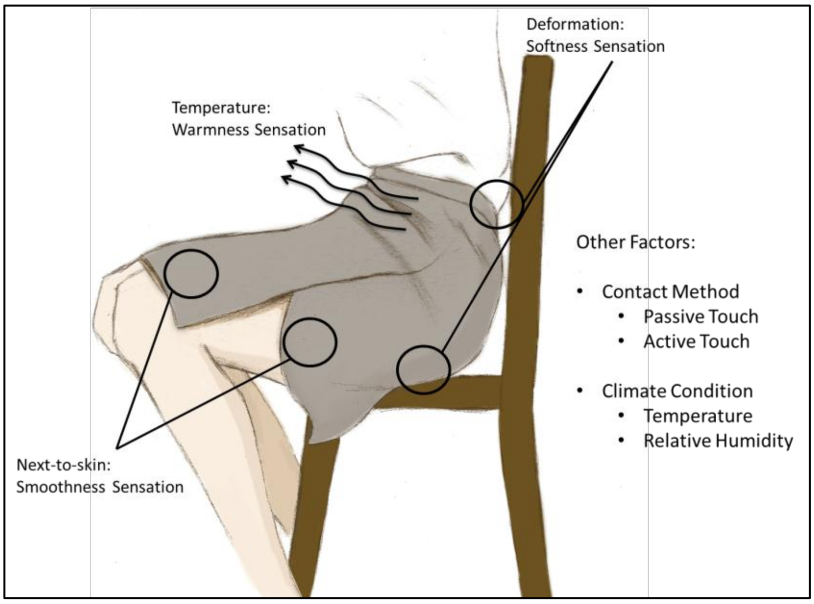

Figure 6-1 Dimensions and Affecting Factors of Touch Sensation

6.1 Experiment

6.1.1 Subjects

The students and staff members of different universities were invited to take part in the study. There were in total 226 participants; 79 (35%) were male and 147 (65%) were female. The average age of the subjects was 24.5 (median: 24) years old with 18 as the youngest age and 60 the oldest. No compensation of any kind was provided to the subjects. The subjects reported no neural diseases or discrimination disabilities that may impact the touch sensation evaluation results. All of the subjective evaluations followed required local laws and regulations.

The procedures were strictly followed in an exact manner for participants in six cities in the East-Asia area as listed in Table 6-1. The average temperature and relative humidity were chosen to represent the climatic conditions of these cities. The listed data were obtained from an online weather-information website. The average values were recorded by calculating from one month before the experiment date of the first subject until the experiment date of the last subject. The subjects invited had been living in the specified cities for at least one month prior to the experiments.

Table 6-1 Average Climatic Conditions of Six Involved Cities

Climatic Condition	City	Average Temperature (°C)	Relative Humidity (%)	Record Period
1	Shanghai	5[a]	72[a]	Jan. 2013 – Feb. 2013
2	Xi'an	-1[b]	52[b]	Dec 2013 – Jan. 2013
3	Hong Kong	15.8[c]	85[c]	Jan. 2012 – Feb. 2012
4	Qingdao	15.9[d]	57[d]	Sept. 2013 – Oct. 2013
5	Nagano	16.8[e]	63.4[e]	Sept. 2013 – Oct. 2013
6	Kyoto	11.2[f]	53.1[f]	Mar. 2013 – Apr. 2013

[a] Data obtained from ("Weather history for Shanghai Hongqiao, SH,"); [b] Data obtained from("Weather history for Xi'an, SA,"); [c] Data obtained from ("Weather history for Hong Kong, Hong Kong,"); [d] Data obtained from ("Weather history for Qingdao, SD,"); [e] Data obtained from ("Weather history for Matsumoto Airport, Japan,"); [f] Data obtained from ("Weather history for Osaka Airport, Japan,").

6.1.2 Stimuli

Twenty different kinds of fabrics were selected as stimuli in this series of experiments. The fabrics used are the same as those described in Chapter 5. The fabric swatches for the experiment had a size of 200 mm x 400 mm with a longer side of the warp direction. The fabric swatches were ironed to remove obvious creases and then stored in a standard chamber (temperature of 21°C ± 1°C and relative humidity of 65% ± 2%) for at least 24 hours before measurements were taken.

6.1.3 Procedure

The subjective evaluation in this study followed the AATCC EP5 (AATCC, 2011). The subjects were required to wash their hands and forearms with hand soap that did not contain moisturizers and then dry off with paper towels. Afterwards, they were taken to the evaluation chamber (temperature of 21±1 °C and relative humidity of 65±2 %) to rest for at least 30 minutes. The conditioned chamber provided an environment that other potential impactors, e.g. air flow, were controlled. The standard condition during evaluation is part of the standardization of the evaluation process. Standardized process would make the experiments, which were conducted in six different host institutes more reliable and comparable. Therefore, the underlying mechanisms of perceiving fabric touch sensations could be evaluated. During resting, they were to avoid any extreme movements and exposure of their hands to different temperatures.

Ten pairs of bipolar descriptors were chosen for the measurement. The scale midpoint was defined as neutral, and there were three scale points around each side of this midpoint. The views of the subjects were blocked during the entire evaluation process. The reference fabric (Fabric A) was considered as having a neutral feel (score: 0) among all the descriptors. One of the hands of the subjects was to touch the reference fabric; the other hand touched the other fabric samples. The subjects were expected to compare the other fabrics with the reference fabric and provide their input by using the ten descriptors. The research staff read out the descriptors and recorded the scorings provided by the subjects. The definitions of the descriptors were given to the subjects in both English and their native language (i.e. Chinese or Japanese). The subjects had to fully understand the meaning of these descriptors before undertaking the evaluation. Descriptors are defined as opposites in negative and positive terms as follows.

- Cool-Warm: the temperature of the fabric.
- Itchy-NonItchy: whether the fabric feels itchy to the skin.
- Scratchy-NonScratchy: whether the fabric scratch the subjects.
- Prickly-NonPrickly: whether the fabric surface gives a prickly sensation.
- Rough-Smooth: whether the fabric is free from coarseness or has projections, irregularities, or unevenness.
- Sticky-NonAdhesive: whether the fabric feels sticky.
- Stiff-Pliable: whether the fabric feels rigid or not flexible or pliant.
- Thick-Thin: extension between opposite surfaces.
- Hard-Soft: the amount of absolute resistance to pressure.

- NonFullness-Fullness: whether the fabric would spontaneously regain its normal bulk after compression

There are two parts of the measurement: passive (forearm) and active (hand) touching. For passive touching by the forearm, both hands were placed on a table with the palms up as illustrated in Figure 6-2. Subjects were requested to keep both arms straight during the experiments. The reference fabric was always placed on the left hand of subjects while the other fabrics were placed on the right hand randomly. With regard to active touching (i.e. hand evaluation), there are four contact positions made by the hand according to AATCC EP5 (AATCC, 2011) as shown in Figure 6-3. These are: use of the hand to stroke, pinch, and grab the sample fabric.

Figure 6-2 Illustration Figure of Passive Forearm Contact for Subjective Measurement

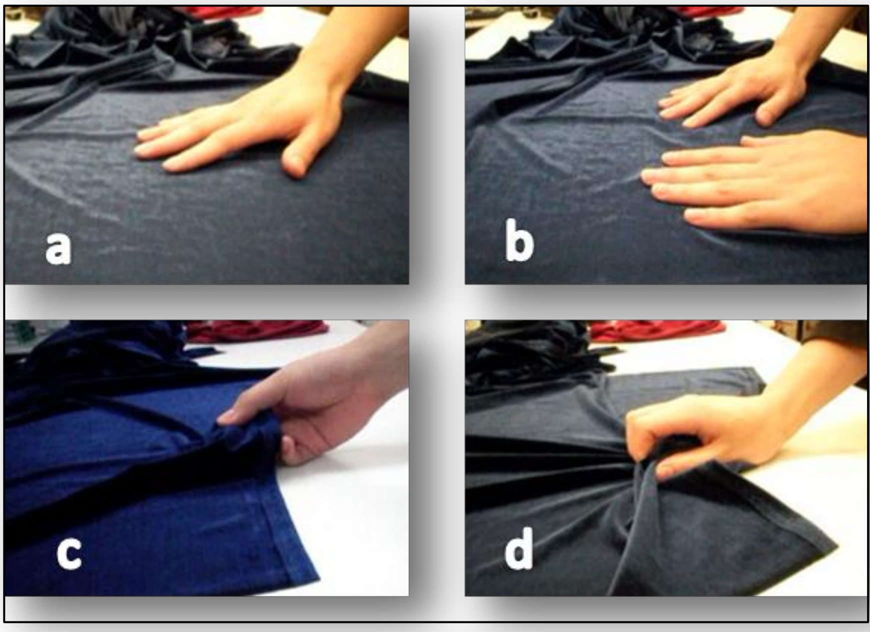

Figure 6-3 Illustration Figure of Active Hand Contact for Subjective Measurement: (a) initial touch, (b) stroke, (c) pinch and (d) grab.

6.2 Results of Psychological Discrimination

The discrimination capabilities of the subjects on these samples with the different descriptors taken into consideration were first examined. Table 6-2 shows the results of the ANOVA testing on passive and active touch respectively. With a probability values (p) less than 0.05, it is clear than there are significant differences between the subjective scoring of the 19 samples. The effect size statistic, shown as the F value, indicates that Hard-Soft, Thick-Thin, and Stiff-Pliable are easier to discriminate while this is not true for Sticky-NonAdhesive. It can also be noticed that these individual descriptors are significantly correlated to each other, see the full table provided in the appendix. This implies that despite that each chosen descriptor stands for a specified kind of "feeling", these "feelings" lead the subjects to obtain many of similar perceptions and therefore, a dimension reduction is needed.

6.2.1 Discussion on Psychological Discrimination

The following figures display the results of subjective scoring on each descriptor respectively. Figure 6-4 shows the results with regard to the Cool-Warm descriptor. Error bar stands for 95% confidence intervals in this figure and following figures in this chapter. Fabric 3, a 100% cotton non-woven fabric, has the highest result, and Fabric 11 (polyester/wool blend flannel woven fabric) has the next highest result. The lowest result was obtained by Fabric 14, a viscose/nylon blend single jersey knitted fabric. Generally speaking, knitted fabrics have a low result for the Cool-Warm descriptor, while all of the silk jacquard fabrics give similar results.

Table 6-2 ANOVA Test of Fabric on Individual Descriptors

Descriptors	df	F Value	p Value
Cool-Warm	18	174.62	0.000
Itchy-NonItchy	18	90.48	0.000
Scratchy-NonScratchy	18	101.56	0.000
Prickly-NonPrickly	18	100.84	0.000
Rough-Smooth	18	174.19	0.000
Sticky-NonAdhesive	18	10.97	0.000
Stiff-Pliable	18	252.30	0.000
Thick-Thin	18	299.02	0.000
Hard-Soft	18	314.83	0.000
NonFullness-Fullness	18	73.08	0.000
Uncomfortable-Comfortable	18	178.85	0.000

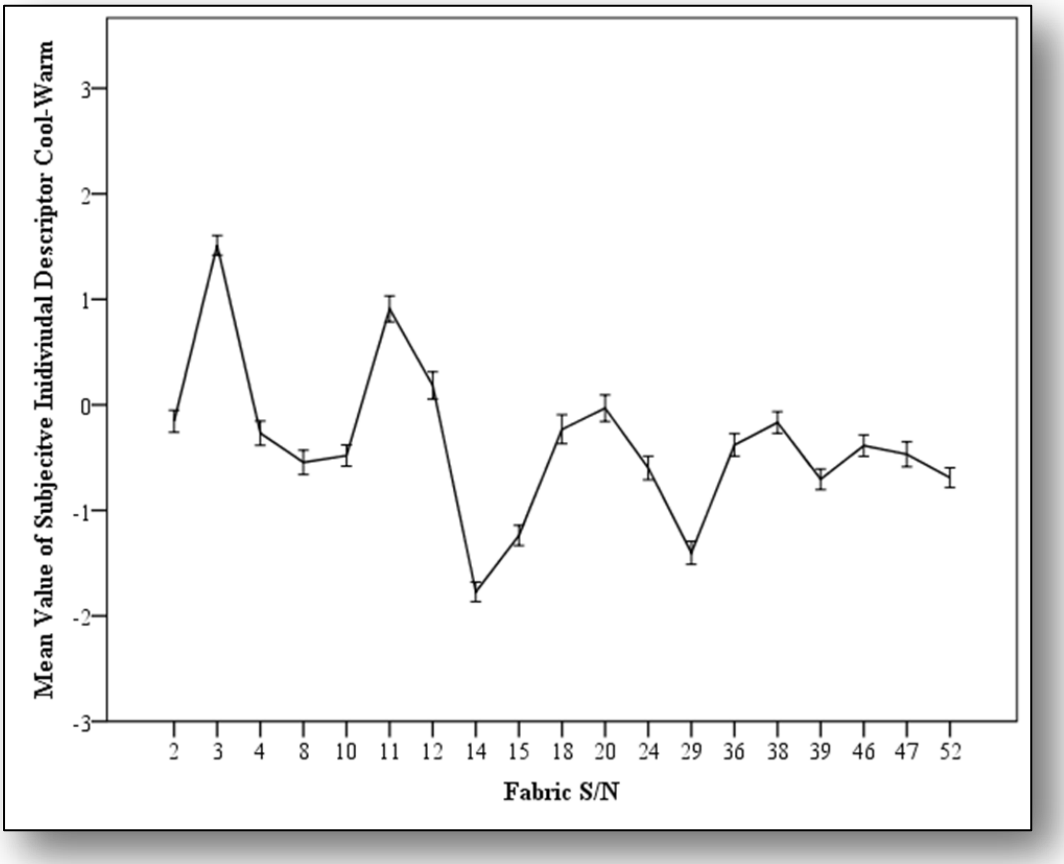

Figure 6-4 Results of Psychological Perception on Individual Descriptor Cool-Warm

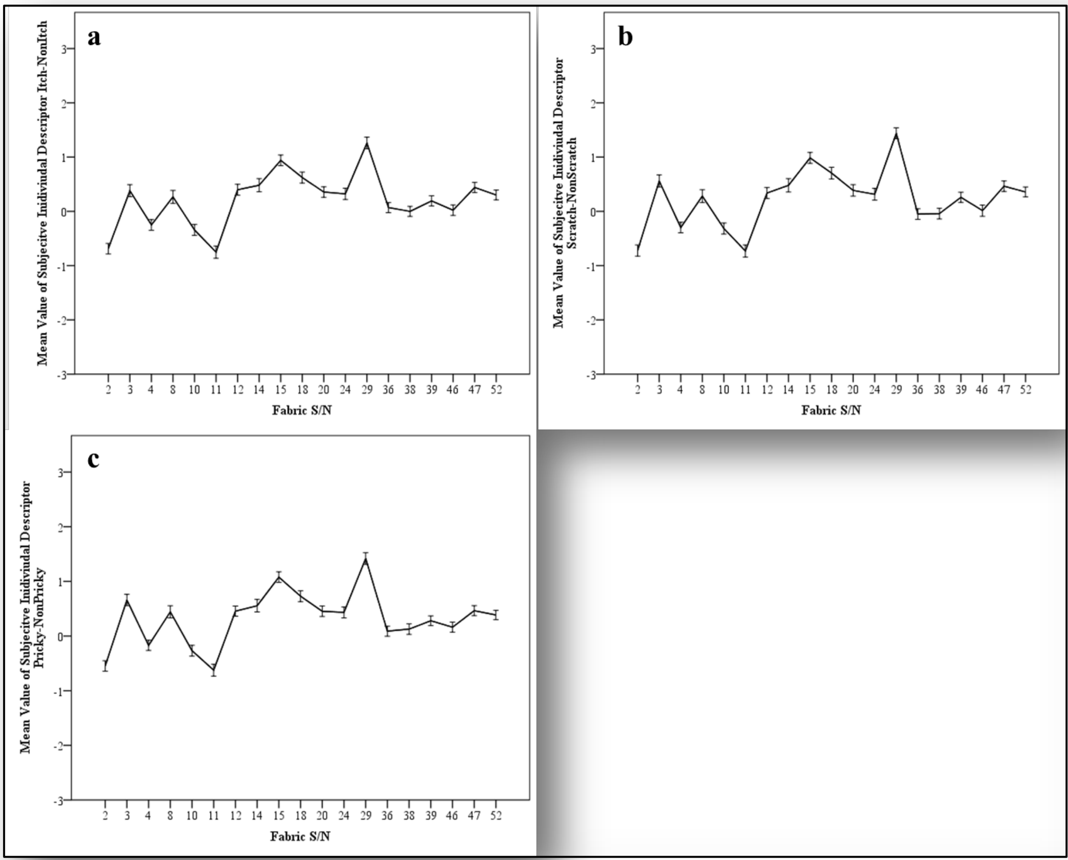

Figure 6-5 Results of Psychological Perception on Individual Descriptors Itchy-NonItchy, Scratchy-NonScratchy, and Prickly-NonPrickly

Figure 6-5 shows the results of three surface-related descriptors: Itchy-NonItchy, Scratchy-NonScratchy, and Prickly-NonPrickly. It is clear that the subjective scores of these three descriptors are almost identical. The highest score was recorded for Fabric 29, a polyester/elastan blend knitted fabric. The lowest score, which means the most uneven fabric, is Fabric 11.

Figure 6-6 shows the results of the Rough-Smooth descriptor. The results are slightly different from the three previous descriptors. Fabric 29 again is considered to be the smoothest fabric while Fabric 2, a 100% linen plain woven fabric, is the most rough.

Generally speaking, the knitted fabrics (Fabrics 12 to 29) are considered to be smooth. Although there are clearly variances among the silk jacquard fabrics (Fabrics 36 to 52), it seems that the subjects could feel the different jacquard patterns on the fabrics and perceive them as having a rough-smooth texture.

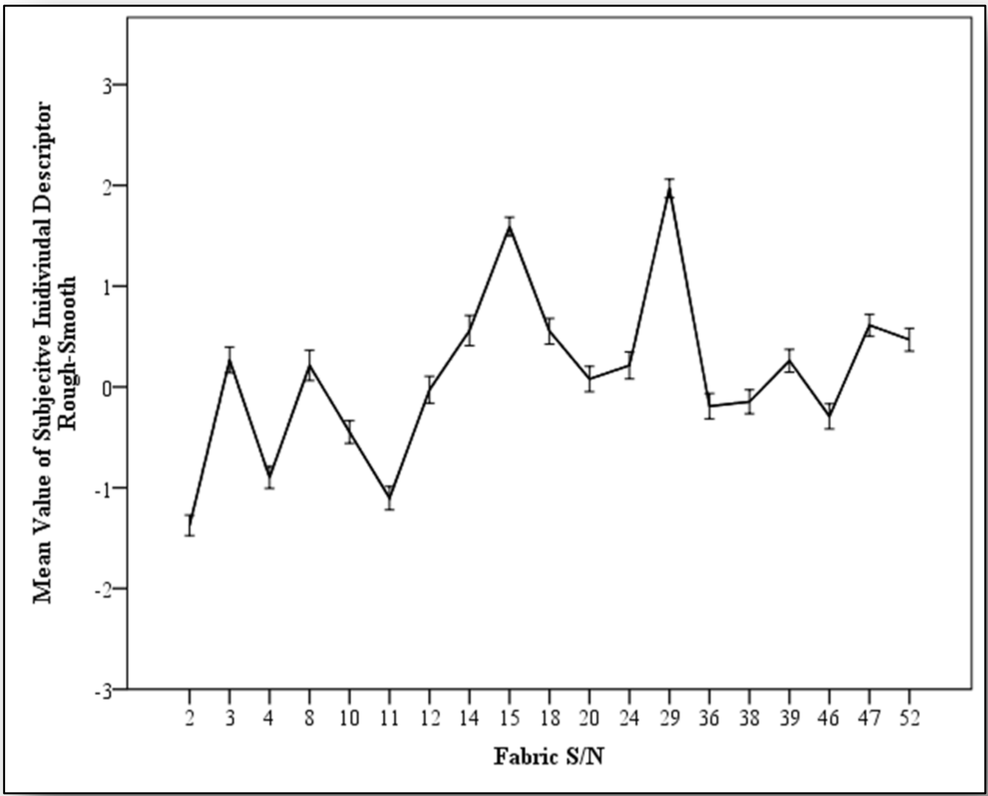

Figure 6-6 Results of Psychological Perception on Individual Descriptor Rough-Smooth

With regard to the Sticky-NonAdhesive discriminator as shown in Figure 6-7, the selected fabric stimuli seem to have limited variance. The average results obtained were within scores of -1 to 1. Fabric 8, a 100% polyester chiffon woven fabric, showed the highest result while Fabric 11, the lowest result.

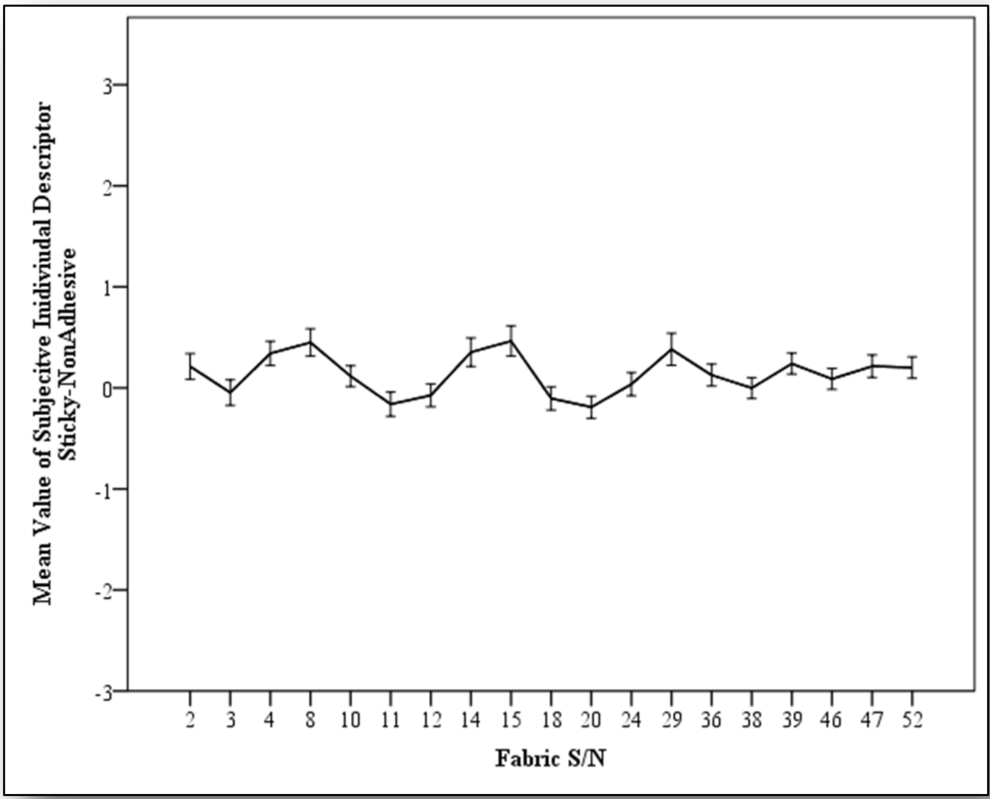

Figure 6-7 Results of Psychological Perception on Individual Descriptor Sticky-NonAdhesive

Figure 6-8 shows the subjective perception of two descriptors: Stiff-Pliable and Hard-Soft. The two curves show that the subjects gave close scores for these two descriptors although they are expected to represent bending and compression rigidities respectively. Fabric 29 is considered to be the softest fabric with both descriptors whilst Fabric 4, a 100% cotton twill woven fabric, is conceivably concluded as the hardest fabric.

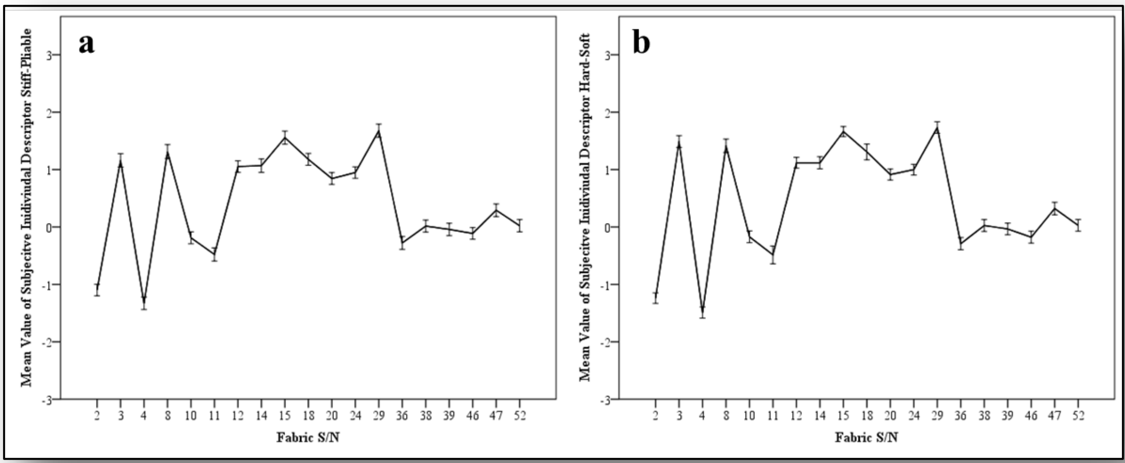

Figure 6-8 Results of Psychological Perception on Individual Descriptors Stiff-Pliable and Hard-Soft

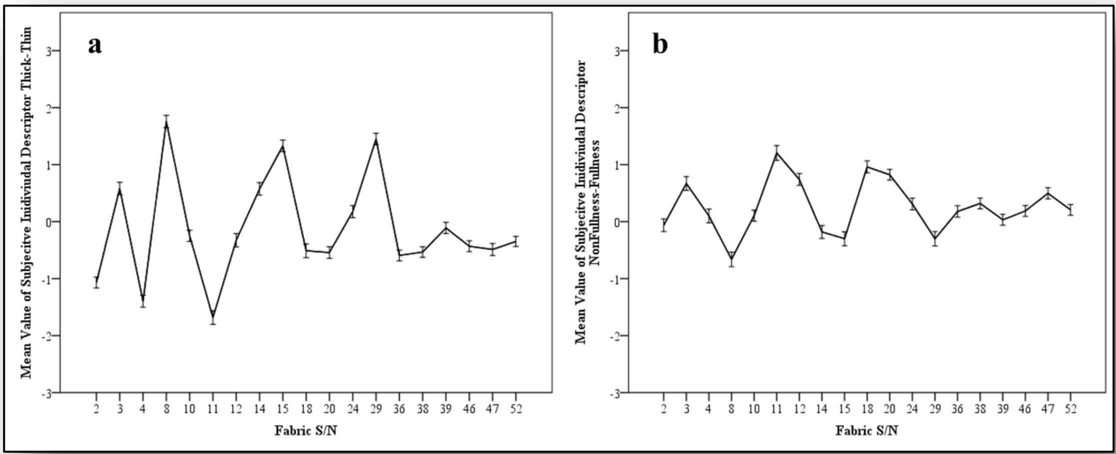

Figure 6-9 Results of Psychological Perception on Individual Descriptors Thick-Thin and NonFullness-Fullness

Figure 6-9 illustrates the results of the last two descriptors: Thick-Thin and NonFullness-Fullness. Fabric 11, as expected, is considered to be the thickest fabric and also the one with the most fullness. It is not surprising that thicker fabrics would give a feeling of more fullness. Fabric E is concluded as the thinnest fabric with the least fullness.

6.2.2 Effect of Active and Passive Touch on Individual Descriptors

Two-way ANOVA testing was conducted to evaluate the effect of touch on the individual descriptors. The results indicated that significant differences exist among most of the descriptors during passive and active touch, as shown in Table 6-3. The effects of the interaction of fabric and active and passive touch further confirmed that all of the descriptors show significant differences.

Table 6-3 Two-Way ANOVA of Fabric and Touch Method on Individual Descriptors

Effect	Descriptor	df	F	Sig.
Main Effect: Contact Method	Cool-Warm	1	827.371	0.000
	Itchy-NonItchy	1	19.322	0.000
	Scratchy-NonScratchy	1	13.835	0.000
	Prickly-NonPrickly	1	1.304	0.254
	Rough-Smooth	1	223.766	0.000
	Stick-NonAdhesive	1	14.720	0.000
	Stiff-Pliable	1	35.549	0.000
	Thick-Thin	1	86.007	0.000
	Hard-Soft	1	56.860	0.000
	NonFullness-Fullness	1	90.006	0.000
Interaction Effect: Stimulus*Contact Method	Cool-Warm	18	17.048	0.000
	Itchy-NonItchy	18	7.605	0.000
	Scratchy-NonScratchy	18	10.141	0.000
	Prickly-NonPrickly	18	8.198	0.000
	Rough-Smooth	18	23.822	0.000
	Stick-NonAdhesive	18	5.220	0.000
	Stiff-Pliable	18	6.415	0.000
	Thick-Thin	18	18.450	0.000
	Hard-Soft	18	9.087	0.000
	NonFullness-Fullness	18	11.629	0.000

In order to more clearly demonstrate the differences between passive and active touch with regard to each type of fabric, one-way ANOVA testing was conducted for each type of fabric to evaluate whether there is a significant difference in the perception by the subjects from passive and active touch. Significant difference count (SDC) is the counting of cases when the fabrics have a significant difference when passively and actively touched. Table 6-4 is a summary of the SDC of the 10 descriptors. The results indicate that passive and active touch would likely confer significantly different feelings with the same stimulus in terms of most of the descriptors, especially for the Cool-Warm, Rough-Smooth, and Thick-Thin descriptors. “p” and “t” represent the probability value and effect size of the general abilities of active and passive touching of all of the fabrics. Significant effects are found for most of the descriptors, except for Itchy-NonItchy, Scratchy-NonScratchy, and Prickly-NonPrickly. The values of the effect size (t statistic) are small. This is because on the one hand, active and passive touch will not be the major impact other than the stimuli themselves; on the other hand, the variances of subjective measurements are normally large, which reduces the value of the effect size by increasing total variances.

Another approach to investigate the impact of passive and active touch is through the discrimination capacities during each instance of active and passive touching. The discrimination capacity is defined as whether the subject could give significantly different scores for two different stimuli. Therefore, post-hoc analyses with Tukey’s method were conducted. For each active and passive touch evaluation, non-discriminated count (NDC) is defined as the number of pairs of fabrics that the subjects could not differentiate significant differences. The following table lists the NDCs during both passive and active touching. A clear advantage can be found in the Cool-Warm, Sticky-NonAdhesive, Thick-Thin and NonFullness-Fullness descriptors. There are also some descriptors that have discrimination advantages during passive touch. However, these values are just slightly lower than those of active touch.

Table 6-4 Summary of Overall Impact of Touch Method and SDC on Individual Descriptors

Dependent Variable	p	t	SDC
Cool-Warm	.000	-4.841	18
Itchy-NonItchy	.607	-.514	8
Scratchy-Nonscratchy	.548	-.601	13
Prickle-Nonprickle	.157	-1.416	10
Rough-Smooth	.000	-3.565	15
Stick-Nonadhesive	.006	-2.757	6
Stiff-Pliable	.003	-2.942	12
Thick-Thin	.052	1.942	17
Hard-Soft	.006	-2.772	13
Nonfullness-Fullness	.022	-2.294	11

Table 6-5 Summary of NDC during both Passive and Active Contact Method

Dependent Variable	NDC during Passive Contact	NDC during Active Contact
Cool-Warm	3.11	2.37
Itchy-NonItchy	3.47	3.58
Scratchy-NonScratchy	3.26	3.16
Prickly-NonPrickly	3.42	3.16
Rough-Smooth	2.68	2.58
Stick-NonAdhesive	8.26	5.95
Stiff-Pliable	2.16	2.37
Thick-Thin	2.84	1.68
Hard-Soft	2.05	2.16
NonFullness-Fullness	5.58	2.68

In short, there exist differences between passive and active touch when the subjects use these means to evaluate fabrics. The descriptors that are likely to show differences include Cool-Warm, Rough-Smooth, and Thick-Thin. Meanwhile, a discrimination advantage is found with active touch over passive touch for the Cool-Warm, Sticky-NonAdhesive, Thick-Thin and NonFullness-Fullness descriptors.

6.2.3 Effect of Climatic Conditions on Individual Descriptors

Two-way ANOVA testing was also carried out to demonstrate the effects of climatic conditions on individual descriptors. Result as shown in Table 6-6 confirms that there are significant differences between subjects who are in different climatic conditions.

Table 6-6 Two-Way ANOVA Test of Climate Condition and Fabric on Individual Descriptors

Source	Descriptor	df	F	Sig.
Main Effect: Climate Condition	Cool-Warm	5	19.535	.000
	Itchy-NonItchy	5	40.916	.000
	Scratchy-NonScratchy	5	68.122	.000
	Prickly-NonPrickly	5	57.758	.000
	Rough-Smooth	5	23.080	.000
	Stick-NonAdhesive	5	18.522	.000
	Stiff-Pliable	5	27.439	.000
	Thick-Thin	5	20.344	.000
	Hard-Soft	5	21.536	.000
	NonFullness-Fullness	5	19.528	.000
Interaction Effect: Fabric * Climate Condition	Cool-Warm	90	3.343	.000
	Itchy-NonItchy	90	2.633	.000
	Scratchy-NonScratchy	90	3.268	.000
	Prickly-Nonprickly	90	3.286	.000
	Rough-Smooth	90	3.747	.000
	Stick-NonAdhesive	90	9.410	.000
	Stiff-Pliable	90	3.457	.000
	Thick-Thin	90	2.173	.000
	Hard-Soft	90	4.451	.000
	NonDullness-Fullness	90	6.044	.000

Table 6-7 Effect of Climate Temperature and Relative Humidity on Individual Descriptors from Dummy Variable Regression

Factor	Descriptor	B	t	Sig.
Climate Temperature	Cool-Warm	-0.062	-4.854	0.000
	Itchy-NonItchy	0.105	8.936	0.000
	Scratchy-NonScratchy	0.121	10.093	0.000
	Prickly-NonPrickly	0.100	8.796	0.000
	Rough-Smooth	0.068	4.839	0.000
	Sticky-NonAdhesive	-0.016	-1.179	0.238
	Stiff-Pliable	0.020	1.563	0.118
	Thick-Thin	0.040	3.349	0.001
	Hard-Soft	0.000	0.006	0.995
	NonFullness-Fullness	-0.114	-9.082	0.000
Climatic Relative Humidity	Cool-Warm	-0.021	-7.145	0.000
	Itchy-NonItchy	0.009	3.250	0.001
	Scratchy-NonScratchy	0.006	2.367	0.018
	Prickly-NonPrickly	0.007	2.719	0.007
	Rough-Smooth	0.004	1.369	0.171
	Sticky-NonAdhesive	-0.010	-3.136	0.002
	Stiff-Pliable	-0.003	-1.216	0.224
	Thick-Thin	0.008	2.854	0.004
	Hard-Soft	-0.011	-3.934	0.000
	NonFullness-Fullness	-0.026	-9.081	0.000
Climatic Temperature * Climatic Relative Humidity	Cool-Warm	0.001	5.161	0.000
	Itchy-NonItchy	-0.002	-8.118	0.000
	Scratchy-NonScratchy	-0.002	-9.314	0.000
	Prickly-NonPrickly	-0.002	-8.346	0.000
	Rough-Smooth	-0.001	-3.787	0.000
	Sticky-NonAdhesive	0.000	1.008	0.313
	Stiff-Pliable	0.000	-0.042	0.966
	Thick-Thin	0.000	-2.222	0.026
	Hard-Soft	0.000	1.330	0.184
	NonFullness-Fullness	0.002	9.173	0.000

The climate temperature and relative humidity as provided above were used to represent the climatic condition. In the following dummy variable regression analysis, fabric was selected as the dummy variable while climate temperature relative humidity as the covariates. The potential impacts of climate relative humidity will be revealed through this analysis. The results of their are summarized in

Table 6-7.

The climate temperature shows a negative effect on the Cool-Warm descriptor and a positive effect on most surface-related descriptors. It also shows a positive effect on the Thick-Thin descriptor and a negative effect on the NonFullness-Fullness descriptor. Meanwhile, the relative humidity shows a negative effect on the Cool-Warm descriptor, but a positive effect on most of the surface-related descriptors. A negative effect of the relative humidity is also found for the Sticky-NonAdhesive, Hard-Soft, and NonFullness-Fullness descriptors, but a positive effect for the Thick-Thin descriptor.

6.3 Identification of Touch Sensory Dimensions

For the purpose of grouping similar descriptors and ease of understanding of the relation between somatosensory neurophysiological mechanisms and psychological touch sensation, identification of the dimensions of the touch sensory is carried out. A factor analysis along with a PCA was used to define the dimensions of fabric touch sensation. The varimax rotation method was selected because it can better distinguish the sensory dimensions.

6.3.1 Effect of Actively and Passively Touch on Sensory Dimension Identification

The following scree plot, Figure 6-10, shows that three dimensions could explain for up to 65.6% of the total variances from the 10 selected descriptors. The first component accounted for the largest percentage of the variances at 32.6% while the other two accounted for 20.5% and 12.4% respectively.

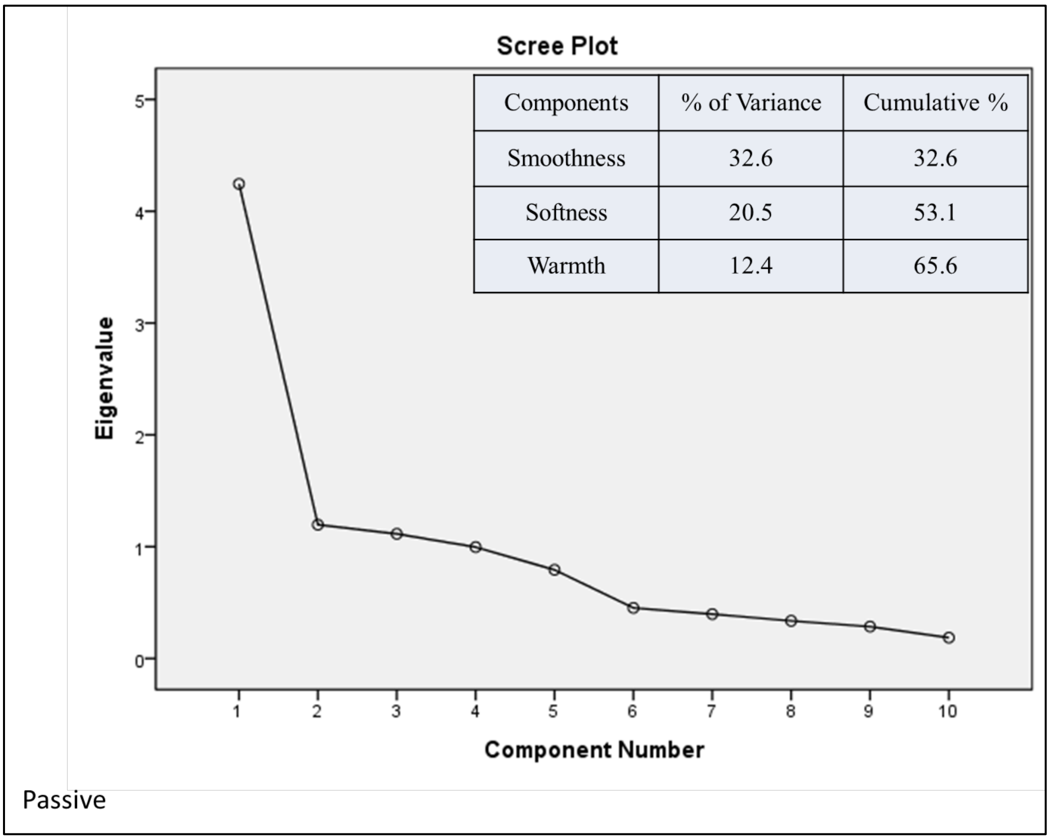

Components	% of Variance	Cumulative %
Smoothness	32.6	32.6
Softness	20.5	53.1
Warmth	12.4	65.6

Figure 6-10 Scree Plot of Passive Touch Sensory Dimensions

These three dimensions are named smoothness, softness and warmth. The constitutions of these three dimensions are summarized in Table 6-8. Only the loadings larger than 0.5 are shown.

Table 6-8 Constitution of Passive Touch Dimensions

Descriptors	Smoothness	Softness	Warmth
Scratchy-NonScratchy	.896	--	--
Prickly-NonPrickly	.889	--	--
Itchy-NonItchy	.868	--	--

Rough-Smooth	.670	--	--
Sticky-NonAdhensive	.201	-.023	-.174
Hard-Soft	--	.814	--
Stiff-Pliable	--	.775	--
Thick-Thin	--	.707	--
NonFullness-Fullness	--	--	.882
Cool-Warm	--	--	.503

Four of the surface-related descriptors comprise smoothness with a larger value means a smoother feeling. They are Scratchy-NonScratchy, Prickly-NonPrickly, Itchy-NonItchy, and Rough-Smooth. These four descriptors are closely related to the texture properties of the fabric surface and texture stimulus as discussed in previous chapters. Hard-Soft, Stiff-Pliable, and Thick-Thin descriptors form the second dimension, which is softness. A larger value in the softness indicates softer samples. These three descriptors represent the mechanical properties of fabrics. There must be force reactions exerted onto the human skin when performing such evaluations. Clearly, this dimension reflects the stimuli in the group of force reactions. There are only two descriptors for the last dimension (warmth): NonFullness-Fullness and Cool-Warm. However, Sticky-NonAdhesive is only descriptor that cannot be easily defined by any dimension. The largest loading that can be found is a positive correlation between Sticky-NonAdhesive and smoothness.

With regard to active touch, the same three dimensions also apply: smoothness (39.4%), softness (19.1%), and warmth (16.5) respectively as shown in Figure 6-11. The loadings of the three dimensions are similar as those from passive touch. Warmth, which represents the thermal stimulus, has a higher percentage of variances compared to that of passive touch.

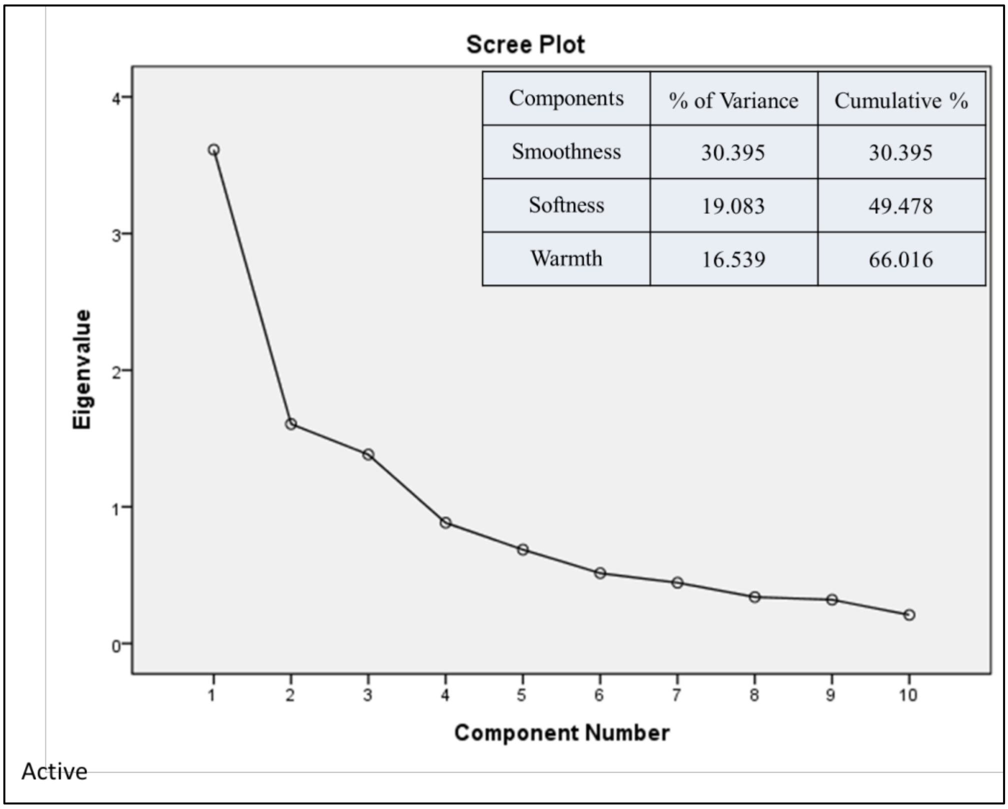

Figure 6-11 Scree Plot of Active Touch Sensory Dimensions

The loadings of each dimension are summarized in as follows Table 6-9. The basic constitutions of the three dimensions of active touch are the same as those of passive touch. It is only during active touch that the Thick-Thin descriptor has a noticeable influence on both softness and warmth. On the other hand, the Sticky-NonAdhesive descriptor still cannot be concretely grouped into any dimensions.

Table 6-9 Constitution of Active Touch Dimensions

Descriptors	Smoothness	Softness	Warmness
Scratchy-NonScratchy	.908	--	--
Prickly-NonPrickly	.876	--	--
Itchy-NonItchy	.854	--	--
Rough-Smooth	.681	--	--

Hard-Soft	--	.822	--
Stiff-Pliable	--	.814	--
Thick-Thin	--	.610	-.558
NonFullness-Fullness	--	--	.788
Cool-Warm	--	--	.737
Sticky-NonAdhesive	.204	-.325	-.388

Table 6-10 One-Way ANOVA Test of Fabric on Sensory Dimensions

Effect	**df**	**F**	**p**
Passive Smoothness	18	59.173	0.000
Passive Softness	18	118.386	0.000
Passive Warmth	18	31.136	0.000
Active Smoothness	18	67.149	0.000
Active Softness	18	218.801	0.000
Active Warmth	18	214.937	0.000

The factor analyses carried out separately based on passive and active touch led to the same three dimensions with similar constitutions. The loadings of the three dimensions still varied during the implementation of these two types of touch. Smoothness counts more for passive touch while loadings of both softness and warmth increase during active touch. A detailed discussion on the effects of touch on sensory dimensions is discussed later. As shown in the Table 6-10, the one-way ANOVA results are summarized for these dimensions based on passive and active touching of fabrics. There are significant differences between these sensory dimensions. The sizes of the effects also indicate that greater differences can be found during active touch.

6.3.2 Effect of Climatic Condition on Identification of Sensory Dimensions

In terms of the probable influences from climatic conditions on the loading of these sensory dimensions, the same factor analyses were individually conducted for each climatic condition. The results showed that the concluded dimensions are similar in their constitutions for each climatic condition, which are smoothness, softness, and warmth as well. The loadings of these dimensions, however, varied for different climatic conditions. In the Table 6-11, the loadings of the three sensory dimensions under different climatic conditions are provided. They all follow a pattern in which smoothness is the most important dimensions; followed next by softness; and finally, warmth as the least important of the three dimensions. However, a clear trend that associates climate temperature or relative humidity with loadings of these sensory attributes cannot be found in this study.

6.3.3 Discussion

Smoothness, softness, and warmth are attributed as factors that contribute to the psychological discrimination of various fabrics with the use of both passive and active touching. The aforementioned studies have stated that three types of stimulus information that could be received by the human skin are texture information, reaction force information from mechanical stimuli, and temperature information from thermal stimulus. The identification of dimensions from psychological behavioral measurements ascertained that humans could discriminate fabric touch sensation in accordance with these three types. From a list of commonly used descriptors for fabric touch sensation, subjective evaluations showed that, as hypothesized, these descriptors could be expressed as the three dimensions through somatosensory neurophysiological mechanisms.

Table 6-11 Summary of Sensory Dimension Loadings during Each Climatic Condition

Contact Method	Climatic Condition	Loading of Smoothness	Loading of Softness	Loading of Warmth
Passive	1	29.9	21.5	10.6
	2	26.3	23.7	11.1
	3	26.5	26.3	10.5
	4	27.6	22.6	10.2
	5	29.9	20.4	10.3
	6	33.7	30.6	10.3
Active	1	29.2	23.3	10.4
	2	26.0	21.0	15.0
	3	25.3	18.8	11.0
	4	26.0	19.5	10.3
	5	28.9	20.8	10.3
	6	32.7	30.0	10.3

The three dimensions show that thermal stimulus should be just as important aspect of touch sensation as other tactile stimuli. Although the loadings of warmth have the smallest value among the dimensions of passive touch, warmth counts for more than half of softness. Furthermore, with evaluation through active touching, there is less than a 3 percent difference between warmth and softness. This chapter therefore echoes the conclusion of those in Chapters 4 and 5: thermal stimulus is an important dimension of fabric touch sensation.

Smoothness is the most important among the three dimensions. This indicates that texture information from mechanical stimuli is the most significant aspect in the evaluation made by the subjects in this study. A number of studies have categorized the responses to reaction forces into amount of stiffness and pressure. However, in this study, the results suggest that the Stiff – Pliable and Hard – Soft descriptors could be grouped as a softness dimension.

6.4 Effect of Active and Passive touch and Climatic Conditions on Sensory Dimensions

6.4.1 Effect of Active and Passive touch on Sensory Dimensions

Similar statistical analyses were again conducted for sensory dimension scores. Two-Way ANOVA test illustrates that although the main effect from contact method did not lead to significant for different fabrics, interaction effects from both fabric and contact method precipitate different scores for all three sensory dimensions.

Table 6-12 Two-Way ANOVA test of Contact Method and Fabrics on Sensory Dimensions

Effect	Sensory Dimension	df	F	p
Main Effect: Contact Method	Smoothness	1	.000	.998
	Softness	1	.001	.978
	Warmth	1	.000	.982
Interaction Effect: Fabric * Contact Method	Smoothness	18	17.862	.000
	Softness	18	5.420	.000
	Warmth	18	26.961	.000

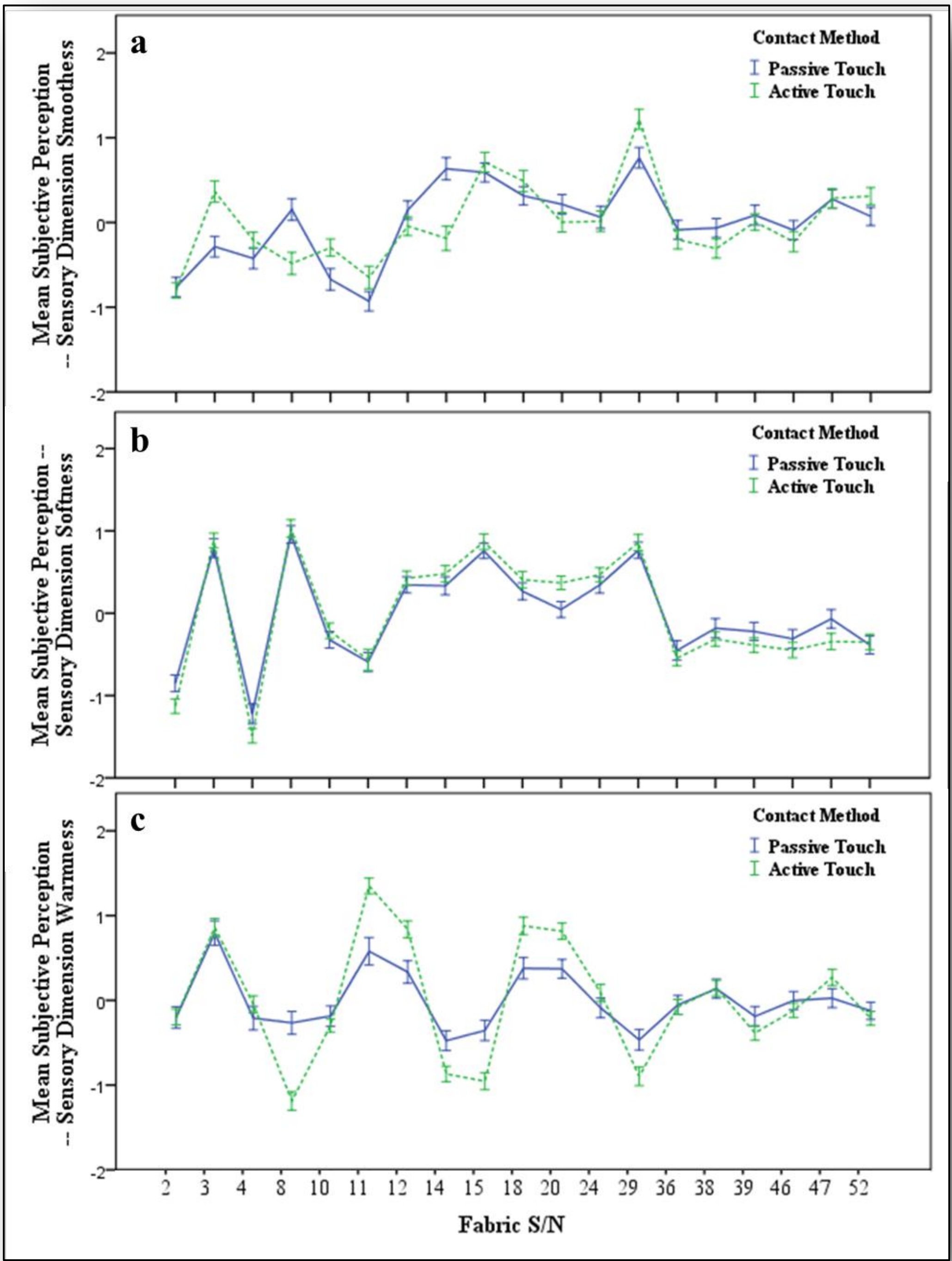

Figure 6-12 Results of Sensory Dimension during Passive Touch and Active Touch respectively

With regard to the perception of smoothness, individual ANOVA test for each sample indicates that 12 out of 19 fabrics show significant differences between by using of passive and active touching. The NDC of passive touch is 4.84 while that of active touch is 4.32. There were only 5 fabrics that showed significant differences as regards softness. The two curves are quite similar as shown above in Figure 6-12. Solid lines represent the results during active touch while dashed lines indicate results during passive touch. The NDCs are also similar. They are 2.84 and 3.58 for passive and active touch respectively. In terms of warmth, 11 fabrics show significant differences between by using passive and active touching. The NDC during passive touch is 6.63 and significantly decreases to 2.84 in active touch.

In summary, conflicting results on subjective perception are likely to be obtained for smoothness and warmth during passive and active touching, although softness does not appear to show significant differences. Active touch shows a remarkable advantage for the discrimination of warmth. The discrimination capacities of the other two attributes seem to be nearly the same; passive touch seems to be slightly better in discriminating softness and active touch in smoothness.

6.4.2 Effects of Climatic Condition on Sensory Dimensions

In Table 6-13, the two-way ANOVA test results of the effect of climatic conditions and fabric are provided. The probability p values of both the main effects from the climatic conditions and effect of the interactions of the climatic condition and fabric suggest that different climatic conditions are likely to cause varying scores on touch sensory dimensions. The size of the effect (F values) shows that warmth is most impacted due to climatic condition.

Table 6-13 Two-Way ANOVA test of Climatic Condition and Fabric on Sensory Dimensions

Effect	Sensory Dimensions	df	F	p
Main Effect:	Smoothness	5	60.445	.000
Climatic Condition	Softness	5	49.006	.000
	Warmth	5	20.253	.000
Interaction Effect:	Smoothness	90	3.581	.000
Fabric * Climatic	Softness	90	4.343	.000
Condition	Warmth	90	4.648	.000

In Table 6-14, the coefficients of climate temperature and relative humidity from the dummy variable regression as stated previously are shown. The outcomes suggest a positive relationship between climate temperature and smoothness, but a negative impact from climate temperature to warmth. The relative humidity of the climate also shows a positive impact on smoothness but negative impact on both softness and warmth.

The series of experiments conducted in six climatic conditions suggests that climatic conditions, such as temperature and relative humidity, have noticeable impacts on touch perception. Temperature could lead to a positive impact on smoothness perception and negative impact on warmth perception while its influence on softness seems to be limited. Meanwhile, relative humidity has significant impacts on all three dimensions: it is positive on smoothness, and negative on softness and warmth.

Table 6-14 Effect of Climate Temperature and Relative Humidity on Sensory Dimensions from Dummy Variable Regression

Factor	Sensory Dimension	B	t	Sig.

Climate Temperature	Smoothness	0.089	9.251	0.000
	Softness	-0.016	-1.936	0.053
	Warmth	-0.07	-7.543	0.000
Climate Relative Humidity	Smoothness	0.005	2.487	0.013
	Softness	-0.005	-2.728	0.006
	Warmth	-0.02	-9.536	0.000
Climate Temperature * Climate Relative Humidity	Smoothness	-0.001	-8.638	0.000
	Softness	0.001	3.599	0.000
	Warmth	0.001	7.851	0.000

6.5 Discussion

6.5.1 Discussion on Active and Passive Touch

Active touch and passive touch describes different cases when we contacting fabrics in daily life. When firstly evaluating the touch sensations of fabrics, we used active touch methods to "manipulate" the sample and conclude the preferences. Whilst when making buying decisions on ready-to-wear garments, especially on those which were usually wore next-to-skin, we would like to try them on. That is a kind of passive touch evaluation. The perception from active touch may be more important in textiles selection while the royalty building would depend more on the passive touch perception, i.e. wearing sensations.

There was no common conclusion on whether passive touch is superior to active touch or vice versa. The experiments conducted in this study indicate that perception through either active or passive touch is not the same in terms of the three different attributes of touch sensation. Based on the nature of passive and active touch, a basic assumption is made here. The author of this thesis work believes that passive touch only stimulates receptors located in shallow skin while active touch allows subjects to gain more information from all skin receptors while manipulating objects.

Figure 6-13 shows the skin anatomy and location of different receptors. Two types of slowly adapting afferents, Merkel corpuscles (SAI) and Meissner corpuscles (SAII), are located shallowly under the skin. Two types of fast adapting afferents, Ruffini endings (FAI) and Pacinian corpuscles (PC), are located deeper under the skin. Some of them are located shallow in the skin so they may be stimulated by passive touch while the others are deeper into the skin, which means they require more skin indentation for stimulation.

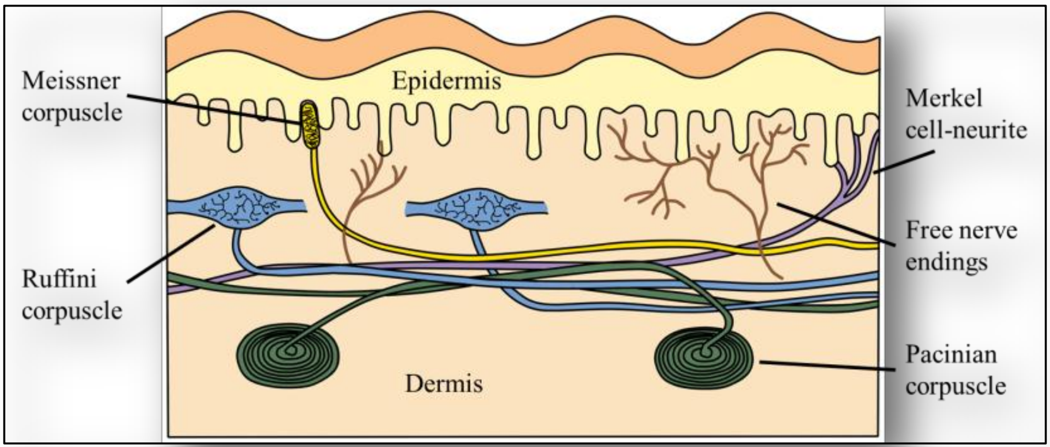

Figure 6-13 Location of Cutaneous Receptors in Human Skin

With regard to the sensation of smoothness, there are differences between perception obtained from passive and active touch yet the discrimination capacities are similar. There are two concluded coding mechanisms of texture information. The first is temporal coding of PC fiber (Pacinian corpuscles) and the second is spatial coding of SA1 fiber (Merkel corpuscles). Temporal coding is considered to be stimulated through vibration caused by surface unevenness (Hollins & Bensmaia, 2007) while spatial coding provides different impulse rates, correlated with the height and width of unevenness, along the surface of objects that are touched (D. T. Blake et al., 1997) (David T Blake et al., 1997) (Yoshioka et al., 2001). Scientists have concluded that temporal codes are more sensitive to unevenness distances less than 200 micrometers, see (S. Bensmaia & Hollins, 2005; Mackevicius et al., 2012). The unevenness of fabrics could be constituted by both fabrication structure (on a millimeter scale) and yarn/fiber unevenness (on a micrometer scale). As a result, it seems possible to stimulate both types of receptors for texture information on fabric. The consequence of this feature of fabrics may lead to results where although the smoothness perception by receptors through passive and active touch tends to be different, the discrimination capacity of passive and active touch is similar.

In terms of softness, there are hardly any differences discerned between active and passive touch whilst the latter shows slightly better discrimination capacity. Neurophysiological studies have revealed that SA1 fiber (Merkel corpuscle) fire strongly in relation to stimulus compliance (Condon et al., 2014). Regardless of the light indentation of skin as a form of passive touch or deep indentation as active touch, these afferent fibers which are located at the epidermis level, could be stimulated. Therefore, there is no difference between active and passive touch.

As regards warmth, the differences are significant and active touch shows an advantage in discrimination. The perception of warmth is unique compared to smoothness or softness. The trigger of thermoreceptors, changes in the temperature, always exists. The human skin has the ability to sense the surrounding temperature. Since the stimuli were conditioned to the surrounding temperature (21 °C) for more than 24 hours, it is reasonable to assume that their surface temperature was around 21°C. With human skin temperature at around 32°C (Freitas, 1999), the perception of the warmth of a stimulus is actually the perception of the stimulus temperature, which is affected by the thermal conductivity of the stimulus. With regard to soft materials like fabric, their thermal conductivities are significantly reduced if they are pressed. Therefore, the perceived warmth of these fabric stimuli is mostly different in passive and active touch. The factor analysis results also confirm that warmth is also affected by fullness and thickness of the stimulus. These two characteristics, however, could hardly be perceived through passive touch, which leads to the advantage of active touch in the discrimination of the warmth of a stimulus.

This comparison study of the psychological results and neurophysiological theories finds that the effect of active and passive touch varies for different dimensions of touch perception. The anatomical location of different receptors means that it may be easier to stimulate them with either active or passive touch.

6.5.2 Discussion on Climatic Condition

The negative correlation found between climate temperature and warmth is in agreement with the temperature acclimation hypothesis. The thermal receptors in the human body can adjust accordingly to different climatic conditions. The study by Mäkinen et al. (Mäkinen et al., 2004) confirmed that the threshold of cold sensation differs according to climate changes. In Figure 6-14, the concept of acclimation is illustrated. Three double-arrow lines represent classification of thermal sensation from cold to hot. When climate condition changes, acclimation could cause the whole perception range shifted, i.e. change on cold/hot detection threshold. Sample α, for instance, is a stimulus that is rated neutral in a climatic condition of a mid-range temperature. Although its temperature remains the same, fabric would be perceived as cooler or warmer respectively when situated in a climatic condition with either a high or low temperature.

A negative correlation between warmth and climate relative humidity may be due to the good heat transition property of water/water vapor. Experiments on mice showed that an environment with lower humidity leads to significantly lower skin conductance (Katagiri, Sato, Nomura, & Denda, 2003). It is highly likely that even though the subjects in this study had been resting in a standard chamber for more than half an hour, the water content of their skin was still under the effect of the local humidity environment, i.e. a lower climate relative humidity leads to lower skin conductance. Since the temperature of human skin is higher than the chamber temperature, heat transferred from skin to ambient air through the fabrics and skin when the subjects were evaluating the samples. Therefore, with the same fabric, lower skin conductance transfers less heat and a warmer sensation could be perceived.

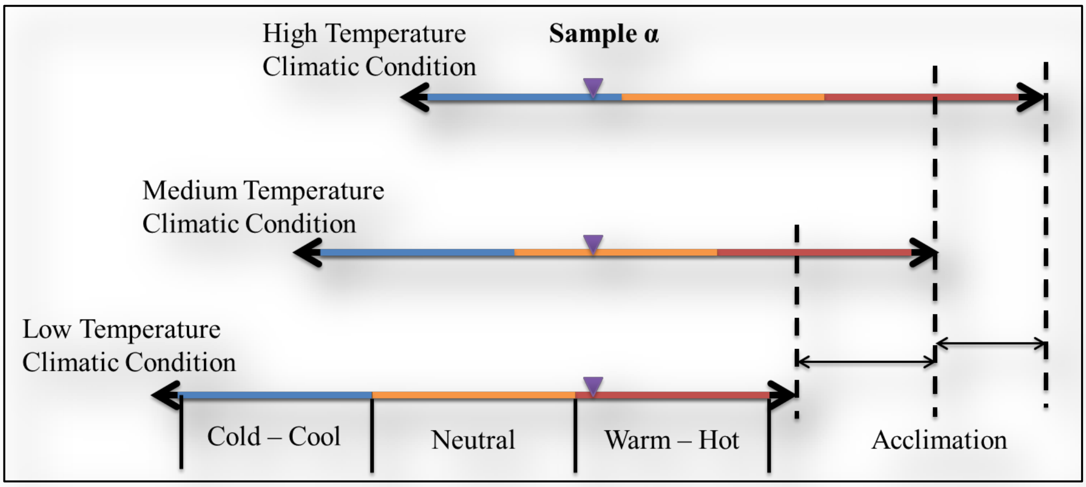

Figure 6-14 Effect of Temperature Acclimation on Thermal Perception

Another significant correlation found here is the negative influence on smoothness from the climate relative humidity. This correlation is much more significant with active touch than passive touch. Besides sensing surface unevenness, the detecting of the forces of relative movement between the skin and stimulus is also a means to perceive smoothness. Previous discussions have stated that climate humidity subsequently have effects on skin humidity (i.e. water content). A higher water content is likely to cause a stickier feeling. A stickier fabric, in terms of sensation, is always referred to as having a rougher feel. This could be the reason why climate humidity has a negative correlation to the sensation of smoothness.

With regard to the correlation between softness and climate temperature and relative humidity, climatic conditions could change the stiffness of skin tissue. The literature has suggested that properties of the stratum corneum, the outermost layer of epidermis, are highly affected by the climate temperature and relative humidity. A higher relative humidity would lead to a less stiff stratum corneum (Xu & Lu, 2011). Meanwhile, the perception of the softness of a stimulus has been mainly detected as cutaneous information through skin indentation (Condon et al., 2014). A stiffer skin would be indented less so under the same pressure, which leads to a softer feel for the stimulus. As a result, a higher relative humidity means that a stimulus will be perceived as harder.

6.6 Conclusion

The objective 4 has been completed in this chapter through subjective measurement, design of experiment of which includes both active and passive touch method as well as six different climatic conditions. Mechanism of psychological discriminations regarding fabric touch sensations are discussed in this chapter.

The effects of active and passive touch and climatic conditions on touch sensation are evaluated in this psychophysical section of the thesis study. Reported study involved a large number of human subjects so that the trends are presented with more accurate. The findings from the psychological experiments here are in agreement with the physiological mechanisms of sensation perception. Two types of coding mechanisms of smoothness, which are temporal and spatial variances, lead to different perceptions of smoothness with the use of active or passive touching, while their discrimination capacities are similar. The responsible receptors that are shallow in the skin makes passive touch preferable for the perception of softness. The perception of warmth, on the other hand, requires multiple types of information other than stimulus temperature, which means that active touch is more sensitive to perceiving warmth. Meanwhile, influences are also found from climatic conditions, such as temperature and relative humidity. Temperature acclimation causes changes in the perception of warmth. Relative humidity influences the skin properties and changes their behaviors when evaluating a stimulus. Climatic conditions could even have impacts when touch perception occurs in a general indoor environment.

Chapter 7 Psychophysical Relationships

The aim of this chapter is to accomplish objective 5 by exploring the relations between psychological sensation and physical stimuli as well as the effects of the interactions of different types of physical stimuli on individual sensory dimensions. Classic psychophysical laws, as they pertain to psychophysical relations, are also investigated.

Three different levels of the perception of touch sensation with fabric are discussed in Chapters 4 to 6. At the physical level, there is the detection of physical stimuli (see Chapter 4). At the neurophysiological level, there is the coding of physical stimuli to neural signals (see Chapter 5). At the psychological level, there is the integration of information passed onto the cerebrum and a conclusion on touch preferences (see Chapter 6). On the basis of the studies at these three levels, prediction methods that link them are subsequently evaluated in Chapters 7 and 8.

Psychophysical approaches are most commonly used to link these different levels of perception. Psychophysical laws, known as the Weber-Fechner law or Stevens' power law, are well known relationships that denote the underlying connections between stimuli and responses. As reviewed in Chapter 2, many other psychophysical approaches have been previously used, including regression, artificial neural network, and fuzzy logic. However, these studies have not completely investigated the psychophysical relations that take into consideration the effects of the interaction of different types of physical stimuli.

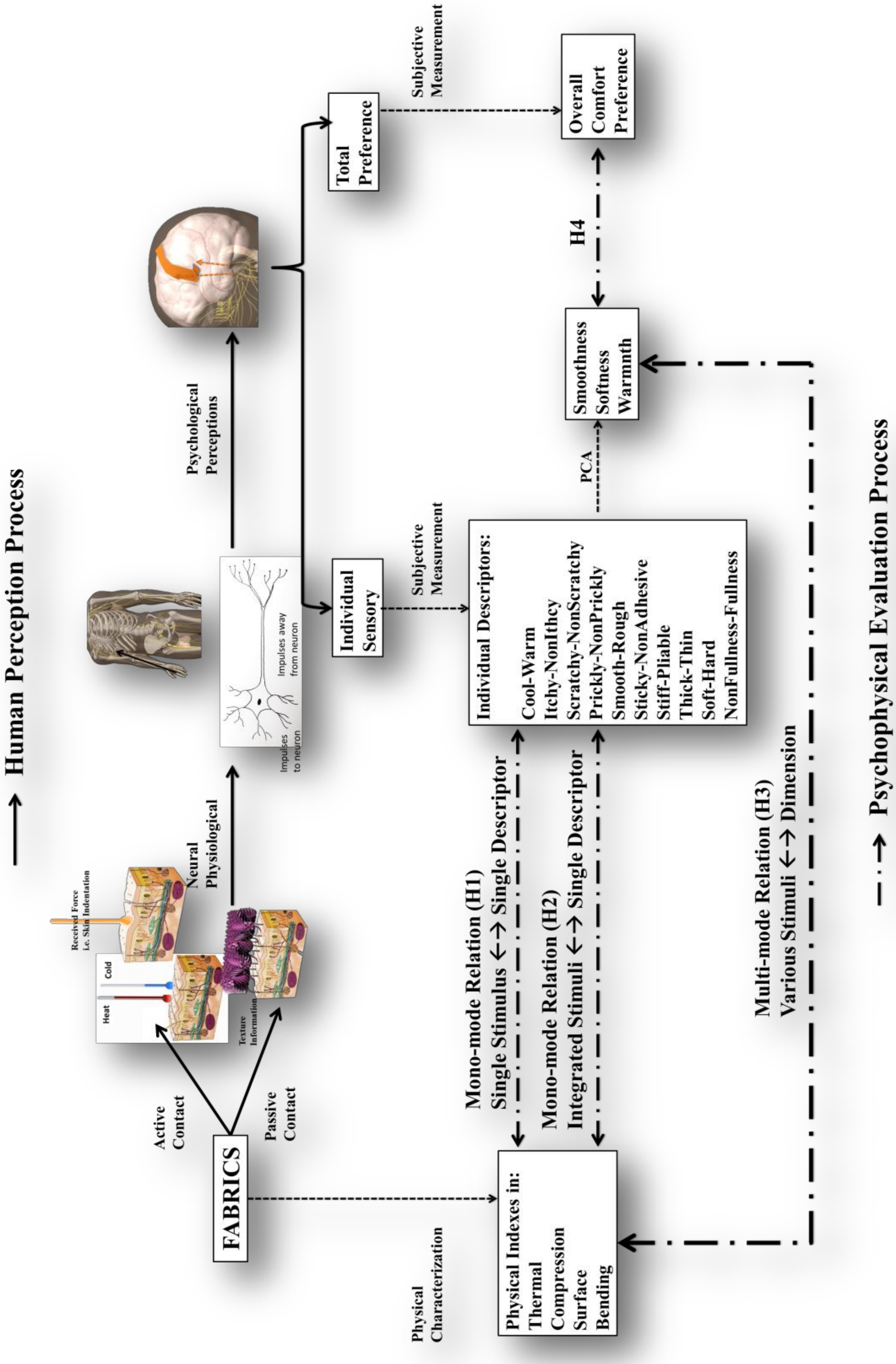

Figure 7-1 Description of sensory perception and simulation of the perception process

Sensory perception begins from the detection of physical stimuli from contacted objects. In this study, the objects are different types of fabrics. Humans can actively or passively touch fabrics. Fabrics then stimulate the corresponding skin receptors. These receptors transduce the stimulations into neural signals. The neural signals are then transmitted to the brain through the central nerve system (CNS). Finally, touch sensation from a fabric is received after contact. This complete process is illustrated in the upper part of Figure 7-1.

The dotted lines on the left in Figure 7-1 show previously reported direct measurements on physical stimuli detection, which have been discussed in Chapter 4. With reference to active and passive methods, which are two ways to perceive stimuli, the characterized physical properties obtained from using the FTT also include indexes for both the face and back sides respectively. Meanwhile, the dotted lines on the right show the psychological perception measurements discussed in Chapter 6. There are two types of subjective results obtained. The first is ten individual descriptors that indicate the direct subjective "feeling" of the fabrics. The other is the overall comfort preference, which is an integrated preference that takes into consideration all aspects of the touch sensation. These ten descriptors were then further grouped into three attributes through a PCA. The three sensory dimensions include smoothness, softness, and warmth. They could better show the different aspects of touch sensation because each sensory dimension refers to a type of skin cutaneous simulation. Smoothness refers to the distribution differences of shallow skin indentations; softness to the received forces that cause deep skin indentations; and warmth refers to the stimulation of the thermoreceptors.

The psychophysical evaluation links physical stimuli and psychologically perceived sensations, shown as dashed lines in the lower part of Figure 7-1. There are generally three levels of relations. First, physical stimuli are evaluated to directly address various subjective "feelings", i.e. descriptors. Mono-mode relations are commonly built based on different assumptions, including psychological laws and linear assumptions. Secondly, the psychophysical relationship between physical stimuli and psychologically perceived dimensions are discussed through a multi-mode relation. Lastly, integration of a sensory dimension is expected to correlate with subjective total comfort. Detailed methods to analyze these relations will be discussed in the next section.

7.1 Methodology

Psychophysical analyses simulate the entire neurophysiological perception process with statistical techniques. The fundamental objective of psychophysical analysis is to explore whether there is a solid relationship between physical stimuli and psychological perception.

7.1.1 Hypothesis 1

Psychophysical laws have provided universal linkages between human sensation and stimuli to these sensations. The Weber-Fechner law indicated that an increase in the intensity of a stimulus would be proportional to an increase in the perception of this stimulus. It is agreed that there is a logarithm relationship. The formula could be transformed as:

$$P = k \, ln \frac{S}{S_0} = f_1(S) \tag{7-1}$$

where P is magnitude of perception, k is an empirical-defined constant parameter, S and S_0 are the intensity of physical stimulus and the minimum perceived physical stimulus intensity (threshold). Meanwhile, Stevens' Power Law revised such relationship with power function as:

$$P = tS^{\alpha} = f_2(S) \tag{7-2}$$

where t is a constant depends on stimulus unit, and α is empirical-defined parameter for different sensation.

Linear relationships, on the other hand, are most commonly used in establishing psychophysical connections. The relationship could be described by using a formula such as:

$$P = mS - mS_0 = f_3(S) \tag{7-3}$$

where m is the coefficient of linear relationship.

7.1.2 Hypothesis 2

There are, however, many ways to characterize the physical properties of stimuli with no general agreement. A hypothesis is consequently offered. The potential relationship between integration of features, through different characterization concepts, of stimulus and individual descriptor is evaluated. Since there are mainly three reported function relations between them, the hypothesized relation formulas are separately defined as:

$$P = \sum k_i \, ln \frac{S_i}{S_{io}} = f'_1(S_i); or \tag{7-4}$$

$$P = \sum t_i {S_i}^{\alpha} = f'_2(S_i); or \tag{7-5}$$

$$P = \sum m_i (S_i - S_{io}) = f'_3(S_i) \tag{7-6}$$

7.1.3 Hypothesis 3

Individual descriptors, as investigated in Chapter 6 and many other reviewed papers, are usually correlated to each other. As a result, sensory dimensions should be more suitable to test the multi-mode relation hypothesis as their independence are ascertained through the use of PCA. A simple multi-mode relation is hypothesized as the following formula:

$$D = \sum a_i f_1(S_i) + \sum b_j f_2(S_j) + \sum c_l f_3(S_l) = f_4(S) \qquad (7\text{-}7)$$

where D is sensory dimension, S_i, S_j, and S_l are different physical stimuli that felt into different function relations as f_1, f_2, and f_3 respectively, a_i,b_j, and c_l are the coefficient of these physical stimuli.

Meanwhile, the neurophysiological mechanism of the human somatosensory system implies that there are effects of the interaction of various physical stimuli on a single perception aspect. The above formula could be revised to involve potential interactions between these physical stimuli as:

$$D = \sum a_i f_1(S_i) + \sum b_j f_2(S_j) + \sum c_l f_3(S_l) + \sum d_{ijl} f_1(S_i) f_2(S_j) f_3(S_l) = f_5(S) \qquad (7\text{-}8)$$

7.1.4 Hypothesis 4

The total comfort describes the overall touch preference of fabrics. They are believed to directly represent the integration of multiple aspects of "feelings". Therefore, total comfort should be related to the integration of various physical stimuli and subsequently various sensory dimensions. The exact description of this relation is too complex to calculate so a simplified relation between total comfort and sensory attributes is proposed as:

$$C = \int S_i = \int P_i \cong \sum W_d D_d = f_6(D) \qquad (7\text{-}9)$$

Where C is total comfort, D_d is sensory dimension score and W_d is the weight of it.

7.1.5 Experiment

As regards this study, the relation between physical stimuli and psychological perception are determined as follows. Per the discussions in Chapter 6, 10 subjective descriptors and total touch comfort were obtained through subjective measurements. Three sensory dimensions were also defined, which are smoothness, softness, and warmth. The mean values from all 226 subjects were included as the subjective perception values. The physical results of the same fabrics are covered in Chapter 4. Their physical properties were measured by using the FTT. The average values of indexes in the warp and weft directions were used.

7.2 Mono-mode Relation between Sole Characterization of Single Stimulus and Individual Descriptor

Psychophysical laws support the basic idea of Hypothesis 1. They propose correlation between a single defined stimulus and individual descriptor would exist and this correlation would follow the same type of monotonic function, that is, either logarithmic or power, for different types of perceptions. Figure 7-2 illustrates how they are connected. Left side of the figure lists defined index of physical stimuli from FTT. Right side of the figure lists measured psychological perception descriptors. The middle box connecting these two sides represents there are three types of hypothesized mono-mode relations. As defined above, f_1, f_2, and f_3 stand for the correlation of logarithmic, power, and linear functions, respectively.

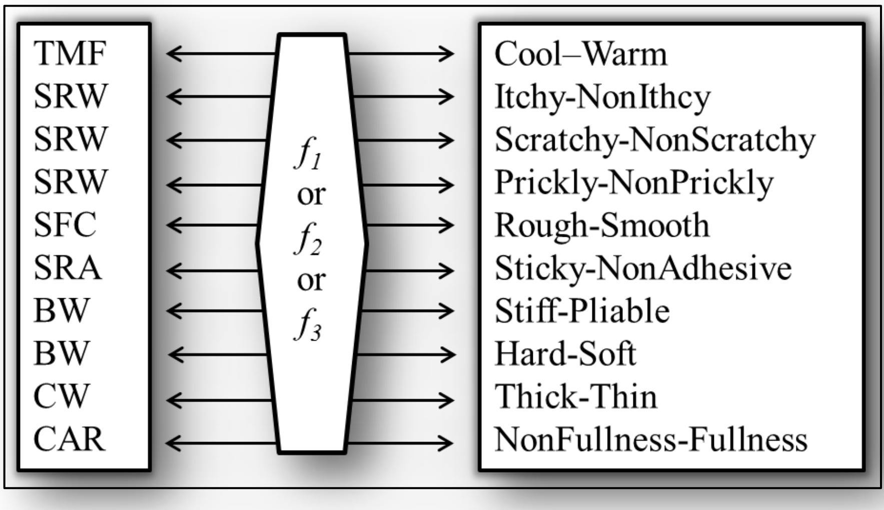

Figure 7-2 Hypothesized mono-mode relation between sole characterization of single stimulus and individual descriptor

7.2.1 Results

In Table 7-1 and Table 7-2, the monotonic correlations between physical stimuli and psychological perception are summarized. Spearman's rho correlation is used to examine for any possible monotonic functions, which usually include power (exponential), logarithmic and linear functions.

Table 7-1 Summary of Model Fits on Mono-mode Relation to Passive Perceived Descriptors (Hypothesis 1)

Descriptor	Statistic	T	CW	CRR	CAR	RAR	TCC	TMF	BAR	BW	SFC	SRA	SRW
Cool-Warm	Coefficient	--	--	--	--	--	--	--	--	--	--	--	--
	p Value	--	--	--	--	--	--	--	--	--	--	--	--
Itchy-NonItchy	Coefficient	--	--	--	--	--	--	--	--	--	--	--	--
	p Value	--	--	--	--	--	--	--	--	--	--	--	--
Scratchy-NonScratchy	Coefficient	--	--	--	--	--	--	--	--	-0.579	--	--	--
	p Value	--	--	--	--	--	--	--	--	0.007	--	--	--
Prickly-NonPrickly	Coefficient	--	--	--	--	--	--	--	--	-0.586	--	--	--
	p Value	--	--	--	--	--	--	--	--	0.007	--	--	--
Rough-Smooth	Coefficient	--	--	--	--	--	--	--	--	-0.562	--	--	--
	p Value	--	--	--	--	--	--	--	--	0.010	--	--	--
Sticky-NonAdhesive	Coefficient	--	-0.597	--	0.608	0.568	--	0.528	--	-0.490	--	-0.487	--
	p Value	--	0.005	--	0.004	0.009	--	0.017	--	0.028	--	0.029	--
Stiff-Pliable	Coefficient	--	--	--	--	--	--	--	--	-0.680	--	--	--
	p Value	--	--	--	--	--	--	--	--	0.001	--	--	--
Thick-Thin	Coefficient	--	-0.483	--	0.483	0.489	--	0.453	-0.522	-0.789	--	--	--
	p Value	--	0.031	--	0.031	0.029	--	0.045	0.018	0.000	--	--	--
Hard-Soft	Coefficient	--	--	--	--	--	--	--	--	-0.716	--	--	--
	p Value	--	--	--	--	--	--	--	--	0.000	--	--	--
NonFullness-Fullness	Coefficient	0.589	0.829	--	-0.833	-0.818	--	-0.838	--	--	--	0.744	0.704
	p Value	0.006	0.000	--	0.000	0.000	--	0.000	--	--	--	0.000	0.001

Table 7-2 Summary of Model Fits on Mono-mode Relation to Active Perceived Descriptors (Hypothesis 1)

Descriptor	Statistic	T	CW	CRR	CAR	RAR	TCC	TMF	BAR	BW	SFC	SRA	SRW
Cool-Warm	Coefficient	0.543	0.857	-0.445	-0.865	-0.765	--	-0.767	--	--	--	0.650	0.623
	p Value	0.013	0.000	0.049	0.000	0.000	--	0.000	--	--	--	0.002	0.003
Itchy-NonItchy	Coefficient	--	--	--	--	--	--	--	--	--	--	--	--
	p Value	--	--	--	--	--	--	--	--	--	--	--	--
Scratchy-NonScratchy	Coefficient	--	--	--	--	--	--	--	--	--	--	--	--
	p Value	--	--	--	--	--	--	--	--	--	--	--	--
Prickly-NonPrickly	Coefficient	--	--	--	--	--	--	--	--	-0.529	--	--	--
	p Value	--	--	--	--	--	--	--	--	0.016	--	--	--
Rough-Smooth	Coefficient	--	--	--	--	--	--	--	--	--	-0.523	--	--
	p Value	--	--	--	--	--	--	--	--	--	0.018	--	--
Sticky-NonAdhesive	Coefficient	-0.534	-0.755	--	0.762	0.695	--	0.713	--	--	--	-0.737	-0.565
	p Value	0.015	0.000	--	0.000	0.001	--	0.000	--	--	--	0.000	0.009
Stiff-Pliable	Coefficient	--	--	--	--	--	--	--	--	-0.693	--	--	--
	p Value	--	--	--	--	--	--	--	--	0.001	--	--	--
Thick-Thin	Coefficient	-0.689	-0.716	--	0.701	0.692	--	0.701	-0.746	-0.922	--	-0.541	--
	p Value	0.001	0.000	--	0.001	0.001	--	0.001	0.000	0.000	--	0.014	--
Hard-Soft	Coefficient	--	--	--	--	--	--	--	--	-0.696	--	--	--
	p Value	--	--	--	--	--	--	--	--	0.001	--	--	--
NonFullness-Fullness	Coefficient	0.672	0.833	--	-0.838	-0.815	--	-0.854	--	--	--	0.741	0.654
	p Value	0.001	0.000	--	0.000	0.000	--	0.000	--	--	--	0.000	0.002

The results show that the Cool-Warm descriptor is monotonically correlated to the thermal index TMF during active touch. The Itchy-NonItchy, Scratchy-NonScratchy, and Prickly-NonPrickly descriptors have no significant correlation to the surface property indexes. The only correlated index is BW. Meanwhile, the Rough-Smooth descriptor is monotonically correlated to the index SFC and Sticky-NonAdhesive descriptor is significantly correlated to the surface index SRA. With regard to the Stiff-Pliable and Hard-Soft descriptors, they are strongly correlated to BW for both passive and active touch. Lastly, the Thick-Thin and NonFullness-Fullness descriptors are correlated to many physical indexes with relatively high coefficients of correlation to CAR and TMF.

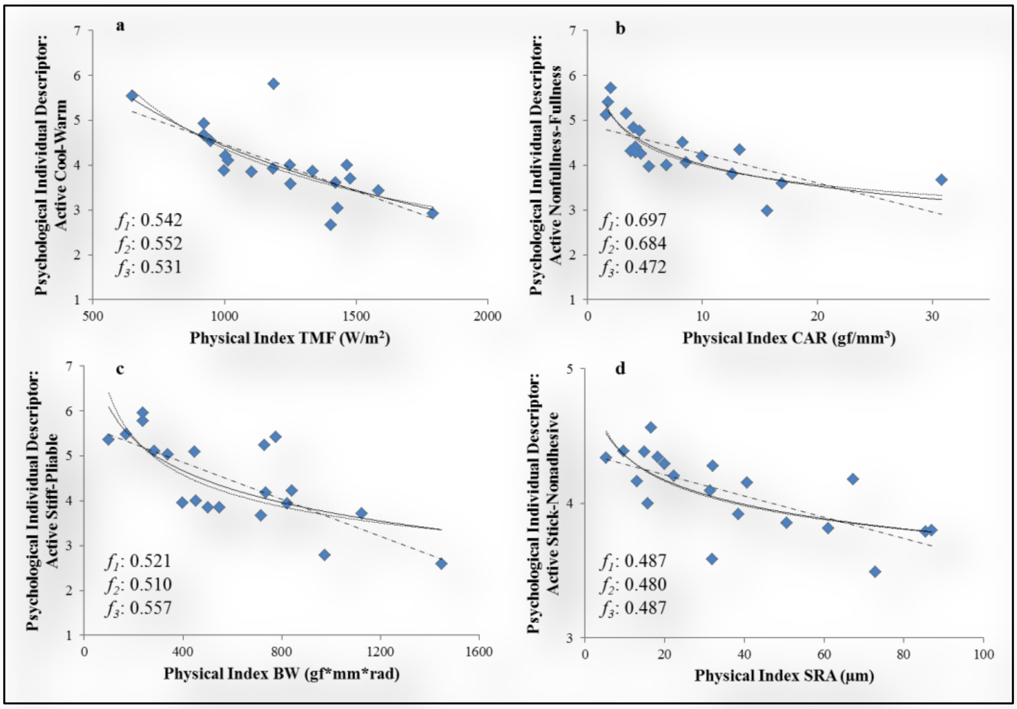

Figure 7-3 Scatterplot between Active Psychological Individual Descriptors and Physical Indexes

A cross-comparison on the mono-mode relation analysis shows that mono-mode relations are generally stronger when associated with the results of active touch rather than passive touch, and the NonFullness-Fullness descriptor has the highest coefficient during both active and passive touch. After obtaining a significant monotonic correlation between pairs of physical stimulus and psychological descriptor, the exact functions are investigated by model fitting techniques.

Figure 7-3 shows the scatter-plots of typical mono-mode relations found between pairs of stimulus and descriptor. Solid line, dot line, and dashed line represent trend-line as logarithmic function (f1), power function (f2), and linear function (f3) respectively. R^2 of all three functions are listed in each figure as well. For the Cool-Warm descriptor and TMF, the power function shows the highest model fit (statistic R^2) while the logarithmic and linear functions both show slightly lower model fit. The logarithmic function is found to have the highest model fit with regard to the relationship between Sticky-NonAdhesive and SRA as well as between the NonFullness-Fullness descriptor and CAR. The linear function is supported when evaluating the relations between the Stiff-Pliable descriptor and BW.

7.2.2 Discussion

The fundamental expectation that psychological perception is significantly correlated to the physical properties of fabric is again proven in this study. Generally speaking, the subjective scoring on specific descriptors is correlated to the anticipated physical property. This finding is in agreement with numerous work in the literature. The finding indicates that the psychological perception of fabrics is related to their physical properties. Hence, a study on fabric touch sensation should be based on the clear physical characterization of the fabrics themselves.

Nonetheless, the functions of these relations vary for different descriptors. Psychophysical laws, including the Weber-Fechner and Stevens' power laws, as well as the assumption of linear functions all demonstrate that they are the best function model for at least one pair of physical stimulus and psychological descriptor. As a result, the abovementioned hypothesis as a universal function relation can hardly be supported by this set of empirical data.

Meanwhile, there are usually several points of views to characterize the physical properties of certain stimuli. For instance, in order to quantify the compressibility of fabric, the CW index uses an energy theory while the use of the CAR index is interpretation of compressibility from the average force. The NonFullness-Fullness descriptor shows monotonic relations with both indexes. Hypothesis 2 discussed in Section 7.3, as a result, is the exploration of the possibility that there is a mono-mode relation between the integration of the characterization of a single physical stimulus and an individual descriptor.

7.3 Mono-mode Relation between Integration of Characterization of Single Stimulus and Individual Descriptor

In the following paragraphs, Hypothesis 2 is discussed as a model for revising the mono-mode relation. The framework of this hypothesis is shown in Figure 7-4. The integration of the characterization of a single stimulus is proposed in which a combination of the defined indexes used on single stimulus could give a better picture of the intensity of this stimulus. By taking thermal properties as an example, the combining of the TMF and TCC indexes takes not only instant energy transfer when humans touch fabrics, but also the energy transfer rate during continuous touch into consideration. f_1, f_2, and f_3 denote the integration of indexes based on the logarithmic, power, and linear functions respectively.

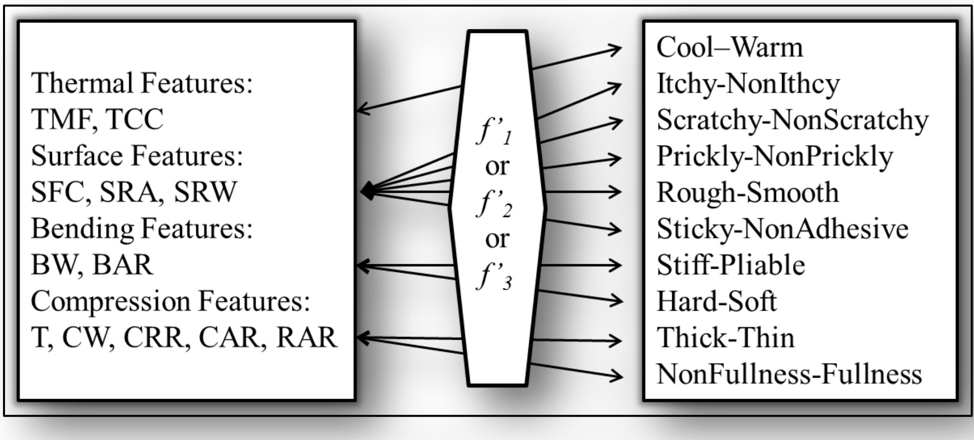

Figure 7-4 Hypothesized Mono-Mode Relation between Integrated Characterization of Single Stimulus and Individual Descriptor

7.3.1 Results

The physical indexes obtained by using the FTT are first transformed by using the logarithmic, power, and linear functions respectively. Linear integration on the transformed indexes is applied. The Weber-Fechner law describes a natural logarithmic function. Meanwhile, in the original study on the Stevens' power law, exponents of various physical stimuli were proposed based on empirical research. There are some related to touch sensation, such as:

- Exponent for Cold Perception (Metal contact on arm): 1;

- Exponent for Tactual Roughness (Rubbing emery cloths): 1.5;
- Exponent for Tactual Hardness (Squeezing rubber): 0.8;
- Exponent for Finger Span (Thickness of blocks): 1.3; and
- Exponent for Pressure on Palm (Static force on skin): 1.1.

In terms of linear functions, since there is no agreement on the slopes and constants of linear formulas, the regression method by using SPSS sofware was used.

For the Cool-Warm descriptor, thermal indexes TMF and TCC were integrated. With regard to the Itchy-NonItchy, Scratchy-NonScratchy, Prickly-NonPrickly, Rough-Smooth, and Sticky-nonAdhesive descriptors, the integration of the surface indexes SFC, SRA, and SRW was checked. In terms of the Stiff-Pliable descriptor, the bending indexes BW and BAR were combined. Furthermore, the compression indexes T, CW, CRR, CAR, and RAR were integrated to check the Hard-Soft, Thick-Thin, and NonFullness-Fullness descriptors.

Table 7-3 summarizes the model fit on individual descriptors. In the table, relationships that share an adjusted R^2 higher than 0.5 are bolded. The results show that relationships as logarithmic functions are significant for most of the psychological descriptors, although their model fit statistics (R^2) vary from the lowest at 0.349 to the highest at 0.736. The results also indicate that the assumption of a power function shows limitations in connecting surface-related descriptors, such as Itchy-NonItchy, Scratchy-NonScratchy, Prickly-NonPrickly, Rough-Smooth and Sticky-NonAdhesive (passive touch only). Similar results as compared to the power function are obtained with the linear function. No significant relations are obtained for the Itchy-NonItchy, Scratchy-NonScratchy, Prickly-NonPrickly and Rough-Smooth descriptors.

Table 7-3 Summary of Model Fits on Mono-mode Relation (Hypothesis 2)

Descriptor	Statistic	Passive Contact			Active Contact		
		Log.	**Power**	**Linear**	**Log.**	**Power**	**Linear**
Cool-Warm	Adjusted R^2	0.349	0.282	0.282	**0.578**	**0.527**	**0.527**
	p Value	0.010	0.000	0.023	**0.000**	**0.001**	**0.001**
Itchy-NonItchy	Adjusted R^2	0.271	--	--	0.322	--	--
	p Value	0.045	--	--	0.026	--	--
Scratchy-NonScratchy	Adjusted R^2	--	--	--	0.328	--	--
	p Value	--	--	--	0.025	--	--
Prickly-NonPrickly	Adjusted R^2	0.309	--	--	0.309	--	--
	p Value	0.030	--	--	0.030	--	--
Rough-Smooth	Adjusted R^2	0.272	--	--	0.442	--	--
	p Value	0.045	--	--	0.006	--	--
Sticky-NonAdhesive	Adjusted R^2	--	--	--	0.395	0.360	0.397
	p Value	--	--	--	0.011	0.017	0.011
Stiff-Pliable	Adjusted R^2	**0.636**	**0.673**	**0.678**	**0.675**	**0.706**	**0.714**
	p Value	**0.000**	**0.000**	**0.000**	**0.000**	**0.000**	**0.000**
Thick-Thin	Adjusted R^2	--	0.443	0.431	**0.542**	**0.578**	**0.568**
	p Value	--	0.018	0.021	**0.005**	**0.003**	**0.004**
Hard-Soft	Adjusted R^2	--	--	--	--	--	--
	p Value	--	--	--	--	--	--
Nonfullness-Fullness	Adjusted R^2	**0.671**	**0.640**	**0.624**	**0.736**	**0.700**	**0.689**
	p Value	**0.001**	**0.001**	**0.001**	**0.000**	**0.000**	**0.000**

On the other hand, logarithmic functions have the advantage of describing the psychophysical relationships of the NonFullness-Fullness and Cool-Warm descriptors while linear functions are observed with better model fit in terms of Stiff-Pliable and Thick-Thin. It is also observed that actively perceived descriptors show better model fit than passively perceived descriptors.

7.3.2 Discussion

The general findings in this part of the thesis are in agreement with the previous findings from Hypothesis 1. Preference of the three different functioning assumptions of psychophysical relations can hardly be concluded.

The confidence of relation hypothesized as a mono-mode with the integration of the characterization of a single stimulus is higher than that with only characterization. Without a clear investigation on the neurophysiological stimulation mechanism, there will always be questions on the type of physical characterization that should be used for psychophysical studies. Integration characterization that combines various physical indexes may overcome this gap and provide better coefficients in building psychophysical relations.

Meanwhile, studies on mono-mode relations have also revealed that psychological descriptors not only show potential relationships of paired physical stimuli, but also demonstrate monotonic correlations to "unexpected" physical stimuli. This kind of cross-effect and even interaction effect cannot be evaluated by using the current psychophysical laws or simple mono-mode linear correlations. The multi-mode relation, as discussed in the next section, proposes a possible solution.

7.4 Multi-mode Relation between Various Stimuli and Sensory Dimensions

To arrive at a method that enables simultaneous prediction, all physical stimuli could be the affecting factors of psychological sensation, regardless whether they are pair-matched. Fabric touch sensation could be divided into three independent dimensions according to type of their stimulation. As mentioned before, these are smoothness, softness, and warmth. Therefore, the subsequent paragraphs will provide information on the investigations on multi-mode relations between various stimuli and these sensory dimensions, as illustrated in Figure 7-5.

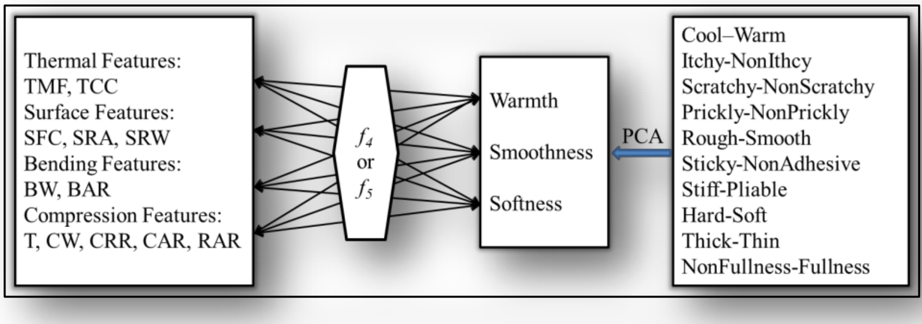

Figure 7-5 Hypothesized Multi-Mode Relation between Various Stimuli and Sensory Dimensions

For the purpose of the identification of potential functions of the correlations between physical stimuli and psychological dimensions, both Hypotheses 1 and 2 were evaluated with the three sensory dimensions. According to the results, the surface related indexes SFC, SRA, SRW were logarithmically transformed before they were involved with the hypothesized function f_4. Thermal indexes TCC and TMF were also first logarithmically transformed. The bending and compression indexes were not transformed because they were expected to express linear relations.

7.4.1 Results

The components in the hypothesized function relation f_4 were selected by the backwards elimination method of linear regression by using the SPSS software.

Table 7-4 is a summary of the statistics of the remaining components with the three sensory dimensions in terms of passive touch.

Table 7-4 Summary of Remained Factors related to Passive Sensory Dimensions

Dimension	Factor	Standardized Coefficient	t	p
Smoothness	TCC (Logarithmic)	1.44	3.37	0.005
	TMF (Logarithmic)	-1.71	-2.73	0.017
	T	-2.49	-2.96	0.011
	CW	0.84	2.20	0.046
	CAR	1.30	3.42	0.005
	BW	-0.38	-1.96	0.072
Softness	SRA (Logarithmic)	-0.51	-2.78	0.014
	SRW (Logarithmic)	0.32	1.95	0.070
	CW	0.47	3.14	0.007
	BW	-0.95	-8.49	0.000
Warmth	SRW (Logarithmic)	0.43	2.24	0.042
	TCC (Logarithmic)	-1.25	-4.09	0.001
	TMF (Logarithmic)	1.30	2.21	0.044
	T	1.94	3.61	0.003
	CAR	-0.77	-2.91	0.011

In passive touch, physical indexes such as the TMF, T and BW show a negative impact on smoothness, while TCC, CW and CAR demonstrate a positive impact. The deformation-related indexes demonstrate a trend in which thinner and softer fabric usually delivers the psychological perception that the fabric is smoother. It can also be noticed that surface related indexes are not included in the regression model building. The adjusted R^2 for relation modeling is 0.553 with an F value of 4.910 and p value of 0.008. The multi-mode relation with the passive softness contains four predictors as listed. Demonstrated by standardized coefficients, physical index BW is the most important predictor. The next two most powerful predictors are the indexes CW and SRA respectively. The adjusted R^2 for this prediction model is 0.820 with the F value of 22.683 and the p value of 0.000. With regard to the perception of warmth with passive touch, five physical indexes can be concluded to have significant impacts. T, TCC, and TMF play the most important roles. The adjusted R^2 for this model is 0.742 with the F value of 11.902 and the p value of 0.000.

Table 7-5 Summary of Remained Factors related to Active Sensory Dimensions

Dimension	Factor	Standardized Coefficient	t	p
Smoothness	SRW (Logarithmic)	0.64	3.46	0.003
	CAR	0.91	4.91	0.000
Softness	SRA (Logarithmic)	-0.28	-2.20	0.044
	TCC (Logarithmic)	0.19	1.76	0.098
	CW	0.49	3.50	0.003
	BW	-1.07	-10.26	0.000
Warmth	TCC (Logarithmic)	-0.47	-2.46	0.026
	T	0.89	3.96	0.001
	CAR	-0.38	-2.54	0.022

Table 7-5 shows the effect of various physical stimuli on sensory dimensions during active touch. Two indexes, SRW and CAR, show a significant impact on the prediction of smoothness with active touch. The adjusted R^2 for this prediction model is 0.547 with the F value of 12.491 and the p value of 0.000.

The factors extracted that link softness with active touch are generally the same as those for softness determined by passive touch, while TCC is added instead of SRW this time. BW and CW have the most influence. These two indexes represent fabric characteristics due to deformation with different methods respectively. As a result, their influences are expected and reasonable. The adjusted R^2 for this multi-mode relation model is 0.846 with the F value of 27.119 and the p value of 0.000.

With regard to the multi-mode relation of warmth through active touch, the compression related physical indexes and thermal conductivity show high coefficients of correlation similar to such for warmth under passive touch. Thicker fabric with lower thermal conductivity has a large probability of being perceived as a warm fabric. The adjusted R^2 for this relation is 0.754 with the F value of 20.420 and the p value of 0.000.

With further analysis, the interactions between the physical stimuli were involved when viewing the psychophysical relations. The interaction factors are defined according to their potential physical meanings, as follows:

1. SRA*SRW means the surface profile of the fabric texture;
2. CW*BW means the deformation response of a fabric;
3. CW*SRA means the surface fiber properties; and
4. CW*BW*SFC means the overall received forces from fabric.

In addition, interactions between the TMF thermal index, and four physical indexes including the CW, BW, SFC, and SRA, were also involved. They indicate thermo-tactile stimuli. A similar backwards elimination method for linear regression was applied to determine the significant factors.

Table 7-6 lists the results of the multi-mode relation to sensory dimensions with passive touch, including interaction factors. Many of the interaction factors remain in the passive touch of smoothness. The adjusted R^2 for this built relation is 0.501 with the F value of 3.389 and the p value of 0.032. In terms of softness in passive touch, the index BW demonstrates the highest coefficient. The interaction of TMF*BW also shows a relatively high impact. The adjusted R^2 for this relation is 0.918 with the F value of 18.804 and the p value of 0.000. Four factors are observed to be significant with regard to warmth in passive touch. The index T and the interaction of CW*SRA show the highest coefficients. The adjusted R^2 for this prediction model is 0.762 with the F value of 13.167 and the p value of 0.000.

Table 7-6 Summary of Remained Factors related to Passive Sensory Dimensions with Interaction Effects

Dimension	Factor	Standardized Coefficient	t	Sig.
Smoothness	SFC (Logarithmic)	-1.07	-2.23	0.047
	TCC (Logarithmic)	2.88	3.83	0.003
	T	-4.91	-3.44	0.006
	BW	-0.58	-2.23	0.047
	CW*SRA	4.15	2.64	0.023
	TMF*CW	-2.34	-2.25	0.046
	TMF*SFC	1.66	2.37	0.037
	TMF*SRA	-0.81	-2.84	0.016
Softness	SFC (Logarithmic)	-3.14	-4.49	0.003
	TCC (Logarithmic)	1.10	3.25	0.014
	T	-3.33	-4.35	0.003
	CRR	-0.44	-2.62	0.034
	RAR	0.91	2.80	0.027
	BW	-10.66	-3.83	0.006
	CW*BW	4.98	3.95	0.006
	CW*SRA	3.00	2.67	0.032
	TMF*CW	-3.76	-3.18	0.015
	TMF*BW	6.82	3.30	0.013
	TMF*SFC	5.48	4.25	0.004
	TMF*SRA	-0.77	-3.92	0.006
Warmth	TCC (Logarithmic)	-1.34	-4.66	0.000
	T	2.21	3.42	0.004
	BW	-0.36	-2.15	0.050
	CW*SRA	-2.16	-2.16	0.049
	TMF*CW	1.93	2.81	0.014

Table 7-7 lists the results of the model fits of the multi-mode relations built for sensory dimensions in active touch. The most important factor related to smoothness with active touch is the index BW while the interaction of TMF*BW also demonstrates relatively high coefficients of correlation. The adjusted R^2 for this psychophysical relation is 0.589 with the F value of 5.544 and the p value of 0.005.

Table 7-7 Summary of Remained Factors related to Active Sensory Dimensions with Interaction Effects

Dimension	Predictor	Standardized Coefficient	t	Sig.
Smoothness	SFC (Logarithmic)	-0.36	-2.13	0.053
	TMF (Logarithmic)	-1.59	-2.61	0.021
	CAR	1.60	4.34	0.001
	BW	-2.48	-2.69	0.018
	TMF*CW	0.71	3.05	0.009
	TMF*BW	2.10	2.49	0.027
Softness	SFC (Logarithmic)	-2.82	-4.47	0.002
	T	-0.72	-2.63	0.028
	RAR	1.12	3.79	0.004
	BAR	0.52	3.18	0.011
	BW	-10.19	-4.79	0.001
	CW*BW	4.15	4.09	0.003
	TMF*CW	-1.29	-2.99	0.015
	TMF*BW	6.33	4.20	0.002
	TMF*SFC	4.78	4.32	0.002
	TMF*SRA	-0.37	-3.28	0.010
Warmth	SFC (Logarithmic)	-1.62	-2.44	0.051
	SFW (Logarithmic)	-2.64	-3.28	0.017
	TCC (Logarithmic)	-3.07	-4.61	0.004
	T	5.97	4.48	0.004
	CRR	0.61	2.88	0.028
	CAR	1.71	3.20	0.019
	BAR	1.36	3.54	0.012
	BW	-1.15	-3.42	0.014
	SRA*SRW	2.59	3.00	0.024
	CW*SRA	-10.28	-4.46	0.004
	TMF*CW	8.05	4.61	0.004
	TMF*SFC	1.99	2.09	0.082
	TMF*SRA	0.91	2.87	0.028

For softness in active touch, the index BW shows the highest coefficient of correlation as it does for passive touch. The interaction of TMF*BW also demonstrates a relatively high coefficient of correlation. The adjusted R^2 for this prediction model is 0.932 with the F value of 27.171 and the p value of 0.000.

As regards the relation to warmth with active touch, the key factors are the interaction of CW*SRA and TMF*CW. The adjusted R^2 for this prediction model is 0.889 with the F value of 12.734 and the p value of 0.003.

7.4.2 Discussion

Multi-mode relations hypothesize towards the successful connection of various physical stimuli and psychological perception. Both relations based on f_7 and f_8 conclude that psychological smoothness is additionally related to thermal indexes when evaluating with passive touch. On the other hand, the compression index T plays an important part when building relations with smoothness in active touch. This implies that humans might gain smoothness sensations with the help of thermal and force stimuli. The importance of the interaction of CW*SRA suggests that the rigidity of free fibers on the fabric surface could be a critical factor that influences the smoothness sensation, especially when humans are perceiving smoothness with passive touch.

The bending and compression properties are, as expected, major factors of physical stimuli related to softness. Therefore, when considering the interaction effects, the interaction of CW*BW which combines the impacts from multiple force-related stimuli, shows high coefficients of correlation. This indicates that the total energy received when deforming fabric is the trigger for the perception of softness. Another noticeable point is that the thermo-tactile factor TMF*BW is concluded as another important interaction factor. Thermal information together with force information again influences the psychological perception of softness as well.

It is concluded that the indexes T and TCC mostly influence the multi-mode psychophysical relation in the perception of warmth since the two indexes together demonstrate the heat energy transfer property of fabrics. When interaction factors are included, it is observed that the interaction of CW*SRA also show relatively high coefficients of correlation. This indicates that the fiber properties of the fabric surface would be worthy of discussion in terms of the thermal perception.

Generally speaking, the psychophysical relation with the interactions, f_5, shows a stronger relation to psychological attributes than f_4. This proves that the interactions between different kinds of stimuli should not be neglected in the study of fabric touch sensation.

7.5 Relation between Sensory Dimensions and Total Comfort

The remaining psychophysical relation is the linking of physical stimuli with total comfort preference. As defined in f_6, a practicable simplified function that links them is the linear summation of the sensory dimensions. The logic of this relation is illustrated in Figure 7-6.

Table 7-8 Summary of Sensory Dimensions' Weights on Total Comfort

Sensory Dimensions	Weights on Passive Comfort	Weights on Active Comfort
Smoothness	0.326	0.304
Softness	0.205	0.191
Warmness	0.124	0.165

In order to test this hypothesis, the estimated scores of the sensory dimension were first determined by using the multi-mode psychophysical relation mentioned above. Their linear summations were then compared to the total comfort scores directly obtained from the subjective measurement. The summation weights of different sensory dimensions, which are the factor loadings described in Chapter 6, are listed in Table 7-8.

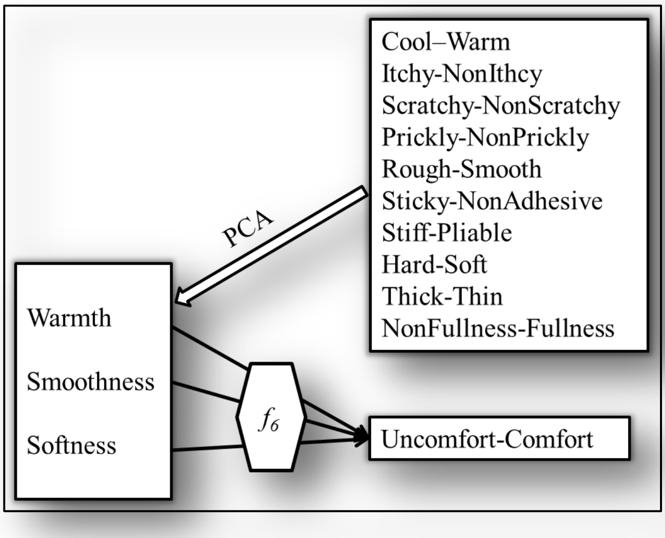

Figure 7-6 Hypothesized Relation between Sensory Dimensions and Total Comfort Perception

Figure 7-7 shows the correlation results of the predicted comfort and psychologically perceived comfort for passive and active touch respectively. Figure (a) and (b) show results for passive comfort and active comfort predicted by linear regression without interaction factors. Figure (c) and (d) demonstrate those with interaction factors. X-axis means the predicted comfort values while Y-axis means subjective comfort perception. Pearson's Correlation Coefficients and probability values are listed in the right-bottom corner of each figure. The probability values show that the correlations are significant. The Pearson's correlation coefficients also indicate that the predicted total comfort, calculated by weighted summation of sensory dimensions, mostly agrees with the overall comfort scores that were subjectively evaluated.

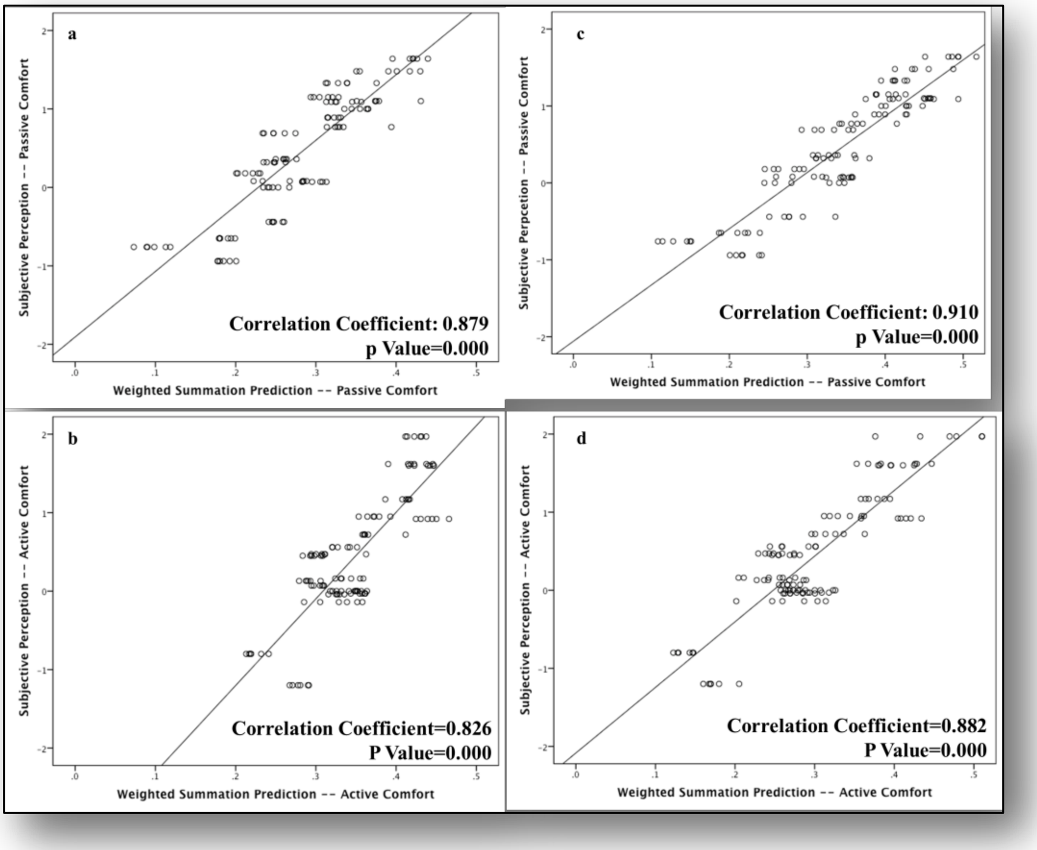

Figure 7-7 Scatterplots Of Predict Comfort Value and Psychological Perceived Comfort

7.6 Conclusion

The objective 5 has been completed by exploring quantitative relationships between primary physical stimuli and psychological perceptions in this chapter. The comparison made between three hypothesized psychophysical relations concludes better correlation capacities through multi-mode relations. For instance, there are obvious limitations of the mono-mode relation to linking surface-related descriptors with only surface related physical indexes. In psychological perceptions, especially for sensory dimensions, multi effects from various physical aspects should be considered. It is also observed that the many interactions of the thermal and tactile indexes have important implications. This finding proves that both thermal and tactile physical stimuli should be involved in the evaluation of fabric touch sensation. It will be inadequate if they are separately studied. Meanwhile, it is found that the weighted summation of the predicted sensory dimensions could successfully identify the overall psychological preference through touch.

Shortages of these psychophysical relations, however, are also obvious. The coefficients of each factor in these models are found based on empirical studies. This makes it difficult to cross-compare the models with one another. The established models may also have limitations when applied to new fabrics. The lack of an underlying mechanism is another weakness of the psychophysical prediction methods. Although linkages could be approximately obtained, the selection of the factors is based on statistical techniques only. The methods for prediction based on the mechanism of perception should be further developed to overcome these shortages.

Chapter 8 Neuropsychological Models

This chapter focuses on the objective 6 to reveal the linkages of the neurophysiological indexes and psychological results. This prediction method in its entirety would innovatively simulate the whole physiological process of sensory perception that takes place in real life. The neuropsychological prediction methods provide an alternate means to address fabric touch sensation on the basis of the underlying neuropsychological mechanisms of the perception process.

A neuropsychological approach is used to evaluate fabric touch sensation in this chapter. The findings from previous physical, neurophysiological, psychological, and psychophysical research work are synthesized together. In this chapter, the aim is to develop neuropsychological prediction models on fabric touch sensation. These models are expected to have better predicting capacities. Moreover, they should clearly address the neuropsychological mechanisms of fabric touch sensation.

In the research work of Chapter 7, commonly used psychophysical methods are applied to link the physical properties of fabric and psychological touch sensation. Nevertheless, the discussed methods are based on establishing statistical correlations between two ends of sensory perception. These methods often have limitations on how to extend the established correlations to different fabrics and more subjects. As reviewed in Chapter 2, the neuropsychological predictions can provide an alternate approach. Neurophysiological indexes, identified in Chapter 5, address the response of the somatosensory receptors in the human skin. These indexes should be linked to psychological sensation in humans, as shown in Figure 8-1. Direct correlations between the physical properties of fabric and psychological perception have neglected the transformation and transport of middle neural information. Neuropsychological prediction methods are, therefore, designed to involve the coding mechanisms of various types of stimuli and represent the complete path of information processing from physical contact to psychological perception.

The lower part of Figure 8-1 shows the neuropsychological process. The physical characterization on the left depicts the identification of fabric physical properties that could stimulate skin receptors. In this Ph.D. study, a new developed instrument, the FTT, was used to quantify the physical properties of fabric as outlined in Chapter 4. The related indexes include four modules: thermal, compression, bending and surface. Subsequently, the neural coding process transduces these physical properties into neural signal intensities. Chapter 5 outlines the transforming of stimuli into three types of neural information including thermal, texture, and received force. On the other hand, the subjective perception results were obtained from psychological measurements. The results include individual descriptors and sensory dimensions, as discussed in Chapter 6.

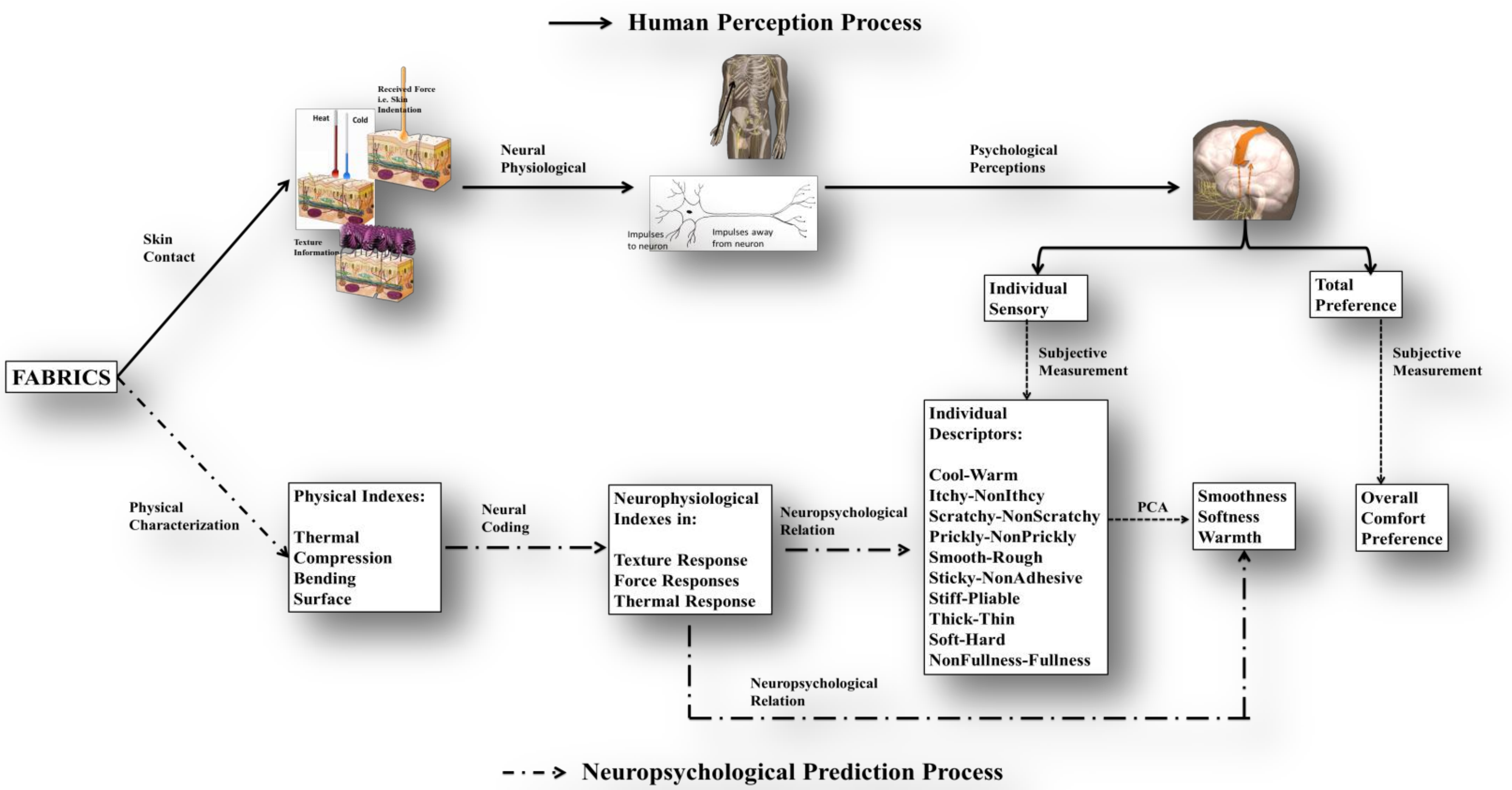

Figure 8-1 Schematic Diagram of Neuropsychological Prediction Method of Fabric Touch Sensations

8.1 Methodology

In this chapter, the aim is to associate psychological perception with defined neurophysiological indexes based on hypothesized neural coding mechanisms. The neurophysiological indexes defined in Chapter 5 address the response of the somatosensory receptors according to various types of stimulation from different fabrics. Each response was expected to be directly linked to a related psychological descriptor. The determination of the categories of the individual descriptors was based on their stimulation tasks. The Cool-Warm descriptor, for example, should be clearly stimulated by the temperature stimulus and related to thermal neural responses.

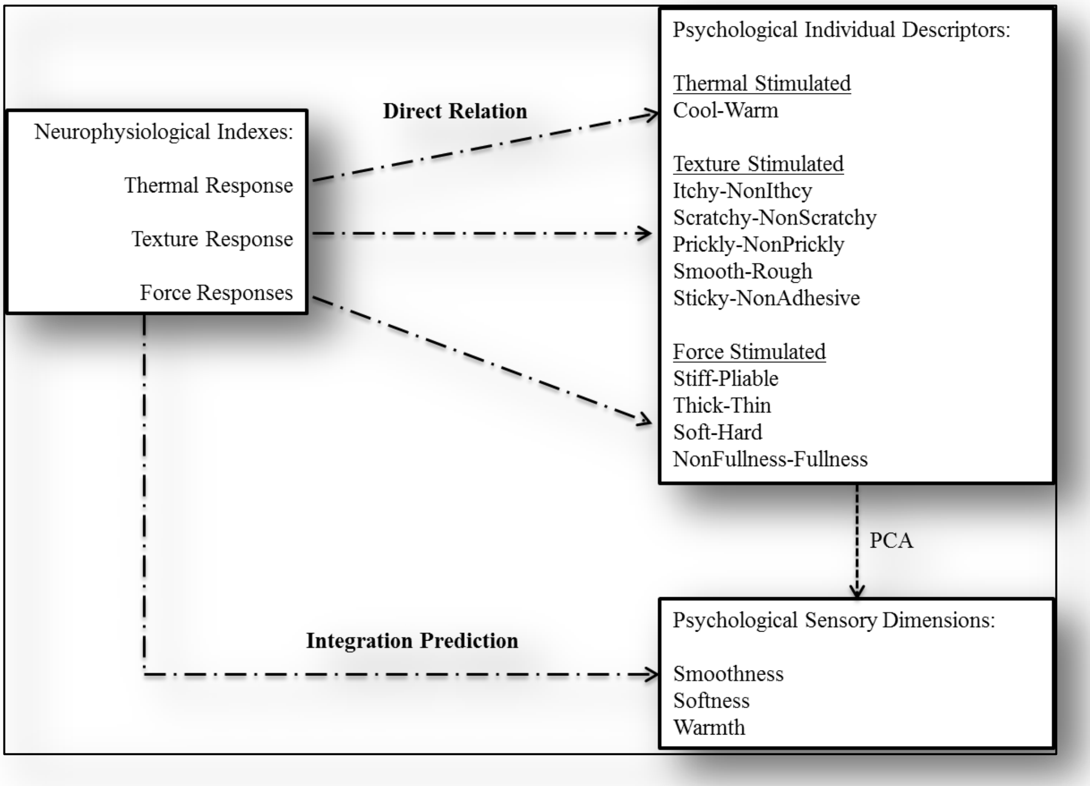

Figure 8-2 Schematic Diagram of Connections between Neurophysiological Indexes and Psychological Perceptions

Their linkages are depicted in Figure 8-2. First, neurophysiological indexes were directly connected to psychological descriptors. Such direct relations would reveal the relations between neurophysiological and psychological responses based on the same physical stimuli. Secondly, the predictions of integration were established from the neurophysiological indexes towards the indicators of psychological sensation. As discussed in Chapter 6, these sensation indicators can indicate major variances measured from the subjects with regard to the touch sensations obtained from the examined fabrics. Consequently, they were expected to be integrated sensations based on multiple stimuli. The psychological and neurophysiological foundations of such assumptions have been discussed in earlier chapters and will not be repeated here. As a result, the responses from all three defined types of stimuli were synthesized together to form prediction methods for these psychological sensory dimensions.

The fabrics involved in this chapter were the 20 types of fabrics that are mentioned in Chapter 7. Their neurophysiological indexes, as provided in Chapter 5, were averaged to be the input for the neuropsychological prediction models. The other end of the prediction models was the mean psychologically measured results from the human subjects as discussed in Chapter 6. For relation exploration, Spearman's correlation analysis was used to verify the correlation coefficients of monotonic correlation. The scatter-plots of the most significantly correlated pairs were also examined to explore the possible functions of these relations. With regard to integration prediction, multiple variance regression methods were used to build relation formulas. Statistical analyses were conducted with IBM SPSS version 20.0 software and Microsoft Office Excel version 2013.

8.2 Relation Exploration between Neurophysiological Indexes and Psychological Individual Descriptors

In the following sections, an exploration of the direct relations of different physical stimuli is carried out. Thermal responses are discussed first, followed by response to texture information and received force information respectively.

8.2.1 Thermal Information

The neurophysiological indexes responsible for the thermal information identified include the indexes that fall under the three different hypotheses on neural transduction. Q_{upsum}, $Q_{downsum}$, and Q_{steady} are defined on the basis of Hensel's model, which contains two components to calculate thermoreceptor response. These two components are absolute temperature as well as change rate of temperature. C_{max}, C_{steady} and C_{diff} are characterized according to the molecular transduction mechanism of the TRPM8 channel, which has been recently considered as the nucleus in innocuous cold temperature sensing. They represent the relative membrane currents of TRPM8 channels under different transient temperature conditions. In addition, Hensel's model is modified into Hypothesis 3 in this thesis, which replaces the absolute temperature with the membrane currents calculated. Similar indexes, Q2upsum, Q2downsum, and Q2steady, are attempts to synthesize the latest molecular findings with classic neurophysiological estimates.

Table 8-1 Correlation Summary between Thermal Neurophysiological Indexes and Psychological Thermal Individual Descriptor Cool-Warm

Index	Statistic	Passive	Active
$\mathbf{Q2_{upsum}}$	Coefficient	--	--
	p Value	--	--
$\mathbf{Q2_{downsum}}$	Coefficient	--	--
	p Value	--	--
$\mathbf{Q2_{steady}}$	Coefficient	--	--
	p Value	--	--
$\mathbf{Q_{upsum}}$	Coefficient	--	--
	p Value	--	--
$\mathbf{Q_{downsum}}$	Coefficient	--	--
	p Value	--	--
$\mathbf{Q_{steady}}$	Coefficient	-0.607	-0.833
	p Value	0.006	0.000
$\mathbf{C_{max}}$	Coefficient	-0.490	-0.866
	p Value	0.028	0.000
$\mathbf{C_{steady}}$	Coefficient	--	-0.838
	p Value	--	0.000
$\mathbf{C_{diff}}$	Coefficient	--	--
	p Value	--	--

Table 8-1 lists the Spearman's correlation coefficients with p values from the neuropsychological comparison. Neurophysiological indexes used in this comparison are those were obtained when the normal pressure was set at 5 gf/cm^2. Comparisons of indexes those were obtained when normal pressures were 42 and 70 gf/cm^2 respectively are provided in the appendix. It can be observed that indexes defined based on Hypothesis 3 show no significant correlation to the individual psychological descriptor, Cool-Warm. Q_{steady} which is based on Hypothesis 1 and C_{max} and C_{steady} which are based on Hypothesis 2 all demonstrate significant negative correlations with regard to psychological scoring in active touch. Q_{steady} and C_{max} also indicate a significantly negative correlation to the Cool-Warm feeling in passive touch.

Figure 8-3 illustrates the comparison of Q_{steady}. Q_{steady} values were calculated with normal pressure at 5gf/cm2. Cool-Warm feeling scores were added 4 to avoid negative values for model fitting. Although the R^2 values are quite similar, the logarithmic functions show slightly higher results than the linear functions. A negative correlation suggests that fabric with stronger intensity of thermoreceptor response will give off a cooler feeling in psychological evaluation, especially during the steady state. This agrees with Hensel's model since it describes the response of cold thermoreceptors. Q_{upsum} and $Q_{downsum}$ describe the features of thermoreceptor responses at the beginning of contact, where bigger variances of the responses would appear. However, neither of them demonstrates a significant correlation to the psychological feeling of Cool-Warm from the evaluation scores.

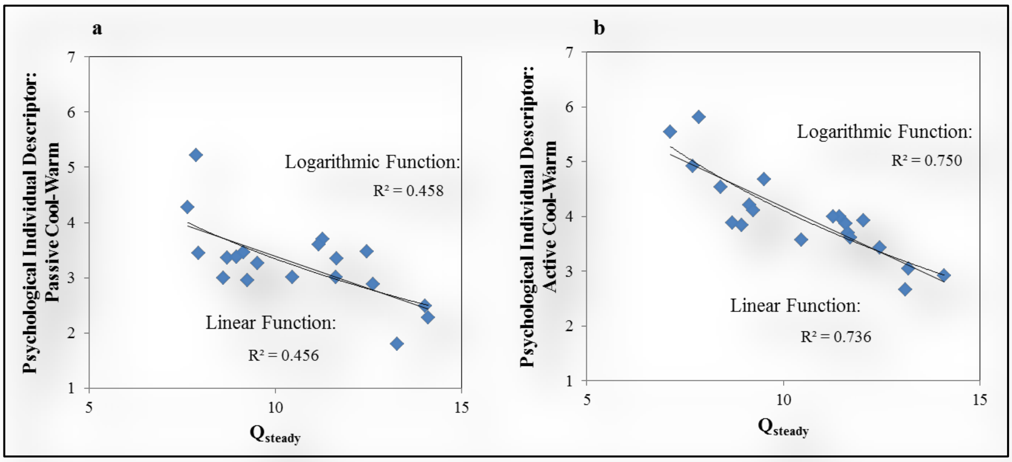

Figure 8-3 Scatterplot of Q_{steady} and Psychological Individual Descriptor Cool-Warm

Figure 8-4 are scatterplots as regards the relative membrane current indexes C_{max} and C_{steady}. Cmax and Csteady values were calculated with normal pressure at 5gf/cm2.

Cool-Warm feeling scores were added by 4 to avoid negative values for model fitting.The logarithmic function shows a noticeably higher R^2 than the linear function this time. C_{max} shows a stronger correlation than C_{steady} with both passive and active touch for feelings of Cool-Warm. Although C_{steady} shows no significant correlation to the feeling of Cool-Warm in passive touch, the scatterplot indicates that the model fits between C_{steady} and feelings of Cool-Warm scores in passive touch is not significantly distinct from those between C_{max} and feelings of cool-warm scores in active touch.

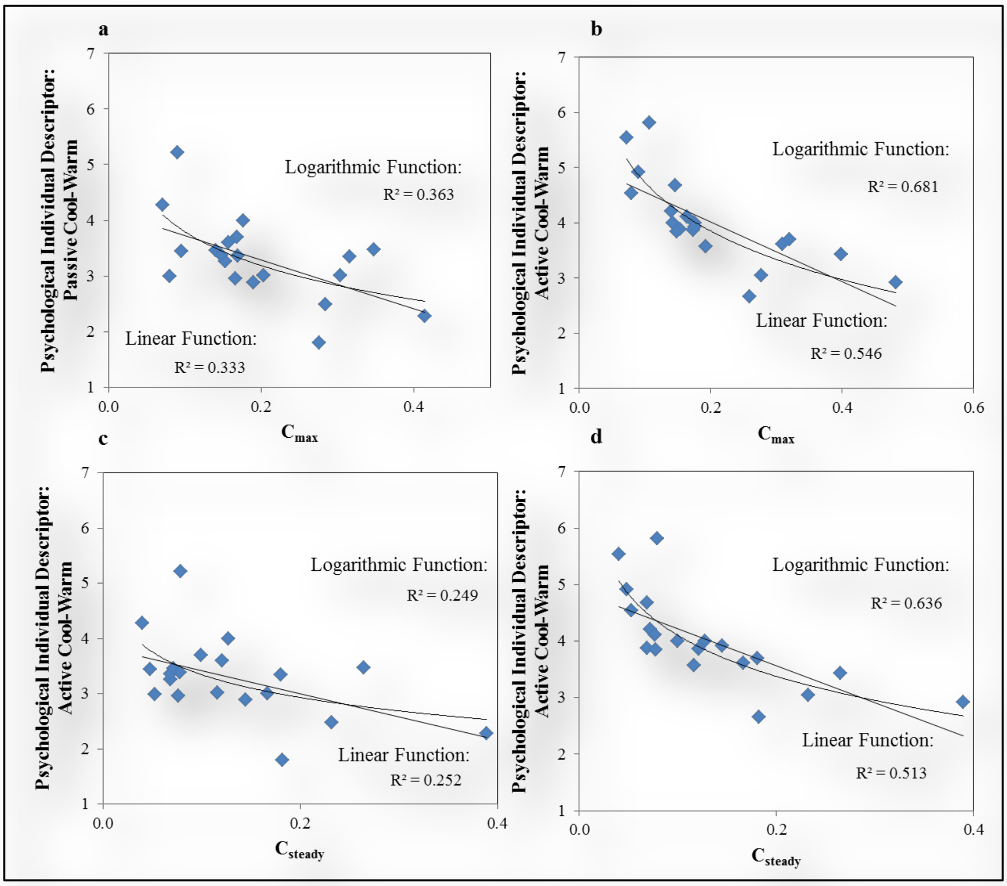

Figure 8-4 Scatterplot of C_{max} and C_{steady} and Psychological Individual Descriptor Cool-Warm

It can also be noticed that the indexes based on Hypothesis 3 do not show significant correlations to the feeling of cool-warm. It seems that the linear combination of relative membrane current and change rate of temperature is not adequate enough to show a neural response from fabric thermal sensation.

By combining the findings from the Q- and C-indexes, it is suggested that the steady state of neural response would be significantly correlated to feelings of cool-warm in active touch. Meanwhile, the maximum relative TRPM8 membrane current also demonstrates a relation with the feeling of cool-warm in passive touch.

8.2.2 Texture Information

Three hypotheses have been examined in Chapter 5: those on impulse responses from SA1 and PC fibers. In Hypothesis 1, a simple linear function is applied to predict the impulse rate of a single SA1 fiber. In Hypothesis 2, the weighted power of PC fiber impulses is determined based on different intensities of different frequencies. In Hypothesis 3, the impulse rate of both the SA1 and PC fiber population is predicted. Spearman's correlation between these neurophysiological indexes and psychological descriptors are summarized in Table 8-2.

Among the defined neurophysiological indexes based on the three hypotheses on texture information coding mechanisms, *I* shows no significant correlation to descriptors of either passive or active touch. This implies that neural responses to a simple sinusoid model of the fabric surface are not directly linked to psychological perception.

Table 8-2 Summary Table of Correlation
between Neurophysiological Indexes and Psychological Individual Descriptors

Neurophysiological Index	Statistic	Psychological Individual Descriptor	
		Passive Rough-Smooth	Passive Sticky-NonAdhesive
I	Coefficient	--	--
	p Value	--	--
W	Coefficient	-0.754	-0.610
	p Value	0.000	0.004
P_1	Coefficient	-0.645	-0.626
	p Value	0.002	0.003
P_2	Coefficient	-0.603	-0.637
	p Value	0.005	0.003
		Active Rough-Smooth	Active Sticky-NonAdhesive
I	Coefficient	--	--
	p Value	--	--
W	Coefficient	-0.794	--
	p Value	0.000	--
P_1	Coefficient	-0.719	--
	p Value	0.000	--
P_2	Coefficient	-0.722	--
	p Value	0.000	--

Table 8-2 shows that the relation with the highest coefficients of correlation is the neurophysiological index *W*, which is identified based on Hypothesis 2 of the fabric texture coding mechanism. Its scatterplots and psychological descriptors are shown in Figure 8-5. Figure (a) and (b) demonstrate relations to passive Rough-Smooth and Sticky-NonAdhesive respectively while figure (c) and (d) display those to active individual descriptors. It is shown that this index has significantly negative correlations to most individual descriptors. With regard to the Rough-Smooth and Sticky-NonAdhesive descriptors in passive touch, and Rough-Smooth descriptor in active touch, a higher value of the weighted power of the PC fibers implies a surface with more stimulating elements, which lead to rougher or stickier sensations. However, there is no significant relation found between the *W* index and Sticky-

NonAdhesive sensation with active touch. This may be the result of the relatively small variances among this descriptor of 20 selected fabrics, as revealed in Chapter 6. It can also be observed that these relations could all be better fitted by using logarithmic functions rather than linear functions. This finding is in agreement with previous reports that have used a similar neurophysiological coding algorithm (S. Bensmaia & Hollins, 2005).

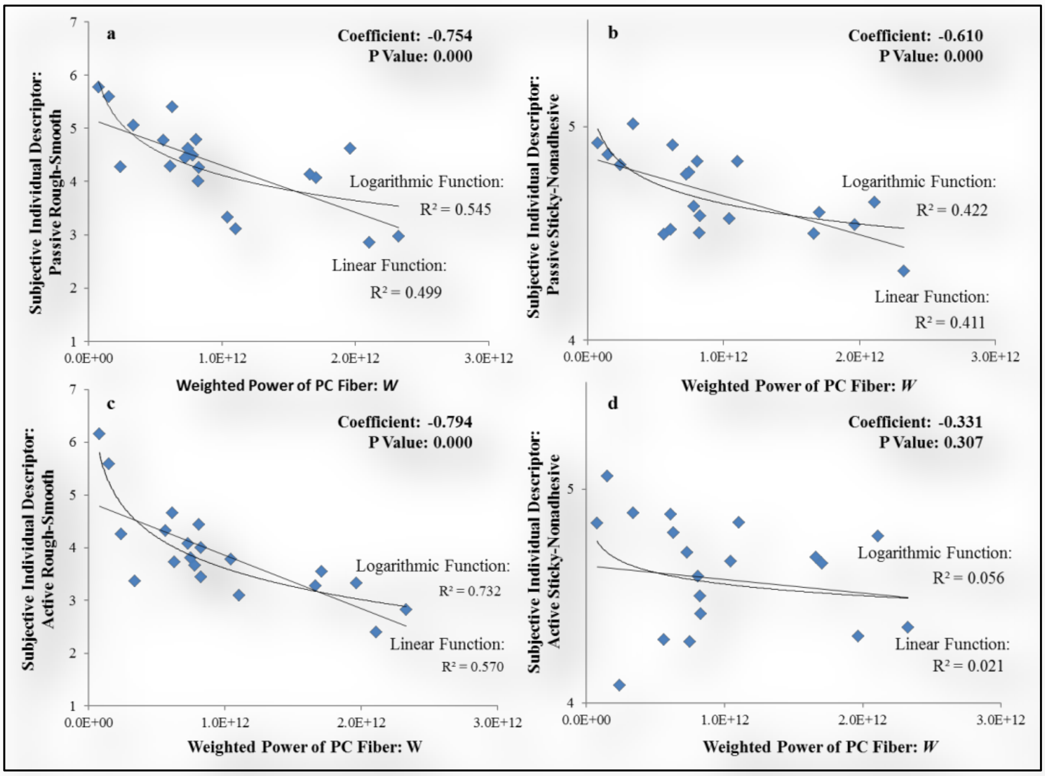

Figure 8-5 Correlation Scatter Plots of PC Fiber Weighted Power (*W*) and Psychological Individual Descriptors Rough-Smooth and Sticky-NonAdhesive

Figure 8-6 and Figure 8-7 demonstrate the relations between indexes based on Hypothesis 3 of texture information coding and related psychological individual descriptors. Figure (a) and (b) of Figure 8-6 demonstrate relations to passive rough-smooth and sticky-nonadhesive respectively while figure (c) and (d) Figure 8-6 display those to active individual descriptors. Similar findings are observed in these figures as well. Except individual descriptor active sticky-nonadhesive, other individual descriptors show negative significant correlations. Meanwhile, linear functions are preferred in these correlation studies.

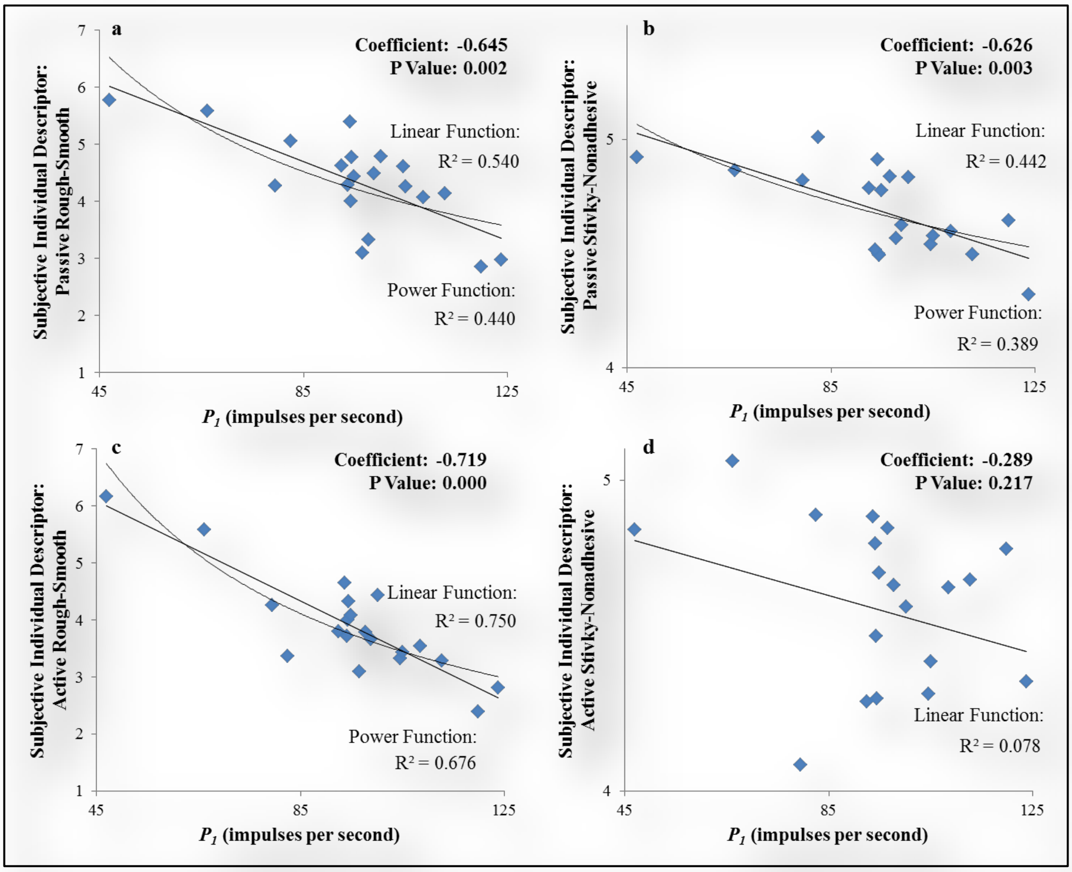

Figure 8-6 Correlation Scatterplots of P_1 and Psychological Individual Descriptors Rough-Smooth and Sticky-Adhesive

In general, the defined neurophysiological indexes, W, P_1, and P_2, are confirmed to be significantly correlated to individual psychological descriptors. The I index demonstrates limited correlation to the psychological results. The W index has the highest correlation coefficient. Among the four examined individual descriptors related to surface sensation, Rough-Smooth with active touch shows the highest correlation coefficient with the neurophysiological indexes. It is also noticeable that the relationships between the *W* index and individual psychological descriptors are better fitted in logarithmic functions.

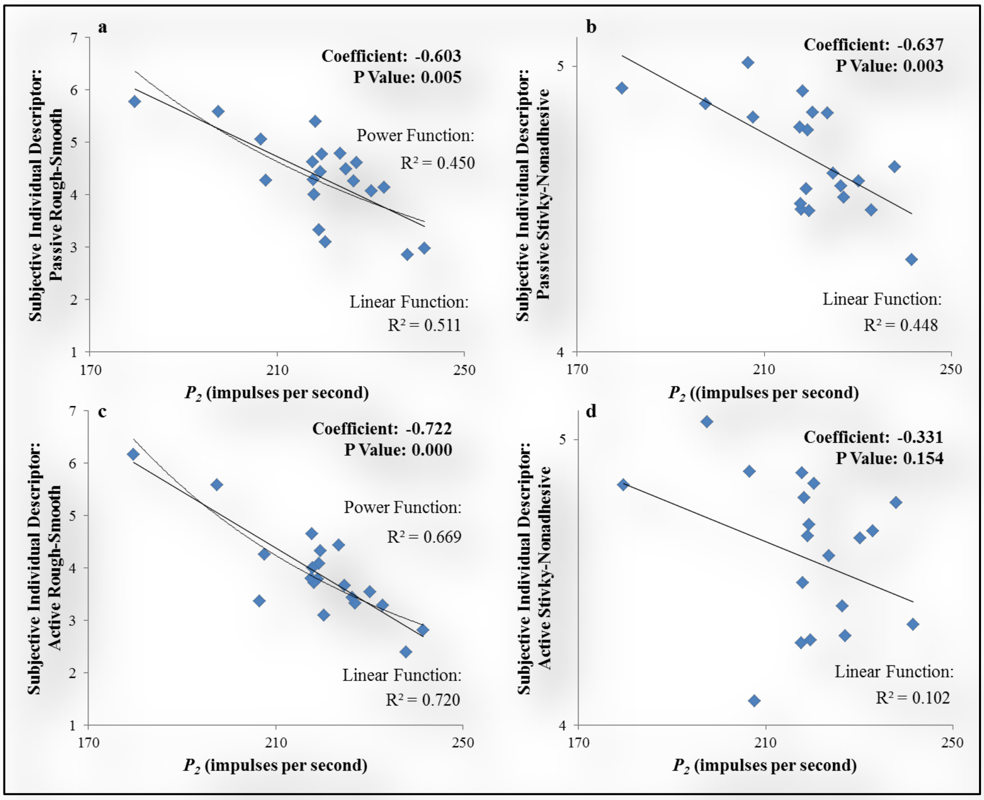

Figure 8-7 Correlation Scatterplots of P_2 and Psychological Individual Descriptors Rough-Smooth and Sticky-Nonadhesive

8.2.3 Received Force Information

The hypotheses proposed in Chapter 5 with regard to the neurophysiological coding of received force information comprise two mechanisms. One of the mechanisms considers neural responses as a function of the force received by the skin. The other mechanism integrates both force received and distance moved by the skin, as cutaneous and kinetic information respectively. Hypothesis 1 involves the calculation of total impulses of SA1 fibers during different deformation stages, which are called T_{c1}, T_{c2}, …, T_{c10}, …, and T_{c20} for compression-recovery deformation and T_{b1}, T_{b2}, …, and T_{b10} for bending deformation. Hypothesis 2 further divides the total impulses of SA1 fibers by the moved distance during each deformation stage. The indexes are defined as R_{c1}, R_{c2}, …, R_{c10}, …, *and* R_{c20} and R_{b1}, R_{b2}, …, and R_{b10} respectively. Exploration of the correlation between SA1 fiber responses to compression deformation and related psychological descriptors is summarized in Table 8-3. In the table, the most correlated neurophysiological indexes are listed for each hypothesis and each individual descriptor. For the Hard-Soft descriptor in passive and active touch, only significant correlations are found for R_{c8} and the coefficients of such relations are relatively low. Meanwhile, for the NonFullness-Fullness descriptor, the indexes based on both hypotheses show satisfactory correlation coefficients.

Figure 8-8 shows the exploration of the relations of neurophysiological indexes on compression based on Hypothesis 1 and a psychological descriptor, NonFullness-Fullness. Figure (a) and (b) demonstrate relations to passive NonFullness-Fullness while figure (c) and (d) display those to active NonFullness-Fullness. The results imply that logarithmic functions could better illustrate their relations than linear functions.

Table 8-3 Summary of Correlation Analysis between Compression Neurophysiological Indexes during Different Compressing and Recovering Stages and Psychological Individual Descriptor Hard-Soft

Hypothesis	Deformation	Stage	Statistic	Psychological Individual Descriptor	
				Passive Hard-Soft	**Active Hard-Soft**
Total Impulses Rate of SA1 Fiber (H1)	Compressing	N/A	Coefficient	--	--
			p Value	--	--
	Recovering	N/A	Coefficient	--	--
			p Value	--	--
Ratio of Total Impulses Rate of SA1 Fiber and Moved Distance (H2)	Compressing	N/A	Coefficient	--	--
			p Value	--	--
	Recovering	8	Coefficient	-0.571	-0.532
			p Value	0.008	0.016
				Passive Nonfullness-Fullness	**Active Nonfullness-Fullness**
Total Impulses Rate of SA1 Fiber (H1)	Compressing	8	Coefficient	0.824	0.830
			p Value	0.000	0.000
	Recovering	1	Coefficient	0.872	0.875
			p Value	0.000	0.000
Ratio of Total Impulses Rate of SA1 Fiber and Moved Distance (H2)	Compressing	10	Coefficient	0.818	0.818
			p Value	0.000	0.000
	Recovering	1	Coefficient	0.850	0.853
			p Value	0.000	0.000

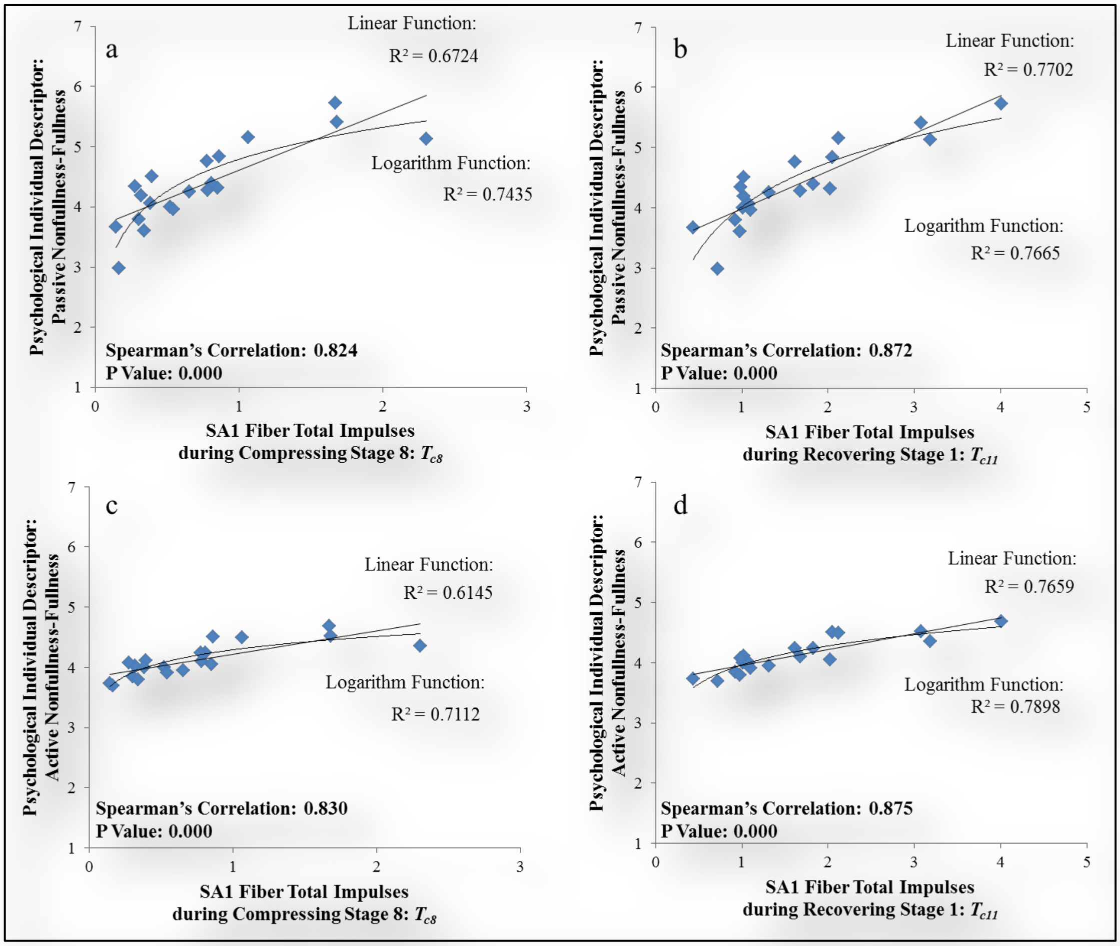

Figure 8-8 Correlation Scatter Plots of SA1 Fiber Total Impulses during Compressing Stage 8 (T_{c8}) and Recovering Stage 1 (T_{c11}) and Psychological Individual Descriptors NonFullness-Fullness

Figure 8-9 shows the scatter plots of the neurophysiological index on compression based on Hypothesis 2. Figure (a) and (b) demonstrate relations to passive nonfullness-fullness while figure (c) and (d) display those to active nonfullness-fullness.Again, logarithmic functions generally have a better explanatory power when conducting model fittings for them. Meanwhile, a comparison between the neurophysiological indexes based on Hypotheses 1 and 2 show no clear preference when linked to the NonFullness-Fullness descriptor. On the other hand, neural responses during the recovery stage are observed to be closer related to psychological perception, especially at the beginning.

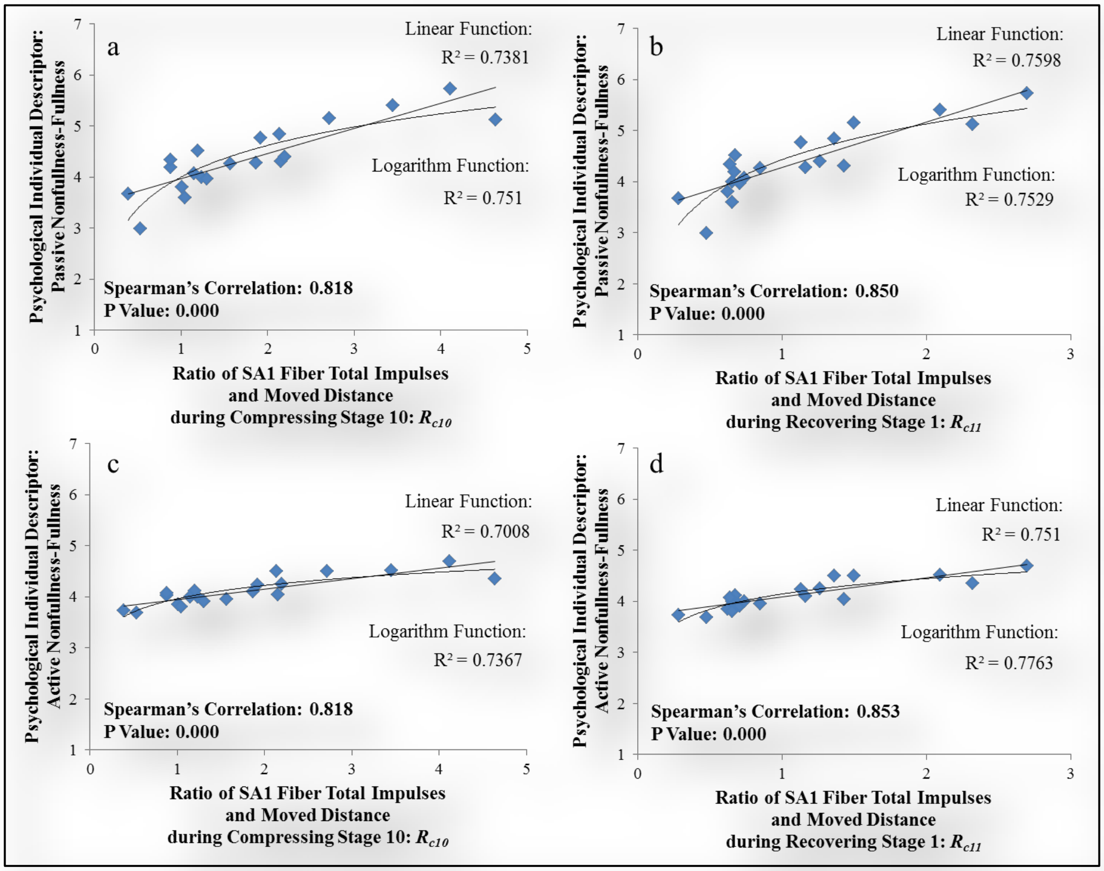

Figure 8-9 Correlation Scatter Plots of Ratio of SA1 Fiber Total Impulses and Moved Distance during Compressing Stage 10 (T_{c10}) and Recovering Stage 1 (T_{c11}) and Psychological Individual Descriptors NonFullness-Fullness

The discussions that follow revolve around the neural responses to bending deformation. Table 8-4 lists the neurophysiological indexes according to bending deformation that have the highest correlations with the Stiff-Pliable and Hard-Soft descriptors. It can be observed that total impulse of the SA1 fibers, which is defined based on the coding mechanism of Hypothesis 1, demonstrates a significant correlation with both descriptors while the ratio of the total impulse of the SA1 fibers and distance moved, defined based on the coding mechanism of Hypothesis 2, show no significant correlation for all of the stages. A comparison of the correlation coefficients further implies that stronger relations could be obtained during the early stage (second stage) of bending deformation when evaluating the bending sensation of fabric with passive touch. At the same time, bending sensations that are perceived by active touch show higher correlation to neural responses during the sixth stage. This is in agreement with the psychological measurement procedures. When conducting evaluation with passive touch, only a few degrees of bending deformation were possible since no hand manipulation tasks were allowed. It is also noticeable that the Hard-Soft descriptor also shows high correlation to neural responses in accordance with the bending deformation.

Table 8-4 Summary of Correlation Analysis between Bending Deformation Neurophysiological Indexes and Related Psychological Individual Descriptors

Neurophysiological Index	**Statistic**	**Psychological Individual Descriptor**	
		Passive Stiff-Pliable	Passive Hard-Soft
T_{b2} (H1)	Correlation Coefficient	-0.791	-0.792
	Sig. (2-tailed)	0.000	0.000
N/A (H2)	Correlation Coefficient		
	Sig. (2-tailed)		
		Active Stiff-Pliable	Active Hard-Soft
T_{b6} (H1)	Correlation Coefficient	-0.774	-0.789
	Sig. (2-tailed)	0.000	0.000
N/A (H2)	Correlation Coefficient		
	Sig. (2-tailed)		

Figure 8-10 illustrates the scatter-plots between total impulse rates of SA1 fibers and the psychological descriptors. Figure (a) and (b) demonstrate relations to passive stiff-pliable and hard soft with neural responses during 2nd bending stage while figure (c) and (d) display active ones with those during 6th bending stage. A clearly negative-monotonic pattern could be found in all four plots. The model fitting shows that it would be better to use linear functions than logarithmic functions.

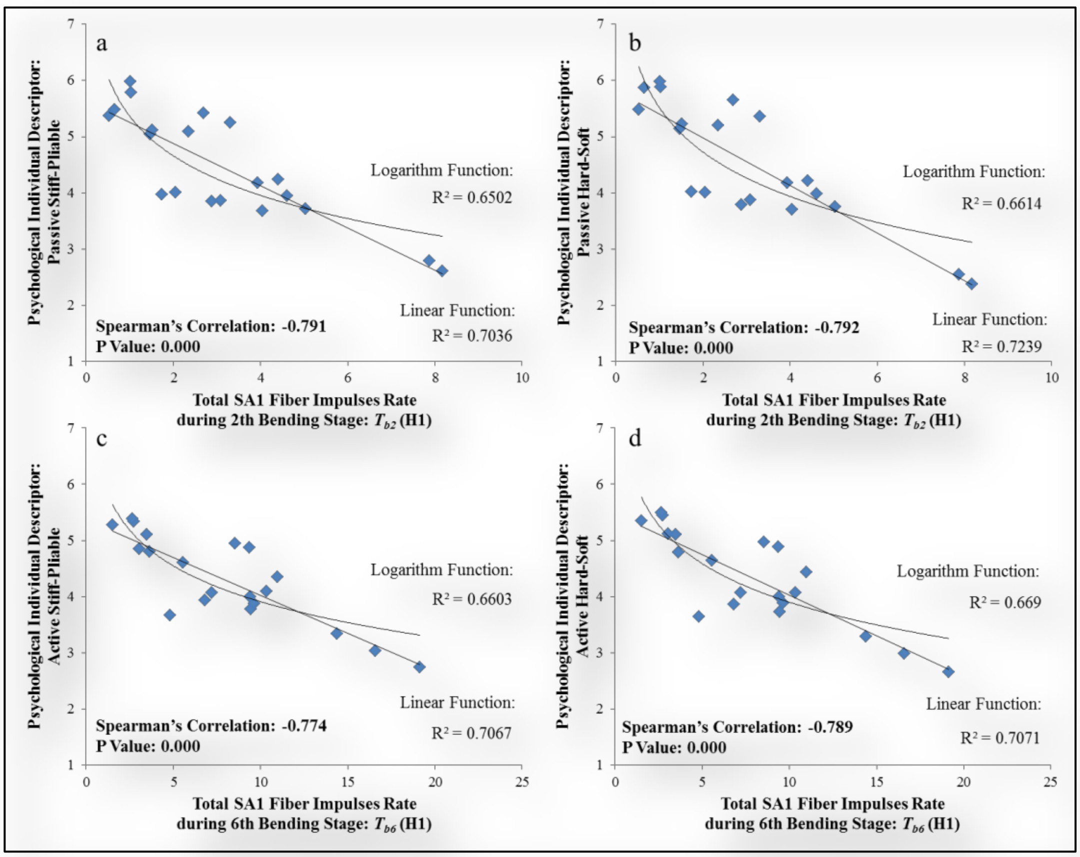

Figure 8-10 Correlation Scatter Plots of SA1 Fiber Total Impulses during Bending Stage 2 (T_{b2}) and Stage 6 (T_{b6}) and Passive and Active Psychological Individual Descriptors respectively

In summary, the neural responses of SA1 fibers based on the hypothesized force coding mechanism could be directly linked to the psychological descriptors. The NonFullness-Fullness descriptor shows higher correlation to neural responses during compression and recovery while the Stiff-Pliable and Hard-Soft descriptors both demonstrate a strong relation to neural responses during the bending process. For compression and recovery, there is no clear preference towards Hypothesis 1 or 2. However, in terms of the bending process, only the total impulse rates of SA1 fibers (Hypothesis 1) are found to be significantly correlated to the psychological descriptors. This finding not only agrees with the neurophysiological conclusions that cutaneous neural information itself could be enough for softness-related sensation discrimination, but also suggests that adding neural kinetic information might even reduce the predictabilities of the indexes in this specific case for fabrics.

8.3 Integration Prediction of Psychological Sensation Dimensions

On the basis of previous analyses, several neurophysiological indexes have been found to be closely related to psychological sensations. For perceptions made by passive touch, they include Q_{steady}, W, T_{c11}, and T_{b2} while C_{max}, W, T_{c11}, and T_{b6} are responsible for perceptions made by active touch. According to previous discussions as regards the exploration of their relation and the psychological descriptors, they are all transformed by first using a natural logarithmic function. Their relations to psychological sensory dimensions are revealed as follows.

Table 8-5 Spearman's Correlation between Neurophysiological Indexes and Their Interactions and Psychological Sensory Dimensions

Index	Statistic	Smoothness	Passive Softness	Warmth
Q_{steady}	Coefficient	--	--	-0.854
	p Value	--	--	0.000
T_{c11}	Coefficient	--	--	0.862
	p Value	--	--	0.000
T_{b2}	Coefficient	--	-0.843	--
	p Value	--	0.000	--
W	Coefficient	-0.693	-0.722	--
	p Value	0.001	0.000	--
Index	**Statistic**	**Smoothness**	**Active Softness**	**Warmth**
C_{max}	Coefficient	--	--	-0.895
	p Value	--	--	0.000
T_{c11}	Coefficient	--	--	0.883
	p Value	--	--	0.000
T_{b6}	Coefficient	--	-0.862	--
	p Value	--	0.000	--
W	Coefficient	-0.737	-0.756	--
	p Value	0.000	0.000	--

Table 8-5 lists the Spearman's correlation coefficients and p values for the psychological sensory dimensions. Smoothness evaluated through passive touch is significantly correlated to the texture-information neurophysiological index W. Softness evaluated through passive touch shows significant correlations to the W index and force-information neurophysiological index, T_{b2}. Last but not least, warmth evaluated through passive touch shows a significant correlation to the thermal-information neurophysiological index Q_{steady} and force-information neurophysiological index T_{c11}. These correlations are the same for perceptions made under active contact, while Q_{steady} and T_{b2} are replaced by C_{max} and T_{b6}.

Based on these observations, the weighted summations of the correlated neurophysiological indexes and their interactions (if any) were built as prediction models. Table 8-6 gives a summary of each model. It can be observed that smoothness evaluated through passive touch share the least adjusted R^2 in all six prediction models while warmth evaluated through active touch show the highest value. It can also be noticed that both smoothness and warmth demonstrate higher model fits for perceptions under active touch than those for perceptions under passive touch, and softness could be better predicted with evaluating carried out by passive touch.

Table 8-6 Summary of Neuropsychological Models on Sensory Dimensions

Dimension	Predictor	Adjusted R^2	F	p
Passive Smoothness	W	0.401	13.695	0.002
Passive Softness	T_{b2}, W, T_{b2}*W	0.787	24.406	0.000
Passive Warmth	Q_{steady}, T_{c11}, Q_{steady}*T_{c11}	0.732	18.335	0.000
Active Smoothness	W	0.615	31.331	0.000
Active Softness	T_{b6}, W, T_{b6}*W	0.726	17.786	0.000
Active Warmth	C_{max}, T_{c11}, C_{max} *T_{c11}	0.814	28.673	0.000

In addition, the best prediction models concluded on Chapter 7 are listed in Table 8-7 for the purpose of comparison. It is observed that smoothness has the lowest adjusted R^2 values in both prediction methods. It is also noticed that the most adjusted R^2 obtained from psychophysical models is higher than those obtained based on neuropsychological models, except for smoothness with active touch. Nevertheless, the F values show results otherwise. Neuropsychological prediction models generally have higher F values.

Table 8-7 Summary of Psychophysical Models on Sensory Dimensions

Dimension	Adjusted R^2	F	p
Passive Smoothness	0.501	3.389	0.032
Passive Softness	0.918	18.804	0.000
Passive Warmth	0.762	13.167	0.000
Active Smoothness	0.589	5.544	0.005
Active Softness	0.932	27.171	0.000
Active Warmth	0.889	12.734	0.003

It is clear that all of the sensory dimensions could be significantly predicted by using the neurophysiological indexes and their interactions. There are only four neurophysiological indexes and their interactions used for building these equations, which span over ten physical indexes as covered in Chapter 7. These indexes have been determined in Chapter 5 based on the neurophysiological coding mechanisms of different types of skin information received during evaluation tasks of objects by hand. They represent the dynamic responses of fabrics within the touch process. Direct comparisons between them and individual descriptors, as well as prediction model building for sensory dimensions, ascertain that they could be used to describe fabric touch sensation just as well as the conventional psychophysical models.

8.4 Model Validation

For the purpose of the validation of the psychophysical prediction models as well as neuropsychological prediction models, another group of samples were evaluated on the basis of the psychophysical prediction and neuropsychological models respectively. Another 32 fabrics were tested by the instrument FTT and subjective experiments. The predicted touch sensation indexes were compared to the subjective obtained touch sensation scores. In the following, there is a discussion on a comparison between the predicted sensory dimension values from these two methods and psychologically obtained values. The two models could be validated through these comparisons.

Figure 8-11 shows the model validation with regard to smoothness with passive touch. Pearson's correlation coefficients and p values are displayed at the right bottom of each figure. The Pearson's coefficient of the neuropsychological model is 0.750 while that of the psychophysical model is 0.563. P values of both models are 0.000 and 0.001 respectively. Results indicate that the subjective obtained scores regarding smoothness sensation for this new set of fabrics can be better predicted by neuropsychological model.

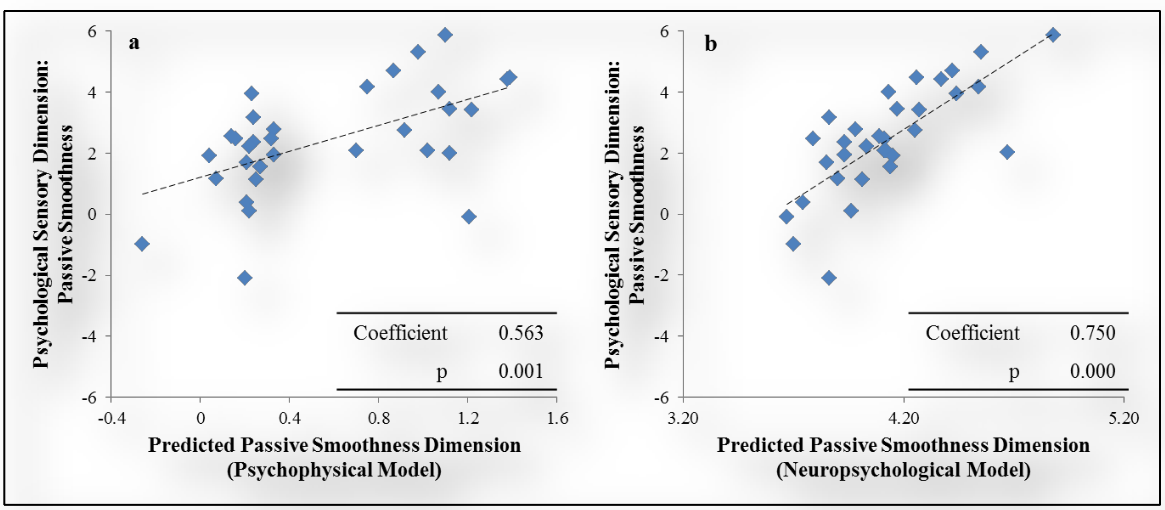

Figure 8-11 Scatterplot of Psychological Sensory Dimension Passive Smoothness and Predicted Passive Smoothness Dimension based on Psychophysical Model (a) and Neuropsychological Model (b) respectively

Figure 8-12 illustrates the results with regard to softness with the use of passive touch. The figure clearly shows better correlation for predicted values from the neuropsychological prediction method as opposed to those of the psychophysical prediction method. The Pearson's correlation coefficient of psychophysical prediction model is only 0.313 and p value is larger than 0.5. Meanwhile, coefficient of neuropsychological model is 0.783. The linear trend line matches much better as shown in Figure 8-12(b).

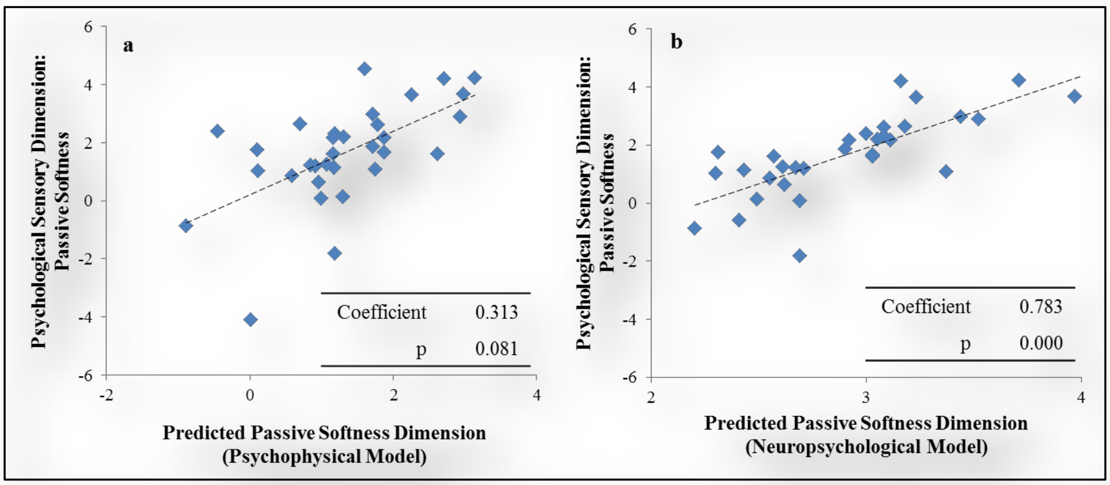

Figure 8-12 Scatterplot of Psychological Sensory Dimension Passive Softness and Predicted Passive Softness Dimension based on Psychophysical Model (a) and Neuropsychological Model (b) respectively

With regard to warmth as evaluated by passive touch, Figure 8-13 indicates that neither prediction method has satisfactory prediction capacity. The predicted values through psychophysical prediction even failed to show significant correlation to psychological values at the significant level of 0.01.

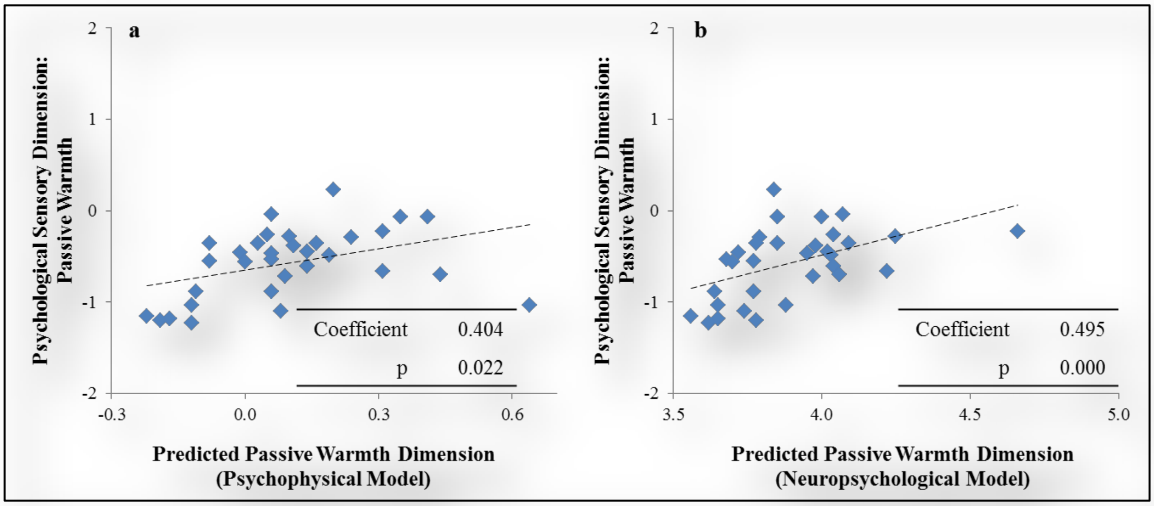

Figure 8-13 Scatterplot of Psychological Sensory Dimension Passive Warmth and Predicted Passive Warmth Dimension based on Psychophysical Model (a) and Neuropsychological Model (b) respectively

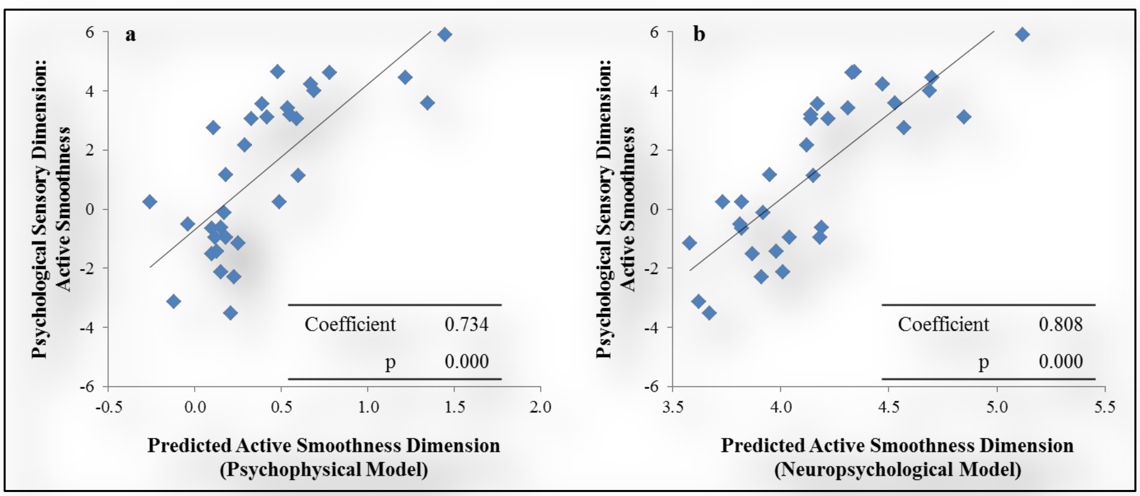

Figure 8-14 Scatterplot of Psychological Sensory Dimension Active Smoothness and Predicted Active Smoothness Dimension based on Psychophysical Model (a) and Neuropsychological Model (b) respectively

With regard to the prediction of smoothness with active touch, the predicted values based on both psychophysical and neuropsychological predictions show significant correlation to psychologically obtained values, as shown in Figure 8-14. Coefficient value of neuropsychological prediction model is 0.808, comparing to that of psychophysical model of 0.734.

Figure 8-15 shows that there is good correlation between psychologically obtained softness values through active touch, and those predicted through psychophysical and neuropsychological predictions. The correlation coefficient for psychophysical model is 0.806. Whilst for neuropsychological prediction, the correlation coefficient is then 0.877, which is the highest value obtained in this study of model validation.

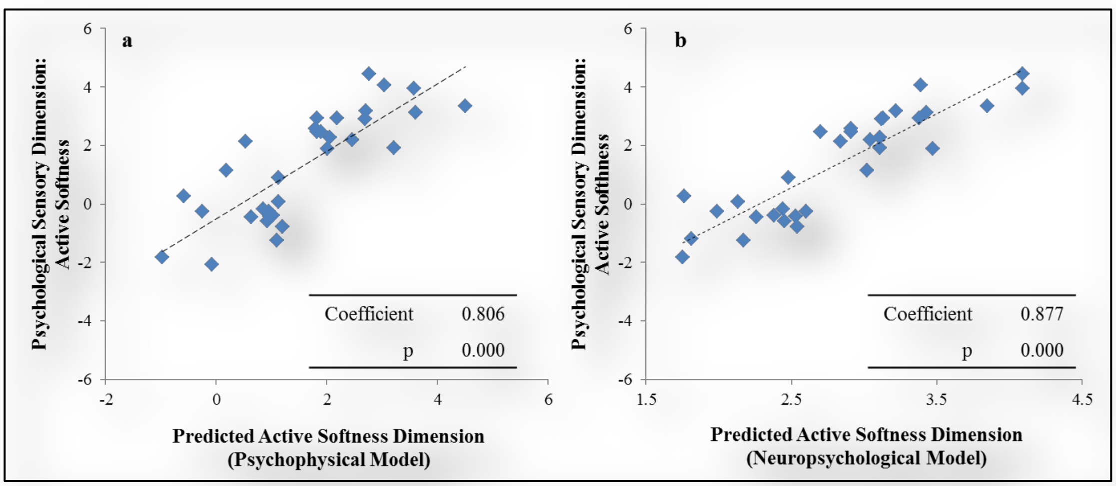

Figure 8-15 Scatterplot of Psychological Sensory Dimension Active Softness and Predicted Active Softness Dimension based on Psychophysical Model (a) and Neuropsychological Model (b) respectively

Figure 8-16 indicates that there is an obvious preference for the neuropsychological prediction model over the psychophysical prediction model. The psychophysically predicted values of warmth with active touch show no significant correlation to the psychologically obtained values. On the other hand, the neuropsychologically predicted value already shows significant correlation to the psychologically obtained feeling of warmth through active touch. The correlation coefficient is 0.783.

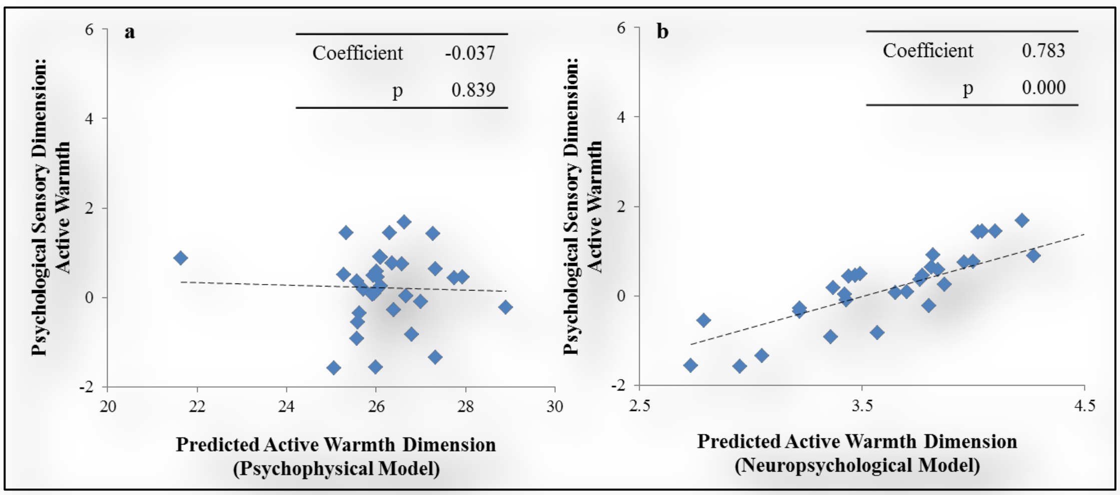

Figure 8-16 Scatterplot of Psychological Sensory Dimension Active Warmth and Predicted Active Warmth Dimension based on Psychophysical Model (a) and Neuropsychological Model (b) respectively

The model validation study discussed ascertains the prediction capacity of the concluded fabric sensation prediction models. Overall speaking, the proposed neuropsychological models present better accuracy to predict fabric touch sensation. Although earlier discussions showed that psychophysical prediction models have higher adjusted R^2 than neuropsychological prediction models, the predicted values based on the former provide lower correlation coefficients to psychological values, especially for the sensation of warmth. Meanwhile, the neuropsychologically predicted values show correlation coefficients that are higher than 0.750 for most sensory dimensions. Among all six sensory indexes, only the prediction capacity for passive warmth is much lower. It is generally agreed that for a sensory dimension subjects could better discriminate, a stronger prediction capacity is obtained. The findings conclude that most fabrics could be precisely predicted by the established neuropsychological models.

8.5 Neuropsychological Mechanism Discussion

Three levels of biologically processing the perception of fabric touch sensation, including at the physical, neurophysiological, and psychological levels, have been discussed in the previous chapters. The explorations, which are carried out through neuropsychological means in this chapter, link neurophysiological neural responses to psychological sensations. On the basis of these discussions, the following synthesizes the three sensation perception processes and neuropsychological mechanisms of fabric touch sensation are proposed.

8.5.1 Psychophysiological Decoding Relation

It is noticed from the findings in Section 8.2 that all of the preferred neurophysiological indexes could be better correlated to psychological sensations after using a logarithmic function. Neurophysiological indexes describe the neural responses, the majority in the format of impulse signals stimulated by external physical information. Such information would be transmitted until it reaches the cerebrum. Current neurophysiological and electrophysiological research has identified different function areas in the human brain. It has been generally accepted that neural signals that reach the cerebrum would excite certain function areas according to their stimulation type. However, the underlying mechanism between brain activity and sensory perceived is still under investigation.

Based on the logarithmic functions between the neurophysiological indexes and psychological sensations concluded in this Ph.D. study, the author proposes a theoretical mechanism between brain activity and perceived touch sensation.

The first feature of a logarithmic function is monotonic change. A monotonic relation is agreed on in most of the previous findings. An increase or decrease in the stimuli intensity would often lead to the same direction of change in terms of the sensory magnitude.

The second feature is the change of the curve slope. The slope of a logarithmic curve decreases with x. This implies that for fabric touch sensory dimensions, smoothness, softness, and warmth, the negative effects of increasing stimuli intensity would be reduced. By taking smoothness as an example, a small reduction in stimuli intensity could cause a relatively larger discrimination towards the sensation of smoothness within a group of relatively smooth fabrics. On the other hand, for a group of relatively rough fabrics, the same amount of reduction in stimuli intensity may not lead to a significant discrimination. On the basis of this theoretical hypothesis, these would be important applications to study the efficiency of methods that improve fabric touch sensation.

In order to determine the "threshold" of the efficiency, mathematical analyses of the relations between neurophysiological indexes and psychological descriptors were conducted. For each neural response index, the most relevant psychological descriptor was used. Two trend-lines in terms of prediction were fitted for each pair, as shown in **Figure 8-17**. The trend-lines of scatters fitted are shown in the figure with solid one stands for logarithmic trend-line while dashed one means linear trend-line. Fitted model of both trend-lines are shown in the right-bottom corner with their R2 values. The "threshold" of efficiency was identified as the point when the slope of the logarithmic function is lower than half of the slope of the linear function. Calculation formula is shown as follows.

$$S_{linear}/_2 = \frac{S_{log} ln(dx)}{dx} \qquad (8\text{-}1)$$

where S_{linear} means the slope of linear fitted model, S_{log} the pre-logarithmic coefficient of logarithmic fitted model. Following table summarizes the results

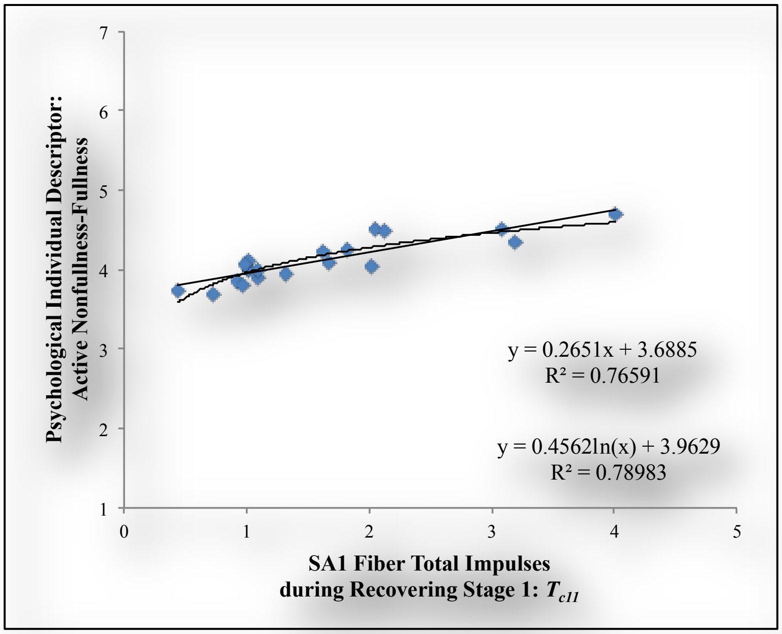

Figure 8-17 Scatterplot between T_{c11} and Psychological Individual Descriptor Active NonFullness-Fullness

8.5.2 Neuropsychological Mechanism

The following is a summary of the neuropsychological mechanism of each sensory dimension of fabric touch. Their perception would all be processed at the physical, neurophysiological, and psychological levels. The neuropsychological mechanisms reveal the principles during each level so that the grounds of fabric touch sensation perceived could be understood.

Figure 8-18 illustrates the neuropsychological mechanism of warmth. It can be seen that the physical grounds of warmth include the thermal and compressibility properties of fabric. The fabric thermal property could be characterized by recording its heat transfer curve during clamping of two plates together at different temperatures. The fabric compressibility properties, on the other hand, could be addressed by monitoring its thickness changes with gradually increasing normal pressure. The corresponding techniques consequently involve finishing materials, which would affect the fabric heat conductance or compressibility. Fabric structure would obviously also influence the fabric thermal and compressibility properties. In addition, the yarn materials used themselves would have inherent affects.

The neurophysiological coding mechanism indicates that both transient temperature and temperature change rate of fabric along with contact time would impact the neural responses to thermal information. Meanwhile, the force needed to change the unit thickness of fabric would stimulate force-responsible neural receptors. Exploration with psychophysiological decoding further implies thermoreceptor responses to fabric at the lowest and most steady temperature are the key factors and total impulse of SA1 fibers determined by resistance force in the very first stage of the compression-recovery process is more correlated. Therefore, to reduce the sensation of fabric warmth, the thermal property should be adjusted to either a relatively high transient thermal conductance or low thermal conductivity at the steady-state. Meanwhile, the changing of fabric so that it would produce low resistance during recovery from the most-compressed state could also be helpful.

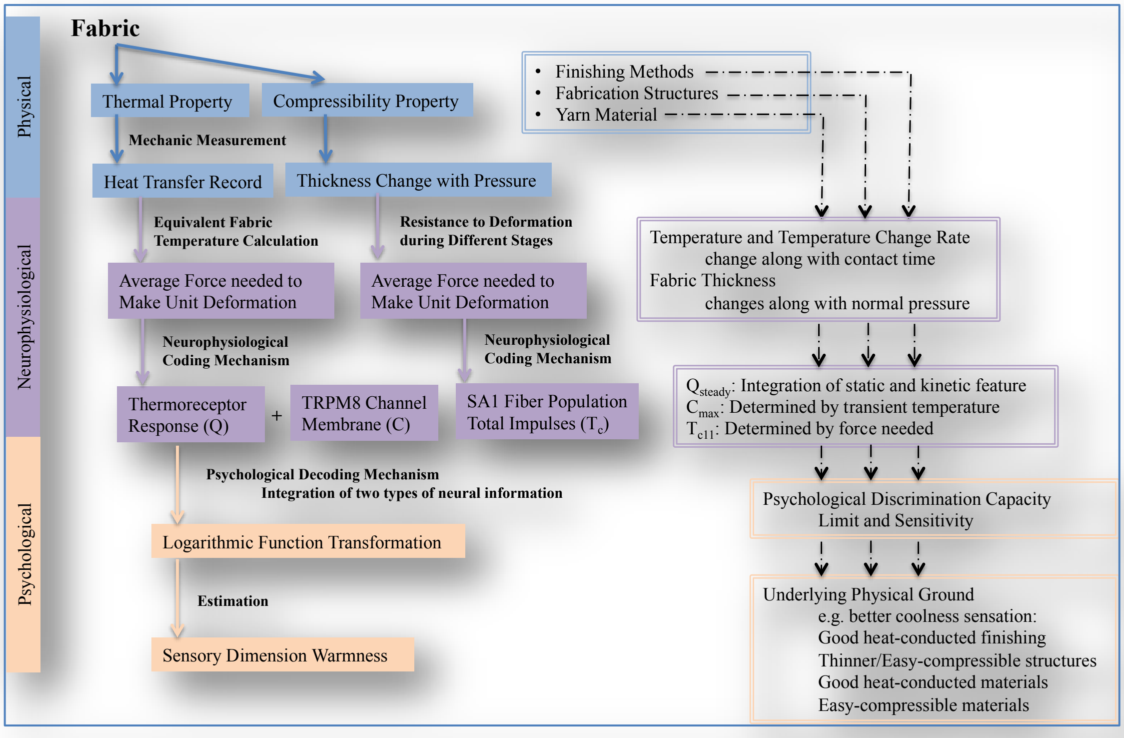

Figure 8-18 Neuropsychological Mechanism of Perceiving Fabric Touch Sensory Dimension: Warmth

The responses of thermoreceptors as well as SA1 fibers could be synthesized to estimate the magnitude of warmth. Based on a natural logarithmic function, the psychophysiological mechanism of the relation between neural responses and psychological sensation is proposed above. The deduction suggests that there would be a turning point of efficiency in order to warrant a sensation of less warmth.

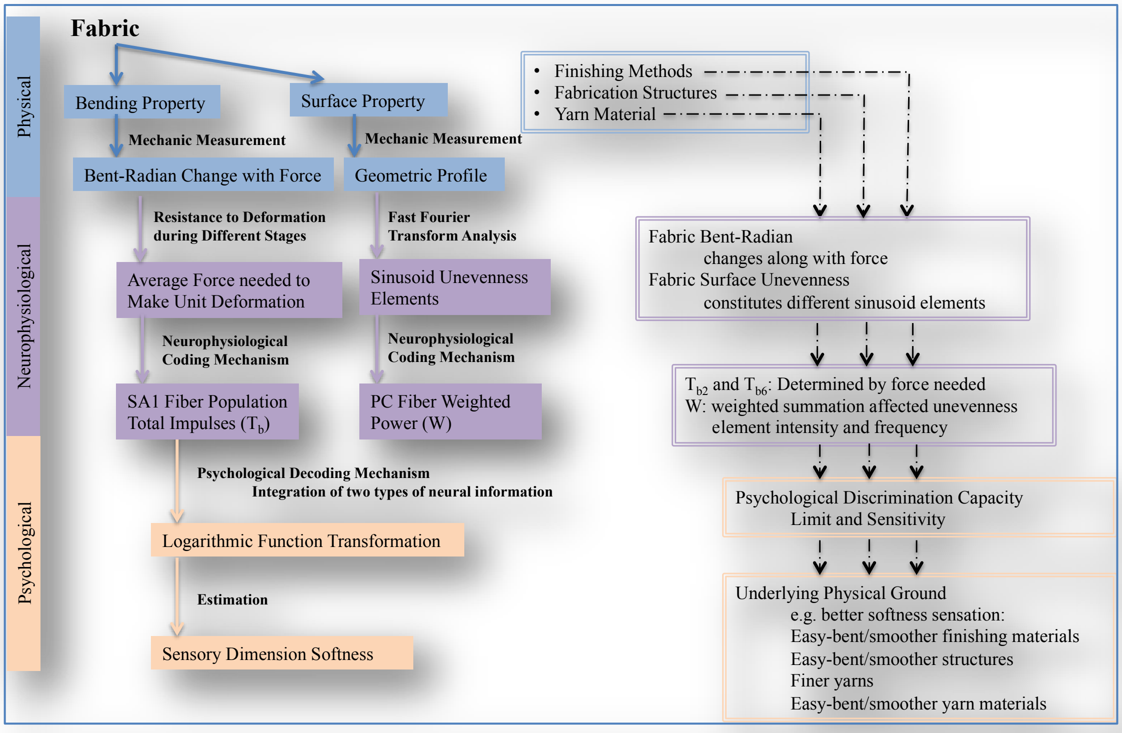

Figure 8-19 Neuropsychological Mechanism of Perceiving Fabric Touch Sensory Dimension: Softness

The neuropsychological mechanism of fabric softness is presented in Figure 8-19. The two concluded physical properties related to softness are bending and surface related properties. Bending could be characterized by examining the force needed to bend 1 radian of fabric while the surface related property could be quantified by exploring its geometric profile. There are also three levels of corresponding fabric physical properties. The finishing materials, fabrication structure, and yarn materials could, to different extents, influence fabric bending as well as the surface.

The neurophysiological coding mechanisms of bending and surface related information are separately analyzed. Similar to compression, force information received during the bending process should also be calculated as the average force needed to make one unit of deformation (i.e. 1 radian). The magnitude of the force received can be linearly correlated to the impulses of the SA1 fiber population. Meanwhile, the geometric profile of the fabric surface should be classified into different sinusoid components with specified intensities and frequencies. The FFT was used to carry out this classification. Subsequently, the influential power of each element was added together with different weight, which was determined by its frequency, to conclude the overall weighted power of the PC fibers. Exploration of decoding from neural responses to psychological sensations suggests that the most important factor of the perception of force is the SA1 fiber responses during the middle bending stage. Based on the physical mechanics of fabric bending deformation, this implies that yarn material should be given more attention.

The logarithmic integration of these neural responses from SA1 fibers to received forces and PC fibers to the fabric surface texture could be used to predict softness. In order to obtain a touch sensation of a softer fabric, efforts could be made to reduce the resistance force of yarns to bending deformation or surface unevenness of fabrics.

Figure 8-20 shows the neuropsychological mechanism of smoothness. It can be concluded that smoothness is solely affected by the surface properties of the fabric. As discussed earlier, the surface properties of fabric should be measured by examining its geometric profile. The physical properties that may influence the geometric profile include surface finishing materials and their distributions, fabric structure, yarn size, and yarn surface texture.

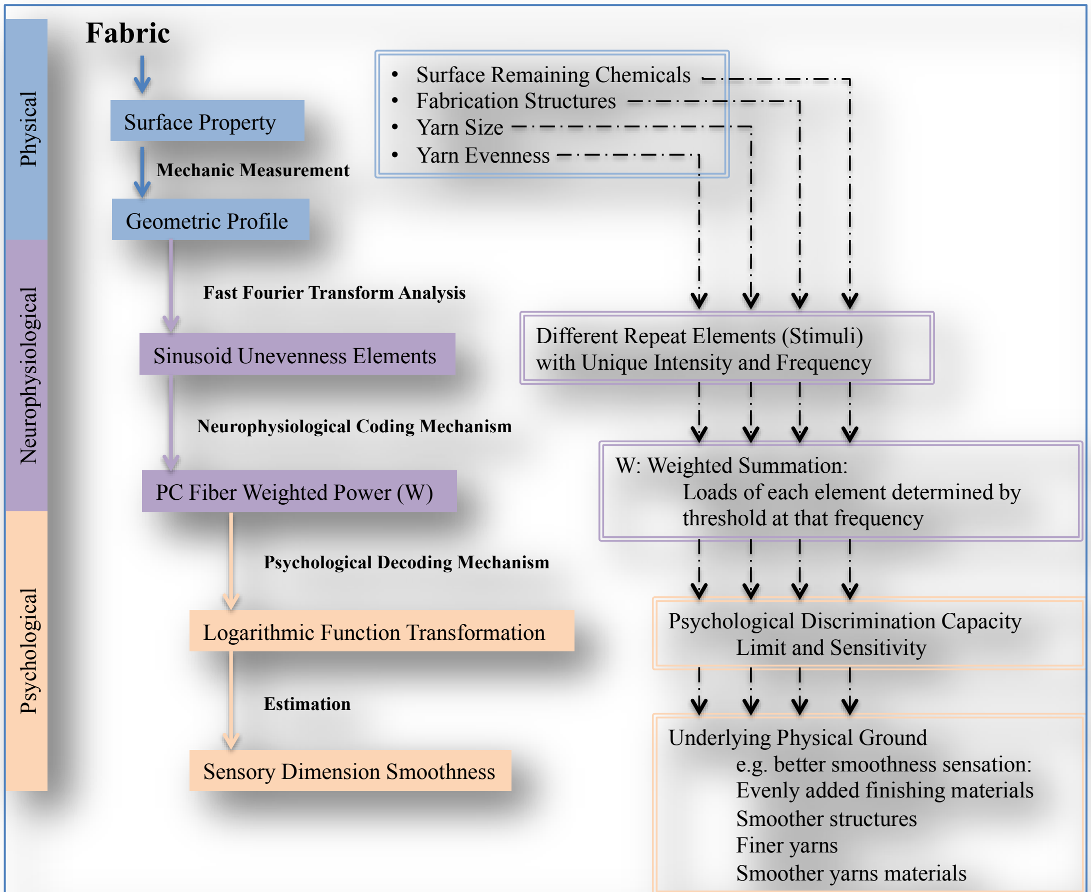

Figure 8-20 Neuropsychological Mechanism of Perceiving Fabric Touch Sensory Dimension: Smoothness

The FFT analysis revealed that geometric profiles could be classified into different sinusoid components with various intensities and frequencies. The neurophysiological coding mechanism indicated that the weighted summation of these elements could be responsible for the response power of PC fibers. The weights of these elements vary according to their frequency. Therefore, since different physical influential aspects are likely to induce different unevenness frequencies, their significances are also different.

Psychophysiological decoding again shows that the logarithmic function is preferred. The physical grounds for smoothness suggest that there are many methods that could be used to improve the touch sensation of fabric smoothness, from finishing materials to yarn surface texture. The efficiency turning point of these improvements has also been proposed from theoretical deduction.

8.6 Conclusion

In this chapter, the objective 6 has been completed by building neuropsychological prediction models of fabric touch sensations. The neuropsychological mechanisms of three sensory dimensions of fabric touch, that is, warmth, softness, and smoothness, have been revealed in this chapter. The discussion in this chapter is focused on linking the three processes of sensation perception. The neuropsychological prediction models of fabric touch sensation further the prediction grounds based on the underlying neural responses. The model validation also demonstrates that the prediction accuracies of these neuropsychological prediction models are better than that of conventional psychophysical models. It is also proposed that similar preferences for logarithmic functions of psychophysiological relations could mean the deduction of a theoretical turning point in the efficiency of modifying fabric properties to improve touch sensation.

Chapter 9 Conclusion and Future Work

9.1 Conclusion

In this thesis, an attempt has been made to study fabric touch sensation. In Chapter 3, a framework of utilizing neuropsychological approach to study fabric touch sensations has been proposed, achieving objective 1. The neuropsychological mechanisms of fabric touch sensation have been comprehensively discussed for different processing stages in later contents. Research has been conducted at the following levels: 1) physical: a simultaneous characterization method has been proposed; 2) neurophysiological: the coding mechanisms of neural responses to fabric touch related stimuli have been concluded; 3) psychological: discrimination psychophysiological mechanism of fabric touch sensation is analyzed; 4) psychophysical: integration of different physical aspects and thermo-tactile influences have been studied; and 5) neuropsychological: neuropsychological mechanisms of fabric touch sensation have been revealed.

In Chapter 4, with regard to the physical detection of stimuli in fabric touch sensation, the objective 2 has been accomplished through proposing the simultaneous detection mechanism of different physical stimuli.

a. The physical detection mechanism of stimuli related to fabric touch sensation is revealed. Biological foundation of skin receptors suggests that simultaneous reception of multiple stimuli is highly likely to take place when humans are doing haptic evaluations on fabrics.

b. A measurement principle that entails the simultaneous characterization of fabric physical properties has been proposed. The method includes measurement of fabric thermal, compression, bending, and surface properties.
c. Indexes to describe the fabric physical properties have been identified accordingly. There are 13 indexes identified based on the transient value at specific moments during measurement and steady value calculated with respect to a period of time.
d. The reliability and repeatability of this new measurement principle have been ascertained through experiments. The results from twelve repeated tests from two operators suggest that the machine variances are under a certain level (less than 10%). In a comparison to instruments within the classic KES-F system, it is found that the results between these two methods are in agreement with each other.

In Chapter 5, with regard to the neurophysiological coding process of fabric touch information, the objective 3 has been completed by building mathematical models to transduce detected physical stimuli into neural responses are developed based on various coding hypotheses.

a. Three types of stimuli information that can be detected by human skin are concluded, which are thermal, texture, and received force information during fabric deformation.
b. The neurophysiological coding mechanism of thermal information is considered to be based on the integration of static temperature and kinetic

temperature change rate and recently hypothesized as the intrinsic changes of the TRPM8 channel due to transient absolute temperature. Due to the special features of fabric heat conductance change with time, the relevant fabric temperature was calculated from the recorded heat flux. Indexes of thermoreceptor responses and relative currents through the TRPM8 channel are determined accordingly to separately represent transient extreme values and average steady values.

c. The neurophysiological coding mechanism of texture information is concluded as the spatial or temporal variances of SA1 and PC fibers. The geometric profile of the fabric surface is considered to have a repetitive sinusoidal form. The neural responses of both types of fibers are determined based on different characterization methods of the sinusoid surface unevenness. An index that refers to the overall/average fiber response is identified for each hypothesis.

d. The neurophysiological coding mechanism of received force information is revealed as the SA1 fiber responses to normal forces applied onto human skin. A linear relation is found between them. Due to the unique non-linear rigidity of fabric deformation, there are ten applications carried out for each deformation task, including compression, recovery, and bending. The indexes are identified as the total impulses that have taken place as well as the ratio between total impulse and distance that the skin has moved during each stage.

In Chapter 6, in terms of the psychological discrimination process of fabric touch sensation, the objective 4 covering sensory dimensions and effects of active and passive touch and climatic conditions have been achieved based on subjective measurements of perception. Ten individual descriptors are chosen for subjective measurement carried out by 226 subjects in 6 climatic conditions.

a. General differences in judging the touch sensation of the samples are observed for passive and active touch. The descriptors that are highly likely to show different subjective ratings include Cool-Warm, Rough-Smooth, and Thick-Thin. Active touch also demonstrates better discrimination capacity of the descriptors including Cool-Warm, Sticky-Non-adhesive, Thick-Thin, and NonFullness- Fullness. In addition, climatic conditions such as temperature and relative humidity are also found to have significant impact on some of the descriptors.
b. The identification of fabric sensory dimensions through a PCA has revealed the three most important attributes: smoothness, softness, and warmth, according to their features. They would count for over 60% of the total variances based on the ten descriptors. Despite that the exact loading of each dimension varies due to active and passive touch and climatic conditions, these three dimensions remain similar in feature and the relative constant loading. It has been noticed that the three concluded sensory dimensions can be perfectly linked to the three types of physical stimuli related to fabric touch sensation.
c. Further analyses also demonstrate the impacts of active and passive touch and climatic conditions on the values of each sensory dimension. Psychophysiological investigations indicate that the different results of the sensory dimensions due to active and passive touch are the result of different

stimulations of the skin receptors during active and passive touching. Their anatomical locations would lead to different information received during passive and active touch. Meanwhile, changes in climatic conditions (i.e. temperature and relative humidity) cause physiological differences in the skin receptors. Such climate acclimation of the skin receptors could take place within one month of being in the new condition and leads to shift in sensation even when the sensation is perceived in a standardized condition.

In Chapter 7, with regard to the exploration of the psychophysical relation of fabric touch sensation, objective 5 has been achieved by examining psychological hypotheses and effects of the thermotactile interaction on fabric touch sensory dimensions through various mathematical models.

a. Mono-mode relations are first explored for linkages between individual psychological descriptors and identified physical indexes. Different mathematic functions are necessary for different types of sensations. The results do not support the recommendation of classic psychophysical laws for a constant type of relation between physical stimuli and psychological sensation.

b. It has been observed that the linkages between psychological sensations of fabrics and their physical properties could be found by using different calculation methods of the physical properties. Physical indexes based on the energy consumed, average force needed, or extreme response received all demonstrate, to different extents, correlation to psychological sensations. This implies that neglecting the underlying neurophysiological coding process from physical stimulus to neural response is a mistake in studying fabric touch sensation.

c. The multi-mode psychophysical relations to fabric touch sensory dimensions provide the features of the best model fit when different aspects of physical indexes and interactions between them are included. Better correlation is observed as regards the integration of different aspects of physical stimuli to predict one single sensory dimension. This is in agreement with the concept of simultaneous perception as well as thermotactile impact of fabric touch sensation.

In Chapter 8, with regard to the development of neuropsychological prediction for fabric touch sensation, objective 6 has been completed by establishing and validating prediction models that are neuropsychologically based on each sensory dimension.

a. An exploration of the relation between the identified neurophysiological indexes and psychological descriptors is first conducted. It is concluded that a thermal feeling would better correlate with a steady thermoreceptor response and maximum relative current of TRPM8; texture feelings could be better correlated by the weighted power of PC fiber responses; and feelings of received force could be better correlated by the total impulses that take place during certain deformation stages (very first recovery from the most-compressed state, second and sixth stages of bending deformation). It is also found that the relations all better fit by using logarithmic functions.

b. Prediction models based on neuropsychological mechanisms are developed. Warmth is expected to be significantly predicted through thermoreceptor and SA1 fiber responses during compression deformation while smoothness to be solely addressed by the texture-induced weighted power of PC fiber response. Lastly, softness is anticipated to be predicted through SA1 fiber response during bending deformation as well as the weighted power of PC fibers due to the fabric surface texture.
c. A comparison between these neuropsychological prediction models and conventional psychophysical prediction models indicates no clear advantages of either type. Model validation from a group of new samples (not used when developing these models), nevertheless, demonstrate obvious better prediction capacities of the neuropsychological prediction models.
d. The relation between the psychological results and neurophysiological indexes suggests that psychophysiological mechanisms adhere to logarithmic functions. This implies that larger differences in fabric touch sensation would be perceived when neural response is relatively low.

Through detailed investigations in the abovementioned stages of the perception process of fabric touch sensation, its neuropsychological mechanism is evident. This study originally constructed the neurophysiological responses of fabric touch sensation and implanted the results into prediction models. This provides an alternative to comprehensively studying fabric touch sensation.

Author has made the best attempts to achieve the research objectives. There are some limitations may need further improvement. The sample selections have included the largest available variance of fabric types during the research while the findings could still be checked with more fabric types.

9.2 Commercial Application

The research findings in this Ph.D. study are directly applicable to the industry, which will benefit future industrial development.

The measurement principle that entails the simultaneous characterization of the physical properties of fabric concluded in the physical study of this research work is already commercialized. Three patents have been filed on the measurement principle. A commercial agreement has also been reached. A product named the "fabric touch tester" is already available in the market.

The effects of active and passive touch in relation to climatic conditions are potential references for product development. Textile products for different usages and different regions would address specific active and passive touch and climatic conditions. Therefore, the considering of the effects of these factors would help to provide better touch-feel products.

The neuropsychological prediction models developed from the neuropsychological study in this paper could provide a better method for fabric touch sensation. These models are found to have better prediction capacities through the use of the data in the study. It is reasonable to assume that they would demonstrate a good performance for other fabrics. In addition, the psychophysiological logarithmic functions are the turning point of efficiency to improve fabric touch sensation in industrial applications. The predicted passive sensory dimensions estimate the perceptions when subjects evaluate the touch sensations during initial choosing. The predicted active sensory dimensions, in the other way, estimate the perceptions when subjects try the garments on. Predicted overall comfort gives a reference to the overall perception of fabrics. However, the overall fabric touch perception would be largely affected by the final garment usages.

9.3 Future Work

This Ph.D. study has revealed the neuropsychological mechanisms of fabric touch sensation at the physical, neurophysiological, and psychological levels. Data obtained through physical and psychological means in the study are measured first-hand. However, the neural responses obtained by the neurophysiological study are not directly measured from cloned organics or animals. Neurophysiological transducing mechanisms of skin receptors are still highlighted while neurophysiological transmission mechanisms continue to remain elusive. Direct investigation of neural responses recorded from neurons would help to improve the findings in this research work.

In addition, the scope of the concluded neuropsychological mechanisms could be extended. This PhD study focused on the steady condition of touch perception and revealed the scientific understanding behind the psychological perception. On the basis of the findings, other physical properties including tensile, shearing, and drape could be further evaluated and extend the boundaries of the concluded models. Moreover, the neuropsychological mechanisms uncovered in this study could be further revised to fulfill the more complicated daily usage, i.e. under sweating conditions or in extreme conditions. The water existing could influence the fabric touch perceptions and pressed condition would induce the pain sensations.

Appendix

Table 0-1 Summary of Correlation within Psychological Individual Descriptors

		Cool-Warm	Itchy-Nonitchy	Scratchy-Nonscratchy	Prickle-Nonprickle	Rough-Smooth	Stick-Nonadhesive	Stiff-Pliable	Thick-Thin	Hard-Soft	Nonfullness-Fullness
Cool-Warm	Correlation	1	-0.615	-0.607	-0.573	-0.627	-0.369	-0.407	-0.34	-0.363	0.515
	p Value		0.000	0.000	0.000	0.000	0.000	0.000	0.000	0.000	0.000
Itchy-Nonitchy	Correlation	-0.615	1	0.995	0.994	0.985	0.577	0.902	0.83	0.892	-0.300
	p Value	0.000		0.000	0.000	0.000	0.000	0.000	0.000	0.000	0.001
Scratchy-Nonscratchy	Correlation	-0.607	0.995	1	0.994	0.989	0.572	0.917	0.841	0.909	--
	p Value	0.000	0.000		0.000	0.000	0.000	0.000	0.000	0.000	--
Prickle-Nonprickle	Correlation	-0.573	0.994	0.994	1	0.981	0.596	0.907	0.845	0.900	-0.292
	p Value	0.000	0.000	0.000		0.000	0.000	0.000	0.000	0.000	0.001
Rough-Smooth	Correlation	-0.627	0.985	0.989	0.981	1	0.566	0.926	0.859	0.915	-0.305
	p Value	0.000	0.000	0.000	0.000		0.000	0.000	0.000	0.000	0.001
Stick-Nonadhesive	Correlation	-0.369	0.577	0.572	0.596	0.566	1	0.489	0.680	0.502	-0.622
	p Value	0.000	0.000	0.000	0.000	0.000		0.000	0.000	0.000	0.000
Stiff-Pliable	Correlation	-0.407	0.902	0.917	0.907	0.926	0.489	1	0.896	0.997	--
	p Value	0.000	0.000	0.000	0.000	0.000	0.000		0.000	0.000	--
Thick-Thin	Correlation	-0.340	0.830	0.841	0.845	0.859	0.680	0.896	1	0.903	-0.456
	p Value	0.000	0.000	0.000	0.000	0.000	0.000	0.000		0.000	0.000
Hard-Soft	Correlation	-0.363	0.892	0.909	0.900	0.915	0.502	0.997	0.903	1	--
	p Value	0.000	0.000	0.000	0.000	0.000	0.000	0.000	0.000		--
Nonfullness-Fullness	Correlation	0.515	-0.300	--	-0.292	-0.305	-0.622	--	-0.456	--	1
	p Value	0.000	0.001	--	0.001	0.001	0.000	--	0.000	--	

Table 0-2 Multi-ANOVA Test Result of Neurophysiological Indexes Q_{upsum}, $Q_{downsum}$, and Q_{steady}

Source	Index	Type III Sum of Squares	df	Mean Square	F	Sig.
Corrected Model	Q_{upsum}	3.0E+05	59	5.1E+03	21.2	0.000
	$Q_{downsum}$	8.7E+05	59	1.5E+04	55.5	0.000
	Q_{steady}	1.9E+03	59	3.3E+01	100.4	0.000
Intercept	Q_{upsum}	4.5E+05	1	4.5E+05	1884.3	0.000
	$Q_{downsum}$	1.4E+06	1	1.4E+06	5210.8	0.000
	Q_{steady}	5.1E+04	1	5.1E+04	155365.8	0.000
Fabric Code	Q_{upsum}	2.9E+05	19	1.5E+04	63.4	0.000
	$Q_{downsum}$	8.0E+05	19	4.2E+04	158.0	0.000
	Q_{steady}	1.6E+03	19	8.5E+01	259.7	0.000
Normal Pressure	Q_{upsum}	1.4E+03	2	7.1E+02	3.0	0.053
	$Q_{downsum}$	4.5E+04	2	2.2E+04	83.8	0.000
	Q_{steady}	2.9E+02	2	1.5E+02	449.4	0.000
Fabric Code * Normal Pressure	Q_{upsum}	1.0E+04	38	2.7E+02	1.1	0.308
	$Q_{downsum}$	2.9E+04	38	7.6E+02	2.8	0.000
	Q_{steady}	2.4E+01	38	6.2E-01	1.9	0.002
Error	Q_{upsum}	7.4E+04	309	2.4E+02		
	$Q_{downsum}$	8.2E+04	309	2.7E+02		
	Q_{steady}	1.0E+02	309	3.3E-01		
Total	Q_{upsum}	8.4E+05	369			
	$Q_{downsum}$	2.3E+06	369			
	Q_{steady}	5.3E+04	369			
Corrected Total	Q_{upsum}	3.7E+05	368			
	$Q_{downsum}$	9.5E+05	368			
	Q_{steady}	2.0E+03	368			

Table 0-3 Multi-ANOVA Test Result of Neurophysiological Indexes C_{max}, C_{steady}, and C_{diff}

Source	Index	Type III Sum of Squares	df	Mean Square	F	Sig.
Corrected Model	C_{max}	19.0	59	0.32	47.6	0.000
	C_{steady}	9.1	59	0.15	82.5	0.000
	C_{diff}	4.1	59	0.07	18.8	0.000
Intercept	C_{max}	52.5	1	52.46	7728.6	0.000
	C_{steady}	17.0	1	17.02	9068.0	0.000
	C_{diff}	8.6	1	8.59	2320.2	0.000
Fabric Code	C_{max}	11.2	19	0.59	87.2	0.000
	C_{steady}	7.0	19	0.37	195.1	0.000
	C_{diff}	2.2	19	0.12	31.3	0.000
Normal Pressure	C_{max}	6.2	2	3.11	457.9	0.000
	C_{steady}	1.4	2	0.72	381.5	0.000
	C_{diff}	1.4	2	0.71	191.9	0.000
Fabric Code * Normal Pressure	C_{max}	1.5	38	0.04	5.9	0.000
	C_{steady}	0.7	38	0.02	10.1	0.000
	C_{diff}	0.5	38	0.01	3.4	0.000
Error	C_{max}	2.1	309	0.01		
	C_{steady}	0.6	309	0.00		
	C_{diff}	1.1	309	0.00		
Total	C_{max}	73.4	369			
	C_{steady}	26.7	369			
	C_{diff}	13.8	369			
Corrected Total	C_{max}	21.1	368			
	C_{steady}	9.7	368			
	C_{diff}	5.2	368			

Table 0-4 Multi-ANOVA Test Result of Neurophysiological Indexes $Q2_{upsum}$, $Q2_{downsum}$, and $Q2_{steady}$

Source	Index	Type III Sum of Squares	df	Mean Square	F	Sig.
Corrected Model	$Q2_{upsum}$	4.4	59	0.07	8.5	0.000
	$Q2_{downsum}$	528.4	59	8.96	9.9	0.000
	$Q2_{steady}$	0.0	59	0.00	4.9	0.000
Intercept	$Q2_{upsum}$	23.4	1	23.39	2667.5	0.000
	$Q2_{downsum}$	1499.5	1	1499.50	1659.0	0.000
	$Q2_{steady}$	80.4	1	80.38	6562591.4	0.000
Fabric Code	$Q2_{upsum}$	4.1	19	0.21	24.5	0.000
	$Q2_{downsum}$	507.6	19	26.72	29.6	0.000
	$Q2_{steady}$	0.0	19	0.00	8.6	0.000
Normal Pressure	$Q2_{upsum}$	0.1	2	0.05	5.8	0.003
	$Q2_{downsum}$	5.4	2	2.70	3.0	0.052
	$Q2_{steady}$	0.0	2	0.00	50.5	0.000
Fabric Code * Normal Pressure	$Q2_{upsum}$	0.2	38	0.01	0.6	0.974
	$Q2_{downsum}$	15.6	38	0.41	0.5	0.998
	$Q2_{steady}$	0.0	38	0.00	0.6	0.975
Error	$Q2_{upsum}$	2.7	309	0.01		
	$Q2_{downsum}$	279.3	309	0.90		
	$Q2_{steady}$	0.0	309	0.00		
Total	$Q2_{upsum}$	30.9	369			
	$Q2_{downsum}$	2307.8	369			
	$Q2_{steady}$	80.8	369			
Corrected Total	$Q2_{upsum}$	7.1	368			
	$Q2_{downsum}$	807.7	368			
	$Q2_{steady}$	0.0	368			

Table 0-5 Correlation of Thermal Neurophysiological Indexes with Normal Pressure of 42gf/cm^2

Index	Statistic	$Q2_{upsum}$	$Q2_{downsum}$	$Q2_{Steady}$	Q_{upsum}	$Q_{downsum}$	Q_{steady}	C_{max}	C_{steady}	C_{diff}
$Q2_{upsum}$	Coefficient	1								
	p Value									
$Q2_{downsum}$	Coefficient	--	1							
	p Value	--								
$Q2_{Steady}$	Coefficient	--	0.639	1						
	p Value	--	0.002							
Q_{upsum}	Coefficient	--	--	--	1					
	p Value	--	--	--						
$Q_{downsum}$	Coefficient	-0.519	--	--	--	1				
	p Value	0.019	--	--	--					
Q_{steady}	Coefficient	--	--	--	--	0.593	1			
	p Value	--	--	--	--	0.006				
C_{max}	Coefficient	--	--	--	--	0.423	0.769	1		
	p Value	--	--	--	--	0.063	0.000			
C_{steady}	Coefficient	--	--	--	--	0.728	0.906	0.854	1	
	p Value	--	--	--	--	0.000	0.000	0.000		
C_{diff}	Coefficient	--	--	--	--	--	--	0.612	--	1
	p Value	--	--	--	--	--	--	0.004	--	

Table 0-6 Correlation of Thermal Neurophysiological Indexes with Normal Pressure of 70gf/cm^2

Index	Statistic	$Q2_{upsum}$	$Q2_{downsum}$	$Q2_{Steady}$	Q_{upsum}	$Q_{downsum}$	Q_{steady}	C_{max}	C_{steady}	C_{diff}
$Q2_{upsum}$	Coefficient	1								
	p Value									
$Q2_{downsum}$	Coefficient	--	1							
	p Value	--								
$Q2_{Steady}$	Coefficient	--	0.697	1						
	p Value	--	0.001							
Q_{upsum}	Coefficient	--	--	--	1					
	p Value	--	--	--						
$Q_{downsum}$	Coefficient	-0.451	--	--	--	1				
	p Value	0.046	--	--	--					
Q_{steady}	Coefficient	--	--	--	--	0.630	1			
	p Value	--	--	--	--	0.003				
C_{max}	Coefficient	--	--	--	--	--	0.641	1		
	p Value	--	--	--	--	--	0.002			
C_{steady}	Coefficient	--	--	--	--	0.735	0.889	0.815	1	
	p Value	--	--	--	--	0.000	0.000	0.000		
C_{diff}	Coefficient	--	--	--	--	--	--	0.611	--	1
	p Value	--	--	--	--	--	--	0.004	--	

Table 0-7 Correlation Results between Neurophysiological Indexes and Corresponding Physical Indexes (Normal Pressure: 42gf/cm^2)

Index	Statistic	TCC	T	Qmax
$Q2_{upsum}$	Coefficient	--	--	--
	p Value	--	--	--
$Q2_{downsum}$	Coefficient	--	--	--
	p Value	--	--	--
$Q2_{steady}$	Coefficient	--	--	--
	p Value	--	--	--
Q_{upsum}	Coefficient	--	--	--
	p Value	--	--	--
$Q_{downsum}$	Coefficient	--	-0.580	0.702
	p Value	--	0.007	0.001
Q_{steady}	Coefficient	--	-0.517	0.876
	p Value	--	0.019	0.000
C_{max}	Coefficient	--	-0.786	0.908
	p Value	--	0.000	0.000
C_{steady}	Coefficient	--	-0.769	0.973
	p Value	--	0.000	0.000
C_{diff}	Coefficient	-0.565	-0.514	--
	p Value	0.009	0.021	--

Table 0-8 Correlation Results between Neurophysiological Indexes and Corresponding Physical Indexes (Normal Pressure: 70gf/cm^2)

Index	Statistic	TCC	T	Qmax
$Q2_{upsum}$	Coefficient	--	--	--
	p Value	--	--	--
$Q2_{downsum}$	Coefficient	--	--	--
	p Value	--	--	--
$Q2_{steady}$	Coefficient	--	--	--
	p Value	--	--	--
Q_{upsum}	Coefficient	--	--	--
	p Value	--	--	--
$Q_{downsum}$	Coefficient	--	-0.615	0.728
	p Value	--	0.004	0.000
Q_{steady}	Coefficient	--	-0.561	0.898
	p Value	--	0.010	0.000
C_{max}	Coefficient	--	-0.831	0.836
	p Value	--	0.000	0.000
C_{steady}	Coefficient	--	-0.795	0.976
	p Value	--	0.000	0.000
C_{diff}	Coefficient	-0.572	-0.457	--
	p Value	0.008	0.043	--

Table 0-9 Correlation Summary between Thermal Neurophysiological Indexes and Psychological Thermal Individual Descriptor Cool-Warm (Normal Pressure: 42gf/cm^2)

Index	Statistic	Passive	Active
$Q2_{upsum}$	Coefficient	--	--
	p Value	--	--
$Q2_{downsum}$	Coefficient	--	--
	p Value	--	--
$Q2_{steady}$	Coefficient	--	--
	p Value	--	--
Q_{upsum}	Coefficient	--	--
	p Value	--	--
$Q_{downsum}$	Coefficient	--	-0.450
	p Value	--	0.047
Q_{steady}	Coefficient	--	-0.811
	p Value	--	0.000
C_{max}	Coefficient	--	-0.765
	p Value	--	0.000
C_{steady}	Coefficient	--	-0.748
	p Value	--	0.000
C_{diff}	Coefficient	--	--
	p Value	--	--

Table 0-10 Correlation Summary between Thermal Neurophysiological Indexes and Psychological Thermal Individual Descriptor Cool-Warm (Normal Pressure: 70gf/cm^2)

Index	Statistic	Passive	Active
$Q2_{upsum}$	Coefficient	--	--
	p Value	--	--
$Q2_{downsum}$	Coefficient	--	--
	p Value	--	--
$Q2_{steady}$	Coefficient	--	--
	p Value	--	--
Q_{upsum}	Coefficient	--	--
	p Value	--	--
$Q_{downsum}$	Coefficient	--	-0.480
	p Value	--	0.032
Q_{steady}	Coefficient	--	-0.805
	p Value	--	0.000
C_{max}	Coefficient	--	-0.615
	p Value	--	0.004
C_{steady}	Coefficient	--	-0.734
	p Value	--	0.000
C_{diff}	Coefficient	--	--
	p Value	--	--

Reference

AATCC. (2000). Appearance of Fabrics after Repeated Home Laundering (Vol. AATCC 124-2001).

AATCC. (2011). Fabric Hand: Guidelines for the Subjective Evaluation of (Vol. AATCC EVALUATION PROCEDURE 5).

Abbott, G. M., & Grosberg, P. (1966). Measurement of fabric stiffness and hysteresis in bending. *Textile Research Journal, 36*(10), 928-930.

Ackerley, R., Hassan, E., Curran, A., Wessberg, J., Olausson, H., & McGlone, F. (2012). An fMRI study on cortical responses during active self-touch and passive touch from others. *Frontiers in Behavioral Neuroscience, 6*(51). doi: 10.3389/Fnbeh.2012.00051

Ajayi, J. O. (1992a). Effects of fabric structure on frictional-properties. *Textile Research Journal, 62*(2), 87-93. doi: 10.1177/004051759206200205

Ajayi, J. O. (1992b). Fabric smoothness, friction, and handle. *Textile Research Journal, 62*(1), 52-59. doi: 10.1177/004051759206200108

Ali, S. I., & Begum, S. (1994). Fabric softeners and softness perception. *Ergonomics, 37*(5), 801-806. doi: 10.1080/00140139408963689

Allen, T. T. (2010). Measure phase and statistical charting *Introduction to engineering statistics and lean sigma: Statistical quality control and design of experiments and systems* (pp. 77-113). London: Spinger.

Anttila, P. (1988). *The tactile evaluation of textiles on the basis of cognitive psychology, compared to physical analyses*. Paper presented at the Proceeding of the XVI World Congress, Minnerpolis, MN.

Arnold, H. L., Odom, R. B., & James, W. D. (1990). *Andrews' diseases of the skin: clinical dermatology* (8th ed.). Philadelphia, PA: W B Saunders Co.

Asaga, E., Takemura, K., Maeno, T., Ban, A., & Toriumi, M. (2013). Tactile evaluation based on human tactile perception mechanism. *Sensors and Actuators a-Physical, 203*, 69-75. doi: DOI 10.1016/j.sna.2013.08.013

ASTM. (1996). Standard test method for thickness of textile materials (Vol. D1777).

ASTM. (2008). Standard practice for conditioning and testing textiles (Vol. D1776).

ASTM. (2009). Standard test methods for mass per unit area (weight) of fabric (Vol. D3776).

ASTM. (2011). Standard test method for thermal resistance of batting systems using a hot plate (Vol. D1518).

Ballesteros, S., Reales, J. M., de Leon, L. P., & Garcia, B. (2005). The perception of ecological textures by touch: Does the perceptual space change under bimodal visual and haptic exploration? *World Haptics Conference: First Joint Eurohaptics Conference and Symposium on Haptic Interfaces for Virutual Environment and Teleoperator Systems, Proceedings*, 635-638.

Barlow, S. M. (1987). Mechanical frequency detection thresholds in the human-face. *Experimental Neurology, 96*(2), 253-261. doi: 10.1016/0014-4886(87)90044-6

Bautista, D. M., Siemens, J., Glazer, J. M., Tsuruda, P. R., Basbaum, A. I., Stucky, C. L., . . . Julius, D. (2007). The menthol receptor TRPM8 is the principal detector of environmental cold. *Nature, 448*(7150), 204-208. doi: 10.1038/Nature05910

Bear, M. F., Connors, B. W., & Paradiso, M. A. (2007). *Neuroscience: exploring the brain*. Philadelphia, PA: Lippincott Williams & Wilkins.

Behery, H. M. (1986). Comparison of Fabric Hand Assessment in the United-States and Japan. *Textile Research Journal, 56*(4), 227-240. doi: 10.1177/004051758605600402

Benali-Khoudja, M., Hafez, M., Alexandre, J. M., Benachour, J., & Kheddar, A. (2003). *Thermal feedback model for virtual reality*. Paper presented at the Proceedings of 2003 International Symposium on Micromechatronics and Human Science.

Bensmaia, S., & Hollins, M. (2005). Pacinian representations of fine surface texture. *Perception & Psychophysics, 67*(5), 842-854. doi: 10.3758/Bf03193537

Bensmaia, S. J., & Hollins, M. (2003). The vibrations of texture. *Somatosensory and Motor Research, 20*(1), 33-43. doi: Doi 10.1080/0899022031000083825

Binns, H. (1926). A comparison between the judgments of individuals skilled in the textile trade and the natural judgments of untrained adults and children. *Journal of the Textile Institute Transactions, 17*(12), T615-T641. doi: 10.1080/19447027.1926.10600023

Bishop, C. M. (1995). *Neural networks for pattern recognition*. Oxford: Oxford University Press.

Bishop, P. (2008). Testing for fabric comfort. In J. L. Hu (Ed.), *Fabric testing* (pp. 231-233). Boca Raton: CRC Press LLC.

Blake, D. T., Hsiao, S. S., & Johnson, K. O. (1997). Neural coding mechanisms in tactile pattern recognition: the relative contributions of slowly and rapidly adapting mechanoreceptors to perceived roughness. *Journal of Neuroscience, 17*(19), 7480-7489.

Blake, D. T., Johnson, K. O., & Hsiao, S. S. (1997). Monkey cutaneous SAI and RA responses to raised and depressed scanned patterns: effects of width, height, orientation, and a raised surround. *Journal of Neurophysiology, 78*(5), 2503-2517.

Bolanowski, S. J., Gescheider, G. A., Verrillo, R. T., & Checkosky, C. M. (1988). 4 channels mediate the mechanical aspects of touch. *Journal of the Acoustical Society of America, 84*(5), 1680-1694. doi: 10.1121/1.397184

Boos, A. G. D., & Tester, D. H. (1994). *SiroFAST, Fabric Assurance by Simple Testing: a system for fabric objective measurement and its application in fabric and garment manufacture*. Geelong, Australia: CSIRO Division of Wool Technology.

Brauchi, S., Orio, P., & Latorre, R. (2004). Clues to understanding cold sensation: Thermodynamics and electrophysiological analysis of the cold receptor TRPM8. *Proceedings of the National Academy of Sciences of the United States of America, 101*(43), 15494-15499. doi: 10.1073/pnas.0406773101

Braun, H. A., Bade, H., & Hensel, H. (1980). Static and dynamic discharge patterns of bursting cold fibers related to hypothetical receptor mechanisms. *Pflugers Archiv-European Journal of Physiology, 386*(1), 1-9. doi: 10.1007/Bf00584180

Brodmann, K., & Garey, L. (2010). *Brodmann's localisation in the cerebral cortex*. New York; London: Springer.
Brown, C., Filion, D. L., & Weiss, S. J. (2011). Measurement of tactile response and tactile perception. In M. J. Hertenstein & S. J. Weiss (Eds.), *The handbook of touch : neuroscience, behavioral, and health perspectives* (pp. 219-230). New York: Springer.
Brown, E. N., Kass, R. E., & Mitra, P. P. (2004). Multiple neural spike train data analysis: state-of-the-art and future challenges. *Nature Neuroscience, 7*(5), 456-461. doi: 10.1038/Nn1228
BSI. (1990). Method for determination of bending length and flexural rigidity of fabrics (Vol. BS 3356).
Burton, H. (2002). Cerebral cortical regions devoted to the somatosensory system: results from brain imaging studies in humans. In R. J. Nelson (Ed.), *The somatosensory system*. *Deciphering the brain's own body image* (pp. 28-72). Boca Raton, FL: CRC.
Byrne, J. H. (2010). Resting potentials and action potentials. In J. H. Byrne (Ed.), Neuroscience Online: An Electronic Textbook for the Neurosciences. Houston, TX: Department of Neurobiology and Anatomy, The University of Texas Medical School at Houston. Retrieved from http://nba.uth.tmc.edu/neuroscience/.
Byrne, M. S., Gardner, A. P. W., & Fritz, A. M. (1993). Fibre types and end-uses: a perceptual study. *Journal of the Textile Institute, 84*, 275-288. doi: 10.1080/00405009308631269
Cahusac, P. M. B., & Noyce, R. (2007). A pharmacological study of slowly adapting mechanoreceptors responsive to cold thermal stimulation. *Neuroscience, 148*(2), 489-500. doi: 10.1016/j.neuroselence.2007.06.018
Campero, M., & Bostock, H. (2010). Unmyelinated afferents in human skin and their responsiveness to low temperature. *Neuroscience Letters, 470*(3), 188-192. doi: 10.1016/j.neulet.2009.06.089
Campero, M., Serra, J., Bostock, H., & Ochoa, J. L. (2001). Slowly conducting afferents activated by innocuous low temperature in human skin. *Journal of Physiology-London, 535*(3), 855-865. doi: 10.1111/j.1469-7793.2001.t01-1-00855.x
Cardello, A. V., Winterhalter, C., & Schutz, H. G. (2003). Predicting the handle and comfort of military clothing fabrics from sensory and instrumental data: Development and application of new psychophysical methods. *Textile Research Journal, 73*(3), 221-237. doi: 10.1177/004051750307300306
Carr, R. W., Pianova, S., Fernandez, J., Fallon, J. B., Belmonte, C., & Brock, J. A. (2003). Effects of heating and cooling on nerve terminal impulses recorded from cold-sensitive receptors in the guinea-pig cornea. *Journal of General Physiology, 121*(5), 427-439. doi: 10.1085/jgp.200308814
Cascio, C. J., & Sathian, K. (2001). Temporal cues contribute to tactile perception of roughness. *Journal of Neuroscience, 21*(14), 5289-5296.
Chaudhuri, A. (2011). *Fundamentals of sensory perception*. Don Mills, Ont.: Oxford University Press.

Chaudhuri, A. (2011). The Somatosensory System: Touch, Feeling, and Pain *Fundamentals of sensory perception* (pp. 83-85). Ontario, Canada: Oxford University Press.

Chen, P. L., Barker, R. L., Smith, G. W., & Scruggs, B. (1992). Handle of weft knit fabrics. *Textile Research Journal, 62*(4), 200-211. doi: 10.1177/004051759206200404

Chen, X. J., Shao, F., Barnes, C., Childs, T., & Henson, B. (2009). Exploring relationships between touch perception and surface physical properties. *International Journal of Design, 3*(2), 67-76.

Chen, Y., Collier, B., Hu, P., & Quebedeaux, D. (2000). Objective evaluation of fabric softness. *Textile Research Journal, 70*(5), 443-448. doi: 10.1177/004051750007000510

Ciesielska-Wrobel, I. L., & Van Langenhove, L. (2012). The hand of textiles - definitions, achievements, perspectives - a review. *Textile Research Journal, 82*(14), 1457-1468. doi: 10.1177/0040517512438126

Clapham, D. E. (2003). TRP channels as cellular sensors. *Nature, 426*(6966), 517-524. doi: 10.1038/Nature02196

Colburn, R. W., Lubin, M. L., Stone, D. J., Wang, Y., Lawrence, D., D'Andrea, M. R., . . . Qin, N. (2007). Attenuated cold sensitivity in TRPM8 null mice. *Neuron, 54*(3), 379-386. doi: 10.1016/j.neuron.2007.04.017

Condon, M., Birznieks, I., Hudson, K., Chelvanayagam, D. K., Mahns, D., Olausson, H., & Macefield, V. G. (2014). Differential sensitivity to surface compliance by tactile afferents in the human finger pad. *Journal of Neurophysiology, 111*(6), 1308-1317. doi: 10.1152/jn.00589.2013

Connor, C. E., Hsiao, S. S., Phillips, J. R., & Johnson, K. O. (1990). Tactile roughness: neural codes that account for psychophysical magnitude estimates. *Journal of Neuroscience, 10*(12), 3823-3836.

Connor, C. E., & Johnson, K. O. (1992). Neural coding of tactile texture: comparisons of spatial and temporal mechanisms for roughness perception. *Journal of Neuroscience, 12*(9), 3414-3426.

Coren, S., & Ward, L. M. (1989). *Sensation and Perception* (3rd ed.). New York: Harcourt Brace Jovanovich Publishers.

Daanen, H. (2003). Finger cold-induced vasodilation: a review. *European journal of applied physiology, 89*(5), 411-426. doi: 10.1007/s00421-003-0818-2

Darian-Smith, I., Sugitani, M., Heywood, J., Karita, K., & Goodwin, A. (1982). Touching textured surfaces: cells in somatosensory cortex respond both to finger movement and to surface features. *Science, 218*(4575), 906-909.

Dejong, S., Snaith, J. W., & Michie, N. A. (1986). A mechanical model for the lateral compression of woven fabrics. *Textile Research Journal, 56*(12), 759-767. doi: 10.1177/004051758605601208

Dhaka, A., Earley, T. J., Watson, J., & Patapoutian, A. (2008). Visualizing cold spots: TRPM8-expressing sensory neurons and their projections. *Journal of Neuroscience, 28*(3), 566-575. doi: 10.1523/Jneurosci.3976-07.2008

Dhaka, A., Murray, A. N., Mathur, J., Earley, T. J., Petrus, M. J., & Patapoutian, A. (2007). TRPM8 is required for cold sensation in mice. *Neuron, 54*(3), 371-378. doi: 10.1016/j.neuron.2007.02.024

DiCarlo, J. J., & Johnson, K. O. (1999). Velocity invariance of receptive field structure in somatosensory cortical area 3b of the alert monkey. *Journal of Neuroscience, 19*(1), 401-419.

DiCarlo, J. J., & Johnson, K. O. (2000). Spatial and temporal structure of receptive fields in primate somatosensory area 3b: effects of stimulus scanning direction and orientation. *Journal of Neuroscience, 20*(1), 495-510.

DiCarlo, J. J., Johnson, K. O., & Hsiao, S. S. (1998). Structure of receptive fields in area 3b of primary somatosensory cortex in the alert monkey. *Journal of Neuroscience, 18*(7), 2626-2645.

Duclaux, R., & Kenshalo, D. R. (1972). Temperature Sensitivity of Type-I Slowly Adapting Mechanoreceptors in Cats and Monkeys. *Journal of Physiology-London, 224*(3), 647-&.

Ekman, G., Hostman, J., & Lindstrom, B. (1965). Roughness, smoothness and preference: a study of quantitative relations in individual subject. *Journal of Experimental Psychology, 70*(1), 18-26. doi: 10.1037/h0021985

El Mogahzy, Y. E., Kilinc, F. S., & Hassan, M. (2005). Developments in measurement and evaluation of fabric hand. In H. M. Beherv (Ed.), *Effect of mechanical and physical properties on fabric hand* (pp. 45-65). Abington Cambridge, England: Woodhead.

Elder, H. M., Fisher, S., Armstrong, K., & Hutchison, G. (1984). Fabric softness, handle, and compression. *Journal of the Textile Institute, 75*(1), 37-46. doi: 10.1080/00405008408658459

Fan, J. T., & Chen, Y. S. (2002). Measurement of clothing thermal insulation and moisture vapour resistance using a novel perspiring fabric thermal manikin. *Measurement Science & Technology, 13*(7), 1115-1123. doi: 10.1088/0957-0233/13/7/320

Fechner, G. T., Boring, E. G., & Howes, D. H. (1966). *Elements of psychophysics* (H. E. Alder, Trans. D. H. Howes & E. G. Boring Eds.). New York: Holt, Rinehart and Winston.

Fernandes, A. M., & Albuquerque, P. B. (2012). Tactual perception: a review of experimental variables and procedures. *Cognitive Processing, 13*(4), 285-301. doi: 10.1007/s10339-012-0443-2

Freitas, R. A. (1999). Navigation *Nanomedicine, volume I: basic capabilities*. Georgetown, TX: CRC.

Friedman, R. M., Hester, K. D., Green, B. G., & LaMotte, R. H. (2008). Magnitude estimation of softness. *Experimental Brain Research, 191*(2), 133-142. doi: 10.1007/s00221-008-1507-5

Fritz, A. M. (1992). A new way to measure fabric handle. *Textile Asia, 23*(7).

Fruhstorfer, H. (1984). Thermal sensibility changes during ischemic nerve block. *Pain, 20*(4), 355-361. doi: 10.1016/0304-3959(84)90112-X

Gao, J. (2003). *The principle of the artifical neural network and simulation*. Beijing: Mechanical Engineering Press.

Ghosh, T. K., & Zhou, N. Y. (2003). Characterization of fabric bending behavior: A review of measurement principles. *Indian Journal of Fibre & Textile Research, 28*(4), 471-476.

Goodwin, A. W., & Wheat, H. E. (2004). Sensory signals in neural populations underlying tactile perception and manipulation. *Annual Review of Neuroscience, 27*, 53-77. doi: 10.1146/annurev.neuro.26.041002.131032

Guest, S., Mehrabyan, A., Essick, G., Phillips, N., Hopkinson, A., & Mcglone, F. (2012). Physics and Tactile Perception of Fluid-Covered Surfaces. *Journal of Texture Studies, 43*(1), 77-93. doi: DOI 10.1111/j.1745-4603.2011.00318.x

Hallos, R. S., Burnip, M. S., & Weir, A. (1990). The handle of double-jersey knitted fabrics: 1. Polar profiles. *Journal of the Textile Institute, 81*(1), 15-35. doi: 10.1080/00405009008658323

Harrell, F. E. (2001). Multivariable modeling strategies *Regression modeling strategies: With applications to linear models, logistic regression, and survival analysis* (pp. 53-85). New York, NY: Springer.

Hatem, S., Attal, N., Willer, J. C., & Bouhassira, D. (2006). Psychophysical study of the effects of topical application of menthol in healthy volunteers. *Pain, 122*(1-2), 190-196. doi: 10.1016/j.pain.2006.01.026

Havenith, G., Vandelinde, E. J. G., & Heus, R. (1992). Pain, thermal sensation and cooling rates of hands while touching cold materials. *European Journal of Applied Physiology and Occupational Physiology, 65*(1), 43-51. doi: 10.1007/Bf01466273

Heidelberger, M. (2004). *Nature from within: Gustav Theodor Fechner and his psychophysical worldview*. Pittsburgh, PA: University of Pittsburgh Pre.

Heinz, M., Schafer, K., & Braun, H. A. (1990). Analysis of facial cold receptor activity in the rat. *Brain Research, 521*(1-2), 289-295. doi: 10.1016/0006-8993(90)91554-T

Hensel, H. (1981). *Thermoreception and temperature regulation*. London: Academic Press.

Hes, L., & Dolezal, I. (1989). New method and equipment for measuring thermal properties of textiles. *Journal of Textile Machinery Society of Japan, 42*(8), 124-128.

Hille, B. (2001). *Ion channels of excitable membranes* (3rd ed.). Sunderland, MA: Sinauer Associates.

Ho, H. N., & Jones, L. A. (2006). *Thermal model for hand-object interactions*. Paper presented at the IEEE Proceedings of the 14th Symposium on Haptic Interfaces for Virtual Environment and Teleoperator Systems, Alexandria, Virginia.

Ho, H. N., Watanabe, J., Ando, H., & Kashino, M. (2011). Mechanisms underlying referral of thermal sensations to sites of tactile stimulation. *Journal of Neuroscience, 31*(1), 208-213. doi: 10.1523/Jneurosci.2640-10.2011

Hollies, N. R. S. (1965). *Investigation of the factors influencing comfort in cotton apparel fabrics*. Paper presented at the US department of agriculture, New Orleans, USA.

Hollies, N. R. S. (1975). *Cotton clothing attributes in subjective comfort*. Paper presented at the 15th Textile chemistry and processing conference, New Orleans, USA.

Hollies, N. R. S., Custer, A. G., Morin, C. J., & Howard, M. E. (1979). A human perception analysis approach to clothing comfort. *Textile Research Journal, 49*(10), 557-564. doi: 10.1177/004051757904901001

Hollies, N. R. S., & Goldman, R. F. (1977). *Clothing comfort: Interaction of thermal, ventilation, construction and assessment factors*. Ann Arbor, MI: Ann arbor science.

Hollins, M., Bensmaia, S., Karlof, K., & Young, F. (2000). Individual differences in perceptual space for tactile textures: Evidence from multidimensional scaling. *Perception & Psychophysics, 62*(8), 1534-1544. doi: 10.3758/Bf03212154

Hollins, M., & Bensmaia, S. J. (2007). The coding of roughness. *Canadian Journal of Experimental Psychology, 61*(3), 184-195.

Hollins, M., Bensmaia, S. J., & Roy, E. A. (2002). Vibrotaction and texture perception. *Behavioural Brain Research, 135*(1-2), 51-56. doi: 10.1016/S0166-4328(02)00154-7

Hollins, M., Bensmaia, S. J., & Washburn, S. (2001). Vibrotactile adaptation impairs discrimination of fine, but not coarse, textures. *Somatosensory and Motor Research, 18*(4), 253-262.

Hollins, M., Delemos, K. A., & Goble, A. K. (1991). Vibrotactile adaptation on the face. *Perception & Psychophysics, 49*(1), 21-30. doi: 10.3758/Bf03211612

Hollins, M., Faldowski, R., Rao, S., & Young, F. (1993). Perceptual dimensions of tactile surface texture: A multidimensional-scaling analysis. *Perception & Psychophysics, 54*(6), 697-705. doi: 10.3758/Bf03211795

Hollins, M., Fox, A., & Bishop, C. (2000). Imposed vibration influences perceived tactile smoothness. *Perception, 29*(12), 1455-1465. doi: 10.1068/P3044

Hollins, M., & Risner, S. R. (2000). Evidence for the duplex theory of tactile texture perception. *Perception & Psychophysics, 62*(4), 695-705. doi: 10.3758/Bf03206916

Hollins, M., & Sigurdsson, A. (1998). Vibrotactile amplitude and frequency discrimination in temporomandibular disorders. *Pain, 75*(1), 59-67. doi: 10.1016/S0304-3959(97)00205-4

Howorth, W. S. (1964). The handle of suiting, lingere and dress fabric. *Journal of the Textile Institute, 55*, 251-260.

Howorth, W. S., & Oliver, P. H. (1958). The application of multiple factors analysis to the assessment of fabric handle. *Journal of the Textile Institute, 49*, 540.

Hu, J., Ding, X., Wang, R., & Cai, C. (2009). Intrinsic differences of sensory analysis from instrumental evaluation on fabric softness by lateral compression. *Fibers and Polymers, 10*(3), 371-378. doi: 10.1007/s12221-009-0371-7

Hu, J. L. (2004a). The Bending Properties of Woven Fabrics *Strucure and Mechanics of Woven Fabrics* (pp. 123-148). Boca Raton, FL: CRC.

Hu, J. L. (2004b). Strucutral properties of fabric *Structure and mechanics of woven fabrics* (pp. 61-89). Boca Raton, FL: CRC.

Hu, J. L., Chen, W. X., & Newton, A. (1993). A psychophysical model for objective hand evaluation: an application of Steven's law. *Journal of the Textile Institute, 84*, 354-363.
Hu, J. L., Xin, B. J., & Yan, H. J. (2002). Classifying fleece fabric appearance by extended morphological fractal analysis. *Textile Research Journal, 72*(10), 879-884. doi: 10.1177/004051750207201005
Hu, J. Y. (2006). *Characterization of sensory comfort of apparel products*. (PhD Unpublished PhD Thesis), The Hong Kong Polytechnic University, Hong Kong.
Hu, J. Y., Ding, X., & Wang, R. B. (2006). A review on the cognitive study of fabric hand. *33*(5).
Hu, J. Y., Hes, L., Li, Y., Yeung, K. W., & Yao, B. G. (2006). Fabric touch tester: Integrated evaluation of thermal-mechanical sensory properties of polymeric materials. *Polymer Testing, 25*(8), 1081-1090. doi: 10.1016/j.polymertesting.2006.07.008
Hyvarinen, J., & Poranen, A. (1978). Receptive field integration and submodality convergence in the hand area of the post-central gyrus of the alert monkey. *The Journal of physiology, 283*(1), 539-556.
Iggo, A. (1988). Sensory receptor, cutaneous. In J. M. Wolfe (Ed.), *Sensory systems II: Senese other than vision* (pp. 109-110). Ann Arbor, MI: Birkhäuser Boston.
ISO. (1993). Measurement of thermal and water-vapour resistance under steady-state conditions (Vol. ISO 11092).
ISO. (1998). Ergonomics of the thermal environment: Instruments for measuring physical quantities (Vol. ISO 7726).
ISO. (2005). Ergonomics of the thermal environment -- Analytical determination and interpreatation of thermal comfort using calculation of the PMV and PPD indices and local thermal comfort criteria (Vol. ISO 7730).
ISO. (2007). Ergonomics of the thermal environment: Estimation of the thermal insulation and evaporative resistance of a clothing ensemble (Vol. ISO 9920).
Iwamura, Y. (1998). Hierarchical somatosensory processing. *Current opinion in neurobiology, 8*(4), 522-528.
Iwamura, Y. (2003). *Somatosensory association cortices*. Paper presented at the International Congress Series.
Iwamura, Y., & Tanaka, M. (1978). Postcentral neurons in hand region of area 2: their possible role in the form discrimination of tactile objects. *Brain research*.
Johansson, R. S., & Vallbo, Å. B. (1983). Tactile sensory coding in the glabrous skin of the human hand. *Trends in Neurosciences, 6*, 27-32. doi: 10.1016/0166-2236(83)90011-5
Johnson, J. H., Turner, C. W., Zwislocki, J. J., & Margolis, R. H. (1993). Just noticeable differences for intensity and their relation to loudness. *The Journal of the Acoustical Society of America, 93*(2), 983-991. doi: 10.1121/1.405404
Johnson, K. O., Hsiao, S. S., & Yoshioka, T. (2002). Neural coding and the basic law of psychophysics. *Neuroscientist, 8*(2), 111-121. doi: 10.1177/107385840200800207

Johnson, K. O., & Yoshioka, T. (2002). Neural mechanisms of tactile form and texture Perception. In R. J. Nelson (Ed.), *The somatosensory system : deciphering the brain's own body image* (pp. 73-101). Boca Raton, Fl.: CRC Press.

Ju, J., & Ryu, H. (2006). A study on subjective assessment of knit fabric by ANFIS. *Fibers and Polymers, 7*(2), 203-212.

Kamalha, E., Zeng, Y. C., Mwasiagi, J. I., & Kyatuheire, S. (2013). The comfort dimension; a review of perception in clothing. *Journal of Sensory Studies, 28*(6), 423-444. doi: 10.1111/Joss.12070

Kang, T. J., Cho, D. H., & Kim, S. M. (2001). New objective evaluation of fabric smoothness appearance. *Textile Research Journal, 71*(5), 446-453. doi: 10.1177/004051750107100513

Kang, T. J., Kim, S. C., Sul, I. H., Youn, J. R., & Chung, K. (2005). Fabric surface roughness evaluation using wavelet-fractal method Part I: Wrinkle, smoothness and seam pucker. *Textile Research Journal, 75*(11), 751-760. doi: 10.1177/0040517505058855

Kang, T. J., & Lee, J. Y. (2000). Objective evaluation of fabric wrinkles and seam puckers using fractal geometry. *Textile Research Journal, 70*(6), 469-475. doi: 10.1177/004051750007000601

Karashima, Y., Talavera, K., Everaerts, W., Janssens, A., Kwan, K. Y., Vennekens, R., . . . Voets, T. (2009). TRPA1 acts as a cold sensor in vitro and in vivo. *Proceedings of the National Academy of Sciences of the United States of America, 106*(4), 1273-1278. doi: 10.1073/pnas.0808487106

Karunamoorthy, S., & Das, A. (2014). Study on thermal resistance of multilayered fabrics under different compressional loads. *Journal of the Textile Institute, 105*(5), 538-546. doi: 10.1080/00405000.2013.827388

Katagiri, C., Sato, J., Nomura, J., & Denda, M. (2003). Changes in environmental humidity affect the water-holding property of the stratum corneum and its free amino acid content, and the expression of filaggrin in the epidermis of hairless mice. *Journal of Dermatological Science, 31*(1), 29-35. doi: 10.1016/S0923-1811(02)00137-8

Kawabata, S. (1980). *The standardization and analysis of hand evaluation*. Paper presented at the The Textile Machinery Society of Japan, Osaka, Japan.

Kawabata, S. (1982). *The development of the objective measurement of fabric handle*. Paper presented at the First Japan-Australia Symposium on Objective Specification of Fabric Quality, Mechanical Properties and Performance, Osaka, Japan.

Kawabata, S. (1984). Development of a device for measuring heat moisture transfer properties of apparel fabrics. *Journal of Textile Machinery Society of Japan, 37*(8), 130-141.

Kawabata, S., & Niwa, M. (1989). Fabric performance in clothing and clothing manufacture. *Journal of the Textile Institute, 80*(19).

Kawabata, S., & Yoneda, M. (1981). *Analysis of transient heat conditions and prediction of warm-cool feeling of fabrics*. Paper presented at the The 2nd Japan Symposuim on Thermophysical Properties, Sapporo, Japan.

Kilinc, F. S. (2004). *A study of the nature of fabric comfort: design-oriented fabric comfort model*. (PhD), Auburn Univeristy, Auburn. (3124275)

Kim, H., & G., W. (1996). Fabric hand as perceived by U.S. and Korean males and females. *Clothing and Textiles Research Journal, 14*(2), 133-144. doi: 10.1177/0887302X9601400204

Kim, J. O., & Slater, B. L. (1996). Objective assessment of fabric handle in fabric treated with flame retardants. *Journal of Testing and Evaluation, 24*(4), 223-228. doi: 10.1520/JTE11444J

Kim, J. O., & Slater, B. L. (1999). Objective evaluation of fabric hand. Part I: Relationships of fabric hand by the extaction method and related physical and surface properties. *Textile Research Journal, 69*(1), 59-67. doi: 10.1177/004051759906900110

Klatzky, R., & Lederman, S. (2003). Touch. In A. F. Healy & R. W. Proctor (Eds.), *Experimental Psychology* (2 ed., Vol. 4, pp. 152-177). New York, NY: Wiley.

Kolb, B., & Whishaw, I. Q. (2003). *Fundamentals of human neuropsychology* (5th ed.). New York, NY: Worth Publishers.

Kornhuber, H. H., & Albe-Fessard, D. G. (1975). *The Somatosensory system*, Stuttgart; Acton, Mass.

Lai, S. S., Shyr, T. W., & Lin, J. Y. (2002). Comparison between KES-FB and FAST in discrimination of fabric characteristics. *Journal of Textile Engineering, 48*(2), 43-49. doi: 10.4188/jte.48.43

LaMotte, R. H. (1977). Psychophysical and neurophysiological studies of tactile sensibility. In N. R. S. Hollies & R. F. Goldman (Eds.), *Clothing comfort: Interaction of thermal, ventilation, construction and assessment factors* (pp. 83-105). Ann Arbor, MI: Ann Arbor Science.

LaMotte, R. H. (2000). Softness discrimination with a tool. *Journal of Neurophysiology, 83*(4), 1777-1786.

Latorre, R., Brauchi, S., Madrid, R., & Orio, P. (2011). A Cool channel in cold transduction. *Physiology, 26*(4), 273-285. doi: 10.1152/physiol.00004.2011

Lederman, S. J. (1974). Tactile roughness of grooved surfaces: the touching process and effects of macro and micro structure. *Perception & Psychophysics, 16*(2), 385-395.

Lederman, S. J., & Klatzky, R. L. (2004). Haptic identification of common objects: Effects of constraining the manual exploration process. *Perception & Psychophysics, 66*(4), 618-628. doi: 10.3758/Bf03194906

Lederman, S. J., & Taylor, M. M. (1972). Fingertip force, surface geometry, and the perception of roughness by active touch. *Perception & Psychophysics, 12*(5), 401-408.

Levitan, I. B., & Kaczmarek, L. K. (2002). *The neuron: Cell and molecular biology* (3rd ed.). Oxford: Oxford University Press.

Li, Y. (1988). *Objective assessment of comfort of knitted sportswear in relation to psychosphysiological sensory studies*. UK: The University of Leeds.

Li, Y. (1998a). Clothing comfort and its application. *Textile Asia, 29*(7), 29-35.

Li, Y. (1998b). Sensory comfort: consumer responses in three countries. *Journal of China Textile University*.

Li, Y. (1998c). *Wool sensory properties and product development*. Paper presented at the The 2nd China International Wool Conference, Xi'an, China.
Li, Y. (2005). Perceptions of temperature, moisture and comfort in clothing during environmental transients. *Ergonomics, 48*(3), 234-248. doi: 10.1080/00140130420003277l5
Li, Y., Hu, J. Y., Liao, X., Li, Q. H., & Wu, X. X. (2012a). China Patent No.: C. P. Office.
Li, Y., Hu, J. Y., Liao, X., Li, Q. H., & Wu, X. X. (2012b). China Patent No.: C. P. Office.
Li, Y., Hu, J. Y., Liao, X., Li, Q. H., & Wu, X. X. (2012c). China Patent No.: C. P. Office.
Li, Y., & Wong, A. S. W. (2006). *Clothing biosensory engineering*. Cambridge: Woodhead Publishing.
Liao, X., Hu, J. Y., Li, Y., Wu, X. X., & Li, Q. H. (2012). *A Comparison Study of Measuring Fabric Smoothness Using KES-FB and PhabrOmeter*. Paper presented at the Textile Bioengineering and Informatics Symposium, Ueda, Japan.
Livesey, R. G., & Owen, J. D. (1964). 47—CLOTH STIFFNESS AND HYSTERESIS IN BENDING. *Journal of the Textile Institute Transactions, 55*(10), T516-T530.
MacKay, D. M. (1963). Psychophysics of perceived intensity: A theoretical basis for Fechner's and Stevens' laws. *Science Science, 139*(3560), 1213-1216. doi: 10.1126/science.139.3560.1213-a
Mackenzie, R. A., Burke, D., Skuse, N. F., & Lethlean, A. K. (1975). Fiber function and perception during cutaneous nerve block. *Journal of Neurology Neurosurgery and Psychiatry, 38*(9), 865-873. doi: 10.1136/jnnp.38.9.865
Mackevicius, E. L., Best, M. D., Saal, H. P., & Bensmaia, S. J. (2012). Millisecond precision spike timing shapes tactile perception. *Journal of Neuroscience, 32*(44), 15309-15317. doi: 10.1523/Jneurosci.2161-12.2012
Mahar, T. J., Dhingra, R., & Postle, R. (1982). Comparison of fabric handle assessment in Japan, Australia, New Zealand and India. In S. Kawabata, R. Postle, & M. Niwa (Eds.), *Objective specification of fabric quality, mechanical properties and performance*. Kyoto: Textile Machinery Society of Japan.
Mahar, T. J., & Postle, R. (1989). Measuring and interpreting low-stress fabric mechanical and surface properties. Part IV: Subjective evluation of fabric handle. *Textile Research Journal, 59*(12), 721-733. doi: 10.1177/004051758905901203
Mahar, T. J., Wheelwright, P., Dhingra, R. C., & Postle, R. (1990). Measuring and interpreting fabric low stress mechanical and surface-properties: Part V Fabric handle attributes and quality descriptors. *Textile Research Journal, 60*(1), 7-17. doi: 10.1177/004051759006000102
Mahieu, F., Janssens, A., Gees, M., Talavera, K., Nilius, B., & Voets, T. (2010). Modulation of the cold-activated cation channel TRPM8 by surface charge screening. *Journal of Physiology-London, 588*(2), 315-324. doi: 10.1113/jphysiol.2009.183582
Mäkinen, T. M., Pääkkönen, T., Palinkas, L. A., Rintamäki, H., Leppäluoto, J., & Hassi, J. (2004). Seasonal changes in thermal responses of urban residents to cold

exposure. *Comparative Biochemistry and Physiology Part A: Molecular & Integrative Physiology, 139*(2), 229-238. doi: 10.1016/j.cbpb.2004.09.006
Makous, J. C., Friedman, R. M., & Vierck, C. J. (1995). A critical band filter in touch. *Journal of Neuroscience, 15*(4), 2808-2818.
Marks, J. G., Miller, J. J., & Lookingbill, D. P. (2006). *Lookingbill and Marks' principles of dermatology* (4th ed.). Philadelphia, PA: Saunders Elsevier.
Masin, S. C., Zudini, V., & Antonelli, M. (2009). Early alternative derivations of fechner's law. *Journal of the History of the Behavioral Sciences, 45*(1), 56--65. doi: 10.1002/jhbs.20349
Mathew, L., Purkayastha, S. S., Jayashankar, A., & Nayar, H. S. (1981). Physiological characteristics of cold acclimatization in man. *International journal of biometeorology, 25*(3), 191-198.
Matsuo, T. (1972). Study on (fabric) hand. *Journal of the Textile Machinery Society of Japan, 25*(11), 742-749.
Matta, J. A., & Ahern, G. P. (2007). Voltage is a partial activator of rat thermosensitive TRP channels. *Journal of Physiology-London, 585*(2), 469-482. doi: 10.1113/jphysiol.2007.144287
Mazzuchetti, G., Demichelis, R., Songia, M. B., & Rombaldoni, F. (2008). Objective measurement of tactile sensitivity related to a feeling of softness and warmth. *Fibres and Textiles in Eastern Europe, 16*(4), 67-71.
McKemy, D. D., Neuhausser, W. M., & Julius, D. (2002). Identification of a cold receptor reveals a general role for TRP channels in thermosensation. *Nature, 416*(6876), 52-58. doi: 10.1038/Nature719
Meng, X. L. (2010). *The objective evaluation model on wearing touch and pressure sensation based on GRNN*. Paper presented at the Information and Computing (ICIC), Third International Conference, Wuxi, China.
Molfe, J. M., Kluender, K. R., Levi, D. M., Bartoshuk, L. M., Herz, R. S., Klatzky, R. L., . . . Merfeld, D. M. (2009). Touch *Sensation & Perception* (2nd ed., pp. 301-303). Sunderland, MA: Sinauer Associates.
Morino, H., Matsudaira, M., & Furutani, M. (2005). Predicting mechanical properties and hand values from the parameters of weave structures. *Textile Research Journal, 75*(3), 252-257. doi: 10.1177/004051750507500311
Morley, J. W. (1998). *Neural aspects in tactile sensation*. New York, NY: Elsevier.
Morley, J. W., Goodwin, A. W., & Dariansmith, I. (1983). Tactile discrimination of gratings. *Experimental Brain Research, 49*(2), 291-299.
Mountcastle, V. B. (1998). *Perceptual neuroscience: The cerebral cortex*. Cambridge, Mass.: Harvard University Press.
Muniak, M. A., Ray, S., Hsiao, S. S., Dammann, J. F., & Bensmaia, S. J. (2007). The neural coding of stimulus intensity: Linking the population response of mechanoreceptive Afferents with psychophysical Behavior. *Journal of Neuroscience, 27*(43), 11687-11699. doi: 10.1523/Jneurosci.1486-07.2007
Namer, B., Seifert, F., Handwerker, H. O., & Maihofner, C. (2005). TRPAI and TRPM8 activation in humans: effects of cinnamaldehyde and menthol. *Neuroreport, 16*(9), 955-959. doi: 10.1097/00001756-200506210-00015

Nilius, B., & Voets, T. (2007). Neurophysiology - Channelling cold reception. *Nature, 448*(7150), 147-148. doi: 10.1038/448147a

Nuffel, D., Vepa, K. S., Baere, I., Degrieck, J., Rouck, J., & Paepegem, W. (2013). Study on the Parameters Influencing the Accuracy and Reproducibility of Dynamic Pressure Measurements at the Surface of a Rigid Body During Water Impact. *Experimental Mechanics, 53*(2), 131-144. doi: 10.1007/s11340-012-9619-z

Okamoto, S., Nagano, H., & Yamada, Y. (2013). Psychophysical Dimensions of Tactile Perception of Textures. *Ieee Transactions on Haptics, 6*(1), 81-93. doi: Doi 10.1109/Toh.2012.32

Osgood, C. E., Suci, G. J., & Tannenbaum, P. H. (1957). Urbana, USA: University of Illinoise.

Owen, J. D. (1966). An automatic cloth-bending-hysteresis tester and some of its applications.

Owen, J. D. (1971). Hand and drape of fabrics. *Shirley Link, 4*(18).

Pac, M. J., Bueno, M.-A., Renner, M., & El Kasmi, S. (2001). Warm-cool feeling relative to tribological properties of fabrics. *Textile Research Journal, 71*(9), 806-812. doi: 10.1177/004051750107100910

Pan, N. (2007). Quantification and evaluation of human tactile sense towards fabrics. *International Journal of Design & Nature and Ecodynamics, 1*(1), 48-60.

Pan, N., Yen, K. C., Zhao, S. J., & Yang, S. R. (1988). A new approach to the objective evaluation of fabric handle from mechanical properties. Part II: Objective measure for total hanlde. *Textile Research Journal, 58*(9). doi: 10.1177/004051758805800907

Pan, N., Zeronian, S. H., & Ryu, H. S. (1993). An Alternative Approach to the Objective Measurement of Fabrics. *Textile Research Journal, 63*(1), 33-43. doi: 10.1177/004051759306300104

Pare, M., Carnahan, H., & Smith, A. M. (2002). Magnitude estimation of tangential force applied to the fingerpad. *Experimental Brain Research, 142*(3), 342-348. doi: 10.1007/s00221-001-0939-y

Park, S.-W., Hwang, Y.-G., Kang, B.-C., & Yeo, S.-W. (2000). Applying fuzzy logic and neural networks to total hand evaluation of knitted fabrics. *Textile Research Journal, 70*(8), 675-681.

Park, S. W., Hwang, Y. G., Kang, B. C., & Yeo, S. W. (2000). Applying fuzzy logic and neural networks to total hand evaluation of knitted fabrics. *Textile Research Journal, 70*(8), 675-681. doi: 10.1177/004051750007000804

Patapoutian, A., Peier, A. M., Story, G. M., & Viswanath, V. (2003). Thermotrp channels and beyond: Mechanisms of temperature sensation. *Nature Reviews Neuroscience, 4*(7), 529-539. doi: 10.1038/Nrn1141

Patterson, A. N. (1947). Causes of changes of "handle" of woolen fabrics. *Rayon Textile Monthly, 28*.

Peier, A. M., Moqrich, A., Hergarden, A. C., Reeve, A. J., Andersson, D. A., Story, G. M., . . . Patapoutian, A. (2002). A TRP channel that senses cold stimuli and menthol. *Cell, 108*(5), 705-715. doi: 10.1016/S0092-8674(02)00652-9

Peine, W. J., & Howe, R. D. (1998). *Do humans sense finger deformation or distributed pressure to detect lumps in soft tissue?* Paper presented at the ASME dynamic systems and control division, Anaheim, USA.

Peirce, F. T. (1930). The "handle" of cloth as a measurable quantity. *Journal of the Textile Institute, 21*(9), 377.

Phillips, J., Johansson, R., & Johnson, K. (1990). Representation of braille characters in human nerve fibres. *Experimental Brain Research, 81*(3), 589-592.

Picard, D., Dacremont, C., Valentin, D., & Giboreau, A. (2003). Perceptual dimensions of tactile textures. *Acta Psychologica, 114*(2), 165-184. doi: DOI 10.1016/j.actpsy.2003.08.001

Pier Giorgio, M. (1995). FAST - Fabric Assurance by Simple Testing. *International Journal of Clothing Science and Technology, 7*(2-3), 43.

Postle, R., Carnaby, G. A., & Dejong, S. (1988). Surface of woven fabrics *The Mechanics of wool structures* (pp. 387). Chichester: Ellis Horwood.

Pruett, J. R., Sinclair, R. J., & Burton, H. (2001). Neural correlates for roughness choice in monkey second somatosensory cortex (SII). *Journal of Neurophysiology, 86*(4), 2069-2080.

Raheel, M., & Liu, J. (1991). An empirical-model for fabric hand .2. Subjective assessment. *Textile Research Journal, 61*(2), 79-82. doi: 10.1177/004051759106100204

Randolph, M., & Semmes, J. (1974). Behavioral consequences of selective subtotal ablations in postcentral gyrus of macaca-mulatta. *Brain Research, 70*(1), 55-70. doi: 10.1016/0006-8993(74)90211-X

Ring, J. W., & de Dear, R. (1991). Temperature transients: A model for heat diffusion through the skin, thermoreceptor response and thermal sensation. *Indoor Air, 1*(4), 448-456. doi: 10.1111/j.1600-0668.1991.00009.x

Roland, P. E., O'Sullivan, B., & Kawashima, R. (1998). Shape and roughness activate different somatosensory areas in the human brain. *Proceedings of the National Academy of Sciences of the United States of America, 95*(6), 3295-3300. doi: 10.1073/pnas.95.6.3295

Rombaldoni, F., Demichelis, R., & Mazzuchetti, G. (2010). Prediction of human psychophysical perception of fabric crispness and coolness hand from rapidly measurable low-stress mechanical and thermal parameters. *Journal of Sensory Studies, 25*(6), 899-916. doi: 10.1111/j.1745-459X.2010.00312.x

Romeli, D., Barigozzi, G., Esposito, S., Rosace, G., & Salesi, G. (2013). High sensitivity measurements of thermal properties of textile fabrics. *Polymer Testing, 32*(6), 1029-1036. doi: 10.1016/j.polymertesting.2013.05.011

Sarda, A., Deterre, R., & Vergneault, C. (2004). Heat perception measurements of the different parts found in a car passenger compartment. *Measurement, 35*(1), 65-75. doi: 10.1016/j.measurement.2003.08.018

Schafer, K., Braun, H. A., & Kurten, L. (1988). Analysis of cold and warm receptor activity in vampire bats and mice. *Pflugers Archiv-European Journal of Physiology, 412*(1-2), 188-194.

Schepers, R. J., & Ringkamp, M. (2009). Thermoreceptors and thermosensitive afferents. *Neuroscience and Biobehavioral Reviews, 33*(3), 205-212. doi: 10.1016/j.neubiorev.2008.07.009

Schiwarz, E. R. (1939). Technical Evaluation of Textile Finishing Treatments. *Textile Research Journal, 9*(6), 7. doi: 10.1177/004051753900900603

Schneider, A. M., & Holcombe, B. V. (1991). Properties Influencing Coolness to the Touch of Fabrics. *Textile Research Journal, 61*(8), 488-494. doi: 10.1177/004051759106100810

Schroder, A. C., Viemeister, N. F., & Nelson, D. A. (1994). Intensity discrimination in normal-hearing and hearing-impaired listeners. *The Journal of the Acoustical Society of America, 96*(5), 2683. doi: 10.1121/1.411276

Shirado, H., & Maeno, T. (2005). Modeling of human texture perception for tactile displays and sensors. *World Haptics Conference: First Joint Eurohaptics Conference and Symposium on Haptic Interfaces for Virutual Environment and Teleoperator Systems, Proceedings*, 629-630.

Shyr, T. W., Lai, S. S., & Lin, J. Y. (2004). New approaches to establishing translation equations for the total hand value of fabric. *Textile Research Journal, 74*(6), 528-534. doi: 10.1177/004051750407400611

Siegelbaum, S. A., & Koester, J. (2013). Ion Channels. In E. R. Kandel, J. H. Schwartz, T. M. Jessell, S. A. Siegelbaum, & A. J. Hudspeth (Eds.), *Principles of neural science* (th ed., pp. 100-108). New York: McGraw-Hill Medical.

Simoes-Franklin, C., Whitaker, T. A., & Newell, F. N. (2011). Active and passive touch differentially activate somatosensory cortex in texture perception. *Human Brain Mapping, 32*(7), 1067-1080. doi: 10.1002/Hbm.21091

Smit, J., Hanekom, T., & Hanekom, J. (2009). Modelled temperature-dependent excitability behaviour of a single ranvier node for a human peripheral sensory nerve fibre. *Biological Cybernetics, 100*(1), 49-58. doi: 10.1007/s00422-008-0280-7

Smith, C. U. M. (2000). *Biology of sensory systems*. New York, NY: John Wiley.

Srinivasan, M. A., & Lamotte, R. H. (1995). Tactual discrimination of softness. *Journal of Neurophysiology, 73*(1), 88-101.

Stanković, S. B., Popović, D., & Poparić, G. B. (2008). Thermal properties of textile fabrics made of natural and regenerated cellulose fibers. *Polymer Testing, 27*(1), 41-48. doi: 10.1016/j.polymertesting.2007.08.003

Stevens, S. S. (1957). On the psychophysical law. *Psychological review, 64*(3), 153-181. doi: 10.1037/h0046162

Stevens, S. S. (1961). To honor Fechner and repeal his law: A power function, not a log function, describes the operating characteristic of a sensory system. *Science, 133*(3446), 80-86. doi: 10.1126/science.133.3446.80

Stuart, I. M., & Baird, K. (1966). A new test for bending length. *Textile Research Journal, 36*(1), 91-93. doi: 10.1177/004051756603600112

Sultan, M., & Sheta, A. (1994). Predicting fabric hand acceptance for a specific end-use. *Textile Information Bulletin, 36*(4).

Symmons, M. A., Richardson, B. L., & Wuillemin, D. B. (2004). Active versus passive touch: Superiority depends more on the task than the mode. In S. Ballesteros &

M. Heller (Eds.), *Touch Blindness and Neuroscience*. Madrid: Universidad Nacional De Educacion a Distancia.

Talavera, K., Yasumatsu, K., Voets, T., Droogmans, G., Shigemura, N., Ninomiya, Y., . . . Nilius, B. (2005). Heat activation of TRPM5 underlies thermal sensitivity of sweet taste. *Nature, 438*(7070), 1022-1025. doi: 10.1038/Nature04248

Tanaka, Y., Tanaka, M., & Chonan, S. (2006). Development of a sensor system for measuring tactile sensation. *2006 Ieee Sensors, Vols 1-3*, 554-557.

Taylor, M. M., & Lederman, S. J. (1975). Tactile roughness of grooved surfaces - Model and effect of friction. *Perception & Psychophysics, 17*(1), 23-36. doi: 10.3758/Bf03203993

Tiest, W. M. B. (2010). Tactual perception of material properties. *Vision Research, 50*(24), 2775-2782. doi: 10.1016/j.visres.2010.10.005

Tiest, W. M. B., & Kappers, A. M. L. (2006). Analysis of haptic perception of materials by multidimensional scaling and physical measurements of roughness and compressibility. *Acta Psychologica, 121*(1), 1-20. doi: DOI 10.1016/j.actpsy.2005.04.005

Tiest, W. M. B., & Kappers, A. M. L. (2007). Haptic and visual perception of roughness. *Acta Psychologica, 124*(2), 177-189. doi: 10.1016/j.actpsy.2006.03.002

Tiest, W. M. B., & Kappers, A. M. L. (2008). Thermosensory reversal effect quantified. *Acta Psychologica, 127*(1), 46-50. doi: 10.1016/j.actpsy.2006.12.006

Tominaga, M., & Caterina, M. J. (2004). Thermosensation and pain. *Journal of Neurobiology, 61*(1), 3-12. doi: 10.1002/Neu.20079

Tominaga, M., Caterina, M. J., Malmberg, A. B., Rosen, T. A., Gilbert, H., Skinner, K., . . . Julius, D. (1998). The cloned capsaicin receptor integrates multiple pain-producing stimuli. *Neuron, 21*(3), 531-543. doi: 10.1016/S0896-6273(00)80564-4

Van Wyk, C. M. (1946). Note on the compressibility of wool. *Journal of the Textile Institute Transactions, 37*(12), 285-292. doi: 10.1080/19447024608659279

Verrillo, R. T., & Ecker, A. D. (1977). Effects of root or nerve destruction on vibrotactile sensitivity in trigeminal neuralgia. *Pain, 3*(3), 239-255. doi: 10.1016/0304-3959(77)90005-7

Voets, T. (2012). Quantifying and modeling the temperature-dependent gating of trp channels. *Reviews of Physiology, Biochemistry and Pharmacology, 162*, 91-119. doi: 10.1007/112_2011_5

Voets, T., Droogmans, G., Wissenbach, U., Janssens, A., Flockerzi, V., & Nilius, B. (2004). The principle of temperature-dependent gating in cold- and heat-sensitive TRP channels. *Nature, 430*(7001), 748-754. doi: 10.1038/Nature02732

Voets, T., Owsianik, G., Janssens, A., Talavera, K., & Nilius, B. (2007). TRPM8 voltage sensor mutants reveal a mechanism for integrating thermal and chemical stimuli. *Nature Chemical Biology, 3*(3), 174-182. doi: 10.1038/Nchembio862

Vriens, J., Owsianik, G., Hofmann, T., Philipp, S. E., Stab, J., Chen, X. D., . . . Voets, T. (2011). TRPM3 Is a Nociceptor Channel Involved in the Detection of Noxious Heat. *Neuron, 70*(3), 482-494. doi: 10.1016/j.neuron.2011.02.051

Wang, X., Liu, X., & Hurren, C. (2008). Physical and mechanical testing of textiles. In J. L. Hu (Ed.), *Fabric Testing* (pp. 116-117). Boca Raton, FL: CRC.

Wang, Z., Li, Y., Kowk, Y. L., & Yeung, C. Y. (2002). Mathematical simulation of the perception of fabric thermal and moisture sensations. *Textile Research Journal, 72*(4), 327-334. doi: 10.1177/004051750207200409

Weather history for Hong Kong, Hong Kong. Retrieved June 15, 2014, from www.wunderground.com/history/airport/Hong%20Kong/

Weather history for Matsumoto Airport, Japan. Retrieved June 15, 2014, from www.wunderground.com/history/airport/rjaf/

Weather history for Osaka Airport, Japan. Retrieved June 15, 2014, from www.wunderground.com/history/airport/rjoo/

Weather history for Qingdao, SD. Retrieved June 15, 2014, from www.wunderground.com/history/airport/zsqd/

Weather history for Shanghai Hongqiao, SH. Retrieved June 15, 2014, from www.wunderground.com/history/airport/zsss/

Weather history for Xi'an, SA. Retrieved June 15, 2014, from www.wunderground.com/history/airport/zlxy/

Weber, A. I., Saal, H. P., Lieber, J. D., Cheng, J. W., Manfredi, L. R., Dammann, J. F., & Bensmaia, S. J. (2013). Spatial and temporal codes mediate the tactile perception of natural textures. *Proceedings of the National Academy of Sciences of the United States of America, 110*(42), 17107-17112. doi: 10.1073/pnas.1305509110

Wheat, H. E., Salo, L. M., & Goodwin, A. W. (2010). Cutaneous afferents from the monkeys fingers: responses to tangential and normal forces. *Journal of Neurophysiology, 103*(2), 950-961. doi: 10.1152/jn.00502.2009

Winakor, G., Kim, C. J., & Wolins, L. (1980). Fabric hand: Tactile sensory assessment. *Textile Research Journal, 50*(10), 601-610. doi: 10.1177/004051758005001005

Wong, A. S. W., & Li, Y. (2002). *Clothing sensory comfort and brand preference*. Paper presented at the IFFTI international conference, Hong Kong.

Wong, A. S. W., Li, Y., & Yeung, P. K. W. (2004). Predicting clothing sensory comfort with artificial intelligence hybrid models. *Textile Research Journal, 74*(1), 13-19. doi: 10.1177/004051750407400103

Xin, B. J., Hu, J. L., & Yan, H. J. (2002). Objective evaluation of fabric pilling using image analysis techniques. *Textile Research Journal, 72*(12), 1057-1064. doi: 10.1177/004051750207201204

Xin, B. X., Hu, J. L., & Baciu, G. (2010). Visualization of Textile Surface Roughness Based on Silhouette Image Analysis. *Textile Research Journal, 80*(2), 166-176. doi: 10.1177/0040517508093779

Xu, F., & Lu, T. J. (2011). Skin Biomechanics Experiments: Measurement and Influence of Different Factors *Introduction to Skin Biothermomechanics and Thermal Pain* (pp. 108-109). Berlin: Springer.

Yang, G. H., & Kwon, D. S. (2008). *Effect of temperature in perceiving tactile stimulus using a thermo-tactile display*. Paper presented at the International Conference on Control, Automation and Systems, Seoul.

Yarnitsky, D., & Ochoa, J. L. (1990). Release of cold-induced burning pain by block of cold-specific afferent input. *Brain, 113*, 893-902. doi: 10.1093/brain/113.4.893

Yoneda, M., & Kawabata, S. (1982). *A theoretical consideration on the objective measurement of warm/cool feeling of fabrics*. Paper presented at the Objective Specification of Quality Mechanical Properties and Performance, Kyoto, Japan.

Yoshioka, T., Bensmaia, S. J., Craig, J. C., & Hsiao, S. S. (2007). Texture perception through direct and indirect touch: An analysis of perceptual space for tactile textures in two modes of exploration. *Somatosensory and Motor Research, 24*(1-2), 53-70. doi: Doi 10.1080/08990220701318163

Yoshioka, T., Gibb, B., Dorsch, A. K., Hsiao, S. S., & Johnson, K. O. (2001). Neural coding mechanisms underlying perceived roughness of finely textured surfaces. *Journal of Neuroscience, 21*(17), 6905-6916.

Zakharian, E., Cao, C., & Rohacs, T. (2010). Gating of transient receptor potential Melastatin 8 (TRPM8) channels activated by cold and chemical agonists in planar lipid bilayers. *Journal of Neuroscience, 30*(37), 12526-12534. doi: 10.1523/Jneurosci.3189-10.2010

Zhang, L. M. (1993). *The model and application of the Artifical Neural Network*. Shanghai: Fudan University Press.

Zhang, S. J., Li, Y., Hu, J. Y., Liao, X., & Zhang, H. T. (2014). Heat transfer in single-side napped fabrics during compression. *Journal of Fiber Bioengineering & Informatics, 7*(1), 103-106. doi: 10.3993/jfbi03201409

Zhou, N. Y. M., & Ghosh, T. K. (1997). On-line measurement of fabric bending behavior .1. Theoretical study of static fabric loops. *Textile Research Journal, 67*(10), 712-719. doi: 10.1177/004051759706701003

Zurek, W., Jankowiak, D., & Frydrych, I. (1985). Surface frictional resistance of fabrics woven from filament yarns. *Textile Research Journal, 55*(2), 113-121. doi: 10.1177/004051758505500207